COMPRESSIVE MEMBRANE ACTION

in

BRIDGE DECK SLABS

by

Paul Austin JACKSON
BSc CEng MICE MIStructE

Submitted to the
Council of National Academic Awards
in partial fulfilment of
the requirements of the degree of:

DOCTOR OF PHILOSOPHY

Sponsoring Establishment:
Polytechnic South West
Department of Civil Engineering

Collaborating Establishment:
British Cement Association

April 1989

COMPRESSIVE MEMBRANE ACTION

in

BRIDGE DECK SLABS

by

Paul Austin JACKSON

ABSTRACT

An elastic analysis of restrained slab strips shows that membrane action enhances serviceability behaviour. However, the enhancement is not as great as for strength and serviceability is critical when membrane action is considered in design.

A relatively simple form of non-linear finite element analysis is developed which is able to model bridge deck behaviour allowing for membrane action. This reduces some of the disadvantages of non-linear analysis which have prevented its use in practice. It uses line elements but, because of novel features of the elements and because it considers all six degrees of freedom at each node, it is still able to model in-plane forces reasonably realistically. It gives acceptable predictions for behaviour.

The tension stiffening functions used in non-linear analysis, which are important to the prediction of restraint, are considered. Explanations are proposed for several aspects of the behaviour and a new function is developed. This gives better results than previous expressions, particularly for deflections on unloading and reloading.

Tests under full HB load have been performed on two half scale bridges. These, and the analysis, show that conventional design methods for deck slab reinforcement are very conservative. They also show that the restraint required to develop membrane action is not dependent on diaphragms; it comes from under-stressed material surrounding the critical areas. Thus, over much of a bridge's span, there is transverse tension in the slab and membrane action does not significantly enhance the resistance to global moments.

Both bridge models failed by a wheel punching through the slab. It is shown that these were primarily brittle bending compression failures which were strongly influenced by global behaviour. This is confirmed both by the analysis and by the higher wheel load at failure in single wheel tests.

Recommendations are made for using the results in design and assessment.

ACKNOWLEDGEMENTS

The research reported in this thesis was undertaken at the British Cement Association, formerly the Cement and Concrete Association, whilst I was an employee of that organisation. I wish to thank the Council, directors and former directors of the Association for instigating the project, for continuing to support it during a difficult period for the Association and for allowing me to submit this thesis. I should also like to thank Gifford and Partners for practical help during the latter phase of the project, particularly for the use of several hours of main-frame computer time.

Thanks are also due to my two supervisors, Professor Robert Cope and Doctor Andrew Beeby, for assistance with different aspects of the study. In particular, I wish to thank Professor Cope for many helpful discussions regarding the analysis.

Too many of the staff and former staff of the Association contributed to the experimental phase of the project to name them all. However, I should like to thank them all. Particular thanks are due to Colin Cook for the instrumentation and to Daran Morahan and Ron Jewel, whose enthusiasm and expertise enabled me to complete the testing in what became a very tight timetable.

Thanks are due to my wife, Sue, for typing some of the text and for proof reading the document. Last, but by no means least, I should like to thank our two sons Andrew and Simon, as well as Sue, for putting up with my absence or preoccupation whilst working on the thesis.

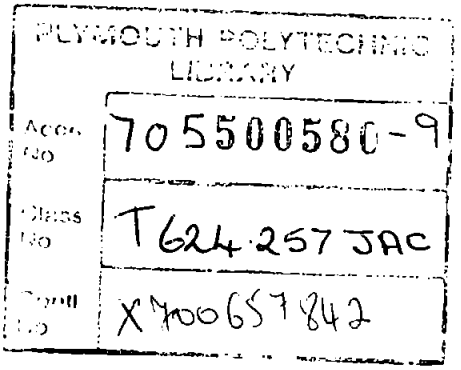

CONTENTS

LIST OF FIGURES

LIST OF TABLES

CHAPTER 1

INTRODUCTION

If in-plane restraint prevents material in the tension region of a beam or slab from expanding as load is applied, a compressive force is developed. This force can lead to greater strengths and stiffnesses than are predicted by normal flexural theory. In a simple steel beam, however, the enhancement is relatively small and arises only when the in-plane restraint is applied below, that is on the tension side of, mid-depth. In concrete, and also in masonry, the low tensile strength and consequent cracking mean that the effect can arise even when the restraint is applied at mid-depth. The enhancement can also be very much greater since the compressive force enables even unreinforced slabs to support large loads.

This effect, which is known as compressive membrane action, arching action or dome effect, has been known since the earliest days of reinforced concrete. It was described by Westergaard and Slater(1) in 1921 and as early as 1909 Turner(2) wrote of his flat slabs "such a slab will act at first somewhat like a flat dome and slab combined". Turner built many flat slabs with reinforcement designed by empirical means. At the time there was good reason to use empirical design methods; the theory of flat plates was not well developed. However, Turner's contemporaries used more conservative design methods and Sozen and Siess(3) report that, in 1910, the weight of steel required in the interior panel of a flat slab varied by a factor of four according to the design method used. As they put it "design methods could not be correct if the variation in results was 400%". When an analysis based on simple statics was published in 1914(4), it suggested that Turner's slabs were grossly under-designed; yet they had behaved well both in service and in load tests. Lord(5) had even measured strains in a load test which appeared to support Turner and defy the laws of statics. Compressive membrane action was an important reason for these discrepancies although there were others, including tension stiffening(3).

Despite the satisfactory behaviour of Turner's slabs, design methods which can be justified by statics are now preferred and purely empirical methods have tended to fall out of favour whenever more rational methods have become available. Thus even flat slabs are now designed using flexural theory, although Sozen and Siess(3) report that the change was gradual whilst Beeby(6) has shown that it is still not complete.

Apart from indirect (and very limited) use in the Soviet design code(7), compressive membrane action seems to have been largely forgotten for many years. Thus, in Braestrup's words(8), "it therefore came as a surprise when Ockleston(9) tested a real structure in South Africa and recorded collapse loads that were three or four times the capacities predicted by yield-line theory". In fact Guyon(10) had found similar results slightly earlier, when he tested a multi-bay continuous slab, but this seems to have been considered a characteristic of prestressed concrete.

Ockleston's results stimulated research into compressive membrane action which has continued ever since. Despite this research, which will be reviewed in Chapter 3, the effect is still not normally used in design. Recently, however, new design rules for bridge deck slab reinforcement, which do allow for the effect, have been developed and incorporated into the Ontario Highway Bridge Design Code(11). These rules lead to major savings compared with conventional design methods; typically a 70% reduction in main steel plus a saving in design time. More recently still, similar rules have been adopted in other parts of the World, including Northern Ireland. The rules used in Northern Ireland(12) were proposed by Kirkpatrick et al(13) for use in the whole of Britain but have not yet been accepted on the mainland.

One objection to these rules is simply that they are empirical. Existing theory shows, as will be seen in Chapter 3, that slabs designed to the rules will have ample strengths under local wheel loads, *provided there is adequate restraint.* It even suggests that there would still be ample strength with no reinforcement at all. This, however, is the limit of the extent to which the rules are proven theoretically. There is also an apparently serious omission from the experimental work on which they are based. An extensive series of tests on laboratory specimens, model bridges and real bridges was undertaken yet none of the tests produced anything approaching the full design global load on a bridge. Thus the integrity of the deck slabs under combined global and local effects is unproven. Also, they may not give the load distribution which is assumed in the design of the beams; particularly as global analysis based on *uncracked* slab properties is recommended(11,14) for use with the rules.

Concrete slab design has come full circle; bridge deck slab design is now in the position which flat slab design occupied in 1914. On the one hand

there is an empirical design method which seems to work and which is very economical yet which could be considered unproven: on the other there is the conventional method which is supported by flexural theory but which seems to be very uneconomical. Just as in 1910 design methods for flat slabs could not be correct when they differed by 400%, so design rules for bridge deck slab reinforcement cannot be correct now when they differ by 300%. There is clearly a need for further research.

In recent years the assessment of existing structures has assumed equal importance to the design of new construction. Current design standards are used in these assessments, but they often suggest that structures which have given many years of satisfactory service are unsafe. In many such cases, compressive membrane action offers the possibility of more realistic assessment which could avoid expensive strengthening and reconstruction work. Previous research, having concentrated on new construction, does not enable this potential to be fully used.

Another problem which has become more important in recent years is reinforcement corrosion. Resistance to this can be greatly improved by increasing cover or by using epoxy coated, or other special reinforcement. Both these approaches would become more economical if membrane action were considered in design. It has even been suggested that satisfactory deck slabs could be built without any reinforcement at all, which would certainly avoid the problem of reinforcement corrosion.

"Localised" reinforcement corrosion is believed to be particularly dangerous(15) but an interesting implication of membrane action, which has not previously been considered, is that this may have no significant effect on the behaviour of slabs.

In the present study the behaviour of bridge decks is investigated in order to develop and justify a rational design and assessment method which can be adopted in British practice but which takes as much advantage as possible of compressive membrane action. The approaches used in the study include tests on large scale model bridges and a simple elastic analysis. However, because model tests alone can produce only empirical results, whilst the behaviour considered is too complex to analyse in full by hand, non-linear computer analyses are also used.

CHAPTER 2

CURRENT DESIGN PRACTICE

2.1 INTRODUCTION

In order to direct this study towards those areas which are important in design, and to ensure that the knowledge gained will be usable in practice, it is necessary to begin the study with a good understanding of current bridge deck design practice. That is, of the way bridges are assumed to behave for design purposes, of the way they are designed, and of the criteria and codes of practice they are designed to. This chapter aims to provide such an understanding. There are also more fundamental reasons for respecting past practice which will be discussed.

Design practice, unlike the real behaviour of bridges, differs significantly between countries. It is not practical, or necessary, to review practice throughout the world. This study is aimed at improving British practice, so this chapter will concentrate on British practice. Much of the most relevant previous research has, however, been undertaken in North America against a background of North American design practice. There are several important differences between British and North American design practice which have greatly influenced the research and render its application in Britain more difficult than might be expected. In order to appreciate these problems it is necessary to review the relevant aspects of North American design practice. Only conventional design methods, which ignore membrane action, will be considered here. The newer empirical design approach, which allows for membrane action, will be considered in the next chapter, along with the research from which it was developed.

2.2 OUTLINE DESIGN

2.2.1 Choice of Form

Before the detailed design of a bridge can be started the form of the bridge has to be decided; for example solid slab, voided slab, beam and slab, box girder or arch. In making this decision, engineers are guided by experience. For particular ranges of span and sets of circumstances, certain forms of structure have been found to be most economical. Over the years these favoured forms change, usually because of changes in construction technology rather than because of advances in analysis. Construction considerations are always very important(16). The desired

erection method nearly always decides the form of the bridge, rather than the reverse. For example, one does not choose to use precast elements in a bridge because it is a beam and slab bridge, one chooses a beam and slab bridge because it is convenient to precast.

The few cases when advances in analysis have changed the form of bridges have arisen when those advances have enabled the analysis of structures which are physically simpler but analytically more complicated. An example of this is the virtual extinction of intermediate diaphragms in beam and slab bridges since load distribution analysis has been in widespread use. These diaphragms served not so much to distribute load between beams as to enable this distribution to be analysed. With modern analytical methods they are eliminated, sometimes at the price of doubling the transverse steel in the deck slab. In terms of material cost this change may be uneconomic, but the difficulty of forming diaphragms in the span is such that eliminating them leads to significant overall savings. Thus if re-introducing these diaphragms solved a problem in using membrane action (and Chapter 3 shows that this is the case) it would still not be economical.

The dominance of construction considerations in the choice of the form of bridges means that a study such as this, which considers only the behaviour of completed structures, is unlikely to alter the form of bridges. It is thus essentially concerned with detailed design rather than with scheme design.

2.2.2 To Stress or not to Stress?

Another decision which has to be taken in the early stages of a concrete bridge design is whether or not to prestress and if so whether to pre- or post-tension.

Again this decision is often dictated by practical considerations of construction. It is not possible to build a glued segmental bridge without post-tensioning and it would be difficult to build any long-span bridge (except an arch) of ordinary reinforced concrete. On the other hand, a small slab is obviously more conveniently reinforced and small precast beams are more easily pre-tensioned on a long line bed. Only over narrow ranges of structures (such as large voided slabs) is the decision marginal,

and therefore sensitive to small changes in the relative costs or quantities of steel required.

In Britain, and most of the rest of the world, it has been found that, because of the extra operations involved, transverse stressing of bridge deck slabs is rarely economical. A large number of tendons have to be fixed, threaded, stressed and grouted, usually with very difficult access. Much of the cost of these operations is fixed so that, even if the required force were greatly reduced, transverse stressing would still be unattractive. Because of this, the present study assumes that deck slabs will not be transversely stressed. Accordingly, the rest of this chapter concentrates on the design of ordinary reinforced concrete. In reality, however, (unlike in most codes of practice) prestressed and reinforced concrete are not fundamentally different. Also bridge deck slabs are often effectively prestressed in the longitudinal direction by the global behaviour of the deck. Thus research on stressed slabs can be relevant and some of it will be considered in Chapter 3.

2.3 DETAILED DESIGN AND CODES OF PRACTICE

2.3.1 The Importance of Codes of Practice

Most major bridge owners, including all of those in Britain, require new construction to be designed to specified codes of practice. The same codes are also frequently specified for use in assessment. Because of this, codes have an importance which they owe as much to their contractual position as to their engineering merit. This alone justifies the extensive reference which is made to them throughout this chapter. It also means that a new design method, such as one which allows for membrane action, will be much more easily put into practice if it can be used within existing codes. Despite this, it is arguable that a research thesis such as this should be concerned only with fundamental requirements of structural behaviour, and not with the sometimes arbitrary provision of codes of practice. Codes do, however, have a considerable engineering, as distinct from contractual, significance which arises from their two different, but overlapping, types of source.

2.3.2 Sources of Code Clauses

The first of these sources is the philosophy, theory and test data on which codes are based. The second is the cumulative experience which they

represent. The latter means that a code can be considered as a set of arbitrary rules which have been found to produce satisfactory structures in the past. Paradoxically, this applies to new codes, as well as to long-established ones, because they are adjusted to make significant changes to past designs only where they are known to be at fault.

The two sources of code clauses each have their faults. Our understanding of structural behaviour and our stock of test results are too incomplete to enable them to be used as the sole basis of a code of practice. On the other hand experience, as a source of code clauses, allows no innovation and shows only where provisions are inadequate, not where they are over-conservative or even unnecessary. It has also been pointed out by Beeby(17) that experience is an unreliable guide to design practice when, as is usual with bridges, the design life is long compared with the time-scale of change in loading, materials and design methods.

Code clauses owe their origins to a complex mixture of theory, test results, experience and the engineering judgement of the code writers. Theories are fitted to test results and to experience. New theories and test results are used to design structures which become part of the stock of experience. Experience is reviewed in the light of new theories, whilst structures which were designed using discarded theories remain in the stock of experience. Finally, when experience shows that a subject needs a code clause but not what the clause should be, and when there is no clear-cut theory or evidence to go on, the code committee makes an arbitrary decision. By now it is often difficult to tell what specific source, or even what type of source, any particular code clause is based on. This may not matter to the ordinary user of the code, but it is important when the code comes to be reviewed in the light of new discoveries.

Even when the source of a code clause can be identified it may be a matter of opinion whether the clause is a logical and fundamental requirement or an arbitrary rule. A classic example of this is the no-tension rule in prestressed concrete, which can easily be traced back to Freyssinet(18). This rule illustrates how the source of a code clause (that is, whether it is a fundamental requirement or an arbitrary rule which has been found to work) affects, or should affect, the way it is reviewed in the light of new discoveries. This will be considered in more detail.

In the 1970's Emerson(19) observed that bridges were subjected to large temperature differentials with non-linear distributions. This implied that many bridges designed to the no-tension rule experienced significant tensile stresses. If the no-tension rule was a logical and fundamental requirement this was an alarming discovery indicating that the prestress in those bridges needed to be increased. On the other hand, if the no-tension rule was simply an arbitrary design criterion which has been found to produce satisfactory structures in the past, the discovery that some of those satisfactory structures do experience tension is no cause for alarm. If anything, it implies that the remainder of the structures designed to the rule, which do not experience tension, have more prestress than they need. It is now widely accepted that the no-tension rule is largely arbitrary [eg. see Low(20)] but at the time it was treated as though it was a rational and necessary requirement. The result was that from the introduction of non-linear temperature distributions into bridge design practice in 1973(21), up to the implementation(22) of BS 5400(23) and the use of a degree of so-called "partial prestressing" in 1983, many bridges were provided with unjustifiably large amounts of prestress.

Research, by providing new theory and test results, can invalidate code provisions which are based on theory and test results. Where new research provides sufficient understanding of the relevant aspects of behaviour it can also supersede code provisions which are based on practical experience. Often, however, the critical design criteria for bridges are difficult to define, let alone check by analysis. A bridge has to survive a long life in an adverse environment and to remain serviceable after experiencing a complex history of loads: environmental, functional and accidental. When we cannot fully analyse these things we rely upon experience to fill in the gaps.

This inability to fully analyse all aspects of behaviour, and the consequent dependence upon experience, tends to make bridge engineers conservative. If code provisions, and hence design methods, are based purely on experience how can we know if it is safe to reduce the steel area in bridge deck slabs? One might think that until we can fully understand all aspects of the behaviour of structures, we have to keep using as much steel as we always have. In truth, however, theory can be used to extrapolate experience and to use experience of one type of structure in the design of another.

If we can prove with new theory that the steel in deck slabs, which is designed for a stress of 345N/mm^2, actually experiences a stress of only, say, 80N/mm^2, it does not prove that it would be safe to design the slab with the new theory. Until we can understand all aspects of behaviour we do not know, from theory alone, that it would be safe or that the behaviour of the slab would be satisfactory. Is it possible that a long-term or cyclic stress of over 80N/mm^2 would cause problems? Our experience of slabs does not answer this question because all the slabs we can observe were designed by the very conservative method which we are trying to supersede. Simply supported beams are statically determinate, however, so we know they experience the stress they are designed for. Thus we do not need to fully understand all the implications of allowing a higher stress to know if it is safe; we know it works in beams. Thus, even if new theory cannot prove that a slab design will be satisfactory, it can show that the maximum stresses the slab will experience are less than those experienced by beams whose behaviour we know to be satisfactory. Thus it enables the reinforcement in slabs to be reduced, refining the safety margins towards, but not below, those already found satisfactory in beams.

2.3.3 Limit State and Working Stress Codes

The great majority of bridges built in Great Britain are designed to Department of Transport standards. The loading standard used is BS 5400: Part 2: 1978(24) as implemented (and significantly modified) by BD 14/82(25) whilst the design standard for concrete bridges is BS 5400: Part 4: 1984(26) which is implemented by BD 24/84(27). These are limit state codes but the Department has only recently changed from using its own standards(21,28,29) which were based on the working stress approach. It is helpful to review what this change in concept means.

The basic idea of a limit state code is that the various ways in which a structure could exhibit unacceptable behaviour are considered in turn. A structure which is on the limit of acceptable behaviour is said to have reached a certain "limit state". Thus a structure which has the maximum acceptable deflection could be said to have reached the limit state of deflection. Checking a design involves checking each limit state in turn. Partial safety factors and the concept of probabilistic design have been introduced at the same time as limit state philosophy but they are not central to the concept or definition of a limit state code.

A working stress code specifies allowable stresses. Checking a design involves using elastic theory to calculate the stresses which exist in the structure under working loads. These stresses are then compared with the allowable stress. It is the code writer's responsibility to set the allowable stress at a level such that compliance with the limit ensures satisfactory behaviour of the structure.

At first sight the two approaches seem quite fundamentally different. It might also be thought, as some engineers have argued(30), that the limit state approach involves the designer in a great deal more calculation than the working stress approach. In practice the difference is far less clear-cut. This is largely because it has never been possible to develop reasonable stress limits which ensure satisfactory behaviour of a structure in every respect. The result is that so called "working stress" codes require separate checks on what are really limit states; such as deflection and crack widths. Conversely, it has been possible to write many limit state codes in such a way that compliance with one limit state (and perhaps some nominal rules as well) ensures compliance with other limit states. In CP110(31) - now BS 8110(32) - this has been taken to the point where it is normally only necessary to check one limit state, the ultimate limit state.

In principle a limit state code needs only to specify the design criteria for each limit state. It could leave the designer free to choose the method used to check compliance. In practice limit state codes do give methods for checking compliance, although these are often optional. The important point is that, in principle at least, the design criteria are fundamental characteristics of structural behaviour (such as strength or deflection) and are independent of the method used to check compliance. This differs from the situation in a working stress code where the design criterion is that the stress, *as calculated using elastic theory*, should comply with the limits. There the design criterion (stress) and the method for checking compliance (elastic theory) are not independent. The result is that the adoption of limit state codes should make the introduction of new methods of analysis and design into practice much easier than it was under working stress codes. It should be simply a case of using the new method to check compliance with the existing fundamental design criteria. In practice it is not this straightforward, because the design criteria in limit state codes are not always truly fundamental or independent of the

methods used to check compliance. This will be considered in more detail for the particular case of BS 5400: Part 4: 1984(26).

2.3.4 BS 5400: Part 4: 1984

BS 5400 is a limit state code and, as far as reinforced concrete is concerned, the major limit states which the designer is required to consider are the ultimate limit state and the serviceability limit states of crack widths and stress limits. There are other considerations, such as durability, deflection and reinforcement fatigue, but these are not normally critical in conventional design. The important limit states will be considered in turn.

a. Ultimate Strength

The need for a check on the ultimate limit state (formerly, and arguably more correctly, known as the limit state of collapse) is obvious. The consequences of failure at this limit state are clearly very serious so the acceptable probability of failure is very low. For this reason the partial safety factors used in BS 5400 for both loads and materials are larger for this limit state than for the serviceability limit state.

In principle, the design criterion for the ultimate limit state is simply that the structure should not collapse under the specified loads. This is a fundamental design criterion so, having specified loads and material strengths, the code is able to give some freedom as to how it is checked. The usual approach is to analyse the structure using methods which will be discussed in 2.4 and then to check sections separately for bending and shear. The bending strength check is done by assuming that plane sections remain plane and using the code specified stress-strain relationship for concrete and reinforcement. There is an additional proviso that the reinforcement should yield at failure which was introduced to ensure a ductile failure mode. As the clause is of questionable value, and has proved difficult to comply with in some sections, the code allows the alternative of providing 15% extra ultimate strength.

b. Crack Widths

The need for the two main serviceability limit states, crack width and stress, is less obvious and requires some explanation. It is desirable to limit crack widths for aesthetic reasons but the restriction in BS 5400 is unnecessarily severe for this purpose. This has arisen because it has

been assumed that there is a relationship between crack widths and reinforcement corrosion. Beeby(33) and others have said that neither the available test evidence nor the accepted theory of reinforcement corrosion support such a relationship. It seems likely, therefore, that the BS 5400 crack width restriction is unnecessarily severe, although at present it has to be complied with in design.

In principle a crack width is a fundamental design criterion which is independent of the method used to calculate it. In practice, however, the available crack width prediction formulae give such widely different results [see Beeby(34)] that the criterion and the method for checking compliance are interdependent. For this reason BS 5400 explicitly states that its criterion is that the crack width *as calculated using the code method* should not exceed the specified values. The particular formula specified in BS 5400 is based on that given in CP 110. The background to this is given by Beeby(34).

The code only requires crack widths to be checked for functional, not environmental, loads. It also only requires 25 units of HB load to be considered, not the full design value of up to 45 units. Tension stiffening is not used if more than half of the bending moment in the section is due to live load. This is to allow for the effect of repeated loading and for the possibility that a section could have been pre-loaded to a higher load than that for which cracking is checked. This differs from CP 110 and makes the crack width prediction formula conservative. Despite this, and unlike under BE1/73(28), it is rarely critical in the design of the main steel for bridge deck slabs.

c. Stress Limits

The provision of stress limits in a limit state code is something of an anomaly. It is contrary to the basic concept of a limit state code. If the deflections, strengths and crack widths are satisfactory it is hard to see how a structure can exhibit unacceptable behaviour due to stress. The stress limits in BS 5400 have been the subject of a study by the author(35). This showed that their purpose is to ensure reasonably linear-elastic structural behaviour. This is not a fundamental design criterion either but it is desirable for two reasons. Firstly, the methods given in the code for checking the other serviceability criteria, such as crack width and deflection, assume linear elastic behaviour. Thus the

check is needed simply as a check on an assumption made in the other checks. Secondly, in a structure which went significantly out of the elastic range, transient loads would cause permanent deformations. This would mean that a structure could be influenced by the cumulative effect of all the loads which it had experienced throughout its life. This would be extremely difficult, if not impossible, to assess. It is much simpler to assume that a structure recovers from transient loads and limit stress so that this is approximately true. It is only because of this restriction that BS 5400 is able to ignore some load cases when checking crack widths.

Because of cracking, the real behaviour of reinforced concrete structures is not linear-elastic. To ensure even approximately linear behaviour it would be necessary to limit the tensile stress to the cracking stress of the concrete, which is not considered practical. This means that a precise analysis of a reinforced concrete structure still requires an assessment of the cumulative effect of all the loadings which it experiences throughout its life. As this is not possible some other approach is needed. The only rigorously safe approach which is practical is to assume that the cumulative damage is total, and hence to ignore the tensile strength of concrete completely. This is done in some calculations, notably in assessing the ultimate strength of sections in flexure. It is also done in BS 5400 when assessing the crack widths which occur in sections loaded predominantly by live load. The approach is not, however, followed rigorously and many of the calculation formulae provided in codes of practice do depend on the tensile strength of concrete(6).

The stress limits in BS 5400 are not fundamental design criteria as they are not independent of the method used to check compliance. This is particularly true of the concrete compressive stress limitation of $0.5f_{cu}$. Concrete is significantly non-linear at this stress but the code writers considered it acceptable to allow some redistribution. This means that the actual maximum stress in a section with a calculated maximum of $0.5f_{cu}$ would be less than $0.5f_{cu}$. Despite this it still only just complies with the code criterion. In axial compression, where there is no scope for re-distribution, the code specifies the much lower limit of $0.38f_{cu}$. This inter-relationship between the code's criterion (the stress limit) and the method of checking compliance (elastic theory) means that, if an alternative analytical method is to be used in design, the design criteria

have to be reconsidered, a fact which has not always been appreciated by non-linear analysts. For example, see Edwards(36).

In routine design to BS 5400 it is not usual to check the stresses in reinforced concrete. The code allows the check to be avoided provided the analysis at the ultimate limit state is elastic without redistribution. The writer(35) has shown that, for normal sections in flexure, this rule results in designs which are similar to those which would be obtained by checking the stress. However, sections designed to this rule which are either heavily reinforced or subjected to axial loads can have calculated concrete stresses which are significantly above the $0.5f_{cu}$ limit. Despite this, such sections behave satisfactorily.

d. Critical Limit State

It can be seen from the preceding sections that ultimate strength is normally critical in the conventional design approach for reinforced concrete. This has led some researchers(37) to the conclusion that research on bridges should concentrate on ultimate strength. In reality, however, ultimate strength is critical in design only because of the conservative approach (elastic structural analysis) which is used to check it. This approach is, in effect, deliberately chosen in order to ensure that ultimate strength is critical and hence to avoid the need to check other considerations, such as the stress limits.

In the case of deck slabs, which are subjected to concentrated wheel loads, elastic theory predicts high moment peaks. In reality these peaks re-distribute. Because of this, a yield-line analysis of a typical deck slab designed by conventional methods shows that the ultimate strength is twice what is required. If, however, the designer opted to use this analysis for design he would have to check the service stress. The writer(35) has shown that, because of this, the maximum saving in steel area which can be obtained from the use of yield-line analysis is only about 11%. Thus, if analysis taking account of compressive membrane action is to result in significant economies, it must indicate improved serviceability behaviour as well as strength.

2.4 ANALYSIS FOR DESIGN - BRITISH PRACTICE

2.4.1 Reasons for Linear Analysis

Linear elastic analysis is nearly always used in design. This is partly because of the code of practice. BS 5400 does allow the use of inelastic methods at the ultimate limit state but, as we have already seen for reinforced concrete design, there is little to be gained from this. Linear analysis is also convenient for another reason; the principle of superimposition applies and, with the great number of load cases which have to be considered, this is a major advantage. It also makes linear analysis much easier to computerise than other methods.

Linear elastic analysis is so widely used in bridge design that designers tend to forget that the real behaviour of reinforced concrete (particularly lightly reinforced concrete) can be highly non-linear even at service loads. However, linear elastic analysis does lead to safe lower-bound solutions which is more important in design than realism. Also, if (as was suggested in 2.3.2) a major justification for the design criteria in codes is the experience that they have led to satisfactory structures, the mere fact that linear analysis was used in the design of those structures is sufficient justification for using it.

2.4.2 Section Properties

Having opted to use linear elastic analysis to analyse a highly non-linear material, such as reinforced concrete, it is necessary to make some gross assumptions to obtain the section properties. Here BS 5400 gives the designer considerable freedom. It allows the use of the gross concrete section, the gross concrete section plus reinforcement transformed on the basis of the modular ratio, or the reinforcement (again transformed) plus the concrete but ignoring concrete which is subjected to tension. In a reinforced concrete frame structure it makes little difference which section properties are used because the relative stiffness of the members is little changed. Bridge decks, in contrast, are often prestressed (and hence uncracked) longitudinally but lightly reinforced transversely. Their transverse stiffness may differ by as much as a factor of 8 between methods whilst their longitudinal stiffness is unchanged. This significantly affects the results but, fortunately, any assumption of section properties will lead to a safe design according to plastic theory(38).

Gross concrete sections are almost invariably used because this enables the final structural analysis to be performed before it has been decided how much reinforcement to provide. It is not always appreciated that the alternative cracked transformed section is not strictly linear in its behaviour. Moment is proportional to curvature, but only if any axial force also varies proportionally. Furthermore the cracked transformed sections in sagging and hogging are different in that, even if the reinforcement is symmetrical, the moment reversal moves the neutral axis. It is this tendency of cracked sections to change their section properties as moment is applied which causes compressive membrane action. This leads to the possibility that an elastic analysis using cracked transformed sections would enable compressive membrane action to be used in design within the existing code. This would avoid the need to solve the complex problem of assessing the cumulative effect of load history on non-linear structures. Such an analysis, which is only linear under proportional loading, will be considered in later chapters.

2.4.3 Global and Local Functions

It is difficult to analyse a whole bridge in sufficient detail to design the deck slab reinforcement. It is convenient, therefore, to divide the behaviour into "global" and "local" functions. The local function of the deck slab is to support wheel loads spanning between the beams. This can be analysed by a variety of elastic methods. These are all based on isotropic plate theory which, as we shall see in later chapters, does not model slab behaviour well. The most popular methods are those due to Westergaard(39) and Pucher(40). In this analysis, the slab may be assumed to be fully fixed-ended or simply supported. Alternatively, an intermediate case is sometimes used.

The global functions of the slab are to distribute load between the beams and to act as the top flange of the beams. A variety of elastic methods have been used for global analysis including methods based on orthotropic plate theory, such as the Morice Little method(41), and several computer methods. The modern trend is to use computerised grillage analysis almost exclusively(42). As a bridge deck is not a true grillage, this requires some approximations, particularly to represent the torsional behaviour, and advice on these has been published by West(43). One fault of grillage analysis for which it is difficult to correct is that it assumes that the main beams are connected together only by transverse beams which are in

the same plane as the main beams. The beams in real beam and slab decks, in contrast, are connected together by their top flanges and the in-plane shear stiffness of these tends to even out the stress between the beams. Ignoring this is conservative and, although the effect on the slab stress is significant [see Hambly(44)], the effect on the beam soffit stresses is quite small. As the latter are critical in design the effect of the error on design is not important.

The calculated global and local transverse moments in the slab are normally simply added together. This is not strictly correct as the end moments assumed in the local analysis should, theoretically, be applied to the global analysis.

In the longitudinal direction the global behaviour imposes an axial force on the slab. It is common practice to ignore this in designing the slab reinforcement. The code explicitly allows this at the ultimate limit state, apparently because it assumes sufficient redistribution capacity. Where the force is always compressive (that is in a simply supported deck) it can be shown that it is conservative to ignore it, even at the serviceability limit state.

2.5 ANALYSIS FOR DESIGN - NORTH AMERICAN PRACTICE

Bridge design throughout North America is strongly influenced, although not always controlled, by the American Association of State Highway and Transportation Officials Standard Specification for Highway Bridges(45) (AASHTO). This differs from the British Standard in philosophy, detailed design methods, loading specification and analytical method adopted. Of these differences the last is the most significant to this study. It is also the least well known so it alone will be considered in detail.

The AASHTO standard does allow global analysis to be performed in a similar manner to that normally used in Britain. However, it is usual to distribute the wheel loads between beams using a table of distribution coefficients provided in the Standard and then to use simple beam theory. This gives a less favourable distribution than the British approach. If the beams are not closely spaced it gives a static distribution, which is certainly conservative.

A table of values is also provided for the local analysis. This is based on Westergaard(39), which is one of the methods often used in Britain, so the results are similar. The most significant difference from British practice is that the main steel in the deck slab is designed only for the local moment. The global transverse moments are not calculated or specifically designed for at all.

Global transverse moments obviously do occur in American bridges so it is interesting to assess their significance. Where a static load distribution is used in designing the main beams, global transverse moments are not needed to maintain equilibrium. Thus, according to plastic theory, the American approach leads to designs with adequate ultimate strength. This does not necessarily ensure satisfactory service load behaviour, but the writer is not aware of any cases of failures in American decks which can be attributed to global moments. This can be explained by the conservatism of the method used for local analysis. The reinforcement designed only for local effects is adequate to resist global moments because the global moments are smaller than the calculated local moments. This would not apply to many British "M" beam deck designs (eg. see Reference 46). The small close-spaced beams lead to higher global, but lower local, moments than the larger wider-spaced beams which are used in North America. The British HB load also gives much higher global transverse moments than does the American design loading. Thus it seems likely that the American design approach would not work for many British bridges. The author also understands that problems have been experienced with some bridge deck slabs in the Middle East, apparently due to a combination of designing British-style decks to AASHTO rules and very poor control of vehicle and axle weights.

2.6 CONCLUSIONS AND IMPLICATIONS FOR THIS STUDY

The basic form of bridges is largely dictated by construction considerations, so it is unlikely to be changed by this study. Accordingly, the remainder of the study will concentrate on the detailed design of the forms of bridges in current use.

The conventional methods of analysis and design which have been reviewed in this chapter assume structural behaviour which is often very different from the real behaviour of reinforced concrete. Nevertheless they have produced structures which have behaved in a satisfactory fashion. They

should be respected for the wealth of experience which they represent. This does not mean that complicated structures, such as bridge deck slabs, which appear to have been over-designed in the past, always have to be over-designed in the future. It is possible to refine analytical methods within existing codes so that effects like compressive membrane action are allowed for in design. This amounts to reducing the safety margins in such structures towards, but never below, the standards already accepted (and found satisfactory) in simple statically determinate structures.

Even if a more radical approach, based on first principles, is to be adopted, this review has important lessons. It shows clearly that ultimate strength is not a sufficient condition for a satisfactory structure. Serviceability criteria and the effect of the complex load history of a bridge have to be considered. It shows too, that a deck slab design needs to consider global, as well as local, effects. Finally it shows that many of the design criteria given in codes of practice are only strictly valid in conjunction with the methods specified for checking them. If other methods are to be used the criteria have to be re-considered. This applies particularly to the serviceability criteria, such as crack width and stress limits, which are less fundamental than ultimate strength.

CHAPTER 3

PREVIOUS RESEARCH

3.1 INTRODUCTION

The stock of evidence showing that conventional flexural theory under-estimates the strength of restrained slabs is vast. It includes tests on real structures(5,9,47,48,49), model structures(10,13,50,51,52) and laboratory specimens(53,54,55,56) under both concentrated(10,13,51,52,55) and uniformly distributed(5,9,50,54,56) loads. Much of this extra strength has been attributed to compressive membrane action. As a result, particularly since 1955 when Ockleston(9) published his test results, membrane action has been the subject of extensive research, both theoretical and experimental. Research has been undertaken in many countries over a long period of time. It is thus not practical to review all the literature in detail. This chapter aims only to establish the present state of knowledge of the subject as it affects, or could affect, the design of bridge deck slabs.

Much of the experimental work which is most directly relevant to this study, including most of the Canadian work mentioned in Chapter 1, has been conducted in the last fifteen to twenty years. Non-linear finite element analysis, capable of allowing for compressive membrane action, has been developed over much the same period. Despite this, there is almost no reference to the non-linear analytical work in the experimental studies so it is convenient to consider finite element studies entirely separately in Chapter 5.

3.2 REINFORCED AND PLANE SLABS

3.2.1 Bending Strength

As it was the realisation that flexural theory under-estimates the strength of restrained slabs which promoted the interest in compressive membrane action, it was natural that research should concentrate on bending strength. Many researchers have extended flexural theories to allow for in-plane forces. Most have used Johansen's Yield-Line Theory(57) as their starting point but a variety of approaches have been used. It is convenient to illustrate each in turn by considering the simplest possible case; a symmetrical restrained slab strip with equal top and bottom reinforcement.

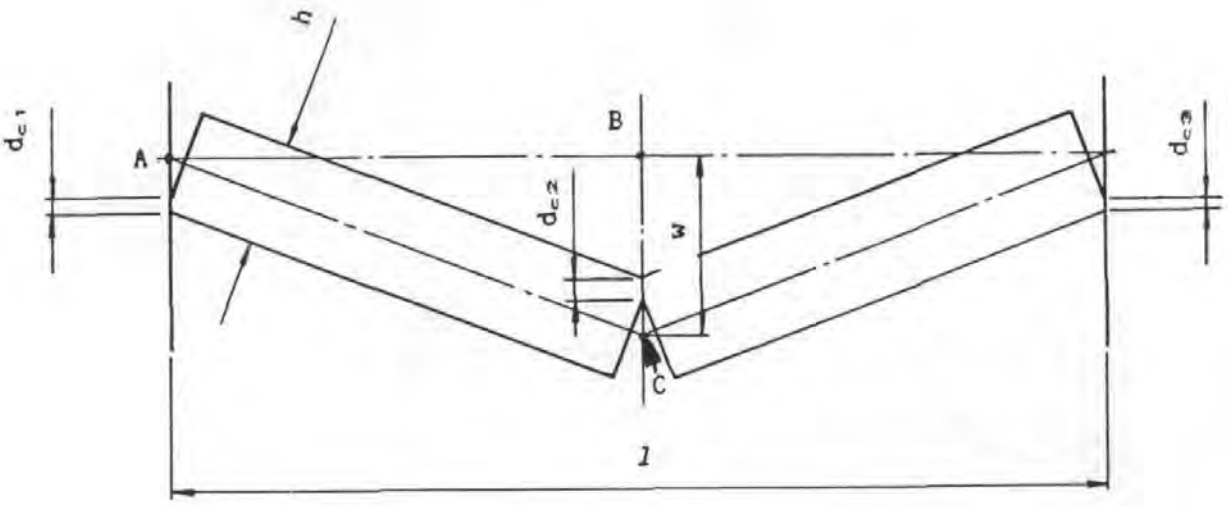

Figure 3.1: Geometry of restrained slab strip

a. Rigid Plastic Deformation Theory

The simplest approach is to assume that the slab material is fully plastic at the yield-lines but rigid elsewhere. This gives the geometry shown in Figure 3.1 and it will be seen that:

$$d_{c1} = d_{c3} \quad \text{by symmetry}$$
$$= d_c \quad \text{say}$$

Also, since both the restraint force, F, and the reinforcement area, A_s, are the same at all sections:

$$d_{c2} = d_c$$

Now;

$$AB^2 + BC^2 = AC^2$$

Hence;

$$(l/2)^2 + w^2 = [l/2 + 2(h/2 - d_c).2w/l]^2$$

Neglecting second order terms, this leads to;

$$d_c = h/2 - w/4 \qquad \text{Equation 3.1}$$

Using a rectangular concrete stress block, considering a unit width of slab and ignoring the tensile strength of concrete, the force in the concrete is

$$= d_c f_c'$$

where f_c' is the "plastic" concrete stress; approximately $0.6f_{cu}$

The tensile force in the reinforcement is

$$= A_s f_y$$

where A_s is the steel area per unit width and f_y is the yield stress.

Ignoring any reinforcement in the compression blocks, this gives restraint force, F

$$= d_c f_c' - A_s f_y$$

The total lever arm for the concrete in the compression blocks, taking the forces to act horizontally, is

$$= h - 2(d_c/2) - w$$

$$= h/2 - 3w/4 \qquad \text{(substituting for } d_c \text{ from Equation 3.1)}$$

and the total lever arm for the tensile steel forces

$$= 2(d - h/2) + w$$

$$= 2d - h + w$$

So the total moment, that is the sum of the support and mid-span moments,

$$= f_c'(h/2-w/4)(h/2-3w/4) + A_s f_y(2d-h+w)$$

By using the virtual work approach, the load-displacement relationship of the slab strip under any symmetrical load case can now be obtained. The result for some typical strips subjected to a single central load is shown in Figure 3.2.

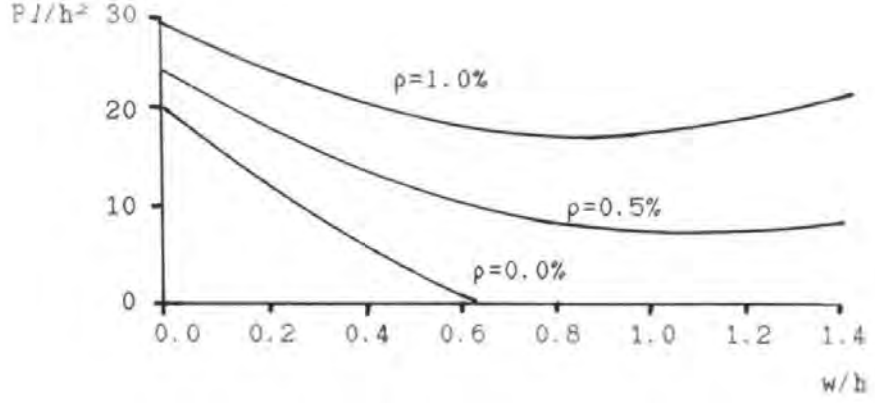

Figure 3.2: Load-displacement relationship of restrained slab strip
(Rigid-Plastic Theory, f_c' = 20N/mm², f_y = 460N/mm², d/h = 0.8)

The unreinforced slab's maximum load, which occurs at zero displacement, is as great as that of a simply supported slab with some 2% reinforcement. It is also equivalent to an unrestrained, but still fixed-ended, slab with about 1% reinforcement. The strength of the slab with 0.5% reinforcement

is greatly enhanced by the restraint, but is only slightly greater than that of the unreinforced slab.

The load on the slabs reduces as the displacement increases. The unreinforced slab will not support any load at all at displacements greater than 0.67h. The reinforced slabs reach a minimum load but then the load starts to pick up again. This is because the slabs start to work by tensile membrane action; the load is supported by the vertical component of the tension in the reinforcement. Eventually the load carried in this way can exceed the initial "ultimate" load.

Real slabs are not rigid between their yield-lines so they do not reach their maximum compressive membrane load at zero displacement. Thus the real peak load is lower than shown in Figure 3.2, and occurs at significant displacement. However, apart from this, Figure 3.2 gives a good indication of the behaviour of slabs, subject to certain conditions which will be discussed in 3.2.2 to 3.2.4. Researchers, such as Brotchie and Holley(56), have performed tests under displacement control and traced the descending and ascending part of the curve after the ultimate compressive membrane load is exceeded.

The ability of reinforced concrete slabs to support significant load by tensile membrane action may occasionally be useful for resisting exceptional accident loads. However, because of the very large displacements required, it is of no practical use in the design of bridge decks. Slabs with realistic span to depth ratios become unserviceable long before they enter the tensile membrane range. In most practical bridge deck slabs a deflection of 0.05h would be excessive.

Although the basic approach of rigid plastic deformation theory is simple, the algebra becomes complicated when the yield-line patterns of two-way spanning slabs are considered. Solutions have been published for only a few cases. One of the first to be solved was the axi-symmetrical case of a fully restrained circular slab with isotropic reinforcement. This was published by Wood(58), who went on to use it to give an approximate solution for square slabs. He then compared the predictions of this theory with the available test data. Because of the elastic deformation, the theory over-estimated the strengths. Wood suggested that this could be allowed for by multiplying the predicted loads by a reduction factor. He found that the measured factors varied from 0.4 to 0.8; the smaller

factors occurring in the more lightly reinforced specimens. This was because heavily reinforced slabs are less sensitive to restraint. If the factor is calculated from the increase in load compared with that given by yield-line theory, rather than from the total load, the range of observed values is much smaller and there is no consistent trend with steel area.
Brotchie and Holley(56) used an alternative approach for correcting the unsafe predictions of rigid-plastic theory. Instead of multiplying the load predicted for zero displacement by a reduction factor, they used the load predicted for the displacement at which rigid-plastic theory gave the same load as an elastic analysis. Since both theories give upper-bound solutions for the load at a given displacement on a structure composed of elastic-plastic materials, it appears that this should over-estimate slab strength. This explains why "theoretical maximum loads are slightly higher than the test results for the thinnest slabs". However, the theory tended to be conservative for the thickest slabs, which had a span to depth ratio of only 5. This was because elastic flexibility has little effect on the strength of such slabs whilst the effect of triaxial enhancement is greater than in shallow slabs. They attempted to allow for this but their correction was conservative.

b. Rigid-Plastic Flow Theory

Plastic deformation theory assumes that concrete develops its plastic compressive stress whenever it is subjected to compressive strain. In reality, not only does the strain have to be significant, it has to be increasing; the stress reduces rapidly if the strain decreases. Equation 3.1 predicts that the neutral axis moves closer to the compression face as the deflection increases. This implies that some concrete, near to the neutral axis, experiences a reducing strain and so will not develop its full compressive stress. The resulting error in the analysis can be avoided by using "flow theory" which assumes that the full stress is developed whenever the strain is increasing. The derivation of Equation 3.1 is then replaced by its first differential with respect to displacement or, more correctly, time. Braestrup(8) has shown that this leads to:

$$d_c = h/2 - w/2$$

and the load displacement relationship for the simple strip can then be calculated in the same way as before.

Braestrup(8) noted that no clear distinction is made in the literature between flow theory and deformation theory. He suggested that, as a result, much of the past research, which is based on deformation theory, is in error.

In Figure 3.3, the results of flow and deformation theory are compared for the unreinforced strip which was considered in Figure 3.2. At large displacements there is a very significant difference but in the practical range of bridge deck slab deflections the difference is not significant. Also, deformation theory is conservative because the extra concrete force it predicts is on the wrong side of the undeflected centre-line and so develops a couple which acts *against* the resistance moment.

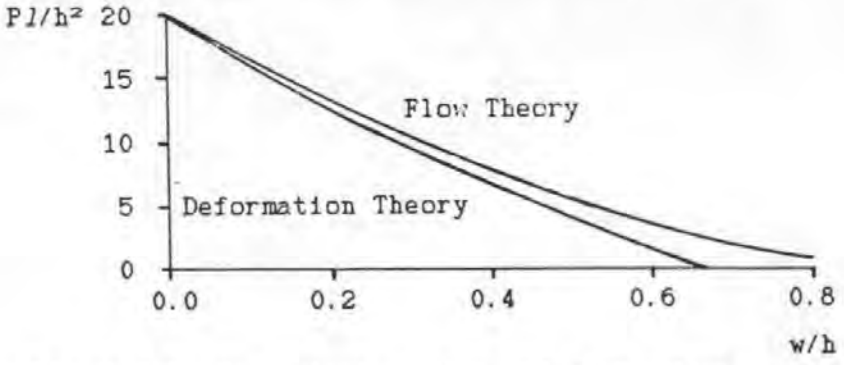

Figure 3.3: Comparison of flow and deformation theory
(ρ = 0, f_c' = 20 N/mm²)

Even in slabs which deflect 0.5h or more before reaching peak load, the difference between deformation and flow theory is not as great as Figure 3.3 suggests because the extra deflection is due to elastic deformation and so does not have the same effect on the neutral axis position. It is only when post-ultimate behaviour is considered that the difference becomes important. Since post-ultimate behaviour is of no practical importance to the applications considered in this thesis, it is reasonable to consider deformation and flow theory as interchangeable.

Morley(59) developed rigid-plastic flow theory so that, in principle, it is general and can be applied to any case. The algebra becomes complicated, however, and he gave only a limited number of solutions. One of these was for polygonal slabs. He compared this solution with some test results, assuming that the true maximum load was that predicted for a deflection of h/2. The choice of this deflection was based on work by Park(60) which

will be considered later. For the slabs which Morley considered the predictions were reasonably good.

c. Elastic-Plastic Theory

Johansen's Yield-Line Theory(57) gives very good predictions for the strengths of unrestrained slabs despite ignoring elastic deformations. This is possible because it predicts loads which are independent of displacement. Thus elastic deformations can significantly increase deflections without affecting strength. When membrane forces are considered, in contrast, there is a relationship between load and deflection even in plastic theory. Thus elastic deformations affect strength and it is useful to consider them in an analysis.

The analysis is particularly sensitive to elastic shortening of the slab because, as will be seen from Figure 3.1, small movements have a large effect on the behaviour, particularly at small deflections. Ideally, however, both in-plane and flexural deformations would be considered. The full equations for this have been formulated by Massonnet(61) and have been applied to rectangular concrete slabs by Moy and Mayfield(62). The mathematical complexity of the equations is such that hand solutions are not practical so Moy solved the equations numerically by computer using a non-linear finite difference approach. Although this approach works reasonably well, it has proved difficult to develop general computer programs. Because of this the approach has been largely superseded by the finite element method, which will be considered in Chapter 5. It would be particularly difficult to develop a finite difference program which could be used by a non-specialist in a wide enough range of circumstances to make it commercially viable. Because of this the finite element method is far more suitable for direct use in design and the finite difference method will not be considered further in this study.

When elastic deformation is included in a hand analysis it is necessary to make some gross approximations to simplify the mathematics. The approach adopted by Park(54), which has been followed by many other studies, was to ignore the flexural deformation and to assume the axial strain to be constant along the length of the strip. Since flexibility in the in-plane restraint has exactly the same effect on the behaviour as the axial flexibility of the strip, it is both useful and convenient to include it in the analysis.

Considering the same simple strip as before, and using deformation theory, this leads to;

$$d_c = h/2 - w/4 - \varepsilon l^2/8w - tl/4w$$

where ε is the axial strain at mid-depth (which is taken to be constant) t is the movement of each support, and the other notation is as before.

Now $$F = d_c f_c' - A_m f_y$$

and, if ε is calculated from the gross concrete properties and the restraints are taken to be elastic such that;

$$F = Kt$$

this leads to;

$$d_c = \frac{h/2 - w/4 + A_m f_y (l^2/8E_c hw - l/4Kw)}{1 + f_c'(l^2/8E_c hw - l/4Kw)}$$

Substituting this result into the expression for the moment, which is otherwise the same as in the rigid plastic theory, the moment and hence the load can be obtained.

In Figures 3.4 and 3.5 the result of this calculation is shown for slabs with 0.5% steel and with span to depth ratios of 10 and 30 respectively. In order to give an indication of the restraint stiffness required this is expressed as a multiple of the axial stiffness of the slab strip.

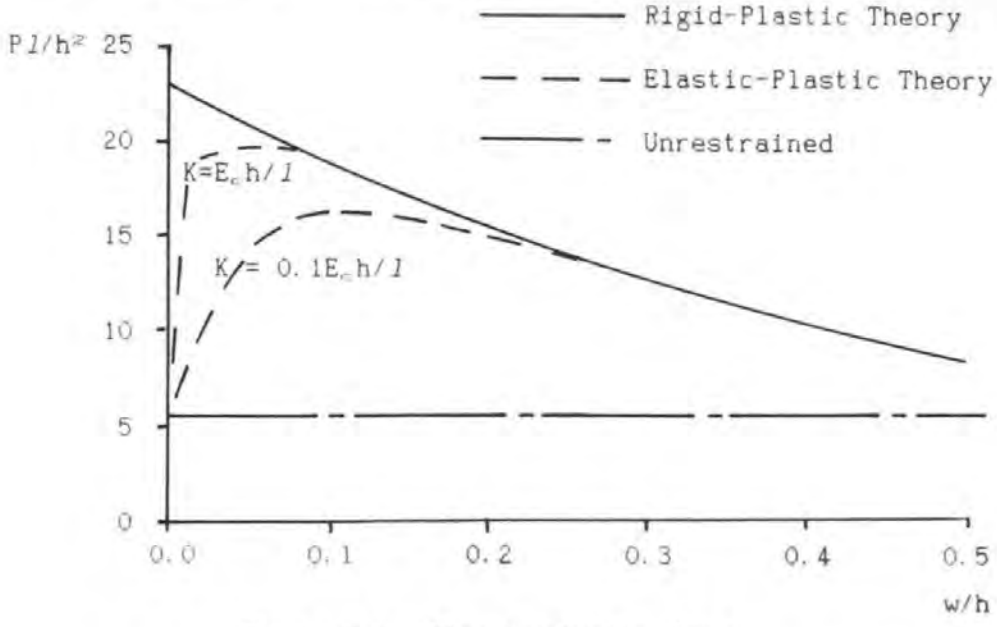

Figure 3.4: Elastic-plastic theory

($l/h = 10$, $\rho = 0.25\%$, $f_c' = 20N/mm^2$, $f_y = 460N/mm^2$, $d/h = 0.8$)

At zero deflection there is no restraint force and the load is as given by normal yield-line theory. The load increases with deflection but starts to reduce again before reaching the value predicted by rigid-plastic theory. Less well restrained slabs support less load and reach peak load at higher deflections. The slab with the larger span to depth ratio is much more sensitive to flexibility of the restraints but restraints which are far less stiff than the slab still have a very significant effect on its strength.

Park(54) considered a more general case and used a different stress block and notation but, apart from this, his theory is the same. However, he gave graphs equivalent to Figures 3.4 and 3.5 which are significantly different; for example, the load at zero deflection is not equal to that given by yield-line theory. This is due to a small algebraic error in the example used to plot his graphs.

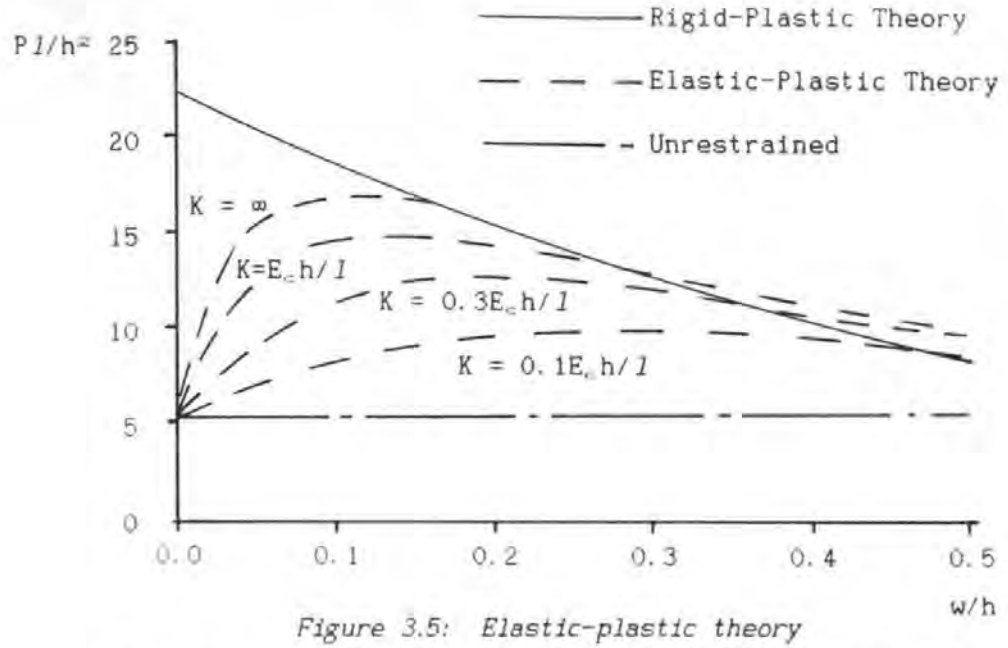

Figure 3.5: Elastic-plastic theory

(*l*/h = 30, ρ = 0.25%, f_c' = 20N/mm², f_y = 460N/mm², d/h = 0.8)

Roberts(53) tested a series of restrained strips. He compared the results with theory similar to the above, which he attributed to Wood. Because of elastic flexibility in bending, the load at low deflections was less than given by the theory. The peak load exceeded the predicted value and Roberts attributed this to the effect of transverse restraint to the concrete at the supports which enhanced its strength. Supplementary tests proved that it was possible to develop stresses in excess of $0.67f_{cu}$. After the peak load was passed the load reduced much more rapidly with

increasing deflection than the theory predicted. This was due to the difference between the real behaviour of concrete and the ideal plastic behaviour assumed in the analysis.

Christiansen(63) developed a theory for restrained beams which is similar except that he added the elastic bending deflection into the analysis. He calculated this using the uncracked section. In addition to applying the theory to beams he also applied it to slabs, including two-way spanning slabs. In these the deflection, and hence the effect of membrane enhancement, varies across the slab width. Christiansen avoided this complication by "considering only arching action across the shorter span at the centre of the longer span." As expected (and intended) this gave conservative answers.

Park(54) used his strip theory to estimate the strength of two-way spanning slabs. He did this by assuming a central deflection and using the strip theory to obtain the moment to use in the virtual work equations obtained from normal yield-line theory. He chose to use a central deflection of h/2, which was based on a study of test results. He acknowledged that this deflection was conservative for slabs with span to depth ratios below about 20. He also acknowledged that it is a greater deflection than his graphs, based on his strip theory, suggest. In fact, because of the error mentioned earlier, his graphs show peak loads which are slightly lower than they should be and which occur at significantly higher deflections than they should. Thus the h/2 used by Park does not agree with the strip theory but Park suggested that this was justified by the elastic bending which the analysis ignores. He showed that the theory gave good predictions for the strengths of slabs subjected to uniform loads. However, because of the use of a deflection of h/2, it is conservative for slabs with short span to depth ratios.

The algebraic complexity of this elastic-plastic theory of two-way spanning slabs makes it difficult to use and gives it a false impression of accuracy. In fact, it is based on gross assumptions. It is quite different from the use of elastic-plastic material properties in non-linear computer analysis. It assumes that the whole depth of the slab is plastic at the critical sections. Elsewhere it is taken to be elastic for axial behaviour but rigid in flexure. The assumption that the axial strain of the slab strips is constant at mid-depth can easily be shown to be wrong,

for example the neutral axis depth at the yield-line is always less than h/2 which implies an axial shortening at this section. Thus the major justification for the equations developed by Park is not the theory on which they are based so much as the fact that they have been shown to give reasonable results. This is significant as it implies that the approach is essentially empirical and thus may not be valid outside the range of cases for which it has been tested.

Mc Dowell et al(64) developed a different form of elastic-plastic analysis. Although intended for use with masonry walls, it is equally applicable to unreinforced concrete. It used the geometry shown in Figure 3.1 and assumed that the strain varied linearly in the span direction, from zero at the crack to a maximum in the compressed region. This was acknowledged to be an arbitrary assumption, and it is easy to prove that it is not correct, but it is just as reasonable as Park's assumptions. Since the total reduction in the slab length at any depth can be calculated from the geometry shown in Figure 3.1, this enables the strain to be calculated at any position. Mc Dowell used the strains at the yield-line positions to calculate the stresses, and hence the bending moments, using an elastic-plastic stress distribution. He assumed that, once the plastic stress had been reached, a subsequent reduction in strain would reduce the stress to zero. This made his approach equivalent to flow theory.

Rankin(65) has successfully applied the approach to unreinforced concrete slabs. He also adapted it to reinforced slabs by adding the effect of the reinforcement. Skates, Rankin and Long(66) used a similar approach although their method for combining the components of the moment capacity due to arching and reinforcement was slightly different. Rankin acknowledged that his flexural and arching analyses assumed different strain fields and the same is true of the approach used by Skates et al. The main consequence of this is that the assumption that the reinforcement yields could be inconsistent with the strains assumed in the arching analysis. Although not stated in the other literature, this is a fault which is shared with all the analyses considered in this section. Rankin suggested that the resulting unsafe predictions could be avoided by limiting the calculated moment capacity to the "balanced" capacity proposed by Whitney(67) which is approximately $0.27f_{cu}bd^2$. This restriction appears to be conservative. Rankin pointed out that, taking d/h as 0.8, the maximum possible arching moment capacity of an unreinforced slab

approximates to this capacity. However, even if it does not yield, reinforcement does increase the moment capacity. Also, in some bridge decks, d/h is significantly less than 0.8. Another conservative aspect of Rankin's analysis is that although the reduction in the concrete lever arm due to deflection is included, the increase in the steel lever arm is not. Thus the analysis would be conservative for shallow heavily reinforced slabs. Despite these faults, Rankin obtained good results and his approach will be considered further in 3.2.4.

3.2.2 Flexural Shear Strength

The theories considered in 3.2.1 assume that flexural failure precedes shear failure. With few exceptions, this assumption is made in the literature without any particular justification. It is therefore necessary to investigate the validity of the assumption and again it is convenient to consider the simple slab strip shown in Figure 3.1.

If the span to depth ratio is less than about 20, rigid plastic flexural theory implies a shear force which exceeds the ultimate shear strength given by BS 5400. However, this ignores the fact that an axial compressive force enhances the shear strength of a concrete section. A simple correction for this, such as that given in the column clauses of BS 5400, suggests that shear failures are only possible if the span to depth ratio is less than about 6. Since the code rules are conservative, and shear strength is further enhanced if the shear span to depth ratio is less than around 2.5 (which is equivalent to a flexural span to depth ratio of 5), this means that shear failures in the type of strip shown in Figure 3.1 are unlikely.

This argument can be extended to show that shear failures are unlikely in practical restrained slabs subjected to uniform loads and explains why no such failures have been reported.

3.2.3 Punching Shear Strength

Even allowing for the limitation on the load imposed by the bending strength of a slab, the shear stress in the vicinity of a concentrated load is much higher than under a uniform load. Because of this, slabs subjected to concentrated loads are likely to fail by punching and test results confirm this(10,13,51,52,55). Despite this, restrained slabs are stronger than unrestrained slabs and, typically, five times stronger than suggested

by conventional design rules which assume flexural failures. Several attempts have been made to analyse the effect.

Aoki and Seki(68) have modified Moe's(69) equation for punching strength to allow for membrane forces. However, the correlation with their test results was not particularly good and they obtained a better relationship using a purely empirical formula. Although this formula worked reasonably well for their tests the author has found that it gives unsafe predictions for many other restrained slabs and it will not be considered further.

The realisation, following research by Young(70), that bridge deck slabs fail by punching at high loads prompted the Department of Highways and Transportation in Ontario to sponsor a major research programme into punching. After largely experimental studies by Tong and Batchelor(51) and Batchelor and Tissington(71), Hewitt and Batchelor(72) endeavoured to develop a theoretical model by modifying an existing theory for punching in unrestrained slabs.

They found that the best available theory for punching in unrestrained slabs was that due to Kinnunen and Nylander(73). Kinnunen observed that the punching failure modes of slabs were approximately axi-symmetrical, even for rectangular specimens, so he used an axi-symmetrical analysis. In this model, which is illustrated in Figure 3.6, outer portions of the slab bounded by a shear crack and two radial cracks are assumed to rotate as rigid bodies. The load is taken by the compressed conical shell above the shear crack which is assumed to be shaped such that the concrete stress is constant. The system is taken to deform linearly with load until a limiting strain is reached and the system fails. The stress in the compressed shell at failure is calculated allowing for the enhancement due to the triaxial stress state. Finally an empirical correction factor of 1.1 is applied to allow for dowel effect in the radial bars which the analysis ignores.

Hewitt and Batchelor applied the theory to 137 test results and obtained good results. They said that they were better than Moe(69) obtained using a purely empirical relationship. However, since Kinnunen and Nylander used empirical factors for limiting strain, triaxial enhancement and dowel effect whilst Hewitt and Batchelor increased the factor for dowel effect from 1.1 to 1.2 to improve correlation, the resulting "theoretical punching load" is largely empirical. In effect, the model was used only to give a

qualitative explanation of the behaviour and to give the form of the equations; the actual values are empirical.

By adding the restraining force and moment acting at the outer edge of the segment into the equilibrium equations, Hewitt was able to correct the theory for known restraint forces. Comparison with the results of tests in which the known restraint was provided by unbonded tendons suggested that the approach gave good predictions.

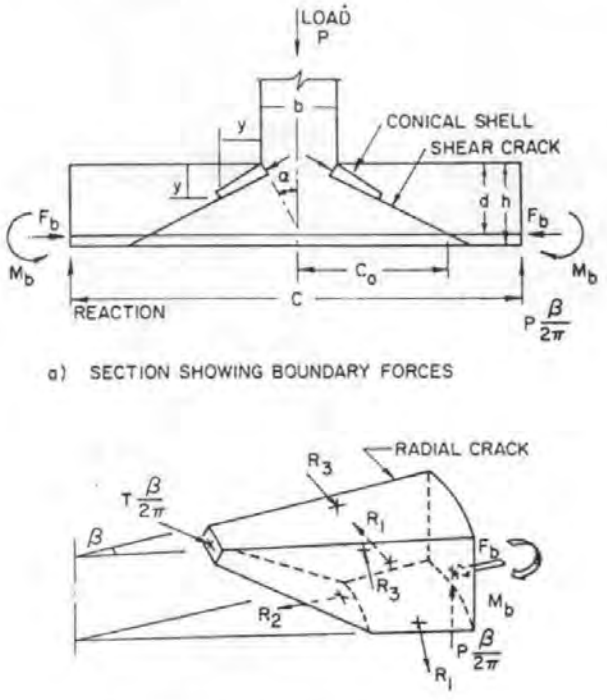

Figure 3.6: Kinnunen and Nylander's model(73)
[as modified by Hewitt and Batchelor(72)]

By adding the restraining force and moment acting at the outer edge of the segment into the equilibrium equations, Hewitt was able to correct the theory for known restraint forces. Comparison with the results of tests in which the known restraint was provided by unbonded tendons suggested that the approach gave good predictions.

For most practical slabs, the restraining force and moment are unknown. Hewitt therefore proposed that the actual boundary forces and moments in real slabs should be expressed as a "restraint factor", R, times the maximum boundary forces and moments. These maximum values were obtained by using "The idealised geometry of displacement as used by Brotchie and

Holley(56)". This gives a neutral axis depth at the support of h/2 - w/4 as in Equation 3.1. However, this assumes that the neutral axis depths at the support and mid-span are equal which conflicts with Kinnunen and Nylander's assumptions. There is also no reason why the actual restraint force and moment should both be reduced by the same percentage relative to their respective maximum values. Thus Hewitt's approach is, in effect, largely empirical and he appeared to acknowledge this, saying "It is not implied that the actual boundary restraint and distribution of stress are known at the instant of failure".

Hewitt obtained the restraint factor values, R, for real slabs by back-calculation from observed failure loads. Although he said "It is a fact that R varies from zero for a simply supported slab to unity with idealised restraint" the highest value he observed was only 0.77. There appear to be two reasons for this. Firstly Hewitt's analysis with full restraint invariably gives a depth to root of crack which is greater than h/2. This is only geometrically compatible with his assumption that the neutral axis depth at the support is h/2 if the supports are jacked closer together. Secondly, Hewitt assumed that the top steel at the supports reaches yield which, except with large deflections, is incompatible with the assumed neutral axis position. Thus "full restraint" in his theory appears to represent the ideal restraint forces, that is the forces which lead to the highest failure load, and not (as some of his statements imply) the forces which arise with ideal (rigid) restraint; R = 1 could only be obtained by prestressing. Another oddity of the model is that it assumes that a volume of concrete, bounded on one side by a shear crack, rotates as a rigid body until a shear compression failure occurs; yet all the descriptions of failures show that the shear crack does not appear until the failure load is reached.

Clearly, although claimed to be a theoretical model, the approach is essentially empirical. Hewitt claimed that it gave acceptable predictions for the strengths of realistic bridge deck slabs and it has been used to develop charts for assessing the strength of existing bridges(11). In order to ensure that these are safe, and to avoid the need for separate charts for use with steel and concrete beams, they are based on a restraint factor of 0.5 even though tests on concrete bridges suggest that values as high as 0.7 give more accurate predictions.

Kirkpatrick, Rankin and Long(13) have developed an alternative analysis of punching in restrained slabs. Like Hewitt's approach, this was developed by modifying a theory for punching in unrestrained slabs. The theory used was Long's(74) "two-phase approach" which gave the strength of a slab which fails in shear before the steel yields as;

$$\frac{4(c+d)d \times 0.42(f_{cyl})^{0.5}(100\rho)^{0.25}}{(0.75 + 4c/l)}$$

where c is the side of the square loaded area, f_{cyl} is the cylinder compressive strength and the other notation is as used previously.

Kirkpatrick et al took the denominator (which is a correction for the effect of the ratio c/l) as constant at 1, arguing that the effect of variation was small. This is reasonably true for the type of specimens originally considered by Long, but the value of the denominator for some of Kirkpatrick's slabs was as high as 1.6 so the stated reason for ignoring this factor is unsatisfactory.

For fully restrained slabs they argued, by reference to test results, that the effect of reinforcement was small and they took the term $(100\rho)^{0.25}$ to represent the influence of flexural strength on shear strength. The value of ρ which they used was the equivalent steel area ρ_e; the area of steel which would be required to give an unrestrained slab the same moment capacity according to normal flexural theory which the fully restrained slab had according to restrained strip theory. The particular theory which they used was that due to Mc Dowell et al(64), although it appears that any of the methods described in 3.2.1 could be used. Because of the fourth root term, the choice of approach has little effect.

Kirkpatrick appears to have accepted that his approach was largely empirical. However Rankin(65) has developed a similar approach, to analyse punching at columns in flat slabs, and he attempted to give it a theoretical basis. He assumed that failure occurred when the compression zone failed in shear. Because compressive stress tends to enhance the shear strength of concrete, he said that the critical position was at the flexural neutral axis. He calculated the shear strength of the compression zone assuming an elastic stress distribution and a critical section at d/2 from the face of the loaded area. Then, arguing that shear was transmitted across the shear crack by aggregate interlock and dowel

forces, he said that the total shear capacity was 2 to 5 times the capacity of the compression zone.

There are many faults with this as a theoretical analysis. Firstly, the shear failure criterion at the flexural neutral axis was based on maximum principal tensile stress. This is not really a failure criterion for the slab at all; it merely suggests that the shear force reduces the neutral axis depth, a fact which is well known from research on beams(75). Secondly, if (as Rankin said and as the observed behaviour suggests) slabs fail as soon as the shear crack appears, dowel forces cannot contribute significantly to the ultimate strength; only to the post-ultimate behaviour. Thirdly, the geometry of the failure mode appears to suggest that there is no shear displacement across the shear crack; it merely opens up. Thus the aggregate interlock force must be small as Chana(75) has found for beams. However, in beams the load continues to increase after a shear crack appears and Chana found that the dowel effect was very significant. Using his approach, it is possible to quantify the force for a punching failure. Because (as Rankin noted) the inclination of the shear crack means that the failure surface is very long at the position of the reinforcement, the dowel force in slabs with conventional quantities of reinforcement is large. The assumption that this force is realised before failure occurs is hard to reconcile with Kirkpatrick's observation (and assumption) that reinforcement has little effect on strength. Although Rankin was a co-author of Kirkpatrick's paper(13), they appear to have differed on this point. Rankin(65) took the dowel force to represent 25% of the shear strength of a reinforced *unrestrained* slab. He therefore assumed that the shear strength of a restrained unreinforced slab with the same depth of concrete in compression at the critical section would be 25% lower. Kirkpatrick, like Skates(66) in a more recent paper, used the full shear stress even in unreinforced slabs. Despite this, differences in their methods for estimating neutral axis depth make Kirkpatrick's formula more conservative than Rankin's for typical bridge deck slabs.

Kirkpatrick said that his formulae gave good predictions for test results and it is informative to compare his approach with Hewitt's. Both are essentially empirical so they can only be compared by comparing their predictions. However, since they were calibrated using sets of data which are not only very similar but which overlap, the absolute value of their predictions give little idea of the relative merits of the approaches. As

might be expected, both give reasonably good predictions for typical slab test results. A better indication of their relative merits is given by the predicted relationship between failure load and the important variables which affect it. These will now be considered in turn.

a. Loaded Area

Since Hewitt considered a critical section at the face of the loaded patch, whilst Kirkpatrick considered a critical section at d/2 from the face, it might be thought that Hewitt's predictions would be more sensitive to patch size than Kirkpatrick's. However, Kinnunen and Nylander's empirical corrections for limiting strain and for triaxial enhancement more than compensate for this.

Taylor and Hayes'(55) results enable the effect of patch size to be clearly identified. They suggest that Kirkpatrick's approach is remarkably good in this respect. However, including Long's original correction for c/l makes it significantly worse, suggesting the factor was removed to improve the results. Hewitt's analysis exaggerates the effect of patch size but it is only with Taylor's smallest patch size (2h/3) that the error is really significant and this is outside the range of c/h ratios which normally occur in bridge deck slabs.

b. Concrete Strength

Because Hewitt and Batchelor's theory assumes a shear compression failure, whilst Kirkpatrick et al's implies a shear tension failure, they differ significantly in their predictions for the effect of concrete strength. Long's two phase approach gave a square root relationship (and he suggested that a coefficient of 0.4 was slightly better) but Kirkpatrick's method of calculating ρ_w increased this up to $f_{cu}^{0.75}$ for very short span to depth ratios. However, it is not clear if this is justified by the theory itself. It is generally accepted that such shear failure loads are proportional to something between $f_{cu}^{0.3}$ (as in BS 8110 and BS 5400) and the tensile strength of concrete (approximately proportional to $f_{cu}^{0.5}$). Also, although Long's original paper implied that the term $\rho^{0.25}$ was purely empirical, Rankin(65) suggested that it was used because, for the relevant reinforcement ratios, the neutral axis depth is approximately proportional to $\rho^{0.25}$. If so, it would be more logical to use the neutral axis depth given by the arching theory (as Rankin did), rather than going indirectly to an approximate value via a hypothetical equivalent reinforcement area.

This would reduce the predicted sensitivity to concrete strength to $f_{cu}^{0.5}$ for short span to depth ratios and less for longer span to depth ratios.

The shear compression failure mode considered by Hewitt and Bachelor might be expected to give failure loads which are proportional to concrete strength. However, the empirical expression for limiting strain reduces this sensitivity. Despite this, the approach predicts a significantly greater sensitivity to concrete strength than Kirkpatrick's as will be seen from Figure 3.7. Unfortunately, in the published studies concrete strength has not been varied sufficiently widely or systematically to determine which is more realistic.

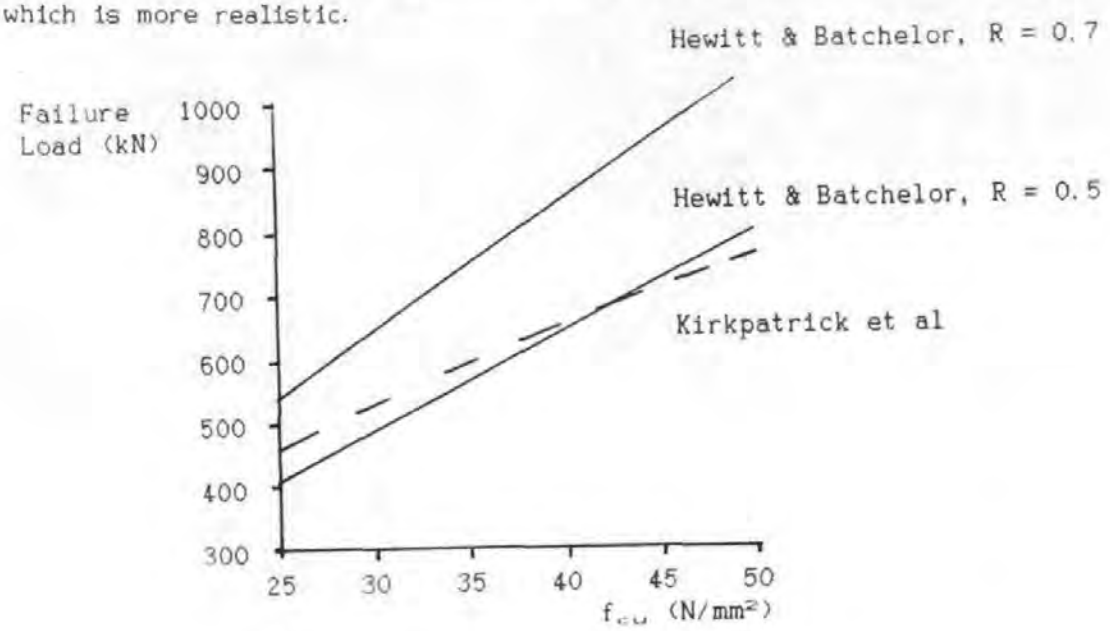

Figure 3.7: Effect of concrete strength
(l = 1.5m, h = 160mm, c = 320mm, ρ = 0)

c. Reinforcement Area

The most obvious difference between Kirkpatrick's approach and Hewitt and Batchelor's approach is that the former ignores reinforcement whilst the latter considers it. However, although Batchelor(76) has criticised this aspect of Kirkpatrick's approach, saying that reinforcement is an "important consideration", his own theory predicts only a small effect for well restrained slabs. For a typical M beam slab, 1% reinforcement increases the predicted strength by around 15%.

A curious feature of Kirkpatrick's approach is that, although the reinforcement is ignored, the prediction is affected by the assumed

effective depth. Since this is clearly illogical, the author has used a hypothetical d of 0.75h for all calculations with the approach.

Analysis of the results of tests on bridge deck slabs appears to give conflicting evidence for the significance of reinforcement area. Kirkpatrick(13) obtained virtually identical failure loads with 0.25%, 0.5%, 1.25% and 1.68% reinforcement. However both Beal(77) and Batchelor et al's(78) results suggest that Hewitt's approach under-estimates the effect of reinforcement. Beal obtained average failure loads, for his model 2, which is illustrated in Figure 3.8, of 11, 26.6 and 31.1kN with 0, 0.23 and 0.35% reinforcement respectively. He also obtained an average failure load of 26.7kN with 0.35% bottom steel and no top steel. The possibility that the apparent contradiction between Beal and Kirkpatrick's results was because small steel areas have a significant effect, whilst increases above some critical area have no effect, can readily be eliminated by reference to other tests such as Taylor and Hayes'(55). They obtained a barely significant difference with 0, 0.9 and 1.8% steel.

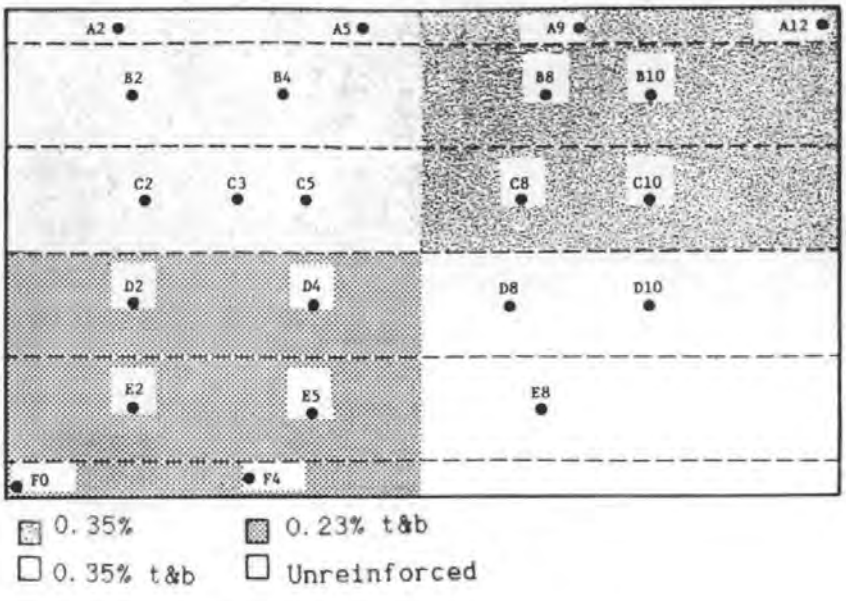

Figure 3.8: Beal's Model Two(77)

As Beal and Kirkpatrick's results appear to be so contradictory it is worth considering them further. Accordingly the author has analysed the two bridges, which are illustrated in Figures 3.8 and 3.9, using both Kirkpatrick's and Hewitt's approaches.

A major difficulty in interpreting the results is that both Beal and Kirkpatrick varied the steel area within the same deck. There are two

objections to this approach. Firstly the restraint may be different in different areas of the structure. This is confirmed by Beal's results, as tests conducted near the centre of the bridge gave consistently higher results than those conducted near the edge. For example, D4 failed at a 36% higher load than E2. The second objection is that reinforcement contributes to the restraint, so reinforcement in adjacent bays may contribute to the restraint available to the area under test. Again Beal's tests show evidence of this as test D8, in the unreinforced area, was stopped when the cracking extended into the adjacent reinforced bay, by which time the load was already 2½ times that at which D10 later failed.

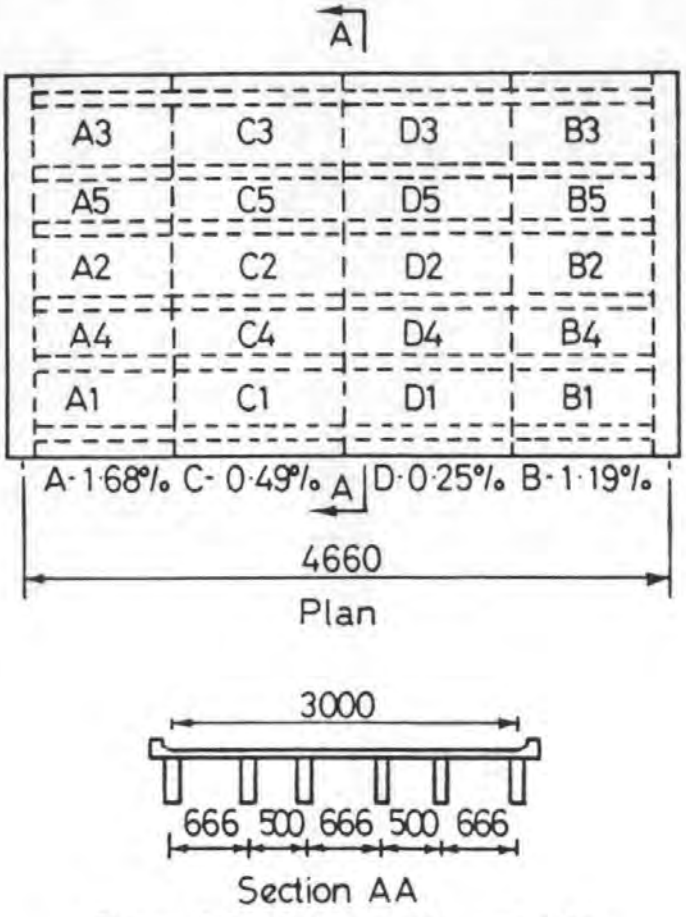

Figure 3.9: Kirkpatrick's model(13)

Kirkpatrick's arrangement of bays might be considered unfortunate as the two lightly reinforced bays were near mid-span, where Beal's tests gave higher failure loads, and they were surrounded by more heavily reinforced areas. Also the bays were rather narrow relative to the slab span. However, by comparing the results for the 0.25% and 0.49% panels and then separately comparing the 1.68% and 1.19% panels, both effects can be eliminated but there is still no trend. Thus it appears that varying

reinforcement genuinely had no significant effect on Kirkpatrick's results. They also show no sign of the difference between the centre bay (bay 2) and the edge (bays 1 and 3) whereas this effect is very significant in Beal's results.

These differences between Kirkpatrick's and Beal's results could be because Kirkpatrick's stiff concrete beams, diaphragms and parapet upstands provided adequate restraint whilst Beal's deck, with its flexible steelwork and no upstands, was more dependent on the slab and its reinforcement for restraint. However, restraint factors back-calculated using Hewitt's approach are little different for the two decks. Those for Kirkpatrick's deck are in the range 0.5 to 0.7 whilst those for Beal's reinforced panels are in the range 0.45 to 0.75. Thus the greater effect of reinforcement on Beal's results cannot be explained by lack of restraint, although it seems likely that the steel girders in Beal's deck did provide less good restraint. The high restraint factors observed near the centre of his deck appear to be the result of global effects which gave the centre portion of the slab a significant biaxial compression.

Beal noted that Hewitt's theory, with a restraint factor of 0.5 as recommended by the Ontario code, gave conservative results. The predictions approximated closely to his results for the outer portions of the deck. He does not appear to have analysed the unreinforced sections but the author has found that Hewitt's theory over-estimates their strengths by a factor of up to just over 2. This is better than Kirkpatrick's predictions which are unsafe by a factor of up to nearly 3. Kirkpatrick's predictions for the reinforced areas are slightly higher than Hewitt's and are thus closer to the average observed values.

Clearly the effect of reinforcement on the strength of Beal's slabs was greater than Hewitt's theory predicts and much greater than was observed by Kirkpatrick. The reasons for this will be considered later.

Beal said that Hewitt's theory ignores "compression steel" so the top steel has no effect on predicted strength. It is true that Hewitt ignored compression steel but he did consider top steel at the support. The reason Beal's had little effect on the predicted strength was that it was very close to mid-depth. According to Hewitt's model, mid-depth steel should have no effect on the strength of a fully restrained slab. However, the fact that his theory still predicts no effect in partially restrained

slabs is merely a consequence of the assumption that the actual restraint forces and moments are proportional to their respective maximum values.

d. Span

The two theories differ significantly in their prediction for the effect of span to depth ratio. This is illustrated in Figure 3.10 for a typical M beam slab. If Long's original expression for the effect of c/l is included Kirkpatrick's analysis suggests that strength increases with span, which seems improbable. This suggests that Kirkpatrick removed it to improve correlation rather than because the effect is small. As the expression was purely empirical this was a perfectly reasonable thing to do.

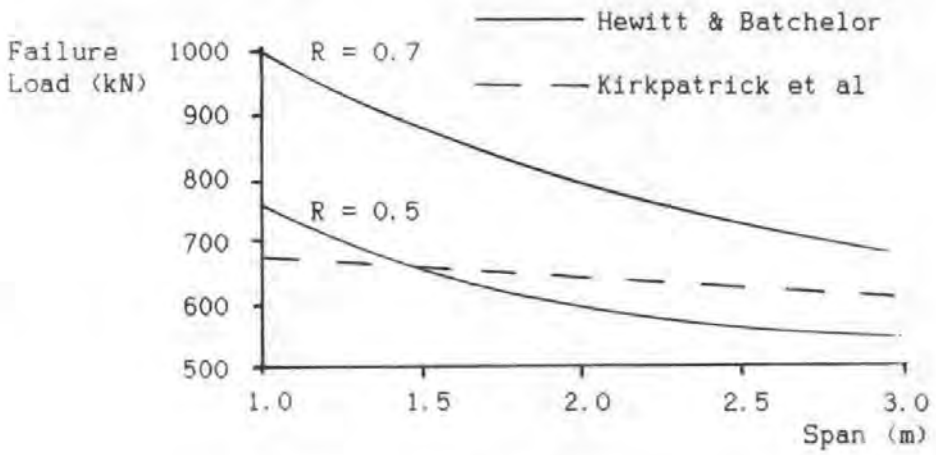

Figure 3.10: Effect of span

(h = 160mm, f_{cu} = 40N/mm^2, c = 320mm, ρ = 0)

Even without the term, Kirkpatrick's predicted effect of span is much smaller than Hewitt's. However there is a fundamental difference between the approaches in that Hewitt's includes a check on the moment equilibrium of the system whilst Kirkpatrick's does not. Within the logic of Long's two-phase approach(74), on which Kirkpatrick's analysis is based, it is clear that a separate check on bending strength should be made and this would be more likely to be critical with longer spans. Kirkpatrick did not detail this check because he considered it would not be critical in normal deck slabs. However, Rankin(65) did detail such a check and this will be considered in 3.2.4.

Batchelor also implied that his predictions were not valid for bending failures. He said that these occur with low reinforcement and poor

restraint but, like Kirkpatrick, he assumed that they would not occur in realistic bridge deck slabs.

It is difficult to clearly identify the effect of span from test results. As with reinforcement area, tests on model bridges appear contradictory. Kirkpatrick obtained virtually identical results for his two span lengths (l/h of 9.4 and 12.5 or 7.2 and 10.2 if only the clear span between the stiff beams is considered) but Batchelor(78) obtained an average 43% higher load with an l/h of 13.7 than with 20.7. However, since Kirkpatrick varied the span within a single model, whilst Batchelor varied it by testing three and four-beam models of the same width, it seems likely that Kirkpatrick's longer spans were better restrained than his shorter spans whilst Batchelor had the reverse situation. Even ignoring the unreinforced bays, Kirkpatrick's analysis over-estimates the strength of Batchelor's longer spans by some 30%. It gives better predictions for the shorter spans although it is still slightly (18%) optimistic for the unreinforced bays.

Despite the differences in the restraint, and consequent difficulties of interpretation, a trend can be detected from the analysis of Kirkpatrick, Batchelor and Beal's results: increasing the span reduces the strength of unreinforced slabs by more than either theory suggests but it also increases the effect of reinforcement. This could easily be explained if the failures were flexural rather than shear failures. In 3.2.1 we saw that the greater deflections associated with longer spans reduce the area of concrete in compression and reduce the lever arm at which it acts, whilst increasing the lever arm at which the steel acts. This effect is allowed for by Hewitt's analysis but it is greatly under-estimated because the deflection is under-estimated. Hewitt's analysis under-estimated Kirkpatrick's small deflection at failure by a factor of 2 and Beal's, which were of the order of h/2, by a factor of up to 10. Kirkpatrick's analysis does allow for the reduced concrete contribution with longer spans but, because of the fourth root term, it under-estimates the effect. Neither Hewitt's nor Kirkpatrick's analyses are capable of allowing for another effect of deflection; it increases steel strain and hence, if the steel has not reached yield, steel force.

It appears that both theories would become unsafe if they were applied to slabs, particularly unreinforced slabs, with very large span to depth

ratios. However, neither are recommended by their originators for use above a span to depth ratio of 18. Within this restriction they are reasonably safe. Although Beal's slab was well within this *l*/h ratio the results which fell below the predictions were for panels which had neither the nominal steel nor the edge stiffening recommended by both Kirkpatrick and Batchelor. It should also be noted that both theories correctly predict that the failure loads of such slabs are so high that their precise values have no practical significance; the safety factors suggested by the tests were in the range 5 to 30.

e. Multiple Loads

Another effect of increasing the slab span is to increase the effect of the other wheels of the HB load. Neither Kirkpatrick's nor Hewitt's analysis enables this effect to be assessed. Kirkpatrick's choice of a critical shear perimeter at d/2 from the loaded area implies that wheels spaced by more than 2c + d centre to centre should have no effect on each other. However, the empirical nature of the approach makes this dubious and Kirkpatrick's own tests confirm this: for the longer spans, two wheels spaced by over twice this distance failed at only 40% more total load than single wheels. Hewitt's analysis implies that wheels spaced by less than *l* could affect each other. This is confirmed by Kirkpatrick's tests. For his shorter spans the HB wheel spacing corresponded to 1.2 *l* and there was no effect. For the longer spans the same spacing corresponded to 0.9*l* and the effect was very significant. However, since the presence of the second wheel violates the assumption that the system is axi-symmetrical, Hewitt's approach does not enable the effect to be quantified.

3.2.4 Ductility

Most of the membrane flexural theories considered in 3.2.1 are based on plastic theories, such as Johansen's yield-line theory. An important assumption of these theories is that the behaviour is ductile.

Reinforcement is ductile, whilst concrete is relatively brittle. Thus, although in reality there is a continuous transition from ductile to brittle behaviour, the assumption of ductility is normally considered valid provided that the tension reinforcement yields before the concrete crushes. This means that sections are considered ductile provided the ratio d_c/d under ultimate moment is less than some critical value. The critical ratio varies slightly according to the material properties.

In the absence of axial forces, the neutral axis depth ratio is a function of the reinforcement percentage. The requirement for ductility thus reduces to a critical reinforcement ratio which is around 1.2%(79). This includes most bridge slabs and nearly all building slabs.

In contrast to the situation in unrestrained slabs, the theory considered in 3.2.1 suggests that the neutral axis depth in a restrained slab is a function of the in-plane restraint. It is also fixed relative to the overall, rather than the effective, depth. Simple calculations show that realistic bridge deck slabs almost never comply with the ductility requirement. In many cases, calculations suggest that the steel stresses should still be quite low when the concrete crushes. This is confirmed by researchers who have found that such slabs fail in a brittle fashion before the reinforcement, often even in the critical areas, has reached yield. Thus it appears that few of the theories considered in 3.2.1 are valid in bridge deck slabs.

Building slabs tend to have larger span to depth ratios, relatively poor restraint and higher effective depth to overall depth ratios. Thus they are more ductile than bridge deck slabs and hence their behaviour is better predicted by plastic theories. Despite this, calculations suggest that the behaviour of some of the slabs which have been tested should be brittle. This was often supported by the behaviour at failure. Yield-line based theories did, however, agree reasonably well with failure loads. To some extent this was mere coincidence; the theory under-estimates the strength of strips so there is some margin for inability to re-distribute the moments. However, it is significant that all the test specimens were loaded by uniform loads. Under such loads the yield-line moment distribution does not differ greatly from the elastic moment distribution so plastic theories do not make great demands on rotation capacity. Under concentrated loads, in contrast, elastic theory predicts local moment peaks so plastic theory depends on very high rotation capacity. Because of this, the theories considered in 3.2.2 tend to over-estimate strengths under concentrated loads. This is presumably why uniform loads were chosen to test most of the theories, although this was not acknowledged.

Amongst the few studies to acknowledge that, because of this lack of ductility, yield-line based analyses may not be valid even in uniformly loaded slabs, are those due to Skates, Rankin and Long(66) and also Niblock

and Long(80). They developed a semi-empirical approach to overcome the problem. In this, the moment capacity of the critical section is calculated as in their analyses considered in 3.2.1. The relationship between the failure load and the moment at the critical section is then calculated using both elastic and plastic theory. Only if the moment capacity is zero, is the plastic relationship considered to be directly applicable. If the moment capacity is equal to that of a plastically balanced section the elastic relationship is used. For all realistic cases, which are between these two extremes, an intermediate solution is obtained by linear interpolation according to the ratio of the moment capacity to the balanced moment capacity. As might be expected, since this approach implies that yield-line theory is only valid in unrestrained slabs with negligible steel areas, the result tends to be slightly conservative.

Skates, Rankin and Long(66) have applied this analysis to slabs subjected to concentrated loads whilst Rankin(65) used it for flat slabs subjected to uniform loads. Because of the great difference between the elastic and yield-line moment distributions for such cases, they are a severe test of a simple linear interpolation. The use of a strip-based method to obtain the moment capacity is also questionable as there is no reason why the distribution of membrane forces across a section should be the same throughout the span. Also, as Rankin acknowledged, the slab analysis implies a different support moment from the strip analysis. It is thus perhaps surprising that they obtained a mean ratio of test result to prediction of 1.16 and a standard deviation of only 10%. However, to achieve this, they used Kirkpatrick's approach as an upper limit imposed by "shear mode failures".

Whilst many brittle bending failures are reported in the literature for uniformly loaded slabs, few such failures are reported under concentrated loads. As there are theoretical reasons for thinking that slabs are more likely to fail in bending before reaching their yield-line moment distribution under concentrated than under uniform loads, this may appear surprising. It is instructive to consider what such a failure would look like.

Elastic theory predicts high moment peaks under the concentrated load. Thus the highest concrete stress occurs in this region, but here the crushing stress is enhanced by the triaxial stress state so the first

crushing is likely to occur around the edges of the loaded area. It may then extend along the potential yield-lines, in which case the failure will be described as "flexural". However, the area where the concrete first reaches its crushing stress is subjected to a high shear stress. Thus, as it approaches its crushing stress, it is liable to fail suddenly under the combined effect of shear and compression, in which case the load will punch through the deck. Thus there is no clear distinction between a punching shear failure and a brittle bending compression failure so an alternative interpretation of the failures considered in 3.2.3 is that they are essentially flexural failures with shear playing a comparatively minor role. It has already been noted that some aspects of the test results can be explained by flexural theory. It is also clear from the descriptions of failure that the characteristic conical shear cracks do not appear until failure. Thus this interpretation is worth further investigation and it will be considered in later chapters.

If the failures considered in 3.2.3 were primarily brittle bending failures, it provides another explanation for the small effect of varying reinforcement on Kirkpatrick's failure loads. Unlike the other researchers, he used the same secondary steel throughout; he varied only the main steel. Increasing this did significantly reduce the deflection at failure, apparently due to the reduced ductility of more heavily reinforced sections. With constant secondary steel this implies that the moments in the secondary direction at failure must have been greater in the more lightly reinforced panels. This in turn implies that the distribution of the primary moments must have been more favourable in the more lightly reinforced panels and this tended to compensate for the reduced strength.

3.2.5 Serviceability

Because of compressive membrane action, restrained slabs have smaller crack widths, deflections and steel stresses than similar unrestrained slabs. Holowka(81), Cairns(82) and others have measured steel strains of the order of a tenth of those predicted by conventional flexural theory whilst Kirkpatrick(49) observed a similar effect on crack widths. There is also wide agreement that compressive membrane action delays the formation of the first crack, presumably because concrete's stress-strain curve departs from linearity before cracks become visible. However, the effect of restraint on acceptable service load is not as great as on strength. Because of this, nearly all the researchers who have considered the

implications of using membrane action in design have acknowledged that serviceability criteria would become critical. Despite this, the theoretical studies have concentrated almost exclusively on the prediction of strength. The design rules which will be considered in 3.2.8 do depend on the enhancement of serviceability due to membrane action but, in this respect, they have no quantitative theoretical basis at all.

Hewitt's approach, which was considered in 3.2.4, is one of the few to have been applied to behaviour at service loads, specifically to the prediction of deflection. However it is very unsatisfactory for this purpose. It is an axi-symmetrical model whilst, although the failure modes of deck slabs are approximately axi-symmetrical, the behaviour at service loads is not. Also the model considers a compressed volume of concrete which is almost entirely arbitrary except in its area at the critical section. In view of these and other faults, some of which were considered in 3.2.4, it appears that any resemblance between the deflections predicted by this approach and those which occur in practice is little more than coincidental. However, because the analysis assumes a linear load-displacement relationship, whilst the observed behaviour is often highly non-linear, it does not under-estimate deflections under service loads as much, or as consistently, as at failure.

Although compressive membrane action tends to improve the ultimate strength of restrained slabs more than their service load behaviour, there are situations in which it may be useful at service loads but not at failure. Yield-line theory assumes that the full plastic bending moment is developed across a wide width of slab. This means that a helpful compressive force across this critical section can only be developed by restraint which is external to the slab, or at least which comes from material well away from the loaded area. However, elastic theory is more appropriate to service load behaviour and this predicts high peaks of bending moment under concentrated loads. Thus a beneficial compressive force across these critical areas could be developed by adjacent areas of less heavily stressed slab. This means that maximum crack widths and stresses could be reduced by compressive membrane action even in unrestrained slabs, such as slab bridges. This possibility does not appear to have been considered before, presumably because of the concentration on strength and the historical development of compressive membrane theory from yield-line theory.

3.2.6 Restraint

Compressive membrane enhancement depends on the availability of adequate restraint strength and stiffness. Thus the prediction of this restraint is important. One reason why membrane action has been so little used in design is the feeling that the restraint available to slabs is unpredictable and perhaps unreliable.

Park is one of the few researchers to give restraint the attention it deserves. His work considered building-type slab and beam systems and he tested many nine-panel specimens(83). When only the centre panel was loaded, peak load was achieved just before the outer panels (which provided the restraint) cracked. This shows that the tensile strength of the concrete in the surrounding structure contributed greatly to the restraint. Park assumed that this tensile strength should be considered unreliable for design purposes, as is usual. Thus, when Hopkins and Park(50) designed a nine-panel floor system allowing for membrane action, they provided extra reinforcement in the beams to resist the restraint forces. They showed that this steel was heavier than that which they had saved by considering membrane action in the design of the slab so they suggested that design using membrane action was uneconomic. This arises because building slabs are designed for all bays fully loaded so the same load case is critical for all bays. Bridge decks, in contrast, are designed for moving loads and hence a different load case is critical for each part of the slab. This means that the critical area is always surrounded by areas for which a different load case is critical. Thus there is always under-stressed steel available to provide the restraint and no extra steel is needed. This means that the scope for economy from using membrane action in design is much greater in bridges, and other structures which are designed for moving loads, than it is in buildings. This is why recent research into membrane action, including this study, has concentrated on bridges.

Park analysed his specimens using his strip approach, which was described in 3.2.1c. He consistently recommended that steel should be provided to resist the full restraint force but he was less consistent in his assessment of the contribution of concrete to restraint stiffness. In reference 83 he used only the steel in assessing axial stiffness, but ignored lateral bowing of the outer slab panels. Theoretically this approach should be conservative where there are wide lightly reinforced

outer panels but unsafe where there are narrower heavily reinforced panels. This is confirmed by the test results. In reference 50 Hopkins and Park used gross concrete properties for assessing restraint stiffness but compensated for this by arbitrarily increasing the axial flexibility of the loaded panel by a factor of 4. This shows that the prediction of restraint flexibility is highly approximate so it is fortunate that, as was seen in 3.2.1c, the strength of slabs is not sensitive to the exact stiffness of the restraints.

Apart from Park's study, very little work has been done on the prediction of restraint. The approach adopted in the Canadian study was to measure the restraint available; not by direct measurement of restraint stiffness or strength, but by observing the behaviour of the slab under a load and back-calculating the "restraint factor" needed in their theory to predict the observed behaviour.

A disadvantage of this approach is that it is only possible to measure the restraint available at the time of the test. The lack of an analytical prediction means that it is not possible to predict any reduction in restraint which might occur in the future. In view of the importance, according to Park's work, of the tensile strength of concrete in providing the restraint this is significant; cracking due to loads previously applied in other positions, or to shrinkage, could reduce the restraint. The Canadians were aware of this so they conducted tests where cyclic loads(84) or pre-loading to failure(78) had occurred in adjacent bays. This seems to have had little effect.

Hewitt obtained restraint factors for laboratory specimens and models by back-calculating from the observed failure loads. However, in the field tests on full size bridges(81), it was not practical to test to failure so the restraint factors were estimated from the deflections at lower loads. In view of the doubts expressed in 3.2.5 about the validity of Hewitt's method for predicting deflections, this approach is less satisfactory. However, the results were similar to those obtained from models although the variation was much greater.

Kirkpatrick assumed rigid restraint which is obviously an unconservative assumption. However, since his approach is essentially empirical and was calibrated with tests on real structures which had less than perfect restraint, this is unimportant from a practical viewpoint except that, as

with the Canadian work, there is no way of allowing for possible future reductions in restraint.

3.2.7 Global Behaviour

Compressive membrane action in bridge decks is normally considered as a mechanism for resisting local wheel loads spanning between webs. However, as was noted in 2.4.3, bridge decks are also subjected to global flange forces and moments. Since slab behaviour is not linear-elastic (and compressive membrane action depends on this non-linearity) the principle of superimposition does not apply. Similarly, because the behaviour of restrained slabs under concentrated loads is not ductile, it is not safe to assume that global forces will re-distribute away from locally over-stressed areas. Thus separate studies of global and local effects cannot prove that behaviour will be satisfactory under combined effects so the interaction of the effects has to be considered.

A global flange force which is compressive has the effect of prestressing the slab. Thus, unless the stress is so high that concrete crushing becomes a problem (which is unusual), it improves the behaviour and can safely be ignored; as it has been by all the previous research.

Tensile flange forces might be expected to have a detrimental effect on slab behaviour. Because of this the Ontario study included tests(78) which simulated the support region of a continuous bridge. The resultant tensile flange force had remarkably little effect on the behaviour which was still entirely satisfactory. It can also be shown that tensile flange forces are unlikely to be serious for another reason: the critical design load case for global flange tension does not impose any local wheel loads in the critical area. Thus, when local wheel loads are imposed, any loss of longitudinal compressive membrane action due to flange forces is more than compensated for by reinforcement provided to resist the non-coexistent worst global moment.

Global transverse moments present a more difficult problem. It was noted in 2.4 that, in some types of deck, these moments can be even greater than the local moments predicted by elastic theory. It is conceivable that these large moments in combination with local effects could cause premature failures in the very lightly reinforced slabs proposed. Previous experimental studies, although comprehensive in other respects, have not

investigated this possibility. Many of the tests were on steel composite bridges with cross-frames which greatly reduce the global transverse moments. Most of the tests were performed using single wheels and some, because of propping off the laboratory floor or reacting against the adjacent beams, did not even model the global transverse moments which a single wheel could cause. Those studies which have considered whole vehicles used loads which were much less severe than HB.

It would be possible to virtually eliminate global transverse moments by providing intermediate diaphragms or cross-frames. However, for reasons discussed in 2.2.1, this solution is unlikely to be economic in concrete bridges, except in the rare cases when beam and slab bridges are built entirely in-situ on falsework. It is more practical in bridges with steel girders where cross frames are, in any case, often required to provide restraint to the compressive flange in construction. Both Kirkpatrick(13) and the Ontario code(11) require such frames to be provided between steel girders although they say that this is primarily to provide restraint.

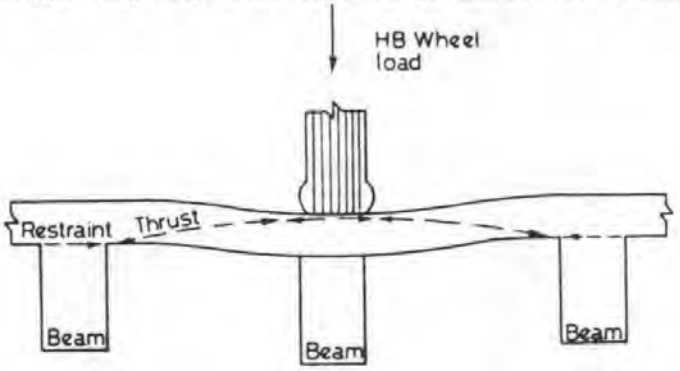

Figure 3.11: Compressive membrane action to resist global moments(13)

Although Kirkpatrick, like all the other researchers, failed to model full global effects in his tests, his background in British practice meant that he was more aware of the problem. He suggested that compressive membrane action improves the ability of slabs to resist global, as well as local, transverse moments as shown in Figure 3.11. This may be true but there are no tests to prove it and there are several reasons for believing that the effect is less pronounced. One of these is clear from Figure 3.11; resisting global moments requires the slab to effectively span at least twice as far as resisting local effects. This doubles the span to depth ratio which reduces the effectiveness of compressive membrane action and, as was shown in 3.2.1c, makes it more sensitive to restraint flexibility. Another reason is that, unlike local moments, global moments act over a

substantial portion of the span length. This means that the ratio of restraining structure to structure requiring restraint is far less favourable.

There is also another effect which is likely to reduce the contribution of compressive membrane action to resisting global transverse moments. It was noted in 2.4.3 that the connection between the top flanges of adjacent beams tends to even out the compressive stresses. This means that the most heavily stressed beam (the one which most requires support from global transverse moments) effectively has a top flange which is wider than the beam spacing. In order to keep a wide compression flange in moment equilibrium about the vertical axis, transverse stresses are required as shown in Figure 3.12. These put the top flange into transverse tension at mid-span and compression at the support: the opposite of what is required to develop compressive membrane action.

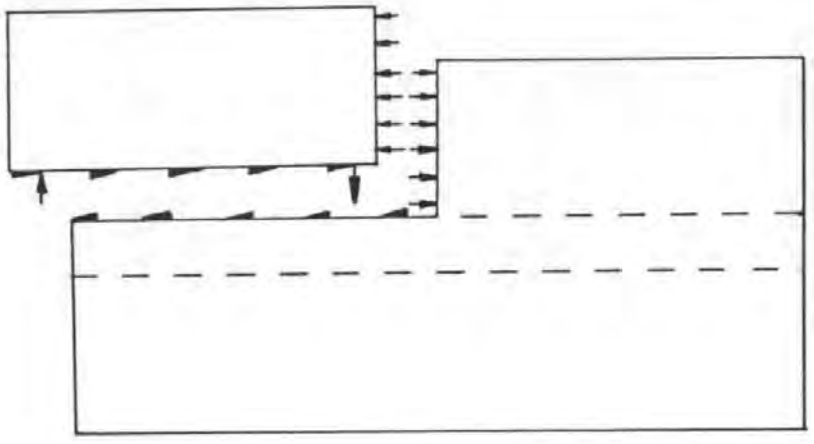

Figure 3.12: Transverse stresses in a wide compression flange

Although it seems likely that the contribution of compressive membrane action to resisting global transverse moments is small, this does not necessarily mean that the slabs themselves will become unsafe or even unserviceable. Once a slab cracks, its stiffness reduces and the global transverse moment starts to redistribute away. However, this leads to a deterioration in the distribution properties of the deck and hence an increase in the moment in the critical beam. This could be a problem as both Kirkpatrick and the Ontario Code use analysis based on *uncracked* section properties to obtain the design moments in the beams. Paradoxically, the Ontario Code introduced this analysis (which is a

departure from conventional North American practice) at the same time as introducing the empirical slab design method.

Theoretically, the problem of worst beam moment increasing above the design value when the slab cracks also arises in decks designed by conventional methods. However, the cracked and uncracked elastic stiffnesses differ by a factor of around three compared with around ten in very lightly reinforced slabs designed allowing for membrane action. Thus the effect is much smaller. Also, conventional design methods provide a safe solution according to plastic theory. Thus, if a beam did start to fail, redistribution would bring the transverse moments back into play. There is no guarantee that slabs designed to the Ontario rules, or even the Northern Irish rules, will be able to act in this way.

3.2.8 Empirical Design Rules

Both the Ontario and the Northern Irish study noted that the available "theory" for restrained slabs predicted only their strength, which is not a critical design criterion. Thus there was no theoretical basis for a design method. However, they considered that there was no need for one either: the observed load-carrying capacity of deck slabs was so high that simple, and probably very conservative, empirical design rules would suffice.

Batchelor et al(78) noted that tests suggested that unreinforced slabs would have adequate strength so they initially recommended 0.2% isotropic reinforcement in each face; the minimum reinforcement recommended by AASHTO(45). This was later amended to 0.3% for reasons which are unclear. Curiously, the percentage is based on the effective depth: there is no logical reason why less steel should be required if it is further from the face. However, this is a fault which is shared with the minimum steel rules in many other codes, including BS 5400 and CP 110 but not BS 8110.

The Ontario Code requires extra steel to be provided in some circumstances. The reinforcement is doubled in the end regions of highly skewed decks. Also, but only in decks with box girders, reinforcement designed by normal means to resist global transverse moments is added to the nominal steel. This rule is rather odd since these moments can be just as great, and just as important, in other types of deck. Also, for

reasons noted in 3.2.7, it still does not prove that behaviour will be satisfactory under combined effects.

Kirkpatrick gave specific recommendations for only one slab thickness; 160mm. This was to provide T12s at 150mm which is approximately 0.6%. The reason for specifying more steel than the Ontario Code was that Kirkpatrick realised that the reinforcement required to resist calculated global transverse moments alone could exceed 0.5% in some slabs which were covered by his rules. It is not clear why he specified the same steel in the longitudinal direction and his rules appear to be unduly conservative in this respect: the author has designed a deck slab to conventional rules which had less longitudinal steel.

Both sets of rules require reinforcement for any deck cantilevers to be designed by conventional methods, which means they are likely to require substantially more steel than the rest of the deck. In his own design Kirkpatrick(13,49) avoided the resulting awkward detailing by not having any cantilevers at all. This was an economic solution for his particular case because the cantilever formwork and reinforcement would have been expensive compared with the cost of an extra beam. This would not apply to longer span bridges and the need to provide extra reinforcement for the cantilevers is a significant limitation on the advantage of using the rules.

The major disadvantage of empirical design rules is that there must be restrictions on their range of applicability. These will now be considered.

a. Span and Depth

Both Kirkpatrick and the Ontario Code specify a limiting span to depth ratio of 15 for the use of their empirical rules. Although there is some evidence that the theories on which they are based (particularly Kirkpatrick's) become unsafe by this span to depth ratio, the observed and predicted strengths of slabs are so high that the limit is conservative. However, it seems to have been considered that this was unimportant because the limit covered normal practice, at least for beam and slab decks. This is not entirely logical; the reason shallower slabs are not used is that they are uneconomical, or even impossible, to design to conventional rules because the reinforcement required increases rapidly with span to depth ratio. This does not apply in slabs designed to the

empirical rules, indeed the required reinforcement *reduces* with slab thickness. Thus, if one was designing a bridge to these rules from scratch (that is, without the restrictions imposed by using an existing range of standard beams), it appears that the optimum solution would always have wide beam spacings and the maximum allowable slab span to depth ratio.

The Ontario Code specifies a minimum slab thickness of 225mm but the Commentary makes it clear that this is not for structural reasons but because shallower slabs are not advised for durability reasons; in Ontario, as in many states in the USA, bare concrete decks are the norm. The restriction on minimum depth, which is not applied in the assessment of existing decks, has the unintended advantage of limiting the problem of global transverse moments since the author's analysis shows that these are most significant in shallow slabs on close-spaced beams.

The Ontario Code also specifies a maximum slab span of 3.7m. This requires a slab depth of only 247mm, compared with the absolute minimum of 225mm, so the range of slab depths which are likely to be designed to the rules is very narrow. There is no advantage in using more than the minimum slab thickness.

A restriction on span is probably justified because longer spans introduce effects which have not yet been researched; significant deadweight stresses and a much greater interaction between the effect of several wheels. However, even with the Ontario Code's allowance for haunches, 3.7m is a modest slab span by the standards of modern long-span concrete box girder bridges. Thus the Ontario rules will not be used for these, indeed the limiting span to depth ratio makes designing them to the rules uneconomic anyway as the extra weight would more than cancel out the saving in reinforcement. There is scope for economy in the design of this type of deck from using membrane action, particularly if this could justify even longer slab spans or shallower slabs than at present, but this requires further research.

b. Restraint

The two sets of rules are very similar in their requirements to ensure adequate restraint. Both require intermediate cross-frames if steel beams are used. Both require diaphragms at the supports if concrete beams are

used. Kirkpatrick also suggests the use of concrete support diaphragms even with steel beams. Both require parapet upstands or edge cantilevers to ensure adequate lateral restraint.

The test results suggest that these requirements are sufficient but give little indication as to whether they are necessary. The outer bays of Beal's deck, which did not comply with the requirements for edge stiffening, did show lesser (but still adequate) strength. All the other decks tested complied with the requirements, as do most of the decks currently designed. Some concrete decks have, however, been built without diaphragms and this has been advocated by Cranston(85) because of the costs of forming diaphragms.

3.3 PRESTRESSED SLABS

One of the earliest, and in some respects still one of the most comprehensive and influential, studies of the effect of compressive membrane action on the behaviour of bridge deck type structures was conducted by Guyon(10). His study is worth reviewing even though he considered only prestressed slabs whilst, for reasons given in 2.2.2, the remainder of this thesis assumes that bridge deck slabs will be constructed of ordinary reinforced concrete.

Guyon's slab was cast integral with longitudinal and transverse beams. It was stressed transversely by concentric wires giving a stress of $1.5N/mm^2$, whilst tendons located in the beams gave a longitudinal stress of $2.4N/mm^2$. These stresses are very low, much lower than the longitudinal stress applied by global effects to many slabs which are not normally considered as being "prestressed".

A jack was used to apply a single central concentrated load to each bay in turn. It reacted, via steel girders, against the beams adjacent to the loaded bay of the slab. Thus only local moments were applied.

Several conventional elastic methods, including Westergaard's(39) and Pucher's(40), were used to analyse the slab. The results were reasonably consistent both with each other and with the initial behaviour of the slab. The strain gauge readings started to show some signs of non-linearity at approximately the load for which the calculated stress equalled the measured flexural tensile strength of the concrete. However, despite the

use of "a powerful microscope", no cracks were visible until the load was increased by a further 30 to 40%.

Once formed, the cracks extended very slowly in both width and length; much more slowly than conventional elastic flexural theory would suggest. Guyon attributed this to a combination of moment re-distribution away from the cracked region and redistribution of the prestress force towards the cracked strips, that is compressive membrane action. Strain gauge readings confirmed this explanation. Initially only the central part of the slab was subjected to a compressive force and tension in the remainder helped to restrain it. As the load increased, the area in compression extended until the whole of the loaded bay was in compression.

Guyon considered that the behaviour was acceptable from a serviceability viewpoint up to a load of over 2½ times that at which the calculated stress equalled the measured tensile stress, or 10 times the load given by Freyssinet's no-tension rule. Removal of the load at this stage caused the cracks to close up, but this is the one aspect of the behaviour of such a lightly stressed slab which could be significantly different from that of a reinforced slab.

With further increases in load the existing cracks grew wider and new radial cracks developed. The load was then carried by "a system of concrete struts", that is pure compressive membrane action. A brittle punching failure occurred at a load of some 25 times the "no tension" load or twice the load given by Johansen's yield-line theory.

In addition to this qualitative description, Guyon developed some simple analyses. He acknowledged that these were based on "debatable assumptions" and in many respects they have been superseded by more rigorous analyses such as those given in 3.2 and Chapter 5. However, they are still useful as descriptions of behaviour. His analysis of the behaviour of strips of slab at relatively low loads is largely confirmed by the form of analysis considered in Chapter 7. Although it is difficult to use in any quantitative way, it is significant because none of the more recent theoretical studies explore the behaviour at low loads.

Guyon extended Johansen's theory to allow for compressive membrane force. Instead of calculating the membrane force required to maintain lateral displacement compatibility, like most of the analyses considered in 3.2.1,

he estimated the maximum available restraint force. His analysis over-estimated the failure load but he attributed this to the fact that he ignored the effect of the vertical displacements on the lever arm at which the restraint force acts. Back-calculation confirms this explanation. He acknowledged that his analysis would not be valid for a slab with a very large area of surrounding restraining concrete and he attempted, largely unsuccessfully, to analyse such a case.

Guyon also gave an axi-symmetrical analysis of the punching failure based on the assumption of rigid lateral restraint. This assumed that the radial struts were elastic and uncracked, except at the outer edge and at the edge of the loaded area, which is analogous to the elastic-plastic analyses considered in 3.2.1c. It also assumed that the force in the struts was constant over their length. This implies that there are no circumferential forces but this was neither mentioned nor justified. Guyon assumed that, at failure, the whole depth of the slab adjacent to the load was in compression. This seems unlikely as there is no mention of cracks closing up in the description of behaviour. Another fault in the analysis is that the calculated concrete stress on the critical section at failure is some 130N/mm^2 and a very large portion of the slab is stressed up to more than the elastic limit. This shows that there were circumferential forces and this axi-symmetrical analysis appears to be the least satisfactory aspect of the study.

As a result of the study Guyon developed a simple design method which he acknowledged to be "much too conservative". This was to analyse the slab using elastic theory but taking Poisson's ratio as zero and taking the slab to be simply supported. The resultant mid-span moment is then shared between the support and mid-span sections and resisted by bending of the prestressed sections. These are analysed ignoring the tensile strength of concrete and the lateral redistribution of prestress, but allowing cracking to extend to the level of the centre-line of the cable. If the cable is at mid-depth of the slab, this gives twice the allowable moment given by the no-tension rule. In the case of a simply supported slab it also gives twice the design load. In fixed-ended slabs the difference is much greater because Guyon's method allows designers to take as much moment as they like at the support, whereas conventional elastic theory only allows a reduction in the mid-span moment of some 15%. The result is that, for a uniform fixed-ended slab, Guyon's method requires only 36% of the

prestress that the no-tension rule requires. In haunched slabs the difference can be greater.

Although less radical than the Ontario approach, this design method is more useful in longer span slabs as it requires no limit on span to depth ratio. The reduction in stressing force is so great that, despite the reservations in 2.2.2, it has had a significant effect on the relative economy of transverse stressing and ordinary reinforced concrete. This has meant that many deck slabs mainly (but not exclusively) in France have been designed using Guyon's rules. These now represent a very significant number of bridge-years of satisfactory experience.

Slabs designed to Guyon's rules are very lightly stressed. They would crack long before the concrete's compressive stress became excessive. Thus their behaviour is not fundamentally different from that of reinforced slabs so the experience of their satisfactory behaviour is significant to this study. However, there is one respect in which stressed and reinforced slabs differ in their behaviour. Once cracked, a reinforced slab's stiffness is greatly reduced for all subsequent applications of tensile stress, however small, but a prestressed slab's stiffness is only significantly affected when the applied tension exceeds the prestress. Thus slabs designed to Guyon's rules may have better restraint than those designed to, for example, the Ontario rules.

3.4 CONCLUSIONS

Previous research shows that bridge deck slabs are far stronger than conventional design methods imply. Slabs designed to the Ontario rules, for example, have very much less steel yet they have behaved well both in service and in load tests.

Two "theories" have been proposed which claim to "predict" the ultimate punching shear strength of bridge deck slabs subjected to wheel loads. These theories are essentially empirical and their predictions are sometimes significantly in error. There is also some indication that the assumption that the observed failures were "shear" rather than "flexural" failures could be incorrect. However, the observed strengths of bridge deck slabs are so high that these faults have no practical significance; typically it is a question of whether the factor of safety is 5 or 7. In practical terms, the only questions over the strength of slabs which are

restrained and which are subjected to single wheel loads relate to span to depth ratios above those for which these theories claim to be valid.

Although it is clear that the restraint available in bridge decks is adequate to develop compressive membrane action, there is no quantitative explanation for this. Similarly, there is no quantitative theory to explain the observed satisfactory service load behaviour of decks designed to the empirical rules discussed. Since service load behaviour is critical in design, this means that there is no theoretical basis for a design method.

Another aspect of the behaviour of bridge decks with very lightly reinforced slabs which has not been proven theoretically is their performance under combined global and local effects. This appears to be a far more serious omission since it has not been investigated experimentally either.

CHAPTER 4

ELASTIC ANALYSIS

4.1 INTRODUCTION

Chapters 2 and 3 showed that serviceability criteria, not ultimate strength, are critical in the design of bridge deck slabs. Elastic theory is more appropriate to the analysis of serviceability than plastic theory but the elastic theory of restrained slabs has not been developed.

The complexity of the behaviour of realistic slabs, particularly under concentrated loads, is such that it is not practical to obtain rigorous analytical solutions, either elastic or elastic-plastic. Thus the solutions considered in 3.2.1 all contained gross approximations, assumptions or empirical factors. It is, however, possible to determine elastic solutions for simple cases by making reasonable assumptions. These cases are not realistic but they do indicate the sensitivity of the behaviour to the relevant variables. Also, by comparison with conventional analyses of similar cases, they give some indication of the significance of membrane action in practical cases. In addition they can be used for checking computer programs which can then analyse more realistic cases.

Since these simple analyses cannot be used directly in design, there is little point in considering a wide range of cases. Thus, in this chapter, only one simple case will be considered; the unreinforced symmetrical slab strip which was considered in 3.2.1, subjected to a single central point load.

4.2 ASSUMPTIONS

The analysis is based on conventional elastic engineer's beam theory. Plane sections are assumed to remain plane and compressive stress is taken to be proportional to strain whilst concrete is taken to have no tensile strength. Unlike the analyses considered in 3.2.1, the deflection is taken to be small relative to the slab thickness but the validity of this assumption will be checked.

Although these assumptions are just as arbitrary as those used in the analyses considered in 3.2.1, this analysis is more rigorous in the sense that the assumed moment, stress and strain fields are made consistent

throughout the structure. The analyses considered in 3.2.1 either used different material properties at the critical sections from elsewhere, as in Park's approach, or, like Mc Dowell, only checked that the assumed strain field and material properties were consistent with the forces at the critical sections.

4.3 STRESS

Since the assumed slab system has no tensile strength, it can only resist vertical forces by virtue of the vertical component of the restraint force. It is thus convenient to consider the system in terms of the line of thrust of the restraint force. This must be straight except at the supports and the point of application of the vertical load.

Because of the assumptions, the slab cracks if the line of thrust goes outside the middle third of the section. Where the slab is cracked, the line of thrust must act at the edge of the middle third of the effective, uncracked, section. This leads to the geometry shown in Figure 4.1.

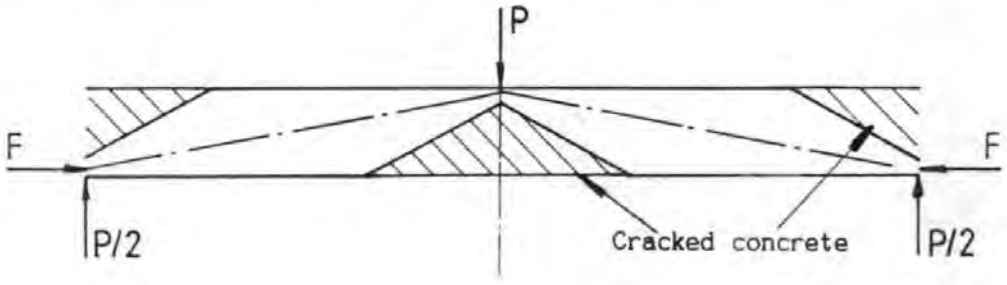

Figure 4.1: Restrained slab strip
(elastic theory)

In Appendix A1 it is shown, by consideration of displacement compatibility assuming rigid restraint, that the depth of concrete in compression at the supports and at mid-span is 0.222h and the maximum stress in the concrete is $2.64Pl/h^2$. Thus, with a concrete stress f_c, the load P

$$= \quad 0.38 f_c h^2/l$$

4.4 COMPARISON WITH OTHER ANALYSES

The rigid-plastic analysis considered in 3.2.1a gave the strength of the equivalent strip as

$$= \quad f_c' \, h^2/l$$

Using the BS 5400 design rectangular stress block this gives;

$$P = 0.4f_{cu}h^2/l$$

Using the BS 5400 elastic stress limit ($0.5f_{cu}$) the elastic solution gives;

$$P = 0.19f_{cu}h^2/l$$

at the serviceability limit state. The ratio of design ultimate to design service load is a function of the load factors and in BS 5400(23) it is

$$= \frac{\gamma_{fg} \times \gamma_{fL}}{\gamma_{fg} \times \gamma_{fL}} \begin{matrix} \text{(ultimate limit state)} \\ \text{(serviceability limit state)} \end{matrix}$$

Considering the case of HB load and load combination 1 (which is usually critical in deck slabs) this is;

$$= \frac{1.1 \times 1.3}{1.0 \times 1.1}$$

This means that a section on the limit of the allowable elastic service stress would have a design ultimate load

$$= 1.3 \times 0.19f_{cu}h^2/l$$

$$\simeq 0.25f_{cu}h^2/l$$

which is only 62% of its strength, confirming that the serviceability check is critical even without allowing for redistribution.

Using the simple BS 5400 design method, the reinforcement required in each face to resist this load would be approximately 0.6%. This is a very significant amount of reinforcement, confirming that membrane action is worth considering.

4.5 CRACK WIDTHS

Unlike most other crack width prediction formulae, the BS 5400 formula can be applied to unreinforced concrete. With the maximum allowable service load derived in 4.4 the calculated crack width for our case

$$\simeq 0.00027h$$

For a 160mm deep slab this is 0.43mm. If it is assumed that the maximum allowable crack width had to be complied with on the surface (which is not strictly required as there is no reinforcement) the limiting value would be 0.25mm. However, this does not have to be complied with under the full HB load; only under 25 units of HB. The result is that crack widths would

not be a limitation in a deck designed for 45 units of HB but they would be in a deck designed for a lower load.

4.6 DEFLECTION

In Appendix A2 it is shown that the analysis given in 4.3 and Appendix A1 leads to a central deflection

$$= \quad 0.173\ P l^2/Eh^3$$

for the load corresponding to a stress of $0.5f_{cu}$ this is

$$\simeq \quad 4.5 \times 10^{-5} l^2/h$$

Now the membrane force acts at a total lever arm

$$= \quad (1 - 0.222 \times 2/3)h$$

$$\simeq \quad 0.852h$$

For small deflection theory to be valid the displacement has to be small compared with this. The error is 1% with an l/h of 13.8, 5% with 30.9 and 10% with 43.6. In practical terms, this means that small displacement theory is valid for the serviceability analysis of local effects. However, if membrane action were used for resisting global transverse moments the effect of displacements could be significant.

4.7 EFFECT OF RESTRAINT FLEXIBILITY

In Appendix A3 the effect of in-plane restraint flexibility is added into the analysis. The result is shown in Figure 4.2 by plotting the load for a stress of 20N/mm^2 against the restraint stiffness expressed as a multiple of the axial stiffness of the uncracked slab. The elastic analysis is very much more sensitive to restraint stiffness than the analysis considered in 3.2.1. Thus restraint is an even more important factor than Chapter 3 suggested.

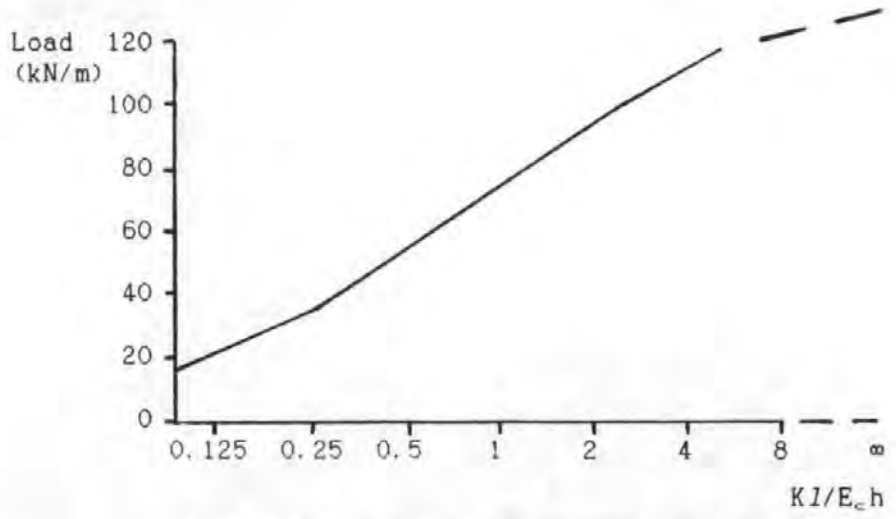

Figure 4.2: Effect of restraint flexibility

(l = 1.5m, h = 160mm, b = 1m)

4.8 CONCLUSIONS

The simple analysis considered in this chapter shows;

1. Compressive membrane action is significant in the elastic range.
2. It is less significant than in plastic analysis, hence serviceability criteria are likely to be more critical in design allowing for compressive membrane action than in conventional design.
3. Small displacement theory is valid for considering local behaviour at the serviceability limit state.
4. The behaviour under service loads is more sensitive than ultimate strength to restraint flexibility.

Despite the extreme simplicity of the case considered, the various test results considered in Chapter 3 suggest that all these conclusions are likely to remain valid for more realistic cases.

CHAPTER 5

NON-LINEAR FINITE ELEMENT ANALYSIS

5.1 INTRODUCTION

The major difficulty with analysis allowing for membrane action, at least as far as flexure is concerned, is not conceptual; it is the complexity of the mathematics. This fact, which is clear from 3.2.1 and Chapter 4, suggests that the subject should be amenable to solution by numerical analysis and the finite element method is the most convenient way of doing this.

The analysis of membrane action has to be non-linear; even the simple analysis considered in Chapter 4 is only linear under proportional loading. Non-linear finite element analysis, NLFEA, is only practical with powerful computers so it is a comparatively recent method which was not applied to concrete until the 1960's(86). Despite this the literature is extensive and, although only a tiny fraction is aimed at the analysis of membrane action, much of it is relevant. It is thus not possible to review all the work in detail. This chapter aims only to introduce the principles and problems of the method. A particular, relatively simple, form will be considered in more detail in Chapter 7 whilst readers requiring a more comprehensive coverage of the state of the art should consult recent specialist works such as reference 87.

5.2 GENERAL APPROACH

The analytical method adopted should be capable of resolving all the problems identified in Chapter 3. Two of the most important of these, the prediction of restraint and the analysis of global effects, require the analysis to consider the whole bridge. Even with very powerful computers, this puts a severe restriction on the form of analysis which can be used. In this study, therefore, only the "smeared crack, distributed steel, layered approach" will be considered. In this, individual cracks are not modelled; the cracks are smeared out into an infinite number of infinitesimal cracks. Similarly, individual bars are not represented; the steel is distributed evenly across the element width. The significance of layering is that it enables the material state to be varied over the element depth whilst still using a two-dimensional element. The stresses are calculated independently for each layer as a function of the strains

which are calculated from the displacements at the "reference plane"; the level at which the elements are implicitly located. The element forces are then calculated by integrating the stresses over the element volume. Thus the forces are calculated directly from the displacements but the correct displacements can only be obtained from the loads by an iterative solution scheme.

Although linear-elastic analyses of slabs, particularly for bridge design, are often performed using alternative structural idealisations, such as grillage analogy, non-linear analysts have assumed it necessary to use plate finite elements. This is because of their desire to produce rigorous and accurate analyses.

5.3 ELEMENT TYPE

5.3.1 Slabs

Early finite element analyses of slab systems used classical thin plate theory which assumes that lines normal to the reference plane remain normal. This approach is being "gradually superseded"(87) by the Mindlin(88) form which assumes that lines normal to the reference plane remain straight but not necessarily normal. This enables shear deformations to be included in the analysis so the theory is sometimes described as "thick plate theory". However, shear causes diagonal cracks in reinforced concrete and the assumption that vertical lines remain straight prevents the realistic modelling of shear failures. Indeed, according to Chana(75), shear failures are sensitive to dowel behaviour at the crack which implies that they cannot be realistically modelled by any form of smeared crack, distributed steel analysis. Despite this, Mindlin's theory does give more realistic predictions than classical theory for the shear forces at a free edge, as has been illustrated by Cope(89). However, it appears that the main reason for adopting it is one of analytic convenience; it requires a lower order of displacement continuity across the element boundaries(87).

The nodal forces in the elements, due to nodal displacements, are calculated using the virtual work approach. To do this it is necessary to assume a displacement field for the whole element from the known nodal displacements. A wide variety of elements can be developed, according to the number of nodes, the displacement field assumed and the method of

integrating the stresses and strains over the element volume. A discussion of their relative merits is outside the scope of this study.

5.3.2 Beams

The beams in beam and slab decks can be modelled using either simple beam elements or an assemblage of plate elements. The latter is far more expensive but it enables inclined web cracking and the transverse bending stiffness of the beam to be modelled. Edwards(36) found the two approaches gave very similar results in a bridge with rectangular beams. However, the transverse bending stiffness of the flange of, for example, an M beam is much greater so there may be more advantage in using plate elements for these. Buckle and Jackson(90) have developed a form of beam element which can model transverse bending. However, because it assumes that plane sections remain plane, it cannot model the warping stresses which contribute to the resistance to torsion.

The beam elements are rigidly attached to the plate elements at the nodes. Since the mesh size is decided by the requirement to model the local slab behaviour, it is smaller than is required to model the beam behaviour. Thus the analysis is not sensitive to the type of beam element used. Buckle and Jackson(90) used a displacement function which will be shown in Chapter 7 to have serious faults, whilst Edwards(36) used a displacement function which was not consistent with that used for the slab. Calculations suggest that neither of these faults had a significant effect on the results.

5.4 MATERIAL PROPERTIES

5.4.1 Steel

The reinforcing and prestressing steel is assumed to be fully bonded to the concrete and to exhibit uniaxial behaviour; that is, it is stressed only by strain in the direction of the bars.

Any stress-strain relationship can be defined numerically and incorporated into a program but it is more usual to use elastic-plastic properties, sometimes with linear strain hardening. Modern reinforcement, and all prestressing, departs significantly from this assumption so there are advantages in using more realistic properties.

When unloading is considered, it is usual to use a straight line parallel to the initial portion of the stress-strain curve which gives a permanent set equal to the previous departure from linearity.

5.4.2 Concrete

a. Uncracked

The enhancement of concrete's compressive strength due to biaxial compression, and the reduction due to orthogonal tension, is normally considered but the effect of vertical stress cannot be modelled in the form of analysis considered here. Despite this, the enhancement can be significant; up to approximately 20%.

A variety of stress-strain relationships have been used. Abdel Rahmen(87) used a simple elastic-plastic relationship with a straight cut-off at a limiting strain whilst Edwards(36) used Popovics' formula(91) for the uniaxial case in beams and Nilson's(92) approach for the biaxial case.

As with steel, unloading is usually modelled with a straight line. The unloading part of the properties are sometimes specified even in analyses under monotonically increasing loads in order to avoid the fault of deformation theory which was mentioned in 3.2.1b. If this is done, the maximum strains have to be stored for all the sampling stations.

The variability of concrete is a major difficulty in a deterministic analysis. This variability is particularly significant to failures, such as punching failures, which are affected by local rather than average concrete strength. The effect is large compared with the difference between stress-strain curves and this, combined with the fact that the relationships are used many thousands of times in the course of an analysis, encourages the use of simple relationships. It also means that the predictions are unlikely to be precise.

b. Cracked

Although smeared crack analysis implies infinitesimal cracks at infinitesimal spacings, real structures have discrete cracks at finite centres. The concrete between the cracks is able to resist tension and this stress contributes to the stiffness of the structure. This effect, which is known as "tension stiffening", is very significant, particularly in lightly reinforced elements and at low loads. It is modelled by an

empirical stress-strain curve which has a descending branch after the concrete has cracked.

Cracks first form in the direction of the maximum principal tensile strain. If this direction subsequently changes, a shear stress is developed across the crack. The shear stiffness is reduced by the crack and can be modelled by another empirical factor called a "shear retention factor". However, even with this reduced shear stiffness, the analysis can imply a tensile stress in other directions which exceeds the cracking stress. Cope et al(93) used an alternative approach in which the "crack" direction rotates to follow the principal strain direction. This appears to give better results in cases where the rotation is significant(94). It may appear illogical that cracks can rotate after they have formed but presumably the explanation is that the crack direction in a smeared crack analysis represents only the average or active crack direction so it can rotate as new cracks form.

The few analysts who have considered unloading in cracked concrete have used widely different assumptions(95,96,97) reflecting the lack of data in this area.

Whatever tension stiffening function is used, the predicted behaviour is very sensitive to the assumed cracking stress. In addition to having an even wider random variation than compressive strength, this varies according to strain rate, strain gradient, curing régime, load duration, number of load repetitions and many other factors. This makes accurate deterministic predictions of behaviour impossible.

Unlike the non-linearity due to reinforcement yielding and concrete crushing, that due to concrete cracking is significant under service loads. Thus it is the only non-linearity which is important to the design of structures for which serviceability criteria are critical. Also, even in strength analysis, it is not realistic to consider only the cracking due to a single monotonically increasing load case since cracking could have been caused by many different service load cases. In particular, cracking due to wheel loads previously applied in other positions could reduce the restraint available to develop membrane action under the case being considered. Thus the lack of an agreed tension stiffening function, particularly for unloading, is a serious obstacle to the use of the analysis in design so the subject will be considered further in Chapter 6.

5.5 APPLICATION TO MEMBRANE ACTION

Several analysts have applied NLFEA to slab systems. Most have considered only monotonically increasing loads, which restricts the application of their analyses, but they do give a useful insight into behaviour. Several analysts have claimed good predictions for the behaviour of restrained slabs but some of these might be considered slightly surprising. For example, Jackson(98) obtained good predictions for Roberts' tests(53) but his analysis used small displacement theory and simple calculations suggest that including the effect of the observed (and predicted) large displacements would have reduced the predicted strength by some 20%. Despite these doubts, non-linear analysis has proved better able to predict the behaviour of complicated slab systems than other methods. At service load levels, the predictions for complicated structures actually appear to be better than those for simple "fully restrained" laboratory specimens. The reason for this appears to be a fault in the tests rather than the analysis; it is difficult to develop full restraint and service load behaviour is very sensitive to restraint as was demonstrated in 4.7.

It is not practical or necessary to consider all these analyses in detail but it is useful to consider a particularly relevant example; that of Cope and Edwards(99). They analysed several of the tests which were considered in Chapter 3, including those of Kirkpatrick. In view of the inherent variability of results which are sensitive to local concrete behaviour, they considered their predictions to be good. However, Kirkpatrick produced enough results to enable the variability to be estimated and this appears to be remarkably small and certainly smaller than the discrepancy between the test results and the non-linear analysis. Despite this, the analysis is reasonably good with the worst error in the failure prediction being some 30% with 15% being more typical. This may not sound that good compared with Hewitt's or Kirkpatrick's "analyses" but they are largely empirical whilst the non-linear analysis obtained the restraint and strength only from the geometry and material properties of the specimen with no empirical corrections.

The brittle nature of the "punching shear" failures was also correctly predicted even though the analysis is incapable of modelling shear. This appears to confirm the suggestion in 3.2.4 that such failures are primarily brittle bending compression failures although the analysis did tend to over-estimate strength slightly, implying that the high shear stress in the

critical region reduced its compressive strength. In practical terms, the good predictions for stresses and deflections at lower loads are more significant as they suggest that the approach is valid for the critical serviceability analysis.

Cope and Edwards' study suggests that NLFEA is able to successfully predict restraint and analyse the local behaviour of bridge deck slabs allowing for membrane action. In theory it can also model the interaction of global and local moments but only Edwards(36) appears to have considered this. He analysed a hypothetical bridge with rectangular reinforced concrete beams and with deck slab reinforcement designed to the empirical rules considered in 3.2.8. His analysis suggested that this reinforcement would be over-stressed under combined global and local moments, confirming the doubts expressed in 3.2.7. However, because of the lack of test data, there is no proof that the analysis was realistic in this respect. The form of deck he considered was also unrepresentative of modern practice since ordinary reinforced beams are rarely used and the moment redistribution behaviour would be very different with prestressed beams.

5.6 USE IN DESIGN

Although NLFE has proved capable of predicting the behaviour of reinforced concrete slab structures, it has rarely (if ever) been used in their design; either directly or for validating simpler design methods. Bedard and Kotsovos(100) have said "The main reason for this appears to be a lack of agreement concerning the numerical description of material behaviour". This reason is supported by 5.4.2b but, in the case of the slabs considered here, it is not a sufficient reason; the analysis would still produce more economical designs than conventional methods if the most conservative conceivable material properties were used. Thus there must be more fundamental reasons and these will now be considered.

a. Cost and Complexity

A non-linear analysis of a given structure with a given element mesh is at least an order of magnitude more expensive in computer time than the equivalent linear analysis. Also, because the principle of superimposition does not apply, every load combination has to be analysed separately. Similarly, global and local effects cannot be superimposed so the whole structure has to be analysed with a fine enough mesh, at least in the

critical areas, to model local behaviour. The result is that the cost in computer time is several orders of magnitude higher than for the analytical methods considered in Chapter 2. More seriously, the analysis is also much more expensive in engineer's time. This discourages its use, particularly under design fee competition.

A related disadvantage, which is perhaps more serious, is the conceptual difficulty; NLFEA is difficult for the ordinary designer to fully understand or control. This makes it potentially dangerous as (at least at the present state of the art) NLFEA is neither fully automatic nor foolproof.

b. Load History Dependence

For reasons which were discussed in 2.3.4 and 5.4, the behaviour of concrete structures, and hence the realistic analysis of such structures, is load history dependent. Since it is impossible to predict and impractical to analyse the load history of a bridge over its entire design life, this could be a serious problem.

c. Incompatibility with Codes

Existing codes of practice were written with conventional analytical methods in mind. If the critical design criteria were clear-cut fundamental requirements, such as ultimate strength, this would not be a major problem. However, Chapter 2 showed that the fundamental critical design criterion for bridges is the very ill-defined one that they should remain "serviceable" for their design life. It is very unclear what this means in non-linear analysis terms, except that it appears to confirm that a whole life analysis is required.

5.7 CONCLUSIONS

Non-linear finite element analysis is a powerful analytical tool which sheds some light on the fundamental behaviour of slab systems and which can give reasonably good predictions for their behaviour. The reported analyses support the suggestion in 3.2.4 that "punching shear" failures may be primarily flexural. One also appears to confirm the doubts about global behaviour expressed in 3.2.7. There are, however, major difficulties in using the analysis in design.

CHAPTER 6

TENSION STIFFENING

6.1 INTRODUCTION

In Chapter 5 it was noted that the lack of an agreed expression for tension stiffening is a serious obstacle to the use of NLFEA. Tension stiffening is particularly significant in lightly reinforced elements and at low loads; that is, at service load, rather than at failure. Since bridge deck slabs designed using membrane action are very lightly reinforced, and since serviceability criteria are critical in their design, tension stiffening is particularly important to these. Also, unlike in most other structures, tension stiffening may still be important at higher loads because of its contribution to the restraint.

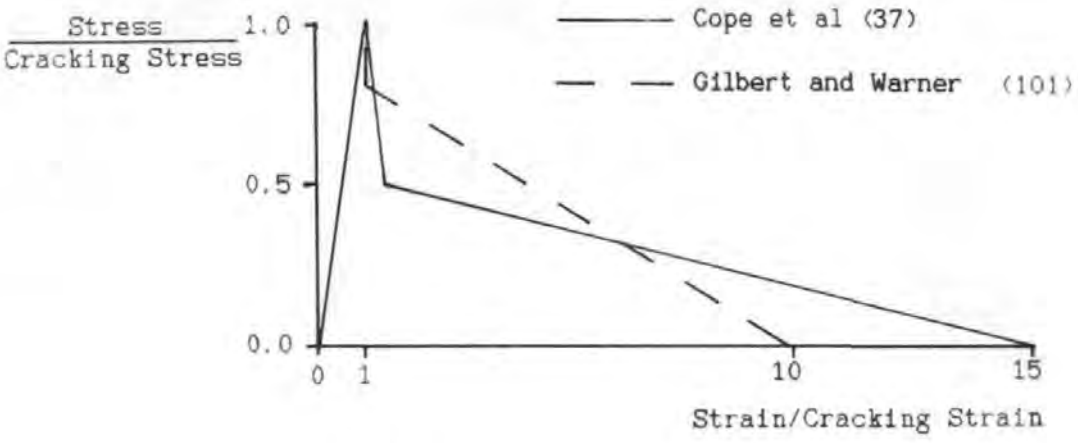

Figure 6.1: Tension stiffening functions

The tension stiffening functions used in non-linear analyses are purely empirical. Many such relationships have been used, two of which are illustrated in Figure 6.1. The dependence of an apparently rigorous fundamental analytical method, NLFEA, on a totally empirical tension stiffening function appears to be a major weakness. Admittedly, all analytical methods depend ultimately on empirically derived material properties. However tension stiffening differs from, for example, the tensile strength of reinforcement in not being a fundamental material property. It is a property of the composite material, reinforced concrete, or even of the structure, not of the concrete or reinforcement. It was therefore decided to investigate this subject at a slightly more fundamental level than is justified by the relatively simple analytical

method subsequently adopted in Chapter 7. The tests reported in this Chapter were also used to calibrate the analysis used in Chapters 7 and 9 as well as to investigate the effect of scale in the half scale models considered in Chapter 8.

6.2 THEORY

6.2.1 Mechanisms

The tension stiffening functions used in non-linear analysis represent stress which is transmitted to the concrete between cracks by two, or perhaps three, mechanisms. The first of these is the bond between reinforcement and concrete. This enables some of the force, which is carried across the cracks by the reinforcement, to transfer to the concrete between the cracks. The second mechanism, which only applies to sections in flexure, is the shear connection between the compression zone and the teeth of concrete between the cracks. The third mechanism which affects tension stiffening is the ductility of concrete in tension. Marthe(102) has shown that even when the strain exceeds that at which the peak stress is developed and cracks have started to form, concrete can transmit significant tension. However the effect is often ignored, which may be justified as the stress is only significant over a narrow range of smeared strains.

Consideration of these mechanisms might suggest that a particular empirical expression for tension stiffening stress would only be valid in a narrow range of circumstances. The bond contribution, for example, might be expected to be sensitive to the bond characteristics, size, quantity and orientation (relative to the cracks) of the reinforcement. In practice, however, many non-linear analysts have obtained satisfactory results using the same function in a wide range of circumstances. An explanation for this apparent paradox can be obtained by considering the way cracks develop in a region of constant moment or constant direct stress.

Prior to the formation of the first crack, the bulk of the load is taken by the concrete (Figure 6.2a). As the stress approaches the effective tensile strength of the concrete, f_{ct}, a crack forms at the weakest point. Here most of the stress is transferred to the steel but beyond a distance, S_o, the stress is unaffected (Figure 6.2b). A further increase in load will cause another crack to form. This cannot occur within S_o of the first crack because the stress is too low. Finally, when all the cracks have

formed (Figure 6.2c), no two adjacent cracks will be more than $2S_o$ apart because otherwise there would be a section between them subjected to a stress in excess of f_{ct}. Beeby(34) has shown that the average crack spacing becomes $1.3S_o$.

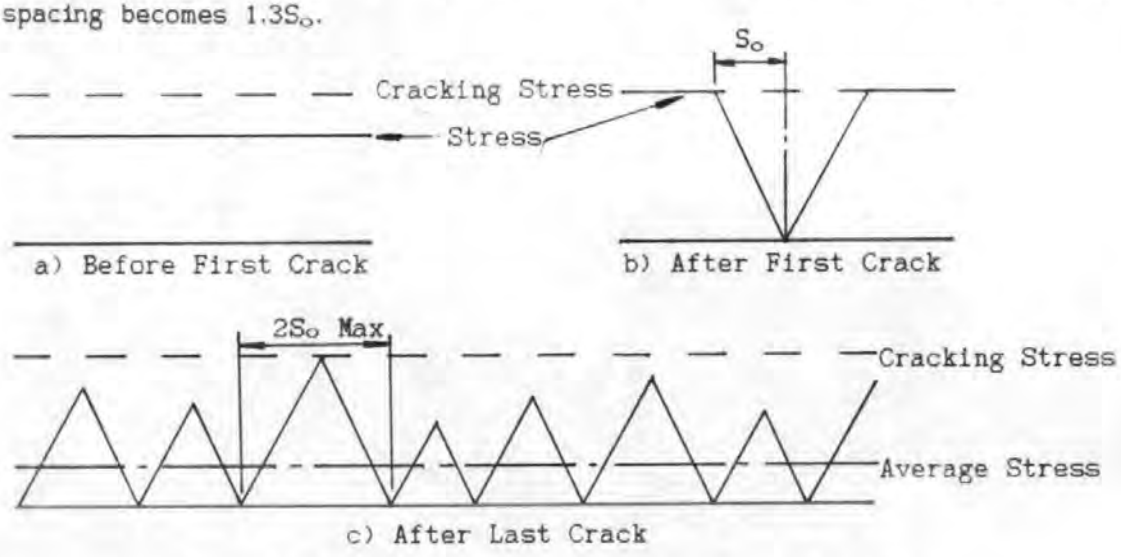

Figure 6.2: Stresses in concrete as cracks develop

This description implies that *anything* which improves the transfer of stress to the concrete on either side of the cracks reduces the final crack spacing. It thus reduces the wavelength of the stress distribution shown in Figure 6.2c, but has no effect on either the amplitude or the average value, which is the stress used in smeared crack analysis.

The above description can be used to obtain an estimate for the tension stiffening when all the cracks have first formed. To do this it is necessary to assume a shape for the stress distribution between the cracks. Vetter(103), in an analysis intended for a different purpose, assumed that the concrete stress increased linearly either side of the crack. He also assumed that the rate of increase of stress either side of the crack was unaffected by the formation of further cracks. From this he deduced that the average stress was approximately $0.5f_{ct}$. However, this was based on the incorrect assumption that the average crack spacing was $2.0S_o$. Using Beeby's crack spacing of $1.3S_o$ the average concrete stress becomes $0.33S_o$.

It has often been assumed that a further increase in strain reduces the tension stiffening stress but it is not clear why it should. For example, where bond is the dominant mechanism, the assumption appears to be inconsistent with the usual design assumption that bond strength is

independent of strain up to at least the yield strain of the reinforcement. It may be argued, therefore, that the smeared stress in the concrete should remain constant after cracking. This assumption is used in some code of practice formulae(104) and is supported by some researchers including Hartl(105).

6.2.2 Steel Stress

An unfortunate consequence of smearing the concrete strain is that the steel strain is also smeared. This means that the peak steel strain, which occurs at the cracks, is not modelled so the load at which the reinforcement yields is over-estimated. This has not previously been a serious problem because the tension stiffening functions used have meant that the effect became insignificant well before the reinforcement became non-linear. If, however, a constant tension stiffening stress were used, as suggested in 6.2.1, the problem would become more serious. Cervenka(106) avoided this by calculating the steel strain independently, ignoring tension stiffening. This approach introduces the reverse error; that is, it is assumed that all the steel is subjected to the strain which only really occurs at the crack position and thus the non-linearity is over-estimated. It appears that it would be more correct to use some form of averaging process between the strains (or stresses) calculated with, and without, allowing for tension stiffening. However, this would be even more inconvenient than Cervenka's approach.

Because of these problems, an analysis using one of the tension stiffening functions shown in Figure 6.1 could give better results than an analysis using a constant tension stiffening stress, even if the constant stress is more representative of the real behaviour of the concrete. This, and the tendency of researchers to concentrate on behaviour at high loads, could explain the preference for the type of tension stiffening function shown in Figure 6.1.

6.2.3 Mesh Dependence

The formation of a crack affects the stress over a distance which is related to the final crack spacing, but in a finite element analysis it affects the stress over a distance which is related to the element size. Because of this it has been suggested that the tension stiffening function should be varied with the element size so that the energy released by a crack is independent of the mesh. However, this was not done in the

analysis considered here and it was found that the results were entirely independent of mesh size. This was because only regions of constant moment or constant direct tension were considered so all the elements cracked simultaneously, unless a variable tensile strength was used. Thus, when a fine element mesh was used, the resulting under-estimate of the energy released at the position of the real cracks was compensated for by the over-estimate of the energy released elsewhere. Consideration of this behaviour shows that this would not occur in a region of varying moment. Ideally, therefore, the tension stiffening stress should be varied both with element size and with the stress state in the adjacent elements. This would be very difficult to do in a general solution procedure so it is fortunate that experience shows that, unless the mesh size is small compared with the crack spacing, a constant function can be used. In view of the variability of tensile strength and tension stiffening, the additional accuracy obtained from a finer mesh would have no real significance. The problem does, however, prevent the use of smeared crack analysis in the study of behaviour which is very local compared with crack spacing.

6.2.4 Cyclic Loading

The contribution of tension stiffening tends to reduce under repeated loading. Indeed the crack width clauses in BS 5400 assume it reduces to zero. Cope and Rao(107) modelled the reduction by reducing the length of the tail of their tension stiffening function, leaving the value of the tensile strength unchanged. This approach cannot be used with the constant tension stiffening stress suggested in 6.2.1. It implies that cyclic loads reduce the tension stiffening stress but do not cause any new cracks. However, it is known that concrete is susceptible to fatigue failures in tension, indeed the conventional design methods for concrete pavement(108) are based on quite well established fatigue relationships. Thus an alternative way of modelling the effect of cyclic loads on tension stiffening would be to reduce the tensile strength used in the tension stiffening expression but to leave the form of the expression unchanged.

6.2.5 Unloading

The bulk of research into both tension stiffening and NLFEA has concentrated on monotonically increasing loading. This means that the tension stiffening functions assume that the tensile strain currently being

experienced is the greatest the concrete has ever experienced. In a complex non-linear structure, this assumption may not be valid even when the structure itself is experiencing a monotonically increasing load. More importantly, for reasons discussed in 5.4.2b, it is not reasonable to consider only monotonically increasing loads in the type of structure considered in this study.

Once concrete has cracked, it never re-acquires its tensile strength. Thus the tensile properties of cracked concrete are not reversible; a separate unloading curve is needed. It seems reasonable that once the crack has fully closed the compressive stiffness of the concrete will be largely unaffected by the crack. It remains only to decide the stress required to close a crack and the amount of strain, if any, which becomes permanent. Although, in reality, the unloading curve may have a complex shape the other errors in the analysis and variability in the behaviour mean that the use of such a function cannot be justified. A simple bi-linear relationship will be used. Unfortunately, at present the values to be used in this relationship can only be obtained empirically.

A variety of expressions have been used. Some researchers, such as Bazant(97), have used a straight line to the origin implying that the cracks close completely at zero stress. At the other extreme, Crisfield(95) used a straight line parallel to the initial, linear, part of the stress-strain curve, implying that the cracks do not close at all. This seems extremely unlikely, particularly if the cracks are wide. Cope(96) used the more reasonable assumption that only the strain corresponding to that at which the concrete first cracks becomes permanent. The wide range of these expressions indicates the lack of data. However many structures, because of relatively heavy reinforcement, or only monotonic loading, are insensitive to the assumptions.

6.3 ANALYSIS OF PREVIOUS TESTS

6.3.1 Direct Tension Tests

Some analysts have derived their tension stiffening functions by obtaining the best fit to the load-displacement response of quite complex structures. This approach is not very satisfactory because tension stiffening is only one of many factors which affect the response. Thus tension stiffening functions are liable to become "fiddle factors" which compensate for a wide variety of errors in the analysis. A better

approach, which has been used by Cope et al(37), is to test simple statically determinate beams with long constant-moment regions. Even with these specimens, however, it is possible to obtain very similar load-displacement relationships with different tension stiffening functions. Only tests which subject the whole specimen to the same smeared strain, that is direct tension tests, give unambiguous results. Unfortunately, because there are theoretical reasons for believing that tension stiffening could be different in flexure and direct tension, direct tension tests cannot be used as the sole basis for deriving tension stiffening functions. However they do give some useful information.

Williams(109) has tested a series of fifteen large slabs in direct tension. The response was approximately linear until the first crack appeared. This occurred at a stress of 0.5 to 0.7 times the tensile strength of the concrete as measured by the split cylinder test. This difference between the effective tensile strength and the split cylinder strength is partly due to the random variation of the tensile strength of concrete; cylinders are constrained to fail on a pre-defined plane whilst a slab is free to crack at its weakest section. Statistical analysis suggested, however, that this alone could not explain the difference. The remainder was presumably due to restrained differential strains which had a greater effect on the slabs than on the cylinders. A restrained strain equal to only some 5% of the total likely shrinkage is sufficient to explain the difference so it could be due to differential shrinkage across the section.

After the first crack appeared, the extension increased rapidly with a relatively slow increase in load. However, tension stiffening remained significant even at a load such that the steel behaviour was non-linear. All the tension stiffening functions previously used by non-linear analysts under-estimate this effect; indeed most (including both of those shown in Figure 6.1) have no effect at all on the results of an analysis performed under load control, as can be seen from Figure 6.3.

The specimens were re-analysed using a constant tension stiffening stress as suggested in 6.2.1. This analysis under-estimated the load in the slabs at extensions just above that required to cause the first crack. This could suggest that the stress between existing cracks was higher at low strains but it seems more likely that it was because of the variation of the tensile strength of the concrete; that is, because not all the cracks

developed at the same load. To investigate this, the computer model was split into several equal elements and these were given a normal distribution of tensile strengths. The number of elements used was ten, which was approximately the final number of major cracks. This approach implicitly assumes that the strengths of the ten elements are independent variables, which is not strictly correct, but it does give a good indication of the effect of concrete variability.

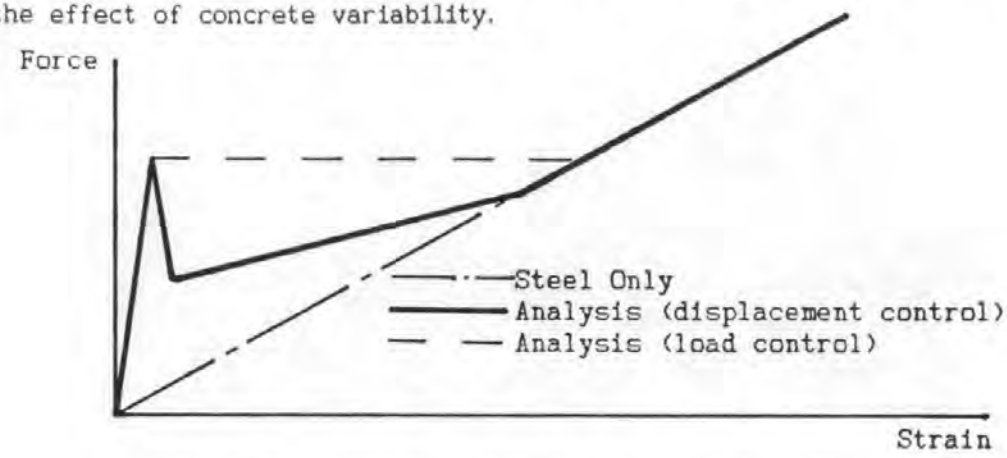

Figure 6.3: Effect of tension stiffening on analysis in direct tension

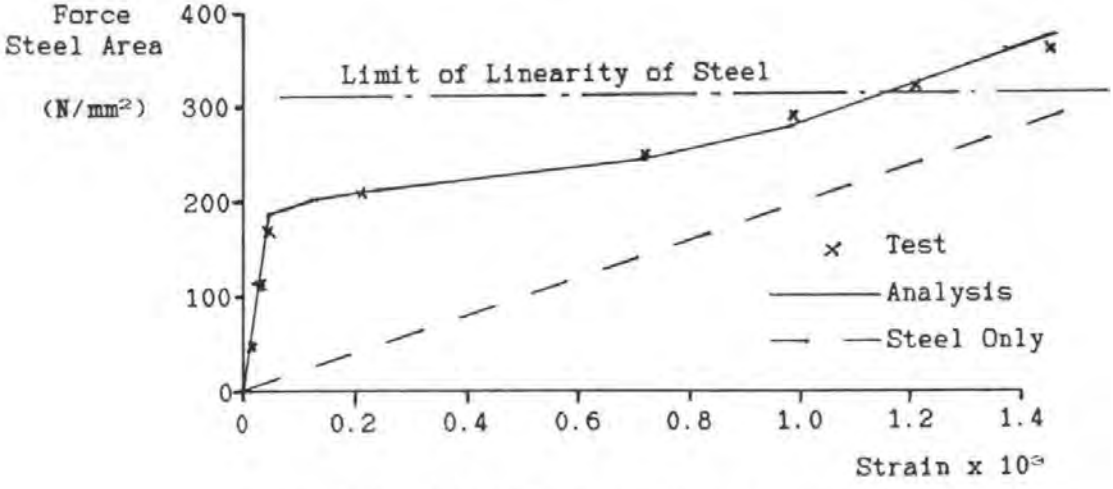

Figure 6.4: Analysis of Williams' Specimen 1
(1% steel)

Analysis with a coefficient of variation equal to that obtained for the split cylinder tests (10%) gave results such as those shown in Figure 6.4. To obtain this excellent relationship, however, the average tensile strength used in the analyses had to be adjusted for each specimen. In the more normal situation, where this cannot be done, the best estimate for the effective average tensile strength of the concrete would be approximately 0.8 times the split cylinder strength. The actual range used

was 0.7 to 0.9. The effect of small errors in the value used for the effective tensile strength of concrete is large compared with the difference between the analysis and test results shown in Figure 6.4 so there is no practical advantage in making further refinement to the tension stiffening function.

Although a coefficient of variation of 10% gave good predictions for the load displacement response, a higher variation and a skewed distribution of strengths were needed to make the analysis model the actual development of the cracks. Analyses which did this exaggerated the rate of decay of tension stiffening with increasing strain. In the tests, new cracks developed with no discernible effect on tension stiffening. This seems to suggest that the stress in the concrete between cracks, even cracks which are within $2S_o$ of each other, increases with strain. This gives further confirmation of the suggestion in 6.2.1 that the tension stiffening effect does not reduce with strain. It is the development of new cracks which causes the apparent decay.

Hartl(105) has also concluded that the tension stiffening stress in direct tension remains constant once the concrete has cracked. He said his tests suggested a tension stiffening stress of 0.4 f_{ct}. However, because he did not consider concrete variability in his analysis, this conclusion is closer to the Author's than it may at first appear. In effect, Hartl concluded that the *average* tension stiffening stress is 40% of the *initial* cracking stress. The Author has concluded that the *average* tension stiffening stress is approximately 30% of the *average* cracking stress. For the analysis considered here this comes to over 35% of the initial cracking stress. In view of the other variables in the analysis this is remarkably close.

6.3.2 Flexural Tests

Clark and Spiers(110) have tested a series of beams and slabs with long constant-moment regions. As it was these tests which were used to develop Cope's tension stiffening function(37), it is not surprising that his function gives a good fit to the results. However, it was decided to re-analyse some of the specimens using the constant tension stiffening function suggested in 6.3.1. The only concession made to the difference between direct tension and bending was to increase the effective tensile strength from 0.8 to 1.0 times the cylinder strength. Predictions using

the two tension stiffening functions are compared with the results of one of Clark's tests in Figure 6.5.

Cope's function appears to give a better fit to the results but it is not possible to tell conclusively from Clark's results which function is more realistic.

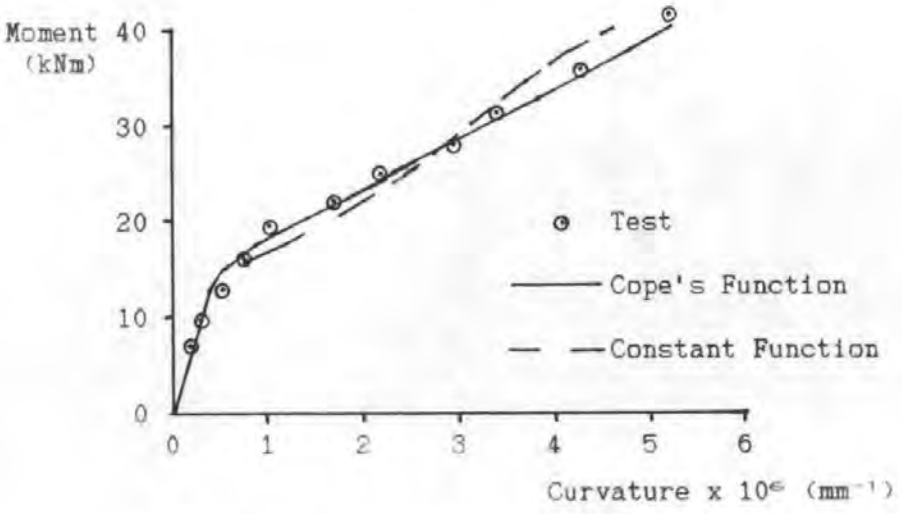

Figure 6.5: Analysis of Clark's Beam 4

6.4 TESTS

6.4.1 Design of Specimens

Because the tests would serve to calibrate the analysis and to investigate the effect of scale for the model bridge tests which will be considered in Chapter 8, it was desirable to make the test specimens as similar as possible to a strip of the proposed slab. It was also desirable to perform identical tests at full and half size. In order to facilitate the cyclic loading of the specimens they were designed so that the full size specimens would fit into a Mayes testing machine. This left very little choice in the design of the specimen which is illustrated in Figure 6.6.

The specimens, like the deck slabs considered in this thesis, were very lightly reinforced which made tension stiffening more significant to their behaviour. They were provided with 0.49% reinforcement. This compares with Clark's most lightly reinforced specimen which had 0.44%. However, as is conventional, this percentage is calculated from A_s/bd. A better indication of the significance of tension stiffening is given by the ratio of uncracked to cracked stiffness. This is a function of $bh^3E_c/A_sE_sd^2$. According to this relationship, the specimens were some 40% more lightly reinforced than any of Clark's. Some slabs used in practice are, however,

more lightly reinforced still, particularly in the secondary direction. Consideration was given to testing more lightly reinforced specimens. It appeared, however, that they would not crack until normal service loads were exceeded so little use could be made of the results.

A single specimen was tested with a higher reinforcement area, more typical of the reinforcement used in current practice, to see if the expression derived from the lightly reinforced specimen was applicable to these.

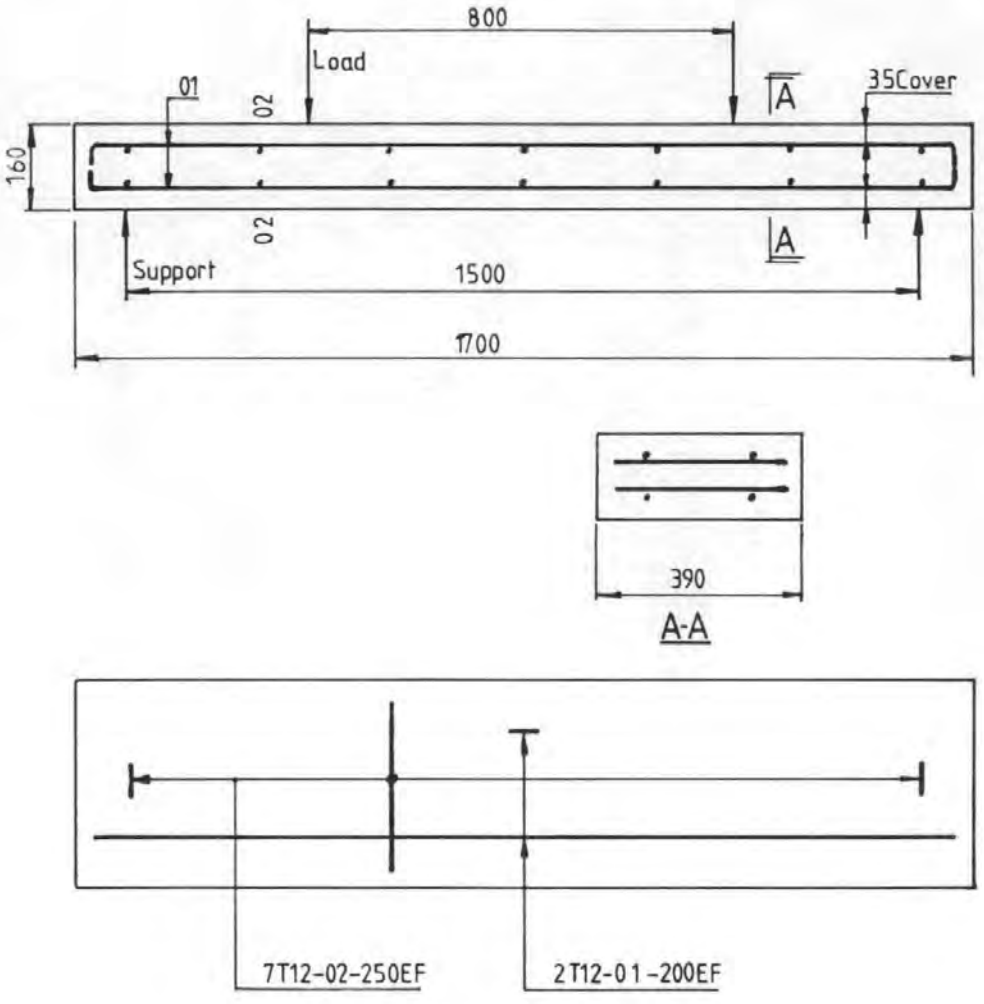

Figure 6.6: Detail of test specimens
(dimensions are for full size specimen)

6.4.2 Loading Rig

All the specimens were tested in the Mayes machine simply supported under two point loading as illustrated in Figure 6.6. A specimen is illustrated under test in Figure 6.7. Consideration was given to applying known in-

plane restraint to the specimens to make the results more directly applicable to membrane action. However, analysis suggested that the results would then be extremely sensitive to the stiffness of the restraint and it was not possible to control this well enough to obtain useful results.

All the tests were performed under load control. Theoretically, more information could have been obtained from tests performed under displacement control. However, the test rig was not stiff enough to achieve true displacement control.

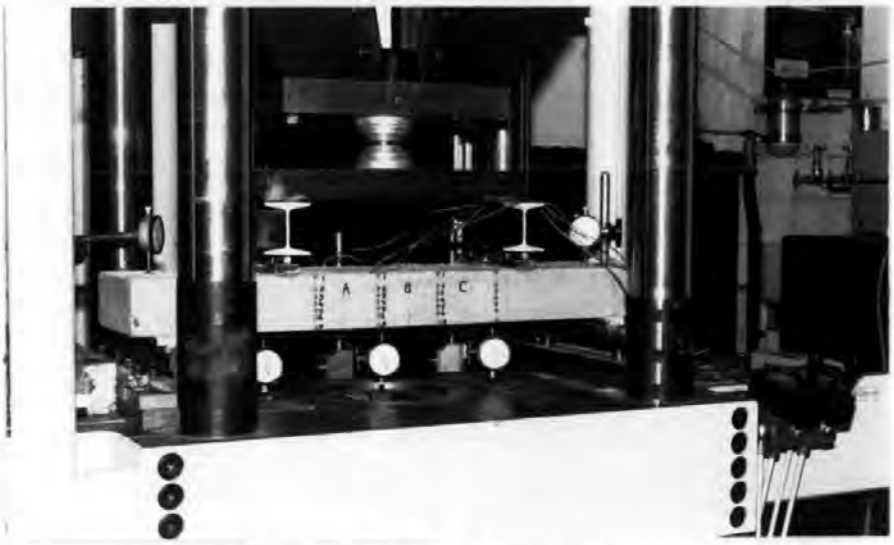

Figure 6.7: Half size specimen under test

6.4.3 Materials

a. Reinforcement

The reinforcement used was GKN "Tor Bar" obtained from normal commercial sources in the required sizes; 6mm and 12mm for the main tests and 16mm for the more heavily reinforced specimen.

A stress-strain curve was obtained for samples of the bar using the same Mayes machine which was used for the tests.

b. Concrete

The mix used for the full scale specimens was intended to be representative of normal practice for bridge deck slabs and to give a strength close to the nominal design strength. These objectives proved to be mutually exclusive; a mix which complied with the minimum cement content normally specified and which had a reasonable workability always

produced significantly more than the nominal strength. The exact mix proportions were varied between specimens as an attempt was made to get closer to the desired results, but a typical mix is detailed in Table 6.1.

Material	Quantity (per nominal m^3)	
	Full Size	Half Size
10-20mm Thames Valley Gravel	780kg	-
5-10mm Thames Valley Gravel	390kg	995kg
Sand (Thames Valley, zone 2 grading)	610kg	726kg
Ordinary Portland Cement	325kg	365kg
Water	≈190l	≈210l

Table 6.1: Typical mixes

The mix used for the half scale tests was intended to be as close as practical to a half scale model of the mix used for the full scale tests. A 10mm maximum size aggregate was used and the proportion of fines was increased to get close to the scaled grading curve. Because of the greater surface area of aggregate in the finer mix, a higher cement content was needed. The water cement ratio was also increased so that the strength, particularly the tensile strength, would be no higher than for the full scale specimens. A typical mix is detailed in Table 6.1. As with the full size mix, modifications were made over the course of the test sequence. However, in order to ensure that this did not affect the relationship between the full and half size mixes, the same modifications were made to both mixes.

The small size of the specimens meant that it would have been practical to mix the concrete in the laboratory using dried aggregate. However, because it was intended to use the tests to develop a mix design for the model bridge tests for which this would not be practical, it was decided to use the same 0.25 cubic metre pan mixer and batching plant which would be used for the model bridge tests.

Cube tests and split cylinder tests for all the mixes were performed using 150mm cubes and 150mm diameter cylinders. Some 150mm diameter cylinders were also tested for Young's modulus in the Mayes machine. All the cubes

and cylinders were cured with the test specimens, under plastic for seven days and then in the laboratory.

The split cylinder tests suggested that the tensile strength of the full and half size mixes were similar. The mean tensile strength of the full size mixes at test age (approximately 28 days) was 3.30N/mm^2 compared with 3.14 for the half sized mixes. Theoretically, it is more correct to compare results for the full size mix tested with 150mm diameter cylinders with results for the half size mix tested with 75mm cylinders. However, since no 75mm cylinder moulds were available, this was not done. Instead, some 100mm cylinders from the full size mix and some 50mm cylinders from the half size mix were tested. The mean results from these tests were 3.94 and 3.49N/mm^2 respectively. Thus, changing from 150 to 100mm specimens for the full size mix gave a 19% higher strength whilst changing from 150 to 50mm with the half size mix gave only an 11% increase. Interpolating between the results for the 150 and 50mm cylinders suggested that the strength of the half size mix measured using 75mm cylinders would be 3.36N/mm^2; 2% higher than the measured strength of the full size mix. The real significance of these results is that they indicate that both the scale effect and the difference between the two mixes were small compared with the random variation in the results.

The compressive strength of the full and half size mixes were also similar to each other but the latter did tend to be slightly lower. Typical figures (actually those for the first pair of specimens and for the mix detailed in Table 6.1) were 54.7N/mm^2 for the full size mix and 47.0 for the half size, both measured with 150mm cubes. Using half size cubes increased the latter to 48.4N/mm^2.

6.4.4 Loading

The first pair of specimens, one full size and one half size, were loaded to a load corresponding to the maximum service moment which BS 5400 would allow. Next, they were subjected to many cycles of a lower load (55% of the first load) corresponding to the maximum HA equivalent load in BS 5400, that is 25 units of HB in a bridge designed for 45 units. However, the number of cycles (over 100,000) and the intensity of the load were deliberately excessive. It was hoped to use the test to justify using a much smaller number of cycles in the model bridge tests. After

the cyclic loads had been completed the specimens were loaded to full service load, unloaded, then loaded to failure.

The second pair of specimens were treated in the same way except that they were first loaded to only the reduced, 55%, load.

The third full size specimen was treated in the same way as the second, except that it was tested upside down to see if this altered the results.

When the third half size specimen was tested, an unloading expression had been developed which gave reasonable results. It was realised, however, that these results were not affected by the stress which was assumed to exist in cracked concrete which was subsequently compressed. It was desirable, therefore, to test a specimen under reversed moment but the apparatus did not enable this to be done. The solution adopted was to load the specimen in the same way as the first but to turn it over after 10,000 cycles and start the test again. It was considered that only the half size specimens could reliably be tested in this way because the dead weight stress involved in turning over the full size specimen would be too great.

The more heavily reinforced specimen was treated in the same way as the first specimen, the loads being increased to allow for the extra reinforcement.

6.4.5 Processing of Results

Three columns of "demec" points were fixed to one side of the constant moment regions. The strain was averaged over the three demec readings in a row and then a linear regression over the rows was performed to give an average curvature and extension. The curvature was also estimated from deflection readings taken from rows of dial gauges. These curvatures differed, typically by 10% but sometimes by as much as 30%. The curvature estimated from a row of dials along the edge of the slab on the side to which the demec studs were attached (that is the three dial gauges nearest the camera in Figure 6.7), was only marginally closer than that estimated from a row at the longitudinal centre-line or on the far side of the slab. It was therefore concluded that the discrepancy was due to variation in curvature over the length of the constant moment region, rather than over the width of the slab. Since the analysis assumes a constant curvature and the regression gives a true average curvature,

whereas the curvature estimated from the deflection readings is weighted towards the curvature at the mid-span of the slab, it was decided to use the demec readings in preference to the dials. The discrepancy does, however, give an indication of the relatively low accuracy which can be expected in the analysis of tension stiffening.

The regression analysis calculated the deviation of the strain readings from the straight line. The root mean square deviations varied between specimens from less than 1% of the maximum strain to over 20%. The former figure indicated that, on average over the gauge length, plane sections had remained plane (as the theory assumes) whilst the latter indicated that they had not. The difference is due to the random nature of the cracking and the fact that the constant moment region was only long enough to accommodate some three main cracks. The best fit was obtained in specimens for which both ends of the gauge length happened to be mid-way between cracks, giving the theoretically desirable exact integer number of cracks. The worst fit occurred in a specimen in which a sloping crack crossed the end of the gauge length. This problem could be reduced by using a longer constant moment region. However, because of the effect of variability of concrete tensile strength, this would give a misleading impression of the shape of the tension stiffening function.

The main reinforcement in most of the specimens was also provided with electrical resistance strain gauges. This provided some useful information but the short gauge length meant that the results were not directly applicable to smeared crack analysis and the gauges were not fitted to the final specimen.

6.4.6 Results and Analysis

a. First Loading

All the tests were analysed using a non-linear program. Because the specimens were essentially beams, in that they were subjected to a constant moment over their width and they were not wide enough to be forced to bend cylindrically (rather than anti-clastically) it was convenient to use beam elements for the analysis. The program used will be described in Chapter 7.

The results of three of the tests are shown in Figures 6.8 to 6.10 along with the results of analyses using the tension stiffening function which

was eventually adopted and which is illustrated in Figure 6.12. To facilitate direct comparison between the figures, the results of the half size tests are expressed as equivalent results at full size.

The experimental results were initially compared with the analytical predictions obtained using a variety of tension stiffening functions. Because of the low steel area, and because the predictions for both the curvature and for the axial extension at mid-depth were considered, this gave a better indication of the shape of the tension stiffening function than previous tests. However, it was still not possible to obtain totally unambiguous results. Both Cope's function and that proposed in 6.2.1 gave reasonably good predictions. A close study of the results suggested, however, that immediately after cracking the true tension stiffening stress was higher than suggested by either function. At high strains (apparently up to and above yield) it appeared to be around 0.1 to $0.2f_{ct}$. An explanation for this behaviour, and its apparent difference from the behaviour in direct tension, is proposed.

When the peak concrete stress is reached in direct tension, a crack forms and the load reduces. A significant increase in extension is needed to get back to the load which caused the crack and no new cracks can form until this has happened. If the specimen was held at an extension just above that at which the peak concrete stress was developed, there would be a significant tensile stress in the concrete even at the sections where the cracks were forming. However, this stress has no effect on the results of a test unless it is performed under true displacement control, which requires a very stiff testing rig.

In a section in flexure, in contrast, there is always a region near the top of a crack where there is a significant tensile stress due to the ductility of concrete. This gives the observed higher tension stiffening stress at lower strains. It also increases the stress in the concrete on either side of cracks and, as we saw in 6.2.1, this reduces the crack spacing. Paradoxically this means that when the strain subsequently increases, and the stress at the cracks reduces to zero, the tension stiffening stress is lower than it would have been without the ductility of concrete in tension. This explains why, at high strains, the tension stiffening stress is lower in flexure than in direct tension.

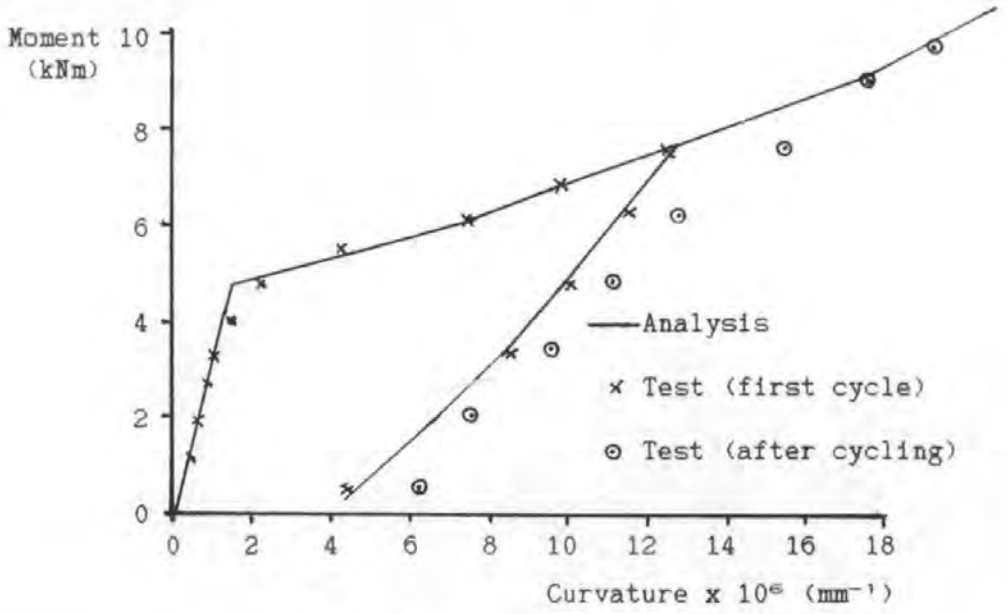

Figure 6.8: Results of first full size test

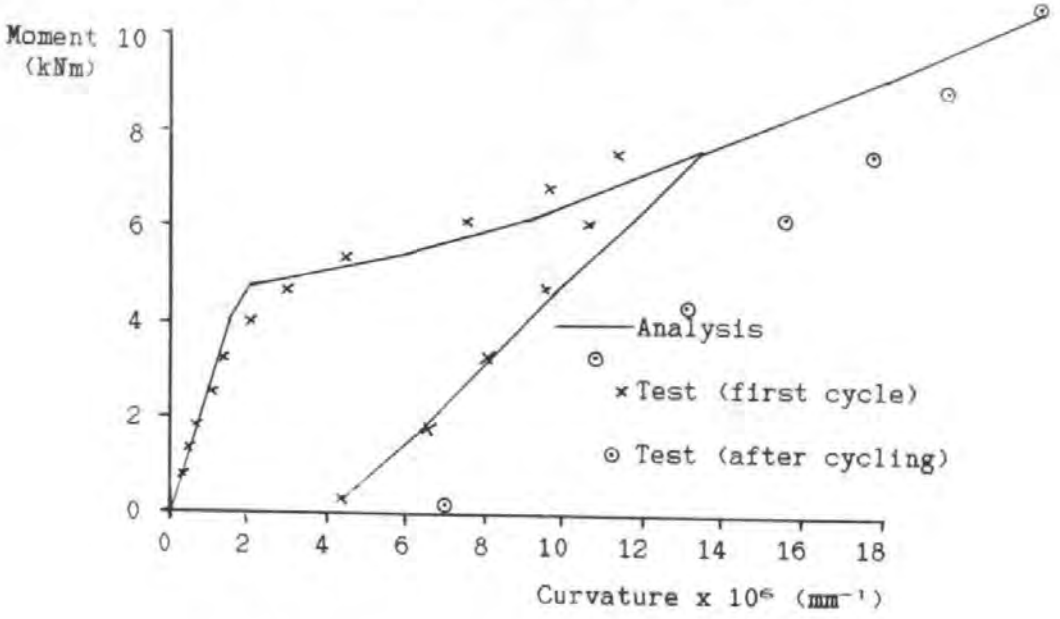

Figure 6.9: Results of first half size test

Theoretically, this effect should be more pronounced where the crack spacing is controlled by the depth of concrete in tension, rather than by the reinforcement. According to Beeby's theory(34), this means it will be more pronounced where the reinforcement is widely spaced. Thus it appears that the tension stiffening stress at high strains should reduce as the bar spacing increases. This has been observed by Clark and Cranston(111), further confirming the theory.

The ductility of concrete in tension also explains why the drop in stiffness visible in Figures 6.8 to 6.10 when the concrete first cracks is far less abrupt than analysis using any normal tension stiffening function suggests. This might have been partly explained by the variability of concrete which means that not all the cracks formed at once. However, analysis using an approach similar to that considered in 6.3.1 showed that this explanation was not sufficient.

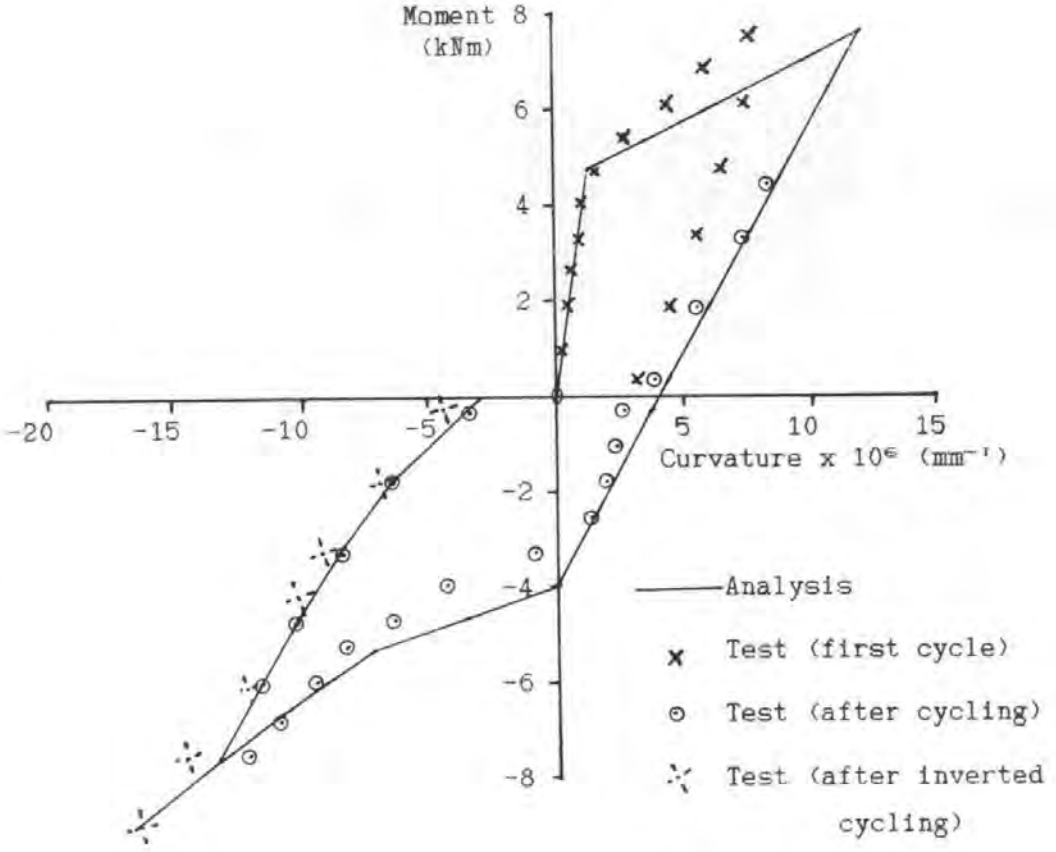

Figure 6.10: Results of third half size test

The first visible crack did not appear in the half scale specimens until the strain was significantly greater than in the full scale specimens; approximately 300 microstrain compared with 200. However, there was not a corresponding difference in the effective tensile strength. Both the full and half size specimens exhibited significant non-linearity before the cracks became visible but this was more pronounced with the half scale specimens. It was considered that this might have arisen solely because the cracks in the half scale specimens were half as wide and so did not become visible until their scale size was greater. To eliminate this possibility, the later half scale specimens were inspected thoroughly for

cracks using a magnifying glass and a crack microscope, whilst the full scale ones were inspected only with the naked eye. This did not alter the conclusion.

The results suggested that the half scale tests would give a reasonably good indication of the load-displacement relationship, and hence of the stresses, in a full scale specimen. They also suggested that the same tension stiffening function could be used at full and at half size. However, the most obvious fault of the analysis, its tendency to exaggerate the abruptness of the loss of stiffness as the concrete cracks, is greater with the half scale model. The results also suggest that the use of a half size model to predict the behaviour of a full size bridge is liable to over-estimate the load at which cracking first appears.

The non-linearity observed before the cracks could be seen suggested that both moment re-distribution and compressive membrane action could start to act before cracks become visible. Thus compressive membrane action should delay the formation of the first visible crack. This has been observed by both Guyon(10) and Kirkpatrick(49). However, it now seems likely that Guyon's specimen, being a small scale model, exaggerated the effect. Similarly Kirkpatrick's slab, being only 160mm thick, would have shown a more pronounced effect than a thicker slab.

Another implication of this non-linearity before cracking is that, in an analysis which ignores the effect, reinforcement could significantly affect the apparent tensile strength. This is confirmed by the fact that the best fit to the results for the lightly reinforced specimens was obtained using an effective tensile strength of approximately 0.8 times the split cylinder strength whilst, for the more heavily reinforced specimen and for Clark's tests, the full split cylinder strength gave better results.

These effects could be modelled by including some non-linearity before cracking in the analysis. It was found, however, that if sufficient non-linearity was included to model these effects, the non-linearity in the moment-curvature response prior to cracking was greatly exaggerated. The explanation for this is that the non-linearity was due to local micro-cracking which had little effect on the strain averaged over a long gauge length.

The best interpretation of the results seemed to be that the tension stiffening function should have the form shown in Figure 6.11. This is essentially a constant tension stiffening function with an expression for the tensile stress transmitted across the crack added on. Theoretically, the latter stress is a function of the width of the crack. This implies that, when it is expressed as a function of strain, it should be affected by crack spacing. However, the variability of the results and the narrow range of crack spacing in the specimens made it impossible to detect this trend.

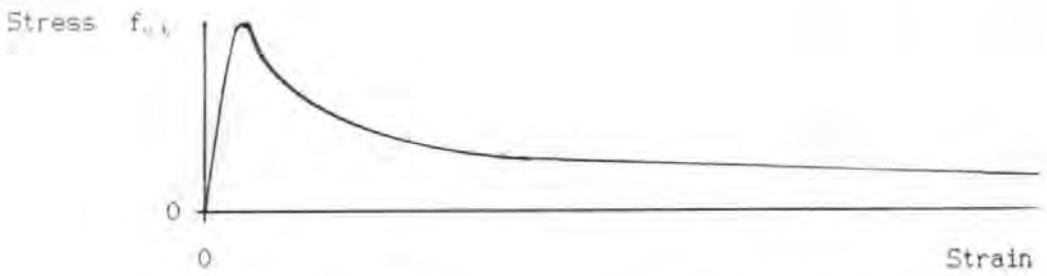

Figure 6.11: Ideal tension stiffening function

Because the stress reduces significantly on cracking, and because the subsequent stress is taken to be a function of the initial cracking stress, the predicted response is very sensitive to the assumed tensile strength. Small changes in the tensile strength have a much greater effect on the results than quite large changes in the assumed shape of the tension stiffening function. This, combined with the problem of steel stress considered in 6.2.2, encourages the continued use of tension stiffening functions of the type shown in Figure 6.1. Even with these, tension stiffening stress in concrete between the neutral axis and the reinforcement could delay the yielding of the reinforcement but, fortunately, the effect is not significant in realistic cases.

For the present study, therefore, it was decided to use the function shown in Figure 6.12. This is essentially a compromise between the constant function suggested in 6.2.1 and the type of function shown in Figure 6.1 and it was found to give marginally better results than either. In most cases, the results could be improved further by stopping the reduction in stress at approximately 0.1 f_{ct} rather than at zero but, because of the risk of artificially delaying reinforcement yielding, this was not done.

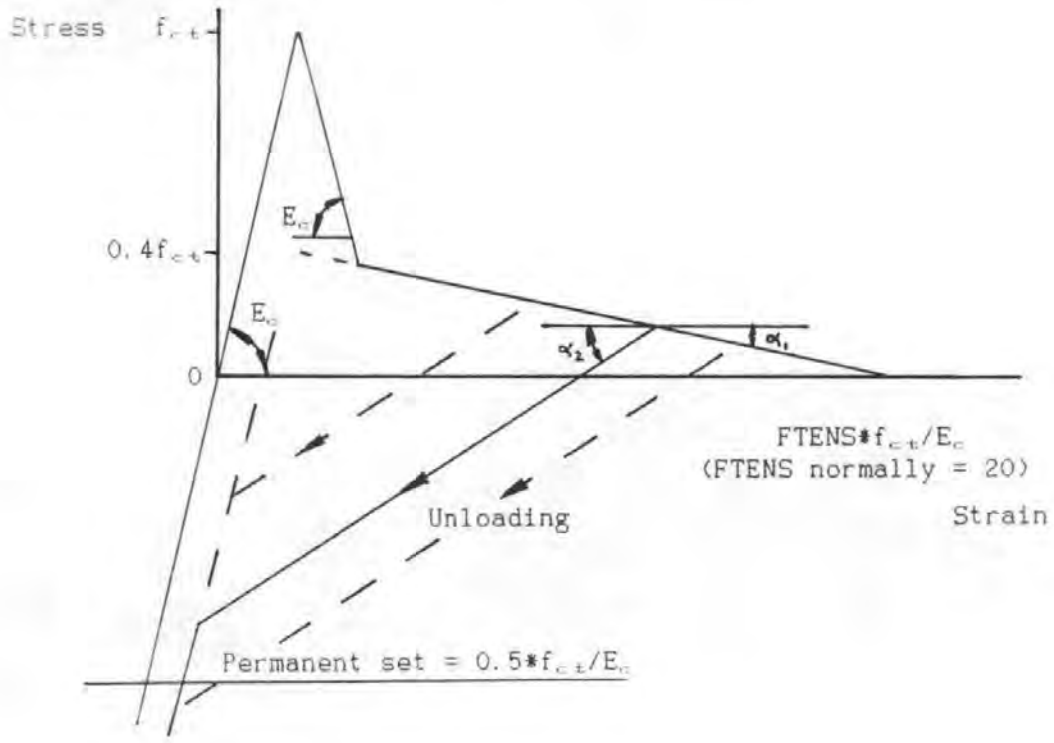

Figure 6.12: Tension stiffening function adopted

In any particular test, the results can be improved by minor adjustments to the tension stiffening function but the behaviour is too variable to justify this. An indication of the lack of repeatability of the tests is given by comparing the maximum curvature on first loading in Figures 6.9 and 6.10. The curvature of two nominally identical specimens subjected to identical loads differed by 47%, even though their measured material properties and dimensions were almost identical.

The tension stiffening expression derived for the lightly reinforced specimens appeared to work equally well in the one more heavily reinforced specimen. However, because the behaviour of this was much less sensitive to tension stiffening, and because only one specimen was tested, this result was not conclusive.

b. Cyclic Loading

The effect of even 160,000 cycles to 55% of the peak load experienced was considered to be too small, compared with the other variables and errors in the analysis, to be worth including. As expected, the effect of the same load cycles on specimens which had not previously been subjected to a higher load was much greater. The static load used in this test was not

sufficient to produce a fully developed crack pattern and new cracks developed during the cyclic tests. This is as would be expected from fatigue theory. Analysis using a reduced tensile strength to allow for fatigue appeared to give good results but tests to a wide range of load cycle intensities would be needed to check this properly. It is also not entirely clear that the degradation was due to fatigue; it could have been largely due to creep since the tests were conducted under sinusoidal load variations which gave a mean moment some 55% of the maximum. However, since no long term static tests were performed, it was not possible to separate the effects of fatigue and creep.

A single cycle to a high stress had a much greater effect than many cycles to a lower stress. In terms of bridge deck design and analysis this suggests that it is reasonable to consider only the worst load cases, the HB load cases, in the stress history analysis and to ignore cyclic loads completely. This is fortunate as it means the stress history of a given point in the structure can, for practical purposes, be recorded by a single number; the maximum historic strain.

c. Unloading and Re-loading

There was a difference between the unloading and the re-loading path, as can be seen from Figures 6.8 to 6.10. However, it was decided that since this was small compared with either the effect of small changes in assumed f_{ct} or the difference between the first loading and unloading path, it was reasonable to ignore it. Thus the ability to store the relevant stress history as a single number was preserved. It should be noted, however, that this approach may not be valid in a dynamic analysis because the difference in the paths, the hysteresis loop, represents energy absorbed by the structure and contributes to the damping.

None of the unloading expressions previously used gave good results. Cope's for example (which was the best of them) under-estimated the curvature which remained when the load was removed; typically by a factor of three. Since these functions were based on data which was either very inadequate or derived from structures which, because of relatively heavy reinforcement, were not sensitive to the expression used, it was decided to ignore them completely. After trying various relationships that shown in Figure 6.12 was adopted, the slope of the unloading path being 3.5 times the slope of the tension stiffening function, that is α_2 equals 3.5α, in

Figure 6.12. This gave reasonably good results such as those shown in Figures 6.8 and 6.9.

A significant deformation remained after the load was removed. This implies that, when a load is applied which is small relative to the maximum previously applied load, the strains and deflections relative to the initial (unstressed) condition can be greater than predicted by a conventional elastic analysis which ignores the tensile strength of concrete. It was found that the deformations (both observed in the tests and predicted by the non-linear analysis) became equal to those predicted ignoring concrete in tension at a load which would correspond to 25 units of HB if the section was fully stressed under 45 units of HB. Since crack widths in BS 5400 are checked under a load of 25 units of HB, this implies that BS 5400 is justified in ignoring tension stiffening in crack calculations in bridges designed for 45 units of HB load even though significant tension stiffening was observed under full load after over a hundred thousand cycles of normal service load had been applied. However, in structures designed for lower HB loads, the assumption is conservative.

Unfortunately, the one specimen which was inverted during the tests was the only one which was sensitive to the amount of strain which was assumed to become permanent after unloading, which was taken to be $0.5f_{ct}/E_c$. The results for this specimen are shown in Figure 6.10 in which moments due to loads applied before the specimen was inverted are shown as positive. The biggest discrepancy in the unloading and re-loading part of the plot is that the analysis failed to predict the earlier initial cracking load under negative moments, that is in the inverted position. This earlier cracking appears to have been the result of the cracks formed by the previously applied positive moments acting as crack inducers since the new cracks all joined the previous cracks. There was no evidence of this earlier cracking in the one specimen which was tested inverted throughout.

d. Failure

On completion of the tests, all the specimens were loaded to failure and they all failed in flexure. The only unusual feature of the failure behaviour was that the low steel area combined with the low d/h ratio meant they did not reach peak load until the top steel yielded in tension. This was predicted by the analysis.

The tension stiffening function used implied that unloading and re-loading to the same load would have no effect on the deflections. In practice it did have some effect, as can be seen from Figure 6.8. However, when the loading was further increased the tension stiffening appeared to recover and the discrepancy was considered acceptable.

6.5 CONCLUSIONS

Because of its sensitivity to a highly variable quantity, the effective tensile strength of concrete, tension stiffening cannot be predicted accurately. However, the functions developed in this chapter appear to be significant improvements over those used in the past, particularly for unloading.

The studies of similar full and half size strips indicated that a half scale model will give a good indication of all aspects of behaviour except the load to produce the first visible crack. The same tension stiffening function can be used as at full size.

CHAPTER 7

A SIMPLER NON-LINEAR ANALYSIS

7.1 INTRODUCTION

Section 5.6 may give the impression that analysis for design is far more difficult than analysis for predicting the behaviour of laboratory specimens. However, designers have a major advantage; they have no need for *accurate* predictions, they need only *safe* predictions. Realistic predictions are desirable because they lead to more economical designs but errors which would be considered excessive to researchers are acceptable to designers, provided they act in the safe direction. Research on non-linear analysis has concentrated on obtaining accurate predictions for the load-displacement response of structures monotonically loaded to failure. From the point of view of the design of the type of structure considered here, this is unfortunate; neither deflection nor ultimate strength are critical design criteria, loads do not increase monotonically and "accuracy" is neither obtainable nor necessary. Indeed, according to both Batchelor(78) and Kirkpatrick(13), slabs with the minimum practical reinforcement have over three times the required ultimate strength. If this is true, an analysis which under-estimates strength by a factor of three is not merely adequate for predicting strength; it is as good as one which is accurate to 0.001%.

The analytical methods considered in Chapter 5 contrast sharply with those currently used in design and considered in Chapter 2. The former are sophisticated and expensive but potentially able to give realistic predictions based on realistic behaviour models even if, at the present state of the art, they are not totally reliable. The latter are cheap and simple but based on unrealistic models of behaviour. Their predictions are not as realistic as those of NLFEA but they are more reliable; they are always safe. In the extreme case of restrained slabs, the two forms of analysis may differ by factors of 5 or even 10 on strength. Clearly, therefore, some intermediate form of analysis (safer, cheaper, easier to understand and more compatible with codes of practice than those considered in Chapter 5 but more realistic than those considered in Chapter 2) would be useful. There is vast scope for making conservative simplifying assumptions compared with the analysis considered in Chapter 5, whilst still maintaining greater realism than the forms of analysis

considered in Chapter 2. This Chapter aims to develop such a form of analysis which could be used in design and assessment.

The Chapter also aims to develop a program which can be used for assessing simpler design methods, such as those considered in 3.2.8. The same program will be used as an analytical tool for investigating the behaviour of bridge decks, including the models which will be considered in Chapter 8. However, because of the fundamental difference between the *safe estimate* analysis needed for design and the *best estimate* analysis needed in research to facilitate direct comparisons with test results some details, including the material models, will differ.

7.2 GENERAL APPROACH

The analysis is essentially a simplification of the approach considered in Chapter 5; that is, it is a non-linear analysis using the smeared crack, distributed steel approach. However, in order to simplify it as much as possible and to make it more similar to the grillage analyses with which most bridge engineers are familiar, simple line elements are used to model both the beams and the slab. This greatly reduces the size of the program enabling it to run on a desk top computer; it is perhaps the first time this form of analysis has been performed on such a machine.

A disadvantage of this "grillage" type of analysis is that it treats the stresses in the two directions as independent so it has to use uniaxial material properties. It thus cannot model the increase in stiffness due to the Poisson's ratio effect in concrete subjected to biaxial compression, nor can it model the enhancement of concrete's compressive strength, or reduction in tensile strength, due to biaxial stress. These faults, however, generally act in the safe direction and are considered acceptable in design, indeed they are shared with all the analytical methods normally used in design.

Another fault is that this form of analysis can only check stresses in the element direction so the maximum principal stress is not modelled if its direction does not coincide with an element direction. Unlike the other faults, this one is not acceptable because it could lead to significant over-estimates of the load to cause cracking or failure. To avoid this, torsionless elements are used forcing the principal moment directions to align with the elements. This is also sometimes done in conventional

linear grillage analyses because it enables the computed moments to be used directly to design the reinforcement without the need to transform them to the reinforcement direction. Because the program uses this principle, the element direction has to be the same as the reinforcement direction. This, and the desirability of using an approximately orthogonal mesh so that the concrete stresses in the two directions are independent, leads to what is probably the major practical limitation on the use of the program; it is difficult to use it to model highly skewed bridges.

The problem of the principal moment direction does not arise in the down-stand beams so these can be given torsional stiffnesses and elastic values are used for this. However, because the program assumes that plane sections remain plane and normal to the reference plane, warping stresses and the effect of transverse bending in the flanges cannot be represented. In the type of beams considered in this study, the predicted torques were not excessive and the increase in stiffness due to the transverse bending stiffness of the bottom flange exceeded any reduction due to cracking. Thus the errors resulting from using elastic torsional properties were conservative as well as small. However, this would not apply in all structures and the program has been altered to enable a limiting value for the torsional strength of beams to be specified(112). This feature was used in the analysis of the second of the models which will be considered in Chapters 8 and 9 and the limiting moment was reached in the diaphragms although not the main beams.

The particular program used was developed from one written by Edwards(36), although the modifications are so extensive that analyses have little more than some basic principles in common.

7.3 DISPLACEMENT FUNCTION

In a beam element which is loaded only at the ends, the axial force is constant whilst the bending moment varies linearly over the length. The displacement function used by Edwards matched this by using constant axial strain and a linear variation in curvature over element length. In a linear-elastic beam element, force is proportional to axial strain and moment is proportional to curvature so this shape function is ideal. In a non-linear element it is not quite as good because the stiffness varies over the length which tends to result, for example, in the analysis under-estimating the moment variation over element length. For use in non-

linear analysis, however, there is a more fundamental fault in the shape function which does not appear to have been considered by other analysts, such as Buckle and Jackson(90), who have used this type of element in non-linear analysis.

The displacements are defined at the reference "plane" or (more correctly for a line element) the reference "line" which, in this study, is at mid-depth of the slab. This means that the strain at the reference plane is assumed to be constant whilst at any other level there is a linear variation in axial strain along the element. This variation is constrained to be proportional to the vertical distance from the reference plane. Since the level of the reference plane is largely arbitrary, this is not satisfactory; even with a perfectly uniform and linear-elastic element, the correct displacement field can only be reproduced if the reference plane is at the neutral axis.

In a typical cracked slab element the actual neutral axis, the level at which there is no axial strain, is well above (that is, on the compressive side of) mid-depth. In the real structure the variation in axial strain along the element is proportional to the distance from the neutral axis but, in the computer model, it is proportional to the distance from mid-depth. Thus, if the variation in curvature over length is correct, the variation in strain along the element is under-estimated for all the material below the reference plane. As a result, unless the element mesh is so fine that the variation in curvature over length is insignificant, the analysis can fail to predict reinforcement yielding in the tension steel and hence can over-estimate strength. There is also a region between the actual neutral axis and the reference plane where the real strain becomes more *tensile* in the direction of increasing curvature but that in the computer model becomes more *compressive*. This means that, if the top of the cracks are in this region (which is often the case) the computer model will indicate that the extent of cracking will *reduce* over element length in the direction of *increasing* curvature, which is clearly incorrect.

One solution to this problem would be to keep the same displacement function but to put the reference plane at the neutral axis. This is not practical because the neutral axis moves as the concrete cracks. The effect can, however, be obtained by introducing a linear variation in axial

strain, as well as in curvature, over element length. The variation in strain due to a linear variation in curvature can then be correctly reproduced at all depths in the element, rather than at only one. In addition, a linear variation in neutral axis depth over element length can be modelled.

Introducing the linear variation in axial strain gives the displacement function illustrated in Figure 7.1. Since the stresses are calculated at only two sections in the length of the elements, it simply means increasing the axial strain at one section and reducing it at the other by the same amount. However, because this linear variation does not alter the element length, it cannot be defined from the displacements of the two end nodes. The modification effectively amounts to introducing a third node at mid-length with only one degree of freedom; the axial displacement δ_c in Figure 7.1.

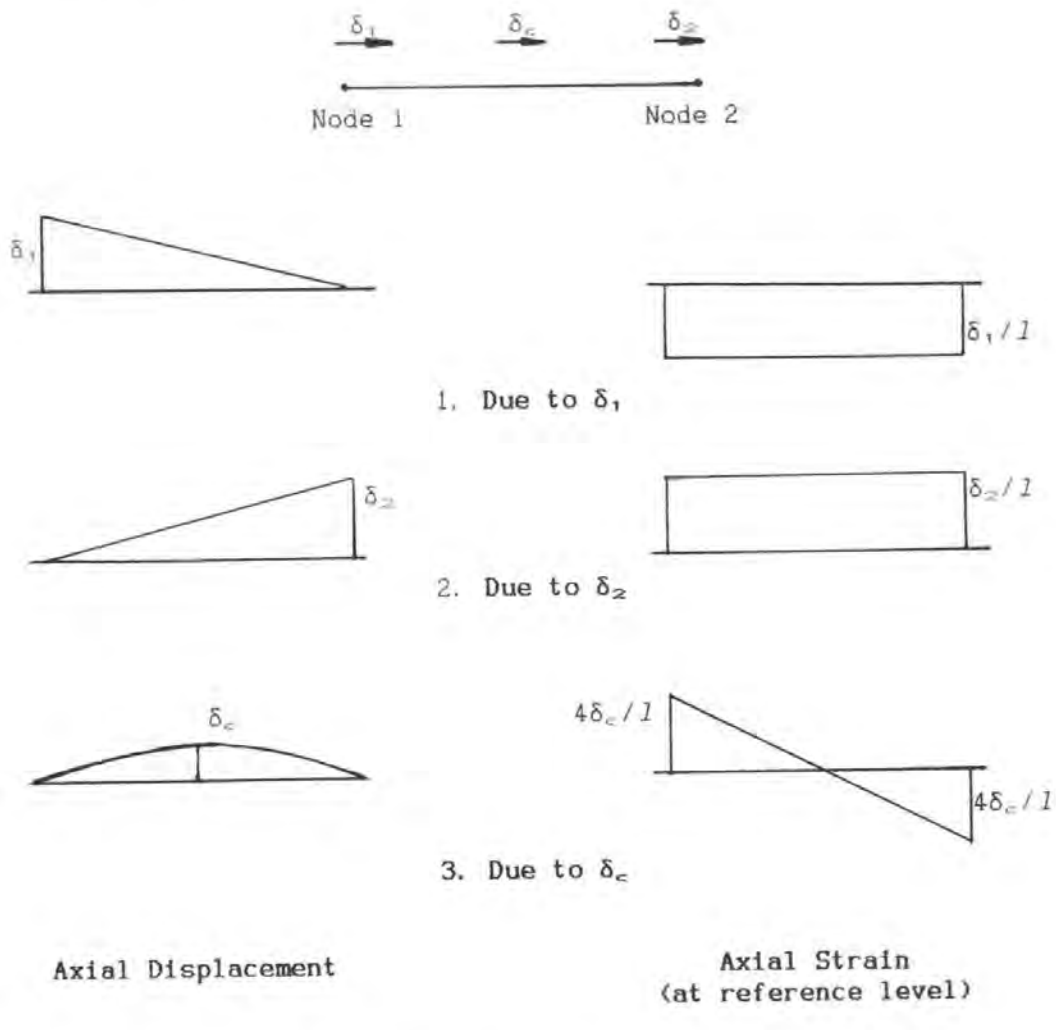

Figure 7.1: Displacement function

Introducing this node into the global stiffness matrix would have complicated the analysis and increased the computer storage space required. This was avoided by considering the internal equilibrium of the elements. The fault in the original displacement function meant that the axial forces calculated for the two sampling sections were not necessarily equal. This leads to a criterion for the correct value of δ_c; the value which equalises the forces. However, this value can only be obtained by comparing the forces at the two sections which requires an iterative calculation. Performing this iterative calculation for every element each time the forces in the structure are calculated would have greatly slowed down the analysis. To avoid this, the number of iterations for δ_c is limited to two, but a vector of δ_c for all the elements is stored and used as the first estimate the next time the element forces are calculated; that is in the next iteration of the whole structure. The modification has effectively increased the number of degrees of freedom in the analysis by some 30% without a proportional increase in the required computer capacity.

The modified version of the program was tested by analysing the simple case considered in Chapter 4 and the results are shown in Figure 7.2. In the Figure the percentage error in predicting the restraint force or displacement, whichever is greatest, is shown for analyses using different numbers of elements. For comparison, the same case was also analysed using the previous version of the program. Because this beam has no tensile strength, and hence the formation of a crack does not release any energy, the problem of mesh dependence which was considered in 6.2.3 does not arise. Thus, as the mesh is refined, both programs converge on the "exact" analytical solution which was derived in Chapter 4. However, the modified form of the program converges very much more quickly and 3 elements with this give better results than 6 with the original program. In most of the structures considered in this study, the improvement is more fundamental because, with the old program, the mesh size required to reduce the discretisation errors to acceptable levels is too fine by the criteria considered in 6.2.3.

Having adopted the principle of defining extra degrees of freedom by considering internal equilibrium of elements, it would be possible to extend it to develop higher order elements. For example, one could use a quadratic variation in both axial displacement and curvature. This would

give two extra degrees of freedom which could be defined by calculating both the axial force and the bending moment at a third section at mid-length and checking that they were consistent with those at the other sections. This would undoubtedly enable a beam to be modelled with a coarser element mesh. However, Figure 7.2 shows that with the existing program a remarkably coarse mesh gives satisfactory results. Even with only 3 elements in a half span in which there is a complete moment reversal, the worst error is around 3% which is small compared with the variability of behaviour observed in Chapter 6. Also, to model slab behaviour with a grillage (even a linear grillage) a finer mesh would be required. Thus the extra complication of higher order elements is not justified.

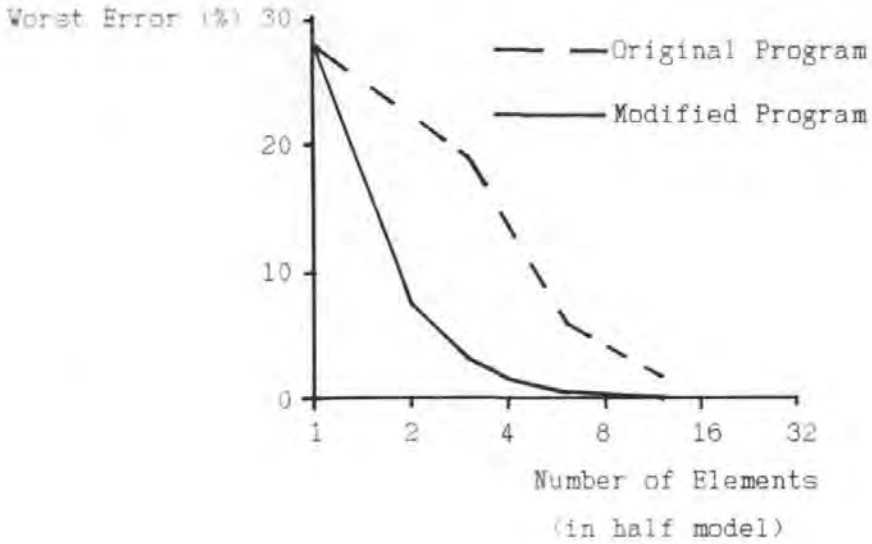

Figure 7.2: Effect of change to displacement function

7.4 ELEMENT INITIAL STIFFNESS CALCULATION

The program calculates the initial stiffness matrix elastically, as in a conventional linear grillage, using the gross-concrete section properties.

Although the displacements are defined from the reference plane at mid-depth of the slab, Edwards' program calculated the initial stiffnesses of the down-stand beams about their own neutral axes. It then treated them as though they were calculated about the reference plane. This did not lead to errors in the final results because the non-linear force calculation correctly calculated the forces from the displacements allowing for the eccentricities. However, because the initial stiffness matrix did not model composite action between the beam and slab, and thus did not

represent the true behaviour even in the elastic range, it did result in very slow convergence. With the simple solution scheme used by Edwards, analyses of structures in which the beams were large compared with the slab would not converge at all. The solution to this was to use a rigid body transformation and this was done by defining the element stiffness about the reference plane by using the stiffness matrix for an off-set beam which is given in Table 7.1.

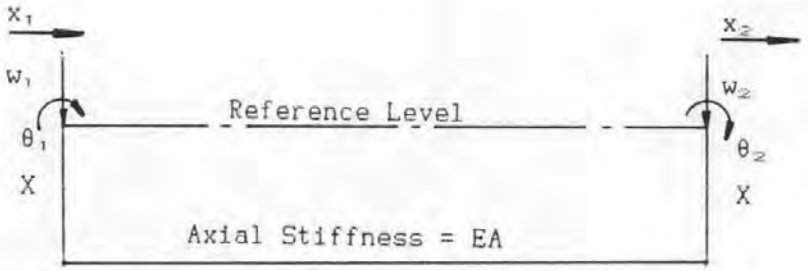

Flexural Stiffness = EI

Length = *l*

	M_1	R_1	F_1	M_2	R_2	F_2
θ_1	$4EI/l + EAX^2/l$	$6EI/l^2$	$-EAX/l$	$2EI/l - EAX^2/l$	$-6EI/l^2$	EAX/l
W_1		$12EI/l^2$	0	$6EI/l^2$	$-12EI/l^2$	0
X_1			EA/l	EAX/l	0	$-EA/l$
θ_2		(symmetrical)		$4EI/l + EAX^2/l$	$-6EI/l^2$	$-EAX/l$
W_2					$12EI/l^2$	0
X_2						EA/l

Table 7.1: Stiffness matrix of an off-set beam element

(For simplicity an element in a plane frame is illustrated)

7.5 IN-PLANE FORCES

Although Edwards described his program as a "grillage" this is not strictly correct. The non-linear analysis leads to axial forces in the elements which a true grillage cannot model. In order to distribute these forces correctly, it is necessary to consider horizontal displacements and the in-plane shear in the slab. Thus Edwards' program considered five degrees of freedom per node instead of three as in a true grillage.

The in-plane shear in the elements was calculated from the relative transverse displacement of the nodes; the horizontal displacement perpendicular to the element direction of the node at one end of the element relative to the node at the other end. This implied that all of this transverse displacement was resisted by shear even though it may have actually been largely due to rotation of the whole element about the vertical axis with no shear deformation, that is as shown in Figure 7.3b rather than 7.3a. It also meant that the complimentary shear and the resulting axial forces, such as the transverse forces illustrated in Figure 3.12, were not modelled. This led to errors in the treatment of in-plane forces which were serious, not so much because they were large (although they could be), as because they tended to act in the unsafe direction. In the finite element programs considered in Chapter 5, this fault is avoided because there are enough nodes in an element to define its horizontal shear deformation from the horizontal displacements of the nodes. However, with only two nodes per element, the shear deformation can only be defined if the rotation of the nodes is also known. Thus, it was necessary to introduce this sixth degree of freedom, rotation about the vertical axis, into the program.

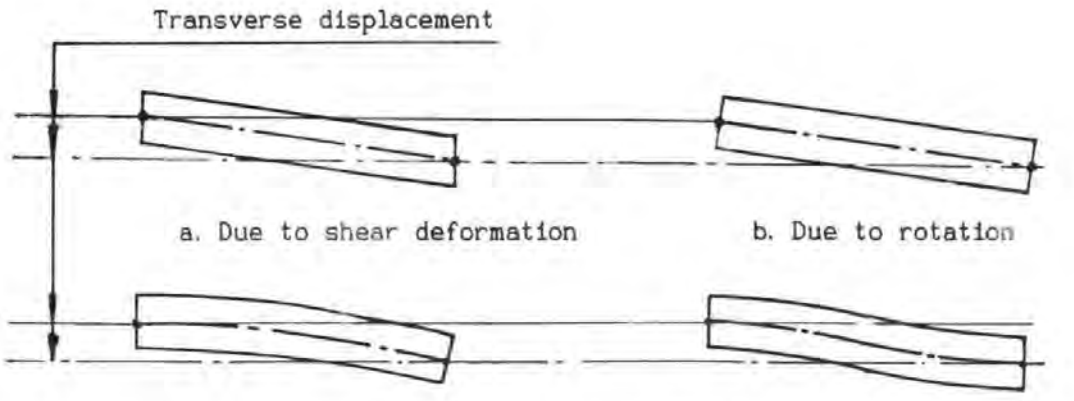

Figure 7.3: Transverse displacements of a line element

If the slab was modelled with normal line elements, as used in a conventional space frame analysis, the transverse shear force would have caused transverse bending in the individual elements as shown in Figure 7.3d; it would have introduced Vierendeel frame type displacements. These displacements do not arise in the real slab because the "elements" cannot bend independently; they act compositely. Thus the displacements due to this local transverse bending of the elements had to be suppressed in the computer model. To achieve this, it is assumed that if the elements are subjected to a transverse displacement without rotation of the nodes (that is as shown in Figure 7.3a and d) the only deformation is due to shear flexibility and the deformation is as shown in Figure 7.3a. The shear force is calculated from this shear deformation, as in Edwards' program, but the moments required to keep the element in equilibrium about the vertical axis (an equal and opposite moment at each end) are applied. In Edwards' program, these moments were not applied to the structure. In effect they were resisted by a totally artificial restraint to rotation of the nodes about the vertical axis.

In order to preserve the basic simplicity of the elements, the individual elements are assumed not to provide any resistance to uniform bending about the vertical axis; they do not resist the form of deformation shown in Figure 7.3c. This means that the stress state can be taken to be constant across the element width and avoids the need to perform a stress integration over width as well as over depth and length. The relatively small moments required to maintain equilibrium with the in-plane shear are the only moments about the vertical axis within the elements. The bending stiffness of the structure about the vertical axis is, however, modelled by the differential axial forces in the elements. The approach is to split the transverse deformation of the elements into two components; a uniform bending about the vertical axis as shown in Figure 7.3c, which is not resisted, and a shear deformation as shown in Figure 7.3a which is resisted by the transverse shear stiffness of the concrete in the slab. The mathematics of the assumed deformation state are given in Appendix B. In practice, a nominal bending stiffness was added because otherwise rotation about the vertical axis is completely unrestrained in some models.

This treatment of in-plane forces is inherently approximate. It might also be argued that including in-plane shear is inconsistent with the reasons given in 7.2 for using torsionless elements since it implies that the

maximum principal tensile stress may not align with the element direction. However, the program is intended for modelling structures whose behaviour is primarily flexural so it is appropriate to use a lower order of analysis for the in-plane forces.

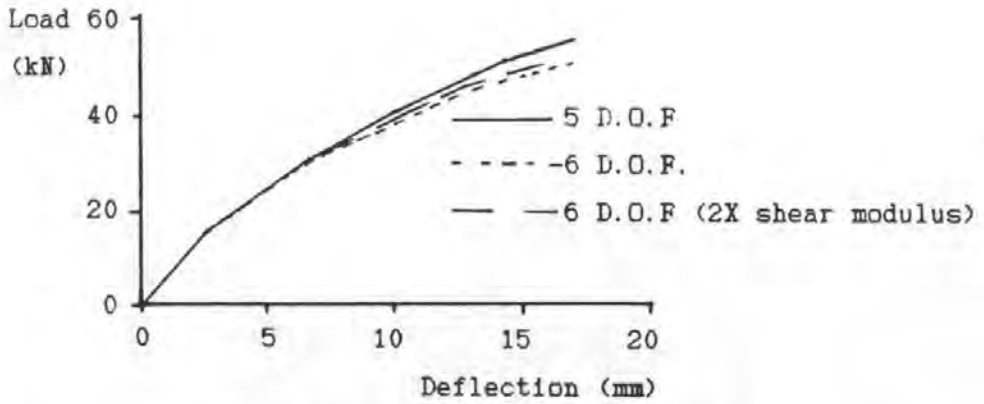

Figure 7.4: Effect of in-plane shear

Figure 7.4 shows the results of the analysis of a simple structure (actually the structure which will be considered in 7.10.3) using the modified program with two different shear moduli and also using the original program. The effect of doubling the shear modulus is small, which implies that errors in the treatment of in-plane shear have little effect and justifies the use of approximate analysis for in-plane shear. Even the apparently fundamental fault in Edwards' program has only a small effect on this particular structure, although the artificial restraint to rotation about the vertical axis is equivalent to more than doubling the shear modulus. However, it is possible that the effect could be greater in some other structures so it was considered prudent to use the modified program for all subsequent analyses to ensure that the results would be safe. For the same reason, and unlike in Edwards' program, a reduced shear modulus is used for cracked concrete.

Because the elements are fixed together at slab level, and because in-plane forces in the slab are represented, the program is able to model both shear-lag and the effect of the shear connection between the beams which was discussed in 2.4.3 and 3.2.7. Unlike Edwards' program, because it checks moment equilibrium about the vertical axis, it also models the resulting transverse stresses which were illustrated in Figure 3.12. The failure of the original program to model this potentially significant effect further justifies the modification.

7.6 LARGE DISPLACEMENTS

When a slab deflects relative to the restraining beams, the lever arm at which the restraint force acts is reduced. Once the deflection becomes significant compared with the thickness of the slab, this significantly reduces the slab's load carrying capacity. Curiously, most of the NLFEA studies mentioned in Chapter 5 did not consider this effect whereas all the (otherwise far less sophisticated) analyses considered in 3.2 did. In this study, it was originally decided to follow the NLFEA studies and ignore the effect and, because the analysis is conservative in other ways, the predictions still tended to err on the safe side. However, for three reasons, it was eventually decided to modify the program to make some allowance for large displacements. Firstly, ignoring the effect nearly always leads to errors which act in the unsafe direction so it is undesirable in a design situation even if the errors are relatively small. Secondly, some of the tests on model bridges which were considered in 3.2.3, notably Beal's(77), reached such large deflections before failing (around h/2) that an analysis of these which assumes the deflection to be small relative to slab thickness is clearly invalid. Thirdly, for reasons discussed in 3.2.8a, it would be desirable to be able to use membrane action in the design of slabs with longer span to depth ratios than the empirical design rules allow. However, financial and time restrictions on this project prevented an experimental study of such slabs. Thus, if their design was to be justified purely by analysis, it was particularly important to ensure that the analysis was safe and, since longer span to depth ratios increase the significance of deflections, this meant allowing for the effect of deflections in the analysis.

Because of the use of line elements, it was comparatively simple to include the deflection in the analysis. It was done within the elements by adding the vertical component of the axial force to the shear force. As is illustrated for a simple case in Appendix C1, this has the effect of modelling the moment in the elements (that is, about the deflected reference level) due to the axial force acting at the undeflected reference level: it models what in a column would be called the "buckling", "added" or "PΔ" moment. The vertical component of the axial force is calculated only from the difference in the vertical displacements of the two nodes. The effect of curvature over the length of the element is not included but this is only significant if an excessively coarse element mesh is used. To

maintain consistency, the vertical component of the in-plane shear was also added and this is calculated from the rotation about the longitudinal axis averaged for the two ends of the element. As an additional allowance for finite displacements, the axial strain in the elements is also corrected for the effect of the slope as detailed in Appendix C2. That is, the axial strain used to calculate the forces in the element allows for the increase in length of the element due to its slope.

These effects are modelled only in the non-linear force calculation, not in the stiffness matrix. This must reduce the convergence rate but was considered acceptable.

7.7 MATERIAL MODELS

7.7.1 Steel

A tri-linear stress-strain relationship is used for steel as indicated in Figure 7.5. In analyses for research purposes, the factors are chosen to give the best approximation to the actual stress-strain curve of the steel. The pre-strain is included primarily to enable prestressing to be modelled but, in simple slabs, a negative pre-strain can be used to represent shrinkage. When modelling prestress, the pre-strain has to be reduced to allow for losses because the program does not consider long-term effects.

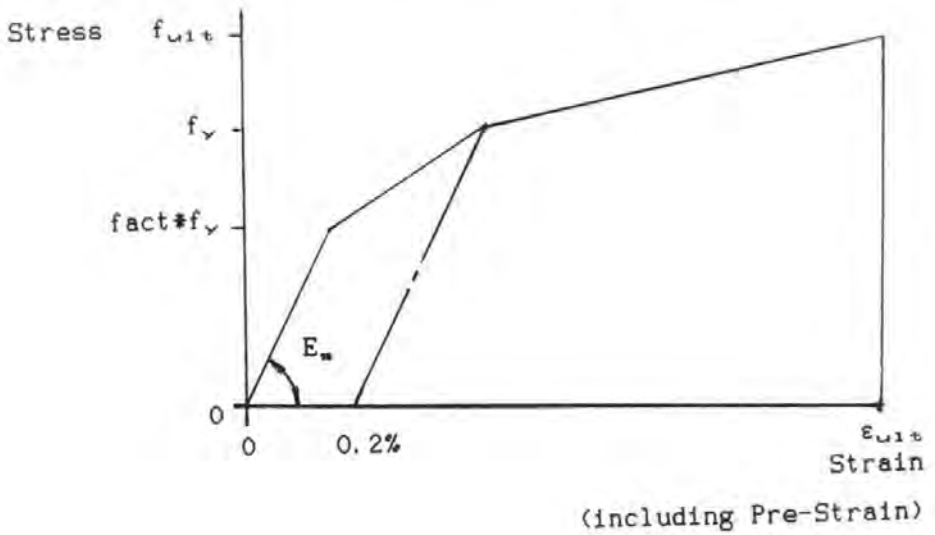

Figure 7.5: Steel properties

The same properties are used in compression as in tension, except for a limit on strain hardening in compression. The stress is taken to be a function only of the present strain. It would be simple to adjust the

program to allow for the permanent set in steel which has been stressed beyond its elastic limit but this would require the maximum strains to be stored for all the steel layers in all the elements. Since none of the structures analysed had steel stressed above its elastic limit, except under the final failure load case when the strain was increasing monotonically, the facility to model permanent set was not implemented.

In analyses for serviceability design, in order to avoid the problem of stress history dependence as much as possible, the steel is taken to be linear-elastic. To justify this assumption, service stress has to be limited to the elastic limit and this becomes a design criterion. Thus no advantage can be taken of re-distribution due to reinforcement yielding under service loads. However, this is not a disadvantage as such yielding is considered undesirable anyway. The approach has the advantage of making the analysis more compatible with current codes of practice.

In analysis for design at the ultimate limit state, the tri-linear stress-strain relationship can be used to represent either the actual steel properties or the code specified properties. It is normally assumed that only reinforcement yielding due to the load case being analysed needs to be considered. This is justified if one assumes that only one load case above design service level is applied. However, in a bridge deck slab, this is not very logical since the design vehicle cannot get to the critical position without first being applied in other positions which are only marginally less severe. Fortunately, this problem (like all aspects of strength analysis) has little practical significance since serviceability criteria are critical.

7.7.2 Concrete in Compression

The stress-strain relationship used for concrete in compression is illustrated in Figure 7.6. Various curves have been proposed which are more realistic, but when one allows for the variability of concrete the improvements are not significant and Abdul-Rahmen(87) used the even simpler elastic-plastic relationship.

It is assumed that when the concrete is unloaded, it follows a line parallel to the initial part of the loading diagram. Thus it takes on a permanent deformation which is equal to the departure from linearity on loading.

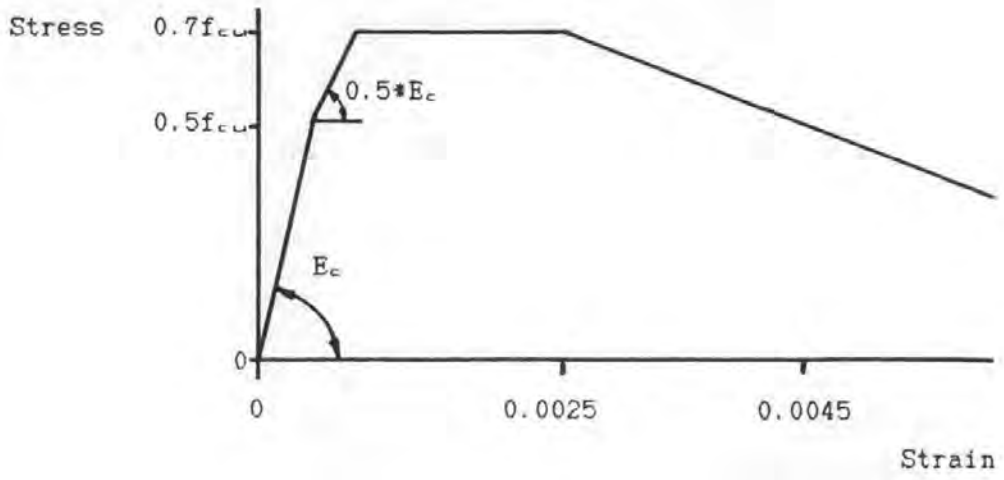

Figure 7.6: Properties used for concrete in compression

The strain at which the stress is taken to start to reduce is lower than in many other analyses. This was a reflection of the results obtained from the cylinder tests and may have been due to the relatively fast speed at which these tests were performed. The rate of reduction of stress after the peak has been passed was intended to represent the true behaviour of the concrete, which can only be observed with a very stiff testing machine, rather than its apparent behaviour. However, because of the nature of most of the structures considered, analyses performed with the more usual form of curve, with a longer plateau followed by a more abrupt cut-off, gave very similar results.

The same basic approach to serviceability design is used as for steel; the material is taken to be linear-elastic and a stress limit is imposed to ensure that this is reasonably true. However, although this limit is also given in codes of practice, it is far less satisfactory than the steel limit. As noted in 2.3.4c and demonstrated in reference 35, even structures designed to BS 5400 can be stressed well above the limits, yet their behaviour is satisfactory. This presents a problem. If the stress limit is imposed on structures designed using non-linear analysis it is unduly conservative; if it is not imposed it will be more difficult to get the approach accepted and it is also difficult to decide what the design criteria should be. A possible compromise is to impose a limit but to make it less conservative. This can be done without departing from the principle of linearity if the increase is justified by the biaxial stress state in the critical area. There is a precedent for explicitly considering enhancement due to multiaxial stress states in BS 4975(113). An

alternative approach is to make a totally arbitrary increase in allowable stress and then to justify it by comparison with test results.

For analysis for design ultimate strength the code specified stress block could be used but a tri-linear approximation was employed. In conventional design methods, the characteristic material properties are used in the analysis of the structure and the design strengths, with the partial safety factors applied, are used only for the analysis of the critical sections. In non-linear analyses, the analyses of the structure and of the critical sections are not separated so this approach, although recommended by BS 8110, is not appropriate. In this study, therefore, the safety factors were applied to all the material. From a statistical viewpoint, this is not justified. However, it is conservative (except for some cases where restraint stresses are dominant) and, since serviceability criteria are critical, this is acceptable. A disadvantage of this approach is that in most codes, including BS 5400, the design ultimate stress in concrete is less than the limit of linearity used at serviceability. Thus, unlike in analyses for research, completely separate analyses have to be performed for serviceability and for ultimate strength.

7.7.3 Concrete in Tension

The properties used for research analyses are illustrated in Figure 6.12 and were discussed in the last chapter.

In choosing properties for analyses for design the major problem is that the desirable characteristics of the properties, that they should be reasonably representative of real behaviour and that they should not be strain history dependent, are mutually exclusive. The simplest solution to this problem is to abandon realism in favour of avoiding strain history dependence and ignore the tensile strength of concrete completely. As was noted in 2.4.2, this approach has the major practical advantage of being compatible with current codes. It is also normally conservative, indeed a disadvantage is that it is liable to lead to an unduly pessimistic prediction of the distribution of moments between the beams. However, it is not possible to prove that the approach is always conservative. A peculiarity of membrane action is that the restraint force, the effect which leads to the enhanced behaviour, is a direct result of cracking. Thus tensile strength, by reducing the extent of cracking, can reduce the restraint force and hence the degree of enhancement. To investigate this,

a simple slab was analysed using concrete tensile strengths of zero and $3N/mm^2$. The latter analysis used the material properties given in Figure 6.12 and the results are shown in Figure 7.7. A half model was used and the load quoted is that on the half model. For comparison, the results of a conventional analysis ignoring the restraint as well as the tensile strength are also shown.

The stresses in the slab which was analysed using a tensile strength of $3N/mm^2$ are calculated in two ways. The lower lines give the stresses directly from the computer program; that is the smeared stresses. These are always less than those calculated ignoring the tensile strength although, once the concrete has cracked, the margin is small. The reason for the discontinuous plot is that in the numerical analysis the cracking advances, both in depth and along the slab, in discrete steps. In the real structure, the cracks can grow more smoothly in depth but the cracked zone can only advance along the slab in discrete steps as individual cracks form. In order to make the analysis as realistic as possible, the element length was matched to the estimated crack spacing giving five elements in a half model. It was found that an analysis using a finer mesh (20 elements in place of 5) predicted very similar behaviour, the deflections being within 2%. However, the smeared steel stress was up to 50% higher. A study of the results revealed that there were two reasons for this. The first was that, on first cracking, the fine mesh predicted unrealistically localised cracking and hence an unrealistically small restraint force. However, because of the tension stiffening function used, the extension on initial cracking was very limited even in the coarse model. The effect of mesh size was therefore far less pronounced than in an earlier analysis performed with concrete tensile strength but without tension stiffening.

The second reason for the effect of mesh size is that the analysis gives the stress only at the last integration station, not at the critical section. In the coarse mesh, the last integration station is 40mm from the critical section and thus is subjected to a 4% lower moment. This might normally be expected to make only a 4% difference to the stress. However, the concrete properties used in the analysis make the moment-steel stress relationship non-linear whilst the 4% difference in moment is not accompanied by a difference in the enhancing axial force. The peak stress predicted by the fine mesh is very localised and the effect is far

less pronounced in the analysis of real slabs because of the finite width of the applied loads.

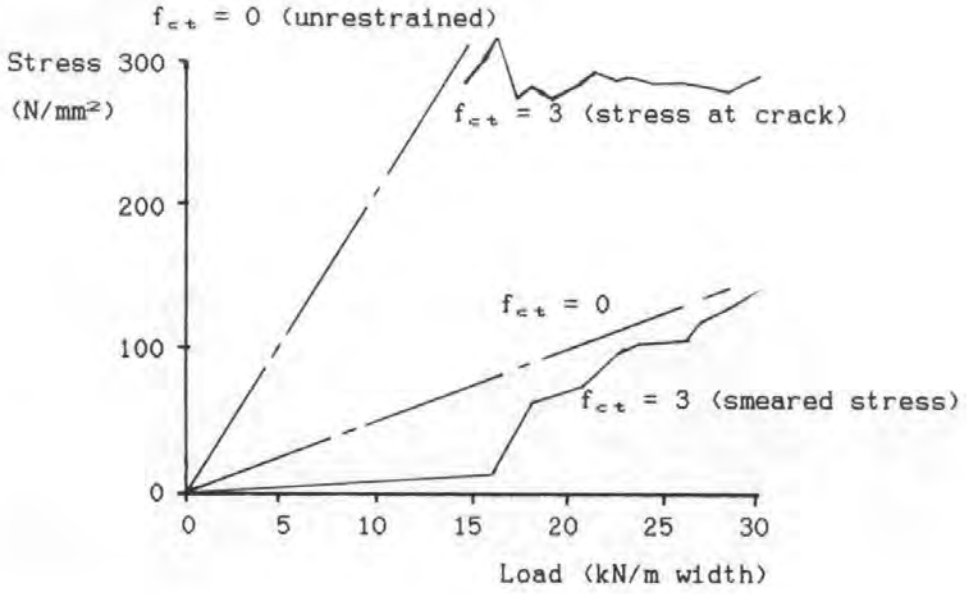

a. Steel Stress

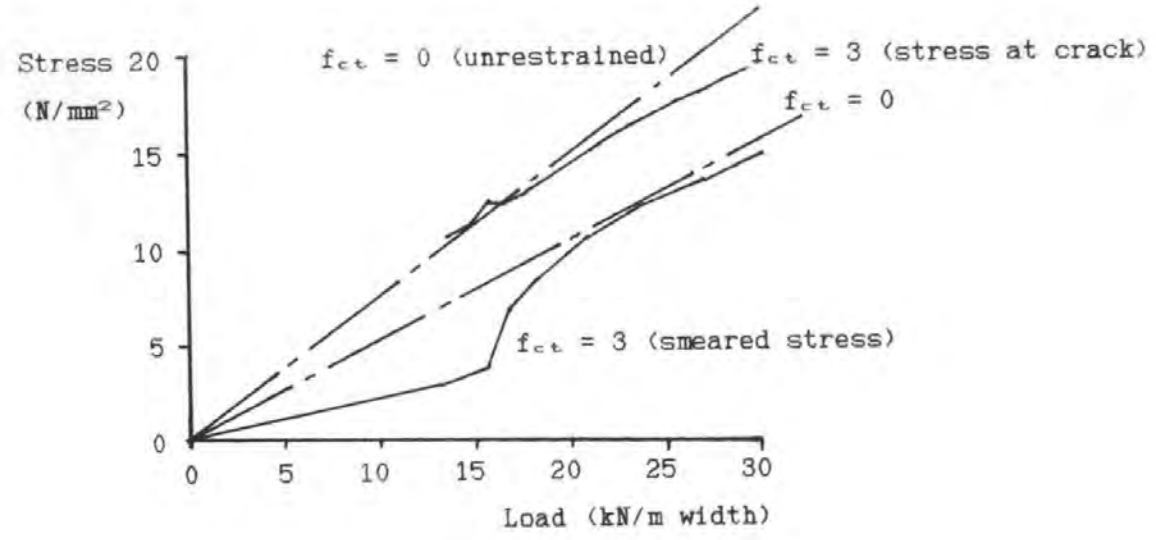

b. Concrete Stress

Figure 7.7: Effect of concrete tensile strength

(Central line load, simply supported but with rigid in-plane restraint
l = 2000, h = 160, d = 119, T12-250 reinforcement)

It was noted in 6.2.2 that smeared crack analysis under-estimates the peak stress in the reinforcement. This is clearly undesirable if stress is to

be used as a design criterion so it appears to be more appropriate to calculate the peak stress at the crack at the critical position using only the forces, not the stresses, given by the computer analysis. This also has the advantage of eliminating one of the effects of mesh size. The stresses calculated in this way are given by the upper solid lines. In accordance with normal practice, the critical section was analysed ignoring both the tensile strength of the concrete and the effect of the top steel. Separate calculations confirmed that the effect of these would be relatively small, provided that the post-peak part of the stress-strain relationship used for the analysis of the structure was not included.

Until the analysis predicts cracking, the stress calculated in this way has no real physical meaning and is not plotted. When the analysis first predicts cracking, the extent of the cracking is very limited. Thus the restraint force is small and the calculated stress at the critical section is similar to that given by the conventional analysis and substantially greater than is predicted ignoring the tensile strength of concrete completely. As the load increases, the extent of cracking (and hence the restraint force) increases disproportionately. Because of this, the steel stress calculated for the critical section does not increase substantially until concrete non-linearity comes into effect and the plot is discontinued because the elastic section analysis used is invalid.

The difference between the various calculation methods is much less for the concrete stress which, using BS 5400 serviceability criteria, is critical for the restrained slabs. The restrained analyses also converge to give similar failure loads of around 70kN compared with 25kN for the unrestrained analysis. Nevertheless, the difference in the allowable service loads implied using the stress at crack approach, 21kN, and the smeared crack approach, 30kN, is disturbingly large and it appears prudent to use the former approach. It should be noted, however, that a substantial part of the difference is due to the aforementioned effect of the difference between the stress at the critical section and at the last integration station. This has two important implications. Firstly the effect will be less pronounced under patch loads (as opposed to point or line loads) so the difference between the two approaches will normally be less than implied by this study. Secondly, the peak concrete stress is too localised for normal material models, based on the behaviour of specimens

in a uniform state of stress, to be valid. Because of this the use of the stress at the critical section is conservative.

The analysis of these slabs appears to confirm that ignoring the tensile strength of concrete may not be conservative. However, the tensile strength of concrete does have a major beneficial effect on real structures which does not arise in the rigidly restrained slabs considered here; it improves the restraint. Thus the tensile strength of concrete is far less likely to have a detrimental effect on the stresses in realistic bridge deck slabs.

7.8 STRESS INTEGRATION

The element forces are obtained by integrating the stresses over the element volume. The stress is taken to be constant over element width and the integration over length is performed using two integration stations at the Gauss points, 21% of element length from each end. The forces at the nodes are then obtained as a function of the forces at the integration stations using the shape functions.

In analyses of this type, it is usual to perform the stress integration over depth numerically with a high order integration function and sometimes as few as five sampling stations. This effectively fits a smooth curve between the stations. As the stress functions used, particularly for concrete in tension, are highly discontinuous it appears that this could lead to significant errors and Ganaba and May(114) have confirmed this. In many of the sections considered in this study, with their very light reinforcement, a five point integration scheme gave only one station in uncracked concrete. This, combined with the fact that the tension stiffening function used was more discontinuous than that favoured by Ganaba and May, suggested that the integration errors would be particularly significant.

Two solutions to this problem were used. For analyses which did not consider stress history, an exact analytical integration was developed. In addition to eliminating integration errors, this was significantly faster than numerical integration. However, neither this solution nor that suggested by Ganaba and May (splitting the integration at the root of the crack), could be used for stress history analyses. It was therefore decided to increase the number of integration stations from five to eight,

to improve accuracy, and to change from high order Newtonian integration to trapezoidal integration to reduce the effect of the discontinuities. The stresses in the down-stand beams were integrated separately using the same integration scheme.

Comparison with the exact analytical version of the program showed that these changes made the integration errors in the analyses of structures insignificant compared with the other errors. However, it appeared that this was partly because the errors were essentially random and so tended to cancel out; the error in the forces calculated for a single element could still be significant. This tendency of the errors to cancel out explains why, despite the large errors observed by Ganaba and May in the forces calculated for individual elements, other analysts [such as Abdel Rahmen(87)] have found their results to be insensitive to the number of integration stations used.

In the analyses of the constant moment regions considered in Chapter 6 there was no scope for the integration errors to cancel out so they could be more significant. Because of this, and because "accuracy" was considered more important for a fundamental study of tension stiffening, a special version of the program was developed which employed 32 point trapezoidal rule integration. This was used for all the analyses in Chapter 6, except those which did not consider stress history and so could be performed with analytical integration. For practical purposes, this eliminated integration errors completely. Indeed, since they were spaced at only a quarter of the maximum aggregate size, the integration points were unrealistically close. However, because the maximum historic strains are stored for all the integration stations, this version of the program required more storage space as well as more computer time and it was not used for the analysis of more complex structures.

7.9 SOLUTION SCHEME

In non-linear analysis, the forces can be calculated directly from the displacements but the displacements can only be obtained from an iterative solution scheme. Incremental iterative schemes are normally used to enable the behaviour of the structure under increasing loads to be studied and also because the behaviour is sometimes "path dependent" so analyses using very large increments could give incorrect solutions.

A detailed study of solution schemes is beyond the scope of this thesis. However, some problems were experienced which are peculiar either to the type of structure considered or to the form of analysis used. These will now be considered along with a brief review of the scheme adopted.

7.9.1 Control

Solution schemes using displacement(97) or arc-length(115) control are now favoured by analysts but this has arisen primarily because of the concentration on ultimate and post-ultimate behaviour. It is difficult to achieve convergence with analyses using load control as failure approaches and impossible to model softening, post-ultimate behaviour or "snap-through". However, with the type of structures considered in this study, ultimate strength is a secondary consideration and neither "post-ultimate behaviour" nor true "displacement control" have much physical meaning because the failures are local and brittle whilst most of the strain energy is stored in the beams. Thus, even if the bridges had been tested under perfect displacement control, the slabs would still have failed suddenly and completely. Also, the temporary reduction in load which can occur under monotonically increasing displacements as cracking occurs has no practical significance since real structures are loaded under load control. There is thus little practical advantage in departing from using load control, at least in a pragmatic study such as this. As structures are designed for specified loads, and neither strength nor displacement are critical design criteria for the type of structures considered here, analysis under load control is far more convenient for use in design.

7.9.2 Initial Stiffness Method

As serviceability criteria are critical there is no need to take an analysis for design up to failure, only to design ultimate load which is just 30% above design service load in BS 5400. Since this is normally well below the actual collapse load, the demands on the solution scheme are comparatively modest so a relatively simple scheme can be used. Edwards used the simplest possible scheme; the initial stiffness method with no accelerators. In this approach, which is illustrated for a single degree of freedom system in Figure 7.8, the initial elastic stiffness matrix is used throughout. The displacements are calculated from the loads using the inverted initial stiffness matrix. The forces are then calculated from these displacements, using the non-linear material

properties, and compared with the applied loads. The difference (which represents the forces released by cracking, crushing and yielding) is then used to calculate a new set of displacements which are added to the first set. A new set of forces is then calculated for these displacements and the whole process is repeated until the forces match the applied loads. The results are then printed out and the next increment of load is applied.

The approach has the advantage of being numerically stable and reliable as well as simple. However, if the actual tangent stiffness matrix of the structure is substantially different from the initial stiffness matrix, the convergence rate is very slow. This normally occurs as failure approaches. However, in the case of some of the slabs considered in this study, the very low steel areas meant that cracking changed the stiffness so much that the convergence rate became excessively slow even before design service load was reached. In a typical analysis of a 25 node model, over a hundred iterations per increment were needed. This, and the desire to use the analysis as a research tool (which meant that failure behaviour had to be considered) meant that the convergence rate had to be improved.

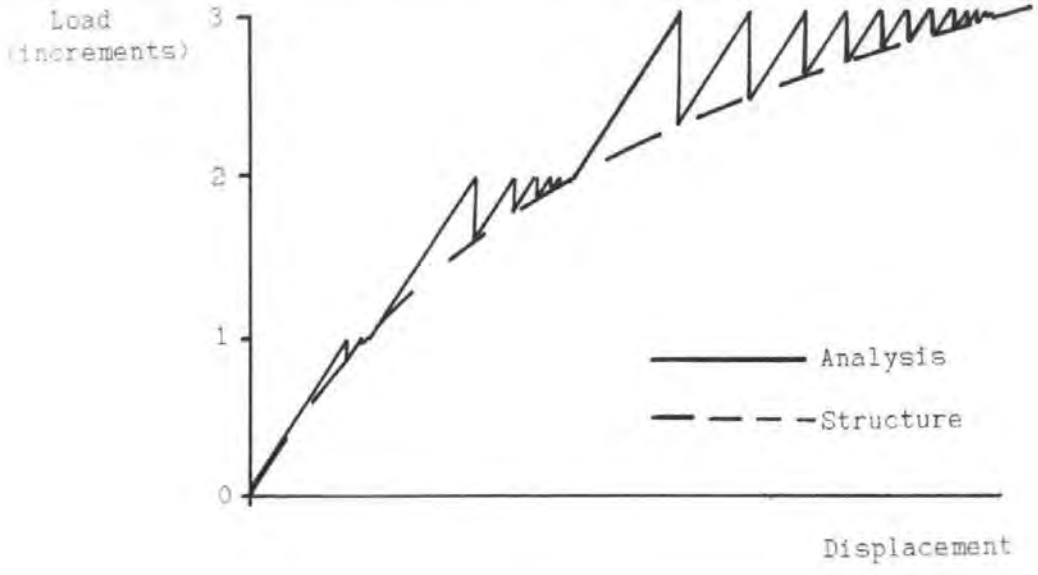

Figure 7.8: Initial stiffness method

7.9.3 Accelerators

The first modification to improve convergence was to use a simple approach suggested by Cope et al(37). In this, the displacements due to the last load increment are used as the first estimate for the displacements due to the present load increment as illustrated in Figure 7.9. Because the

stiffness of the structures considered tended to degrade reasonably progressively, this meant that the first estimate was much closer than it would have been if calculated from the initial stiffness matrix. Thus the number of iterations required to achieve convergence was much reduced. This approach is particularly effective in analyses using very low or zero tensile strength for concrete because the displacements due to each increment are then equal until reinforcement yielding or concrete crushing occurs.

Although this modification greatly reduced the number of iterations required, it was still excessive so a number of acceleration schemes were considered. Some were found to be very effective on some structures but they had erratic results and prevented analyses of other structures from converging altogether. Eventually, it was decided to use a "line search" procedure instead. In this, the displacement vector calculated from the stiffness matrix is multiplied by a scalar factor and this factor is optimised. In co-ordinate geometry terminology, the stiffness matrix is used only to obtain the search direction in "n" dimensional space and the line search attempts to find a scalar multiplier for this vector such that the component of the error energy in that direction is zero.

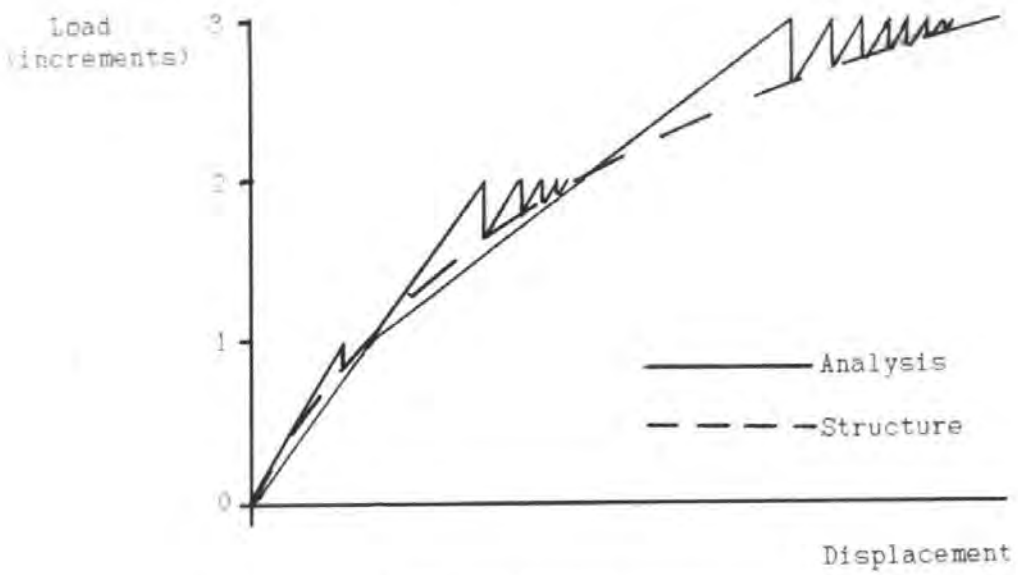

Figure 7.9: Modified initial stiffness method

Since the value of this scalar can only be obtained iteratively, which involves calculating all the element forces for each iteration, exact calculation would require excessive computation. However, by using a very slack optimisation criterion, the number of iterations or "searches" can be

reduced. In this study, the criterion used was that attempts to obtain a better scalar factor were made only if the sum of the error forces multiplied by their respective iterational displacements, that is the error energy in the search direction, was in excess of 60% of a similar summation performed using the error forces from the previous iteration.

The line search procedure greatly reduced the number of iterations required. However, because of the computer time used in the line searches, the effect on the time to achieve convergence was less dramatic although still very significant. Perhaps more importantly, the procedure means that when the structure has failed the analytical deflections become very large. With a pure initial stiffness scheme, failure was sometimes indicated only by failure of the analysis to converge which made it difficult to distinguish failure of the structure from numerical problems with the program.

Line searches are used in most recent NLFEA programs, sometimes in combination with other more sophisticated acceleration schemes. However, for the analysis of cracking, they do have a theoretical fault which does not appear to have been fully resolved. When a crack first occurs, the true displacement is greater than predicted by the stiffness matrix so a line search factor substantially greater than one is applied to *all* the displacements. This can cause cracking in elements which were previously uncracked and in perfect equilibrium. The cracking leads to error forces which are eventually reduced by the iterative solution scheme. However, this could be done by increasing the deformations until the force is taken up by the reinforcement, rather than by returning the element to its uncracked state. The fundamental problem is that there can be two different deformation states in a section which give the same forces; one cracked and one uncracked. The initial stiffness method always underestimates displacements and so always arrives at the uncracked equilibrium state first. However, once a line search is included in the analysis, it is theoretically possible for the analysis to predict cracking in concrete which has never been stressed up to its tensile strength. In practice it was found that this did not occur in the analysis of highly redundant slab systems; analyses with the line search converged on the same solution as those without. However, it did arise in the analysis of direct tension tests using variable tensile strength. For this reason, the line search was not used in the analyses for 6.3.1.

Line searches, and other accelerators, can give displacements (and hence strains) within an iteration which exceed the final equilibrium values. If these strains were used in the stress history analysis, false results could be obtained. For example, concrete could be taken to have cracked, and thus to have lost most of its tensile strength, as a result of strains which only occurred in iterations which had over-shot the true solution. To avoid this, the maximum strains are updated only after convergence has been achieved.

7.9.4 Stiffness Recalculation

With these improvements, the convergence rate was acceptable for small problems and for analyses for design. However, it was still too slow to use the program to analyse large computer models up to failure. It was therefore decided to depart from using the initial stiffness method and a numerical recalculation of the stiffness matrix was added into the program. Ideally, this should calculate the exact tangent stiffness for the current deformation state so that the stiffness matrix truly represents the structure's response to small changes of load. Some analyses(98) have been performed using a "Newton-Raphson" approach, in which the stiffness matrix is recalculated for every load increment or even every iteration. This approach gives a much reduced number of iterations but the computer time required to recalculate and invert the stiffness matrix more than uses up that saved by reducing the number of iterations. In the analyses of cracking, the true current stiffness matrix can also contain negative diagonal terms which would lead to numerical instability.

For these reasons, in the present study the tangent stiffness was calculated only infrequently and approximately and the concrete was always given a significant positive stiffness; usually not less than 3% of the full elastic value. It appears that most studies have attempted to obtain a closer estimate and used a lower tangent stiffness for cracked concrete. This is possible in an analysis under monotonically increasing loads. However, when unloading is considered, it leads to complications since the material models used give different tangent stiffnesses according to whether the strain is increasing or decreasing. Thus the exact tangent stiffness matrix can only be calculated if the direction of change, as well as the value, of the strain is known for all the sampling stations. It

proved much simpler to use only an approximate calculation giving a stiffness matrix which could be used for both loading and unloading.

Having adopted periodic recalculation of the stiffness matrix, it is necessary to adopt a criterion to decide when to do this. The usual approach is to recalculate at the beginning of an increment if some "current stiffness parameter" is substantially different from that implied by the stiffness matrix currently in use. However, in the present study, it was found that this approach did not work very well. If extensive cracking occurred in a particular increment the stiffness matrix was always recalculated for the next increment. However, if little further cracking occurred in that increment, the use of the displacements due to the last increment as a first estimate for the displacements due to the current increment meant that the analysis would converge quickly whatever stiffness matrix was used; provided the previous increment had converged. Thus recalculating the stiffness merely wasted time. If, however, the previous increment had not converged, it would have been better to make it converge by recalculating the stiffness matrix earlier. Thus it was found more satisfactory to recalculate during the increment. It was decided to do this at iteration eight if the convergence rate was slow and the remaining errors were significant.

The choice of iteration eight was a compromise between early recalculation, which could mean unnecessary recalculation, and delaying recalculation until much computer time had been used up in iterations using the old stiffness matrix. However, late recalculation has the advantage that the deformation state, and hence the calculated tangent stiffness, is closer to that in the final equilibrium state so the final convergence tends to be faster.

The stiffness matrix recalculation improved the rate of convergence although not by as much as the line search. However, the greater effect of the line search may not indicate that it is a superior method; rather it appeared to be due to the line search having been incorporated first. The recalculations had a much greater effect on the convergence rate of analyses performed without the line search. It was also apparent that the effect of recalculating the stiffness matrix varied greatly between structures, being generally greatest where the softening was due to cracking in the beams. This implies that the details of the optimum

solution scheme, such as when to recalculate the stiffness matrix, are different for different structures. It was thus clear that the solution scheme adopted was not the optimum for all the structures considered and there was certainly scope for improvement. However, the convergence rate achieved was considered acceptable for the project.

7.9.5 Convergence Criteria

In an iterative solution scheme, it is necessary to adopt a criterion to decide when the solution is sufficiently accurate to stop the iterations, without knowing the exact solution. Criteria based on out-of-balance forces, iterational displacements or the product of the two (that is energy) can be used. It is also possible to consider either overall or local convergence. Analysts tend to favour overall energy criteria, primarily because finite element analysis is an energy based approximation method and there is a useful norm with which to compare the error energy; the work done by the loads on the structure. However, in the present study two difficulties were experienced with energy criteria. Firstly, as Cope and Cope(94) have noted, the in-plane forces tend to be the last to converge and, since the in-plane stiffness is large compared with the flexural stiffness, the energy associated with these is small. Thus significant in-plane error forces can remain in analyses which have converged according to energy criteria. Although these forces might be considered unimportant, since eliminating them usually has little effect on the displacements, they can represent a significant force in the critical elements. Thus, if local stresses are to be used as design criteria, it is important to limit the error forces.

The second problem encountered is a peculiarity of the type of structure considered. The failures were local and brittle. The energy associated with a failure, an individual wheel load multiplied by the displacement of the slab relative to the beams, thus represented only a small fraction, typically 1%, of the total work done by the loads. The combined effect of these problems was that there could be significant local force errors in an analysis when the error energy was less than 0.0001% of the work done by the loads.

Another disadvantage of both energy and displacement criteria is that they depend on the iterational displacements which (unlike the out-of-balance

forces) are a function of the solution scheme used as well as of the displacement. Thus, if the initial stiffness method is used, it is desirable to use a tighter energy convergence criterion because the iterational displacements systematically under-estimate the true displacement errors.

The major difficulty with force criteria is defining a norm with which to compare the out-of-balance forces. The standard of comparison for moments and axial force has to be different otherwise the criteria become dimension dependent. The out-of-balance moments could be compared with the maximum element moment. However, in the type of structure considered here, this would lead to either unduly slack criteria for the slabs or unduly severe criteria for the beams. Comparing in-plane forces with maximum element forces is even less satisfactory because the axial force in a slab element is obtained from the difference between similar tensile and compressive forces. In the early stages of a slab analysis, when the cracking is not extensive, the in-plane forces are very small so a criterion based on a percentage of these forces would be unduly severe. Conversely, in an analysis of a beam and slab deck, the axial forces in the down-stand beams are too large to use as a standard of comparison.

Consideration of these problems led to the decision to use both an overall energy and a local force convergence criterion. The iterations were stopped only when both criteria were satisfied. The energy criterion was based on comparison with the total work done by the loads on the structure whilst the force tolerances were specified by the user. To avoid dimensional problems, separate force and moment criteria were specified.

Despite using a very tight energy criterion, typically 0.01%, and the slackest force criterion considered reasonable, the in-plane force criterion was nearly always the last to be satisfied.

7.10 CALIBRATION

Although the program was not intended to be highly accurate, it was considered desirable to check it by comparison with test results and other analyses to ensure that the results were reasonable. In addition to the studies mentioned in 7.3, 7.7, and also Chapter 6, as well as a check against a linear grillage to ensure that the program was at least

numerically correct, a number of structures which had been tested by others were analysed to investigate the behaviour.

7.10.1 Duddeck's Slabs

Duddeck(116) tested a series of three square corner supported slabs under single central point loads. These have been analysed by both Abdel Rahmen(87) and Cope and Cope(94) using non-linear plate finite element programs. Thus they enabled the program to be compared both with test results and with more sophisticated analyses.

Two of the slabs were analysed using a four by four node quarter model. The results for the first slab, which had 0.7% isotropic reinforcement, are shown in Figure 7.10 and, for comparison, Abdel Rahmen's results are also shown. Duddeck gave little material data so Abdel Rahmen used Mueller's estimate(117) for the tensile strength. In order to make the analysis directly comparable the author used the same figure, but it is improbably low for the quoted compressive strength which probably explains why Abdel Rahmen's analysis under-estimates stiffness. At low loads, the present study under-estimates stiffness still more. This might be expected because of the torsionless elements, particularly as the principal moment direction in the critical area is at 45° to the elements, the worst possible direction.

Both analyses give good predictions for the failure load. The present study is marginally conservative but this is not significant compared with material variability.

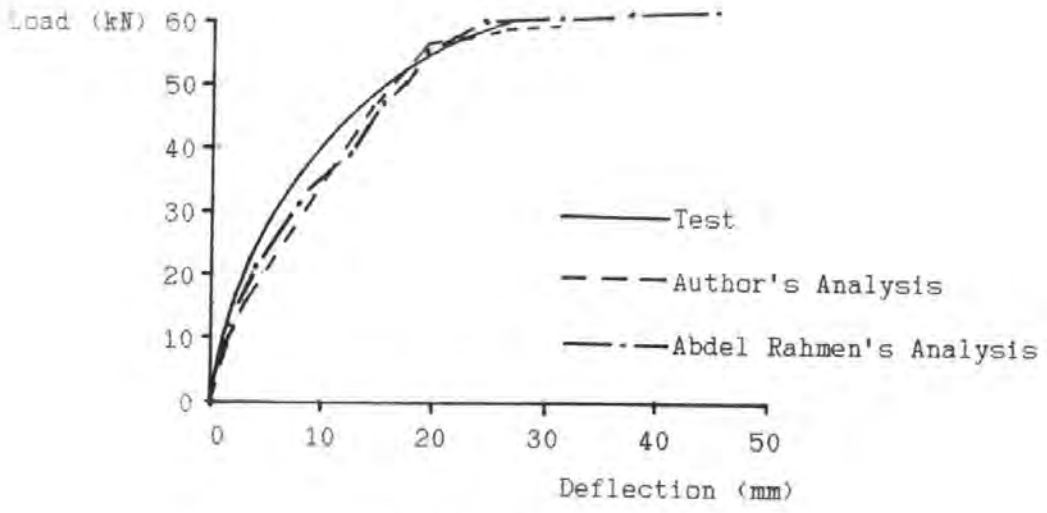

Figure 7.10: Analysis of Duddeck's slab 1

Duddeck's second and third slabs had the same total quantity of steel as the first but in orthotropic arrangements. The results for the third slab, which had 1·0% steel in one direction and 0·4% in the other, are shown in Figure 7.11. Abdel Rahmen's results for this are far less satisfactory; they significantly over-estimate the strength. In contrast, the present study gives better results for this slab than for the first. Both these changes are due to the fact that, as failure approached, the direction of maximum principal moments rotated towards the direction of the heavier reinforcement. Since the use of torsionless elements in the present study means that the principal moments in the analysis act in this direction from the outset, the rotation improves the realism of the analysis. Conversely, Abdel Rahmen's analysis correctly predicted that the principal moments in the uncracked slab, and hence the initial cracks, would be at 45° to the reinforcement. However, it assumed that the crack direction was then fixed. As failure approached, and the principal moment direction rotated, the shear retention factor in the analysis gave a significant shear stress across these cracks which implies a significant tension in the reinforcement direction. In fact, new cracks formed which were approximately perpendicular to the secondary steel and, as this steel yielded, they became very wide. Thus the real concrete was incapable of resisting tension in this direction so the slab was weaker than Abdel Rahmen's analysis suggested. Cope and Cope(94) have shown that this fault can be avoided, either by using a shear retention factor which becomes very low at high smeared tensile strains or by using a rotating axis material model. However, Abdel Rahmen failed to identify the cause of the error and it illustrates the danger of using this form of analysis in the design of even simple slabs without some calibration against tests.

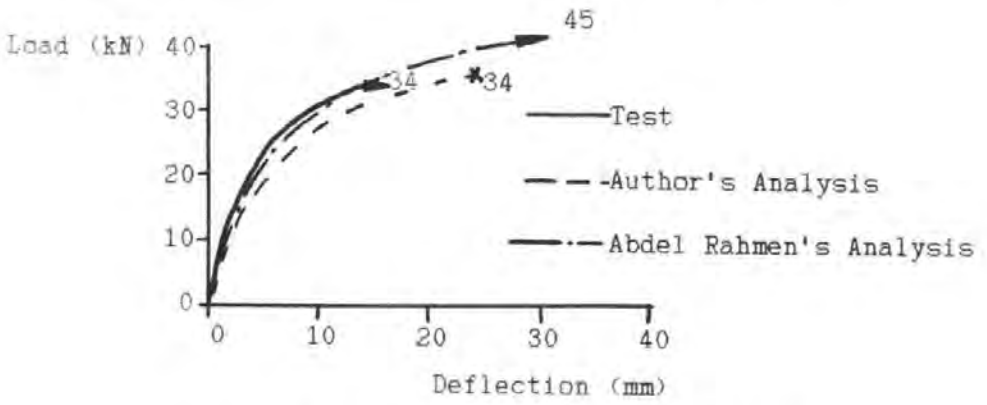

Figure 7.11: Analysis of Duddeck's slab 3

Abdel Rahmen noted that both the tests and his analysis gave failure loads for all three slabs which were higher than predicted by yield-line theory. He attributed this to the contribution of the tensile strength of concrete. However, even with the tensile strength set to zero, the author's analysis gave failure loads which were higher than yield-line predictions. The reason for this is that, as in the slab strips considered in Chapter 6, the depth of concrete in compression was substantially less than the depth to the top steel. Thus the strength was enhanced by the *tensile* force in the top steel.

Although, with the top steel removed, the non-linear analysis gave almost identical failure loads to yield-line theory, it did not give the same moment distribution. At peak load, it predicted a moment in the element under the load which was substantially above the yield line value; the extra strength coming from a net compressive force on the element. This force was resisted by tension in outer elements which resisted lesser moments. Thus the analysis suggested that compressive membrane action affected the behaviour of even these unrestrained slabs. This appears to be confirmed by other test results. For example, Regan and Rezai-Jorabi(118) measured strains in the reinforcement of a one-way spanning slab subjected to a single concentrated load. The strains in the transverse reinforcement indicated that there was a very significant transverse curvature. Thus the longitudinal curvature must have varied significantly over the slab width; yet the strain in the longitudinal reinforcement did not vary significantly over slab width. The only possible explanation for this appears to be that the neutral axis depth varied across the slab width because of the compressive membrane force in the centre of the slab and the tension at the edge.

7.10.2 Taylor and Hayes' Slabs

Taylor and Hayes(55) tested a series of square slabs under single central concentrated loads. These enable the program to be assessed, by comparison with test results, for both restrained and unrestrained slabs.

a. Unrestrained Slabs

Taylor and Hayes tested a series of slabs with two different reinforcement percentages (0.9% and 1.8%) under patch loads of three different sizes. These were all analysed using both a four by four and a five by five node quarter model. A typical load displacement relationship is shown in

Figure 7.12. It will be seen that the displacements at low loads are predicted well. The two analyses gave very similar deflections but, because it modelled the stress concentration under the load, the finer mesh always gave a slightly lower failure load; the difference being greater with the smaller load patches and the heavier reinforcement.

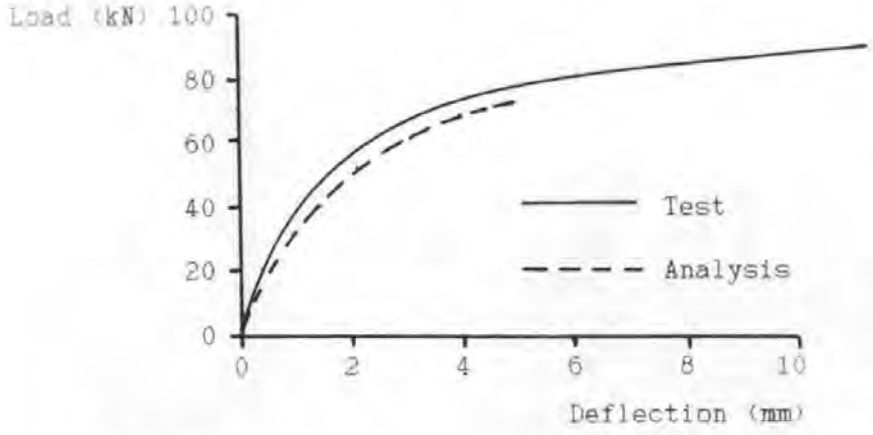

Figure 7.12: Analysis of Taylor and Hayes' slab 2S4

The predicted failure loads were generally lower than the actual failure loads, which is desirable in an analysis for design. However, the discrepancy was up to 30%, which might be considered excessive. Nevertheless, the analysis still gave failure loads which were typically 30% higher than are implied by the elastic analyses currently used in bridge design. Thus, even though arguably excessively conservative, the use of the analysis in bridge design would still lead to significant economies compared with current practice.

Although the ratio of predicted to actual failure load was reasonably consistent, with a coefficient of variation of approximately 7%, a systematic fault could be observed in the results; the analysis under-estimated the effect of load patch size. It gave errors in the unsafe direction in only one case; the heavily reinforced slab with the very small load patch. This was a rather extreme example with a load patch only 50mm across, compared with the slab thickness of 75mm. This, combined with the heavy reinforcement, resulted in very high stresses round and under the loaded area at failure. The calculated shear stress on the critical section at the face of the load reached $6N/mm^2$ and the vertical stress under the load was $31N/mm^2$. It is thus not surprising that an analysis which ignores these stresses over-estimates the strength. However, an alternative explanation is that since even the finer mesh gave

elements which were over twice as wide as the load patch, the analysis had failed to model the stress concentration round the load. To test this, the slab was re-analysed using a nine by nine node quarter model. This gave a significantly lower failure load, below the actual value. For other slabs, with larger loaded areas, it gave only a very slight reduction in failure load. It thus appears that in order to correctly model failure load without a separate shear check there is an additional criterion for the size of the elements in the critical area; they should not be much bigger than the loaded area. This criterion would be difficult to comply with in the analysis of complicated structures. However, further tests showed that a rather coarser mesh can safely be used if the concentrated load is applied at a single node, rather than being distributed in an attempt to model the patch size as it was in the analysis of Taylor and Hayes' slabs.

In contrast to Duddeck's slabs, the failure loads for Taylor and Hayes' unrestrained slabs were lower than predicted by yield-line theory. They said that this was because the slabs failed in punching shear, rather than flexure. However, the analysis suggested that the failures were essentially brittle bending compression failures. Because of the lower grade concrete (typically 30N/mm^2 compared with 43N/mm^2), as well as the higher steel percentage, the slabs were effectively far more heavily reinforced than Duddeck's. However, they were still only just outside Petcu and Stanculescu's(79) ductility requirement for using yield-line theory. The analysis predicted, apparently correctly, that the behaviour would be less ductile than Petcu and Stanculescu assumed because the critical section, under the load patch, would be subjected to a net compressive force. This effect does not appear to have been considered previously, apparently because this type of failure has been attributed to shear. The analysis slightly over-estimated the detrimental effect of this loss of ductility on strength. Other reasons why the analysis was conservative for these slabs, and more so than for Duddeck's, include the under-estimate of concrete crushing strength due to ignoring the multi-axial stress state (which has a greater effect in a more heavily reinforced slab), the torsionless elements' failure to model the diagonal hogging moments in the corners (which do not arise in a corner supported slab) and the use of a finer element mesh relative to load patch size in analysing Taylor and Hayes' slabs. Despite all these faults, the analysis

was entirely satisfactory from a design point of view and its use would lead to significant economies compared to current practice.

b. Restrained Slabs

In addition to the unrestrained slabs, Taylor and Hayes tested restrained slabs. They tested a series to match the unrestrained set plus a set of otherwise similar unreinforced slabs. These were also analysed and typical results are shown in Figure 7.13.

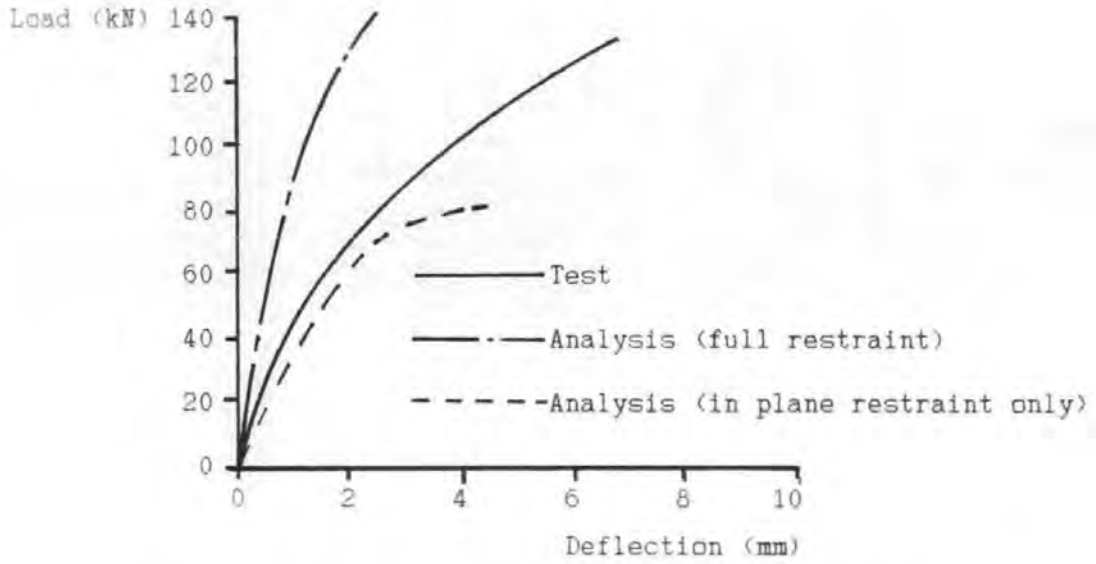

Figure 7.13: Analysis of Taylor and Hayes' slab 2R4

In the tests, the restraint greatly increased the failure loads. The initial analysis predicted a much smaller effect. This appears to be due to differences between the real and assumed restraint conditions. Taylor and Hayes used a steel frame to provide the restraint and the slab was inserted just prior to the test, the gaps being packed out with mortar. This was apparently intended to give full in-plane restraint with negligible rotational restraint so these restraint conditions were used in the analysis. In fact, there clearly was significant rotational restraint; hence the greater than predicted increase in strength. However, when full rotational restraint was used in the analysis, it over-estimated strength. It appears that the steel frame gave partial restraint to both in-plane and rotational movement. This could not be predicted satisfactorily by the analysis.

7.10.3 Batchelor and Tissington's Specimens

The analysis of Taylor and Hayes' slabs confirmed, as had been found in designing the specimens for Chapter 6, that it is difficult to produce known restraint conditions artificially. It therefore appeared that it was not possible to check the analysis of compressive membrane action for simple laboratory specimens before going on to use it to analyse complicated bridge structures. However, Batchelor and Tissington have tested a series of simple bridge models with only two beams each and these provided a useful intermediate case. They also had the advantage of having been analysed by Cope and Edwards(99) so they enabled the analysis to be compared with a plate type finite element program.

Batchelor and Tissington's largest specimen is illustrated in Figure 7.14 and the load-deflection response under a single central load is illustrated in Figure 7.15. It will be seen that Cope and Edwards' analysis gives good results whilst the author's, as expected and intended, is conservative.

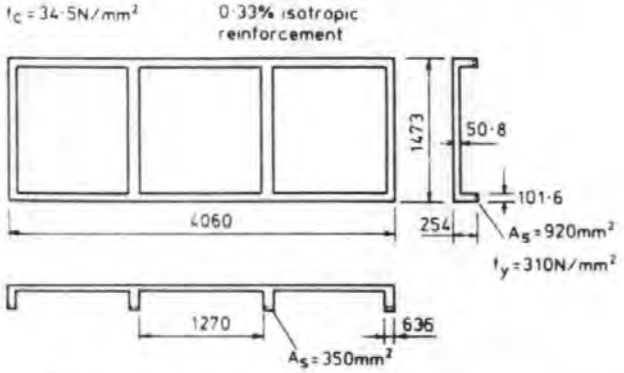

Figure 7.14: Batchelor and Tissington's specimen

The analysis also gave good predictions for the cracking response. It predicted cracking due to hogging moments along the edge of the slab, where these moments are resisted only by torsion in the beams. It also predicted, as observed in the tests, that just before peak load was reached the main beams would crack right through under the restraint forces.

Unlike Taylor and Hayes' slabs Batchelor and Tissington's, with their large span to depth ratio, reached deflections which were significant compared with their thickness before failing. Thus the displacements had a significant effect on the lever arm at which the restraint force acted. However, in order to make the analysis directly comparable with Cope and Edwards', the correction for this, which was described in 7.6, was not used in the analysis shown in Figure 7.15. The analysis was, however, repeated

with the correction. This increased the deflection at a load of 20kN by only 1% and at 30kN by 6%. However, it reduced the failure load by some 25%. This implies that both the author's and Cope and Edwards' analyses under-estimated the basic static strength of the slab. This may have been due partly to under-estimating the material strengths since Batchelor and Tissington gave little data for this; for example, they gave no indication as to whether the reinforcement strain hardened.

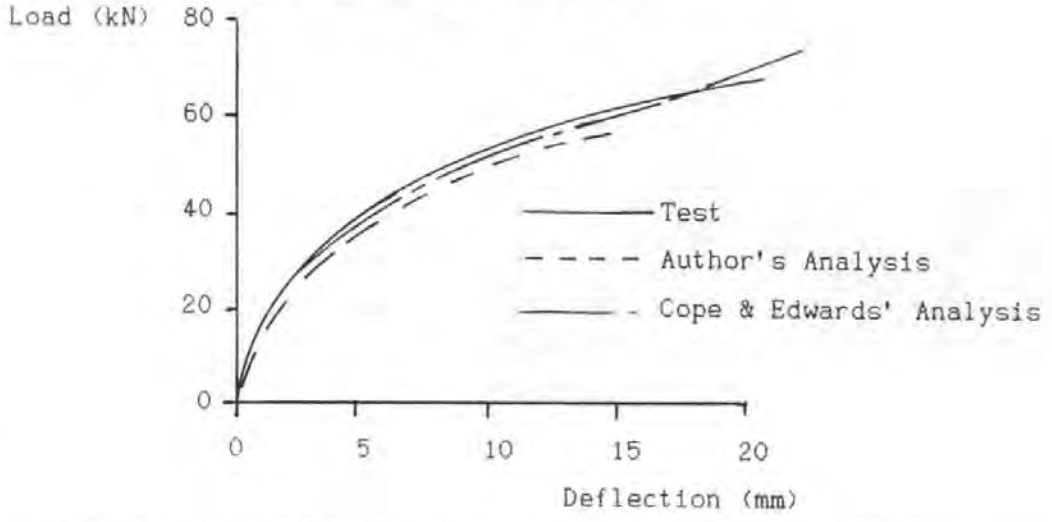

Figure 7.15: Analysis of Batchelor and Tissington's Specimen

7.10.4 Kirkpatrick's Model

Kirkpatrick's bridge model, which was considered in Chapter 3, enabled the program's prediction of local bridge deck slab behaviour to be compared both with test results and with Cope and Edwards' analysis.

A major problem with the analysis of this type of structure is the size of the computer model required. In order to model local effects safely the element mesh has to be fine. In order to obtain the correct restraint the whole of the bridge should be represented, even in an analysis for local effects. To reduce the computer time required, a half model was used which restricted it to the analysis of symmetrical load cases. The computer model was also banded so that only the half of the loaded slab span was modelled with a fine enough mesh to represent local behaviour. Despite this, a model with 288 nodes was required. The banding, combined with the variety of reinforcement areas and different slab spans used by Kirkpatrick, meant that the model required 53 element types.

The result of the analysis of bay C2, which had 0.5% reinforcement, is shown in Figure 7.16. The analysis gave conservative predictions for

deflection and strength. It was slightly more conservative than Cope and Edwards', although this was partly due to including the effect of large displacements. The analysis of bay A2, which had 1.7% reinforcement, also gave conservative deflection predictions but over-estimated failure load by some 10%. Although a 10% error would normally be considered acceptable, as it is small compared with the variability of concrete behaviour, in combination with the 20% under-estimate for C2 it indicated that the program over-estimated the effect of increasing the reinforcement percentage. However, a study of the results revealed that much of the increase was due to the contribution of the top steel, not only in tension over the beams but also in compression under the load. The latter is unusual; in a thin bridge deck slab the cover required usually means that the steel on the compression face is too near the neutral axis to make a significant contribution.

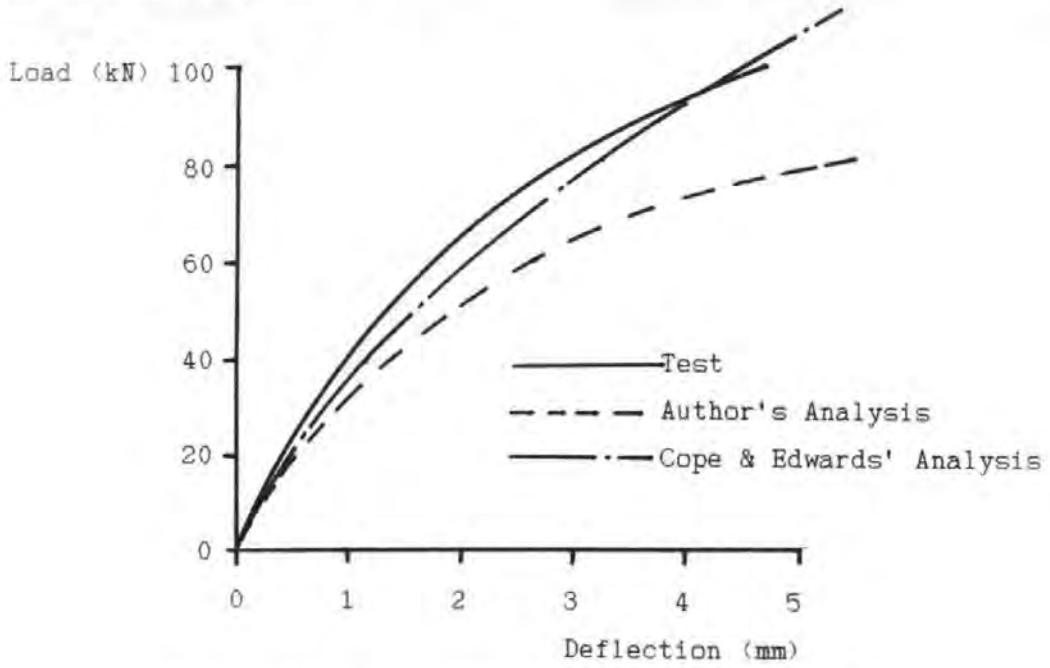

Figure 7.16: Analysis of Kirkpatrick's panel C2

The steel in Kirkpatrick's model was given only 6mm cover which is equivalent to 18mm at full size; approximately half the cover required by BS 5400. Kirkpatrick was careful to maintain and check the bottom cover but attributed less significance to the top cover. Thus the true top cover is uncertain and the effect of the top steel is very sensitive to its position. The steel would need to drop only a few millimetres to explain the discrepancy. Another effect of having significant compression steel is that, unlike the other analyses, the analysis of this bay was

sensitive to the assumption made for the stress in concrete at high compressive strains. Other analyses failed soon after the compressive stress in the critical region started to reduce. However, in this bay the load continued to increase as compressive force transferred to the reinforcement. Thus the unsafe prediction could have been avoided by using a concrete model which gave an abrupt reduction in stress at a relatively low strain. This may explain why the tendency to exaggerate the effect of reinforcement was less pronounced in Cope and Edwards' analyses. The greater ductility given by the relationship shown in Figure 7.6 may be more representative of the behaviour of concrete loaded uniaxially under displacement control. However, the critical concrete in these slabs was subjected to biaxial compression and also to shear which reduced its ductility. Thus it may be prudent, in the analysis of such a slab, to impose a limit on the strain at which concrete can carry compressive stress. A limit of approximately 0.0045, which is still higher than used in most analyses, would eliminate the unsafe prediction for this bay but have little effect on any of the other analyses. However, given that this bay had more effective compression reinforcement and as much tensile reinforcement as any practical bridge deck slab, the analysis can be considered safe for practical slabs despite over-estimating the effect of steel. It also appears, once again, that a flexural analysis has proved capable of predicting a "punching shear" failure. This suggests that the failures were primarily brittle bending compression failures, although the shear force did precipitate the final collapse.

Although the reasonably good predictions for the failure load of these slabs are reassuring, they have little practical significance. Kirkpatrick acknowledged that design should be controlled by serviceability criteria. Applying conventional BS 5400 stress criteria to the element forces from the analysis of bay C2 suggested an allowable service load of approximately 22kN. This compares with a design service 45 unit HB wheel which, at this scale, is 13.75kN. This is interesting as the reinforcement in this bay was similar to Kirkpatrick's eventual recommendation. Thus the analysis has given further support to Kirkpatrick's proposals. However, it remains to consider the influence of global transverse moments.

From Kirkpatrick's observations of the behaviour of his model, and of his full scale bridge, it would appear that, in the absence of any global effects, the behaviour of this bay would certainly be satisfactory under a

service load significantly above 22kN. Thus it may appear that the analysis was unduly conservative. However, to put this into perspective, it should be noted that a conventional analysis of this bay, using Westergaard and BS 5400, gives an allowable service load of only 9kN and implies a failure load of less than 14kN.

7.11 CONCLUSIONS

The form of analysis considered in this chapter gives satisfactory predictions for the behaviour of realistic slab structures. Provided an element mesh is used which is fine enough to model local stress concentrations around the applied loads, it appears to give safe predictions for the failure loads even of slabs which fail in "punching shear".

In some cases the analysis under-estimated strengths by up to 30%. The allowable service loads calculated from the analysis also appear to be conservative. However, despite this, the use of the program in design and assessment would still lead to significant economies compared with current practice.

CHAPTER 8

MODEL BRIDGE TESTS

8.1 INTRODUCTION

The analytical methods considered in Chapters 5 and 7 are potentially very useful, but they have not yet reached the point where they can justify radical changes in design practice without some calibration against tests. It was therefore necessary to perform some tests. These were designed to investigate the key areas identified in Chapter 3 as requiring further research; service load behaviour, restraint and the effect of global moments.

8.2 DESIGN OF MODELS

8.2.1 Scheme

Although small scale models have proved successful for predicting the strength of slabs(51), the cracking behaviour of concrete does not scale well. Thus, in order to obtain reliable predictions of service load behaviour, it is desirable to use the biggest practical scale. Ideally, full size models would be used. However, financial constraints on this project, combined with the need to model a whole bridge and a whole HB load, made this impractical. It was therefore decided to use half scale models of relatively small M beam type bridges. Analysis suggested that these were the type of structures in which global transverse moments would be most significant.

The first model, which is detailed in Figure 8.1 and illustrated in Figure 8.2, was designed to be a worst case for restraint so it had four beams (the minimum practical number for a bridge of this type), no parapet up-stands and no diaphragms. The last point is particularly significant since 3.2.8 noted that previous researchers have said that diaphragms are needed to provide the restraint, yet no tests have been performed on decks without diaphragms to confirm this. Also, analysis using the program described in Chapter 7 suggested not only that diaphragms were not needed to provide the restraint but also that, because of the effect illustrated in Figure 3.12 and discussed in 3.2.7, the slab near the ends of the bridge would be subjected to transverse compression when the full HB load was applied near mid-span.

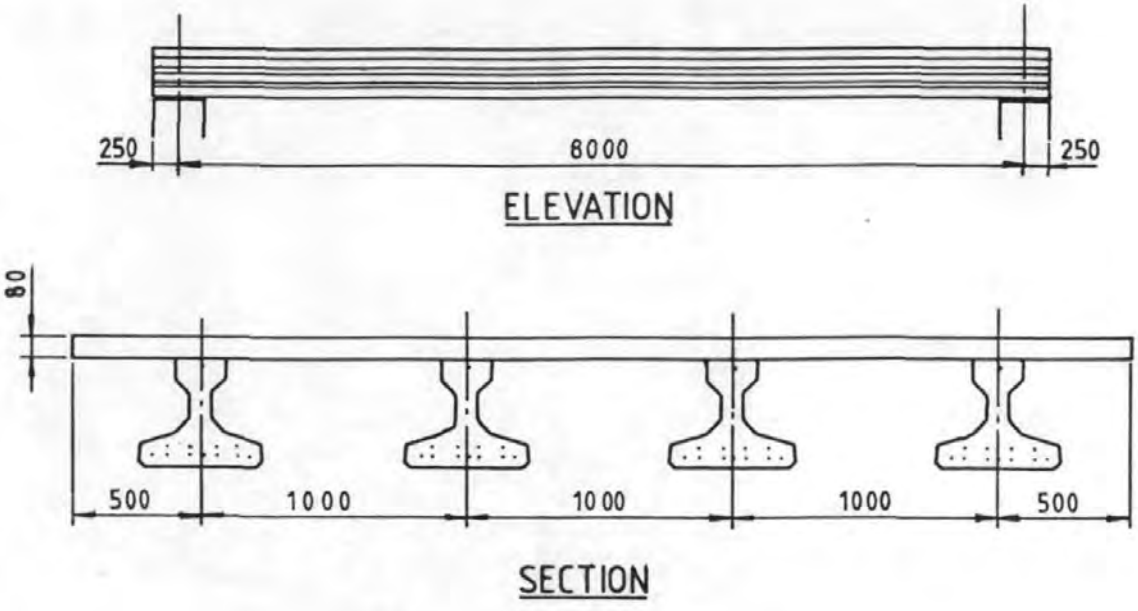

Figure 8.1: Details of first deck

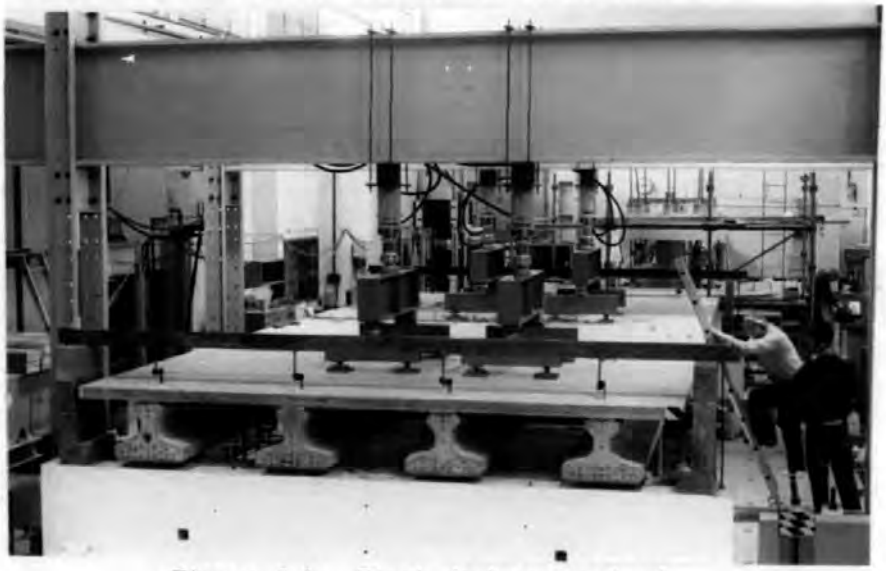

Figure 8.2: First deck under test

To give a worst case for local effects, the maximum practical beam spacing was used with the standard slab thickness, 160mm at full size. The spacing of the beams was limited by their shear strength under the design 45 unit HB vehicle and the slab's span to depth ratio, although greater than normal for this type of deck, was quite modest at 12.5. However, analysis suggested that larger, wider spaced beams would be a less severe test because of the smaller global transverse moments. As these moments were a key area requiring investigation, it was considered better to use a deck which was a severe case for these.

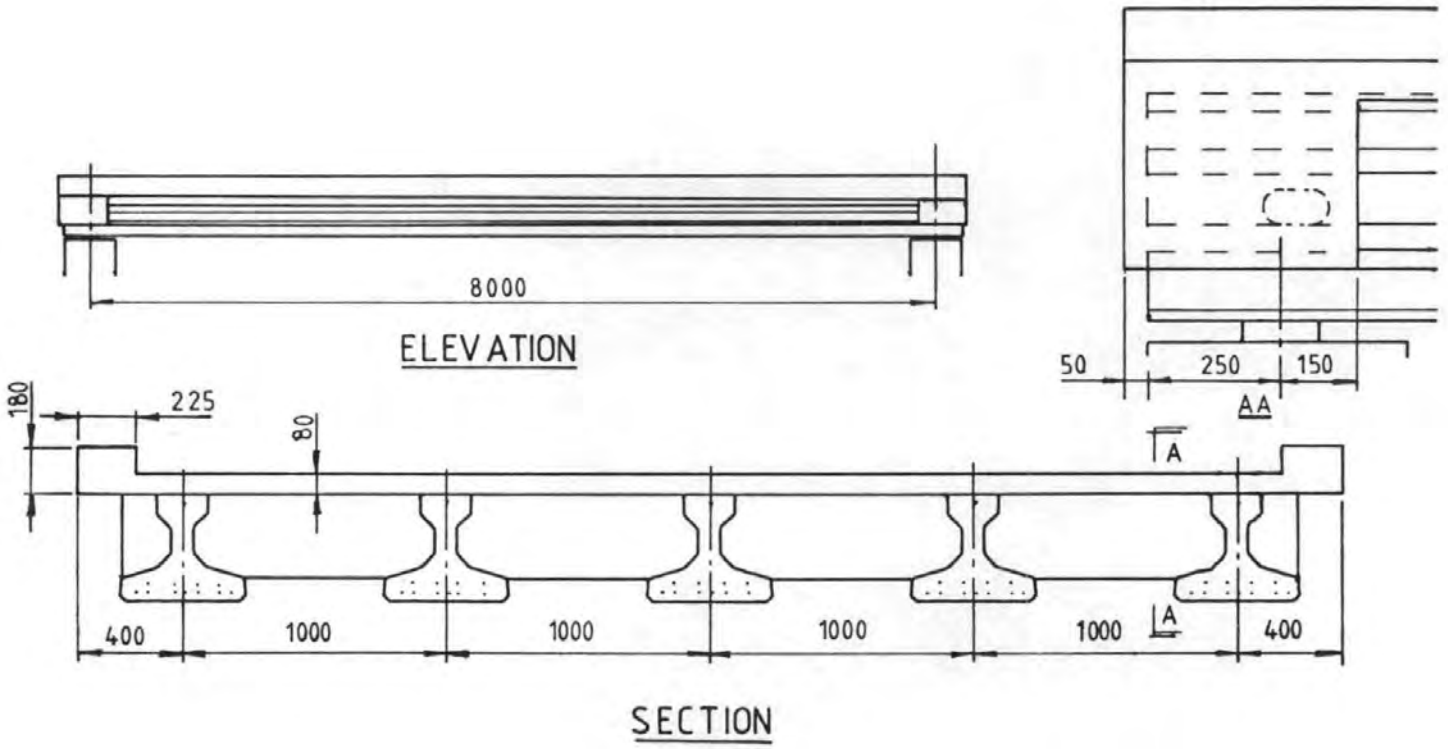

Figure 8.3: Details of second deck

The second model, which is detailed in Figure 8.3 and illustrated in Figure 8.4, was designed to be more typical of current practice so it had parapet up-stands, support diaphragms and an extra beam. The same beam spacing was used as for the first deck and the overall width approximated, at full size, to that of a two lane bridge with neither footways nor hard shoulders. It thus represented the narrowest bridge which is likely to be designed for 45 units of HB load. Although a narrow bridge is the worst case for restraint, analysis suggested that global transverse moments would have been greater in a wider deck. However, it was considered that the behaviour of a wider deck could safely be predicted with the aid of the results of tests on the deck and the program described in Chapter 7. It was not possible to test a wider deck in the laboratory.

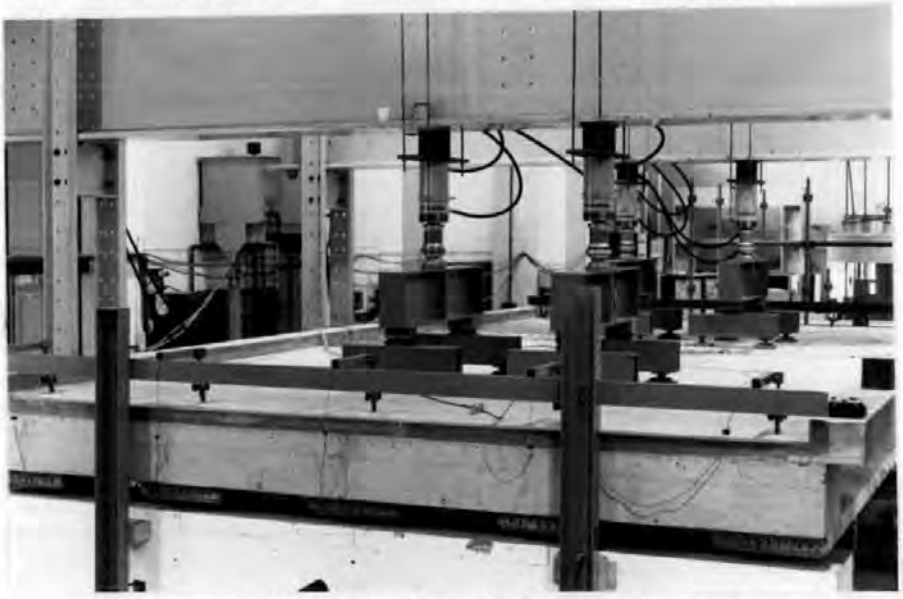

Figure 8.4: Second deck under test

After the two models had been tested, a single beam with the appropriate width of slab was tested on its own to help calibrate the analysis.

8.2.2 Beams

Since the slab behaviour was the main concern of the project, perfect modelling of the beams was not required. However, pre-tensioned beams were used so that the global behaviour was reasonably similar to that of the prototype bridge. Standard inverted T beams were used as approximate half scale models of M beams. These had the same advantage in the research project which they have in practice; the multiple use of formwork makes them much cheaper than specials.

In Figure 8.5 the section of the inverted T beam is compared with a true half scale M beam. The thicker web of the inverted T beam was considered an advantage as it was desirable to avoid shear failures. However, the lack of rebates for the slab formwork was a disadvantage, not only because they were needed to support the formwork, but also because their absence improved the support to the slab. Thus non-standard rebates were provided as shown in Figure 8.5.

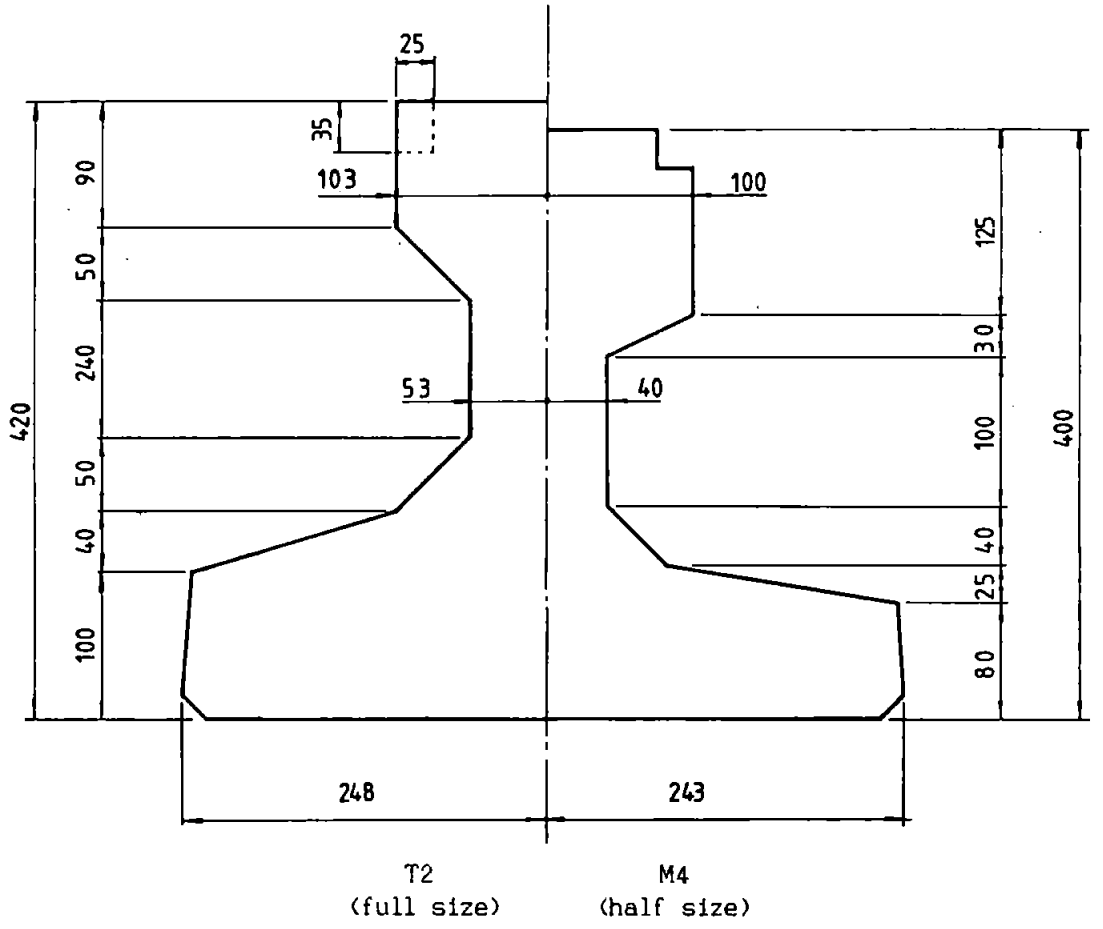

Figure 8.5: Comparison of full size T2 and half size M4 beams

When the design of the beams was fixed, which was very early in the project, it was considered desirable to avoid global failures so the beams for the first deck were provided with approximately 25% more prestress than the conventional BS 5400 based design method required. The beams for the second deck were provided with the same prestress which, because of the improvement in distribution properties due to the diaphragm, meant they had approximately 35% more steel than BS 5400 would have required.

Because of the interest in the interaction of global and local effects under service loads, it was desirable to provide a realistic beam size near

the minimum which could be used, within the code, for this type of deck. Thus the beam size was not increased to match the over-provision of prestress so the beams were stressed at transfer to a higher stress than would normally be allowed.

The shear reinforcement was designed to the normal BS 5400 rules. Because Hughes(119) has found that these are conservative for this type of beam, the shear reinforcement was not increased to match the over-provision of prestress.

The beams for the second deck were provided with standard transverse holes to accommodate reinforcement for the diaphragms. In order to get the diaphragms down to the correct scale size, the holes had to be nearer to the end than is recommended by Green(120), so extra links were provided to control the expected cracking.

8.2.3 Diaphragms

The diaphragms for the second deck were designed to the conventional BS 5400 rules. However, a considerable variety of approaches are used for calculating the torsional inertia used in the analysis to obtain the design moments. This significantly affected the design. It was decided to follow the recommendations of Clark and West(121) and use half the Saint Venant value for the gross-concrete section.

8.2.4 Slab Reinforcement

Because global behaviour and restraint were major areas requiring investigation, it was considered that using bays with different reinforcement percentages was undesirable. The more heavily reinforced bays would have provided extra restraint and distribution which would have given an optimistic impression of the behaviour of the lightly reinforced bays. This meant the choice of steel area was important.

The original idea was to provide the first deck with 6mm high tensile steel bars at 100mm centres (that is T6-100) main steel and T6-125 secondary steel in both faces. This compares with Kirkpatrick's recommendations(13) which are equivalent to T6-75 at this scale. However, later analysis suggested that even T6-100 was slightly excessive and it was decided to reduce the main steel to T6-125 as well. This meant the deck was 20% less heavily reinforced than the strips considered in

Chapter 7. However, since doubling the reinforcement appeared to have had little effect on the tension stiffening, this was unimportant. It appeared that the secondary steel could also have been reduced. However, smaller reinforcement was considered undesirable for practical reasons whilst 125mm was the largest spacing which complied with the code maximum (300mm at full size) and which kept the reinforcement spacing in phase with the beam spacing.

The reinforcement is detailed in Figure 8.6. The reason for providing an 8mm longitudinal bar over each beam was to provide a proper anchorage for the 8mm links projecting from the beams. Since these links stopped short of the edge of the top flange of the beam (as is usual because they have to fit inside the formwork when the beams are cast) it was considered that they would not greatly affect the slab's flexural behaviour and they were ignored in its analysis.

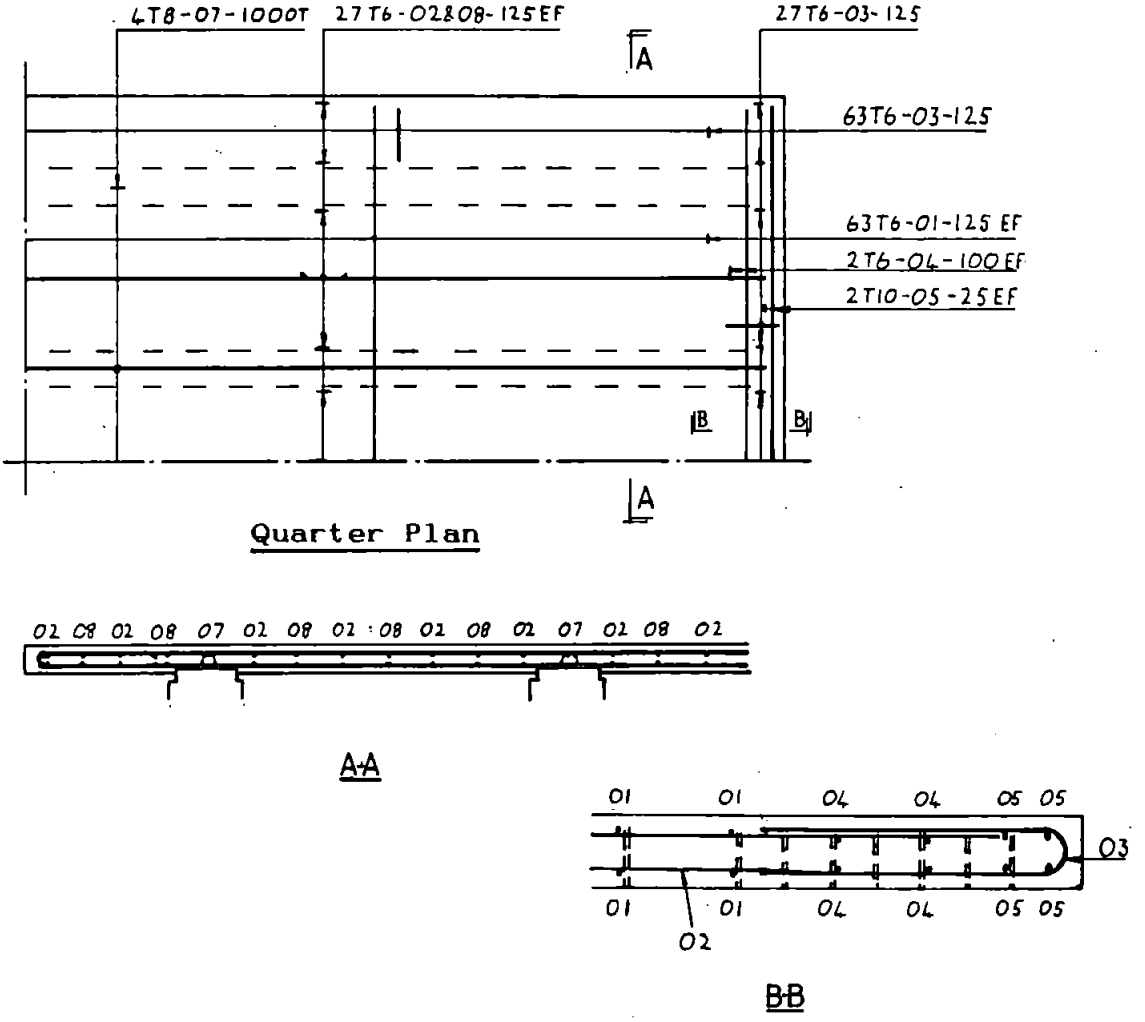

Figure 8.6: Detail of reinforcement in slab of first deck

The real bridge would have to support wheel loads right up to the end of the deck, where there were no diaphragms and where membrane enhancement would be reduced. It was therefore assumed that extra reinforcement would be required. It was also considered desirable to loop the secondary steel round these bars to provide the correct detailing for a free edge. Because of the very thin slab the resulting detail, which is shown in Figures 8.6 and 8.7, was slightly awkward.

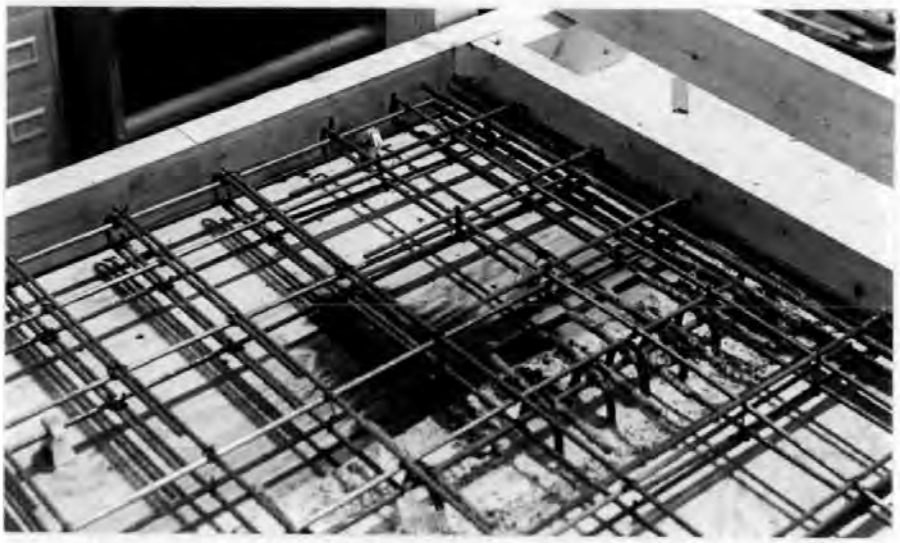

Figure 8.7: Reinforcement in corner of first deck

It was clear that the diaphragms in the second deck would make it stronger than the first. Since the first slab had behaved well, it was decided to reduce the steel area in the second. The opportunity was taken to look into the possibility of using only one layer of steel each way. This has advantages for durability, since it greatly increases the cover, and it also halves the steel fixing cost. It had been rejected by Beal(122) but it seemed probable that the thinner slab in the type of deck considered here would make it more viable.

The main steel was increased to T8-125 giving nearly 90% of the total steel area in this direction used in the first deck. However, since both the first test and the analysis suggested that the secondary steel would be very lightly stressed, this was not increased and just one layer of T6-125 was used.

One effect of diaphragms is to apply a support moment to the most heavily stressed beam. This relatively small moment is frequently ignored in design and the steel in the deck slab would normally be ample to resist it. However, the longitudinal reinforcement in this deck was so light that

it was necessary to provide some designed reinforcement to resist this moment.

It was also decided to use the second deck to conduct a small test, which has been described briefly elsewhere(123), on the effect of local reinforcement corrosion on deck slabs. To simulate the effect of severe local corrosion, eight adjacent main slab bars were cut right through at mid-span of the slab. This was done using using bolt croppers before the slab was cast. The position of the cuts was chosen so that the "damage" would have the minimum effect on the behaviour under the load case used for the initial failure test. However, it would be possible to conduct a service load test with one wheel of the HB vehicle immediately over the cut bars. It was also hoped to perform a failure test using a single wheel over the area if it was in reasonably good condition after the failure test.

8.2.5 Bearings

The beams were supported on normal commercial laminated bearings which were PSC"370132"(124); the smallest size of this type made. These had a greater movement capacity than a single span bridge of this type would require. As a result, they were less stiff than a true half scale model of bearings for a single span bridge. Their behaviour was close to that of the bearings which would be required for a two-span bridge.

The stiffnesses of the bearings were checked in the Mayes machine, first under concentric loading, which gave results very similar to the specified stiffness, then under eccentric loading to measure the flexural stiffness.

8.3 MATERIALS

8.3.1 Concrete

The mixes used for the deck slabs and for the other in situ concrete were similar to those used in the half scale beam strips considered in Chapter 6 and the nominal mixes are detailed in Table 8.1. The mix for the first deck used a realistic cement content but even with a high water content, giving a very wet-looking mix with a slump of some 100mm, it gave a 28 day cube strength of 44N/mm^2 obtained from 150mm cubes stored with the model. The cement content was reduced for the second mix giving a 28 day strength of 33N/mm^2 with a lower water content and a more typical slump of around 40mm. The change in properties between the two mixes was much

greater than the change in the nominal mix proportions would suggest. However, this was a consequence of the long delay between the tests (which meant that both the cement and the aggregate came from different batches) and the use of a normal commercial type batching plant without the advantage of using dried aggregate as in smaller scale tests.

Material	Quantity (per nominal m^3)	
	First Deck	Second Deck
5-10mm Thames Valley Gravel	875kg	905kg
Sand	900kg	930kg
Ordinary Portland Cement	300kg	275kg
Water	≈1651	≈1601

Table 8.1: Mixes for in situ concrete

Similar control specimens were used as for the beam strips considered in Chapter 6. In addition, two sets of six 150mm cubes were tested, one cured in a tank in accordance with BS 1881(125) and the other cured with the specimens. The second deck used 12 batches and a pair of cubes, one for each of these sets, was taken from every other batch. The test results are shown in Tables 8.2 to 8.4. The BS cured 150mm cubes gave higher crushing stresses than the dry cured cubes of either 70 or 150mm size showing that curing had a greater effect than size.

Because the beams were 500mm deep, compared with only 80mm for the slab, and because the precise reproduction of their behaviour was less important, it was considered acceptable to use 20mm aggregate for these so a normal commercial mix design was used. This is detailed in Table 8.5, and the results for the control specimens are given in Tables 8.6 and 8.7. Although the beams were cast in four separate pours, there was so little difference between the test results for the different pours they have all been considered together in the tables. Although it was nominally a 50N/mm^2 mix, the actual strengths were much higher with a characteristic strength of over 65N/mm^2. This arose in part from the specified minimum cement content and in part from the mix being designed to achieve transfer strength, 40N/mm^2, in the minimum time.

Age (days)	Test	Size (mm)	Number	Mean (N/mm^2)	Variation (%)
28	Cube	150	3	43.8	
	Cube (wet cured)	150	3	53.2	
61 (start of tests)	Cube	150 70	3 3	46.0 48.2	
	Indirect tension	150Ø 100Ø 50Ø	3 3 3	3.66 3.42 3.66	
	Elastic modulus	150Ø	1	27000	
90 (end of tests)	Cube	150 70	6 3	49.8 45.3	5.0
	Cube (wet cured)	150	6	60.3	1.6
	Indirect tension	150Ø 100Ø 50Ø	3 3 3	3.66 3.20 3.76	
	Indirect tension (wet cured)	150Ø	3	3.92	
	Elastic modulus	150Ø	1	29000	

Table 8.2: Test results for slab concrete from first deck

Age (days)	Test	Size (mm)	Number	Mean (N/mm^2)	Variation (%)
28 (start of tests)	Cube	150 70	6 3	33.4 33.0	5.2
	Cube (wet cured)	150	6	35.1	4.5
	Indirect tension	150Ø 50Ø	6 3	2.52 3.42	14.8
	Elastic modulus	150Ø	1	28500	
43 (end of test)	Cube	150 70	3 3	36.2 33.5	
	Indirect tension	150Ø 100Ø	3 3	3.01 3.20	
	Elastic modulus	150Ø	2	24400	

Table 8.3: Test results for slab concrete from second deck

Element	Test	Size (mm)	Number	Mean (N/mm^2)
Diaphragm (right-hand end of deck in figures)	Cube	100	3	34.2
	Elastic modulus	150Ø	1	23100
Diaphragm (left-hand end)	Cube	100	3	37.2
Parapet	Cube	100	4	33.3
	Elastic modulus	150Ø	2	23500

Table 8.4: Test results for other in situ concrete from second deck
(all tested at end of test; approximately 40 days old)

Material	Quantity (per nominal m^3)
10-20mm Crushed Limestone	819kg
5-10mm Crushed limestone	352kg
Fines; Crushed Limestone	629kg
Rapid Hardening Portland Cement	400kg
P2 additive	1.121
Water	≈1701

Table 8.5: Mix for precast concrete

Age (days)	Test	Size (mm)	Number	Mean (N/mm^2)	Variation (%)
2-5 (transfer)	Cube	100	8	43.6	6.0
28	Cube (wet cured)	100	12	71.6	2.6
180+ (start of tests)	Cube	150	3	70.1	
	Indirect tension	150Ø	3	4.08	
	Elastic modulus	150Ø	1	35500	
210+ (end of tests)	Cube	150	6	71.5	2.2
	Indirect tension	150Ø	3	3.92	
	Elastic modulus	150Ø	1	37900	

Table 8.6: Test results for precast concrete from first deck

Age (days)	Test	Size (mm)	Number	Mean (N/mm^2)	Variation (%)
2-4 (transfer)	Cube	100	8	43.6	6.0
28	Cube (wet cured)	100	12	71.6	2.6
320+ (end of tests)	Cube	150	5	72.4	2.4
	Indirect tension	150Ø	3	3.87	
	Elastic modulus	150Ø	2	39500	

Table 8.7: Test results for precast concrete from second deck

8.3.2 Reinforcement

The reinforcement for the deck slabs was GKN Tor-Bar in 6, 8 and 10mm sizes. The first of these sizes is no longer available commercially and sufficient steel was in stock for the main steel of the first deck only. For the remaining 6mm steel, all secondary steel, hard drawn wire was used. In order to give reasonably similar bond characteristics to the normal steel, this was specially indented.

Stress-strain curves for all the steel were obtained using the Mayes testing machine and these are shown in Figure 8.8 in which each line represents the average of three test results. The hard drawn wire had a significantly higher yield stress than the equivalent Tor-Bar. Although it appeared that this would have little effect on the behaviour of the slab because the secondary steel was lowly stressed, the different properties were modelled in the computer analyses.

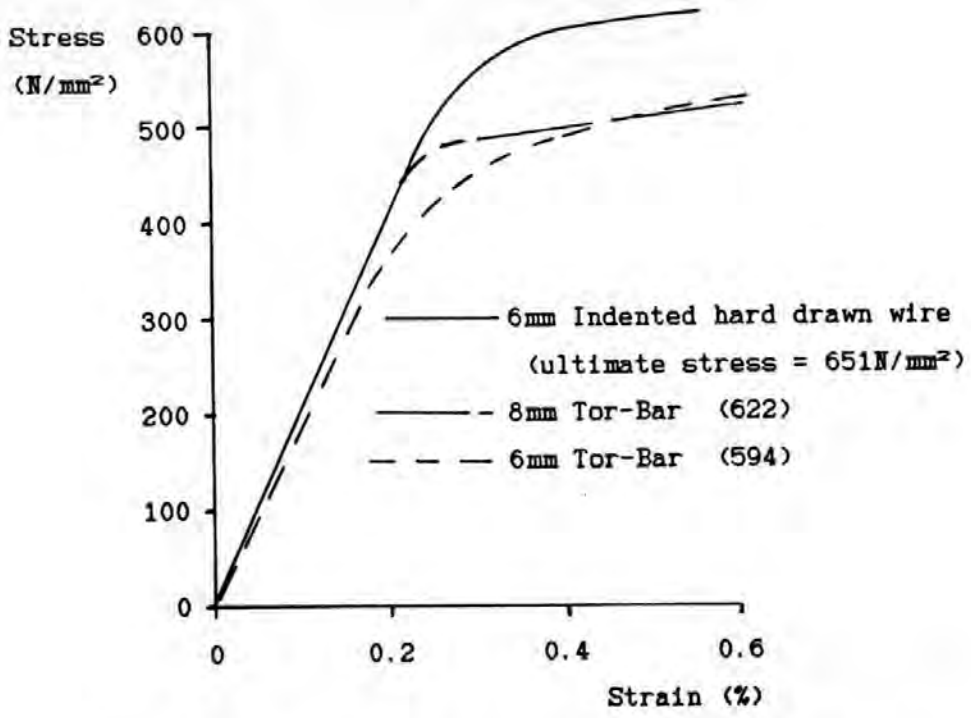

Figure 8.8: Stress-strain relationship for reinforcement

8.3.3 Prestressing

The prestressing was provided by 12.7mm Bridon Dyform strand stressed up to 70% of characteristic strength at transfer. It was intended to take a stress-strain curve for this using exactly the same procedure as for the reinforcement. However, two problems were experienced with this. Firstly the steel was too hard for the points on the clip-on 50mm gauge length strain gauge. It was therefore necessary to attach demec points with Plastic Padding as in the concrete tests. Secondly, the jaws on the machine caused premature failures. This problem could have been solved by using normal commercial wedge anchors but these would not fit in the jaws of the testing machine. It was therefore decided to obtain the material properties for the computer analysis from the 0.2% proof stress, the stress at 1% elongation and the ultimate strength given on the manufacturer's certificates. The results obtained in the laboratory were used only for the elastic modulus, E_s. In the event, this was the only important property since the structures failed before the steel was fully stressed.

8.4 CONSTRUCTION

The beams were cast by Costain Concrete, South Wales, in the normal commercial manner. Demec points were attached to the centre section of

the beams and were read before and after stressing, as well as at the start of the tests, to enable prestress losses to be estimated. The beams were transported to the laboratory, stored outside until required, and placed on the bearings in accordance with the bearing manufacturer's instructions(124).

The slabs were cast on plywood formwork supported off the beams. Thus the stresses due to the normal unpropped construction were reproduced but, because of the lack of deadweight compensation, they were under-estimated by a factor of two compared with a full size bridge.

In the case of the second deck, the diaphragms were poured first, then the slab and finally the parapet up-stands. In both cases, the deck slab was cast in one pour and this required some 12 batches of concrete, slightly more than would be used in a real deck where the batches would normally be $6m^3$ truck mixer loads. The concrete was placed by skip and Figure 8.9 shows the first deck under construction.

Figure 8.9: First deck under construction

It was considered very important to give the slab an even and correct thickness since analysis suggested that the local strength would be very sensitive to this. Two spare beams of each type were cast and those used were selected for equal camber. In the event the cambers of the beams, although greater than normal due to the high prestress, were unusually equal and this precaution was unnecessary. The formwork was adjusted to give as flat a soffit as possible and the concrete was finished using a

screeding rail which spanned the full width of the deck. After completion of the tests, the thickness of the slab was checked by drilling a number of holes and measuring through. The mean thickness of the 17 depths measured on the second deck was 79.65mm and although there was a significant variation, from 76 to 84mm (which was a considerably greater variation than was observed in the first deck), this appeared to be entirely random with the mean depths for four bays being 80.0, 80.5, 79.8 and 78.3mm. It was therefore decided to base the analysis on the nominal dimensions.

The top of the concrete was covered in plastic for seven days then uncovered whilst the soffit formwork was struck after a minimum of four days. Real bridge decks of this type are normally constructed using permanent formwork but access to the soffit was required to enable the cracking to be observed and the surface strain gauges to be attached. For the same reason, neither water-proofing nor surfacing were provided. This made the tests conservative and Cairns(82) has found that surfacing alone reduces the live-load steel stress by some 30%.

No attempt was made to match the curing conditions which would be experienced in a real bridge. The lack of permanent formwork or water-proofing, the small scale, the unusually wet concrete (particularly in the first deck) and the dry laboratory air all had the effect of increasing the shrinkage of the slab whilst the beams were rather older than usual when they were placed. Thus the shrinkage of the slab, and the differential shrinkage between the slab and the beams, was significantly greater than in a real bridge. Because of this, if (as has been suggested) shrinkage has an adverse effect on the development of membrane action, the test results would be conservative.

8.5 LOADING

8.5.1 Loads Applied

Since the slab behaviour was of prime concern, and since analysis indicated that HA load would have a relieving effect on the slab whilst dead weight would have an insignificant effect, only the HB load was applied with no HA load or dead weight compensation. These loads would have increased the moments in the beams, thus the degree of over-strength in the beams was slightly greater than that due to the over-provision of prestress.

The loading sequence was designed to first apply the design service HB load in a critical position, then to simulate the full load history due to the service life of a real bridge before returning the load to its original position. The service load would then be re-applied, enabling the effect of cracking and loss of restraint due to other load cases to be assessed. The load on the HB rig would then be increased until failure occurred.

Whilst the design static service load which should be applied to the deck was well established, and defined in BS 5400, the loading required to simulate the service life of a bridge was less clear. BS 5400 Part 10(126) defines fatigue loads. However, these are intended for use with defined fatigue relationships for steelwork details whilst the primary concern in this project was the cracking behaviour of the concrete. This is much more sensitive to small numbers of large load cycles, as has been found in Chapter 6. Thus if the fatigue loads had been used, they would have been used well outside the range for which they were intended or calibrated. When relatively small numbers of cycles are considered, the design fatigue loads can be locally more severe than the design ultimate load. This does not matter in normal fatigue assessment, since these small numbers of cycles have little effect on the cumulative damage calculations. However, it is clearly illogical to require a structure to resist a thousand cycles of a load in excess of design ultimate. Since bridge deck slabs are likely to be most sensitive to the few loads of near design service level which are applied in their life, it was decided to base the cyclic loads on BS 5400: Part 2 loads.

Unlike the long span HA loading, the HB loading and the short span HA loading, which are relevant to these decks, have no statistical base(127). It was therefore necessary to make some gross assumptions in order to decide how many cycles, and of what magnitude, to apply. It was initially assumed that the design service loads should have the same chance of occurrence as their long span HA equivalents; that is a 5% chance of occurring once in 120 years(127). This implied that only one cycle of this loading should be applied. However, it was decided to apply a more severe sequence to ensure that the tests would be conservative.

Another difficulty with simulating the load history of a bridge was that real bridges are subjected to rolling loads whilst the loading rig was only able to apply pulsating loads at discrete positions. In order to ensure

that this would be at least as severe as applying the intended load at all positions along the length of the deck, the test load was increased. A load of 1.2 times design service load was therefore applied to all the positions. The original intention was to apply two cycles of this load followed by 10000 cycles of a reduced load, simulating 25 units of HB (again with a 20% excess) then 100 cycles of design service HB. The significance of the 25 unit HB load is that it was used to represent HA in the then current loading standards(23,24). Finally, a cycle of 1.2X design service load would be applied, enabling the effect of the cyclic loads to be assessed by comparing the behaviour then with that under first loading. In the event, the 10000 cycles had very little effect so, after the first position, the number applied was reduced to 5000. However, because the critical parts of the slab were subjected to wheel loads under two different load positions, these were subjected to at least 10000 cycles of wheel loads.

The maximum load applied in the service load tests was approximately equal to the design ultimate load. This, combined with the nature of HB load (which is particularly severe for this type of structure and probably unrealistic), the lack of surfacing and the large number of load cycles applied, meant that the load history to which the bridges were subjected was excessively severe and made the tests conservative, as intended. However, Perdikaris and Beim's work(128), which was published after these tests were completed, suggests that rolling loads are more severe than fixed pulsating loads. They suggested that one passage of a rolling load could have the same effect on the fatigue life of a slab as 34 to 1800 cycles of a fixed load. As they considered the number of cycles to 60% of static strength to cause failure, whilst the tests considered here are investigating the effect of cycles of service load level, their conclusions may not be applicable here. Also, the difference they observed appeared to be related to the crack patterns; pulsating loads gave local radial patterns whilst rolling loads gave extensive grid-iron patterns. This was a consequence of the use of large single wheel loads. Under the HB service loads used in the author's tests, the cracking extended over a greater length of the bridge but was purely longitudinal. There is thus no reason to anticipate that rolling loads would have led to a fundamentally different crack pattern. However, even if (as Perdikaris and Beim suggested for this type of reinforcement) one pass of a rolling load was equivalent to 34 cycles of a static load, the use of 20% over-load

meant that the load history used was still conservative. One application of 1.2X design service load had more effect than 100 applications of design service load.

8.5.2 Loading Rig

The 16 wheels of the HB load were loaded by four one-hundred tonne hydraulic jacks acting through spreader beam systems which are illustrated in Figure 8.10. The four jacks were interconnected and connected to a hydraulic pump system which enabled cyclic loads to be applied. This system was rated at only 40% of the hydraulic pressure for which the jacks were designed. Although this enabled a load of 400kN per jack to be applied, equivalent to 2.7 times the design ultimate load, calculations suggested that a slightly higher load would be required to fail the deck. Separate hand pumps were therefore provided for the final failure test.

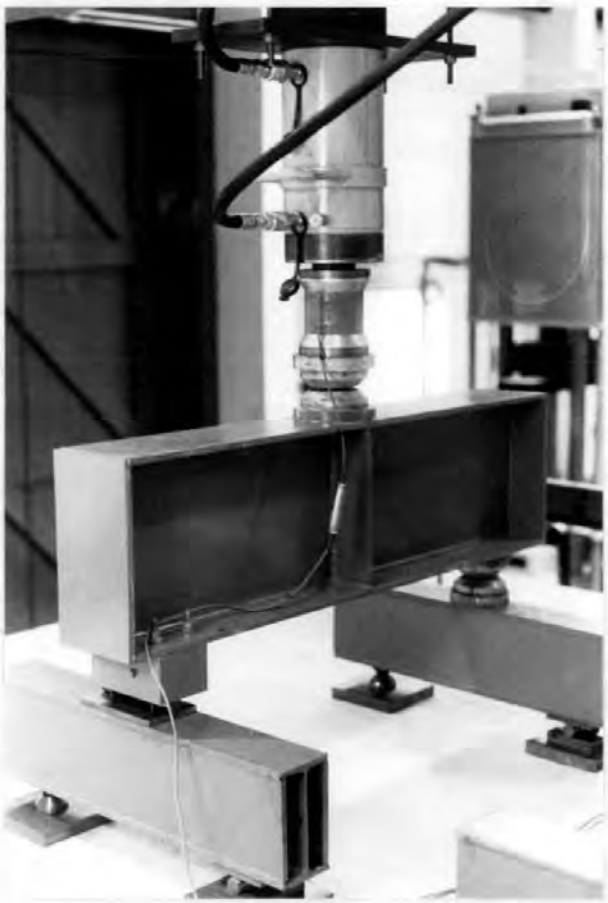

Figure 8.10: Spreader beam assembly

The jacks reacted against two large steel universal beams which were supported by double channel stanchions bolted down to the strong floor of the laboratory. The loading frames can be seen in Figure 8.2. Because the anticipated loads were close to the calculated capacity of the floor, it was necessary to position the bridge to minimise the moments in the floor under the load case which would be used for the failure test. It was also desirable to spread the load on each leg of the frame evenly between four floor bolts. Since the standard spacing of the HB bogies did not match up with the bolt centres, it was only possible to achieve this for the legs of one of the bogies. The load from each of the other two legs was therefore spread unevenly amongst six bolts.

The HB bogies could easily be moved sideways to any required position by moving the spreader beams and jacks. However, to move them longitudinally it was necessary to move the whole loading frame. It could have been moved to any position but this would have required a re-arrangement of the anchorage system. In practice it proved adequate to move the bogies only by multiples of the bolt spacing.

8.6 INSTRUMENTATION

The loads were measured using four 800kN load cells located below the jacks. Separate figures were recorded for the four cells but no facilities to adjust the relative loads were incorporated in the system.

A 50mm travel linear voltage displacement transducer was provided under the centre of each beam. In addition, 10mm travel transducers were provided over each bearing and under some wheel positions. The transducers under the wheels were supported off the top flanges of the beams and thus measured only the slab displacement relative to the beams.

Vibrating wire strain gauges were used both on the surface and in the concrete at selected positions. These have the advantage of remaining stable over long periods, which was important as it was intended to record the total strains due to the application of several different load positions. However, their strain capacity was not sufficient to use them to measure smeared strains in cracked concrete. Thus "portal" gauges developed by Cook(129) were used in positions where cracking was expected. Because it was considered undesirable to estimate curvatures or extensions in concrete sections from top and bottom gauges with different gauge

lengths and other characteristics, portal gauges were also used in some positions where cracking was not expected.

A disadvantage of surface strain gauges is that because their thermal inertia is much less than that of the specimen, they are very sensitive to temperature changes; unlike demecs, the portals have a significant coefficient of expansion since they are made of aluminium. However, although the laboratory was not air conditioned, it proved possible to keep the temperature constant to within some 2°C for the tests for which the strain data was used. In order to avoid the problem of sunlight warming the gauges directly, all the blinds on the South side of the laboratory were closed for the duration of the tests.

Because portal gauges have not previously been used for long-term tests, it was decided to monitor their long-term performance using readings off demec points mounted as close as possible to each portal. The original idea was to use the portals only to record the change of strains during a test and to add these on to long term changes recorded by the demecs. In practice, the changes of reading in the portals were close to those in the demecs so this extra complication proved unnecessary.

The reinforcement under one wheel in the first test and two in the second was also strain gauged, using electrical resistance gauges. Unfortunately, some of these gauges were damaged during the construction of the deck and few of the results were usable.

Two gauge lengths were used for the portal gauges: 200mm for the beams, which is the largest size made, and 100mm for the slab. The latter length was a compromise between the requirement for a short gauge length, to monitor local peaks in the bending moment distribution, and a long gauge length to make the results comparable with smeared crack analysis. However, the latter objective was not achieved since the crack spacings were greater than 100mm. Thus it is more realistic to consider the gauges as indicating only the movement of individual cracks. Similarly, the gauges on the reinforcement represented only the strain at their particular location and were not directly comparable with smeared crack analysis.

All the electronic instrumentation, a total of 74 channels, was connected to a "Compulog" data logging system which converted the results to digital

strain, displacement and force readings before storing it on disc and tape for later processing. Some key strain and deflection readings, as well as the load cell readings, were printed out whilst the tests were in progress.

8.7 TESTS ON FIRST DECK

8.7.1 Global Service Load Tests

a. First Load Position

The loading frame was first positioned to apply the HB load in the position indicated in Figure 8.11. The design service load was then applied in ten approximately equal increments. The structure was carefully examined for cracks after each increment. However, despite studying the critical areas of the slab with an illuminated magnifying glass, no cracks were seen until the full load had been applied. Under the previous increment the strain measured by the portal gauge immediately under the wheel nearest the centre of the deck was 575 microstrain; some three times the strain at which cracking normally first becomes visible. This was partly a consequence of the thin slab and high strain gradient. However, this also applied to the half scale specimens considered in Chapter 6 which cracked at lower strains. Another explanation is that under the concentrated load the scope for stress redistribution, both by moment redistribution and by membrane action, was so great that the concrete in the critical area was effectively being stressed under strain control, even though the structure was loaded under load control. Thus the cracks did not become visible until the concrete stress had dropped significantly below the normal cracking stress.

The crack widths were measured using a crack microscope. Under full service load the maximum width, which occurred under wheel 10 in Figure 8.11, was 0.05mm; equivalent to 0.1mm at full size. This would certainly be acceptable in practice and may appear to be very small considering that conventional design methods implied that the slab should have failed by this stage. However, other studies, notably Kirkpatrick et al's(49), suggested that the slab should have been uncracked under this wheel load. The fact that the outer bay of the slab (where global transverse moments were less significant) was indeed uncracked, suggested that global transverse moments were the reason for this difference from Kirkpatrick's result.

After this test, the deck was unloaded and the cracks closed up so completely that they were invisible even using the microscope. However, Figures 8.12 and 8.13 indicate that the local strains and deflectionss under the critical wheels did not fully recover. The strain reading under wheel 10 was marginally greater than under wheel 9 and the reason for plotting the deflection under wheel 9 (rather than 10) in Figure 8.13 was that the displacement transducer under wheel 10 failed.

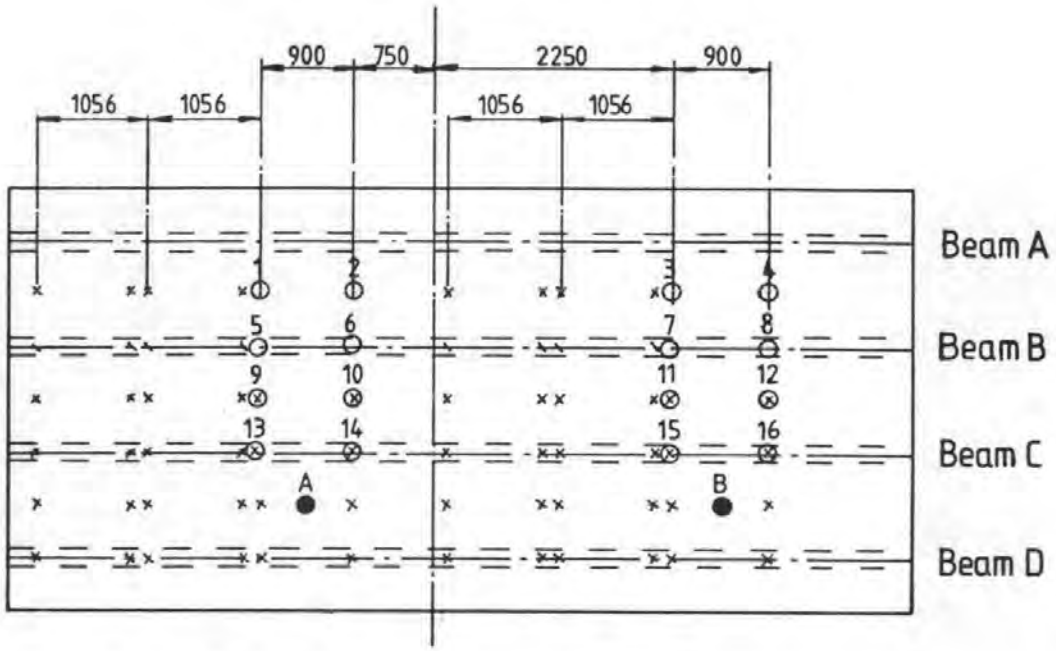

○ HB wheel positions for first and last service load test and for failure test.

× Other HB wheel positions.

● Single wheel test positions.

Figure 8.11: Load positions for first deck

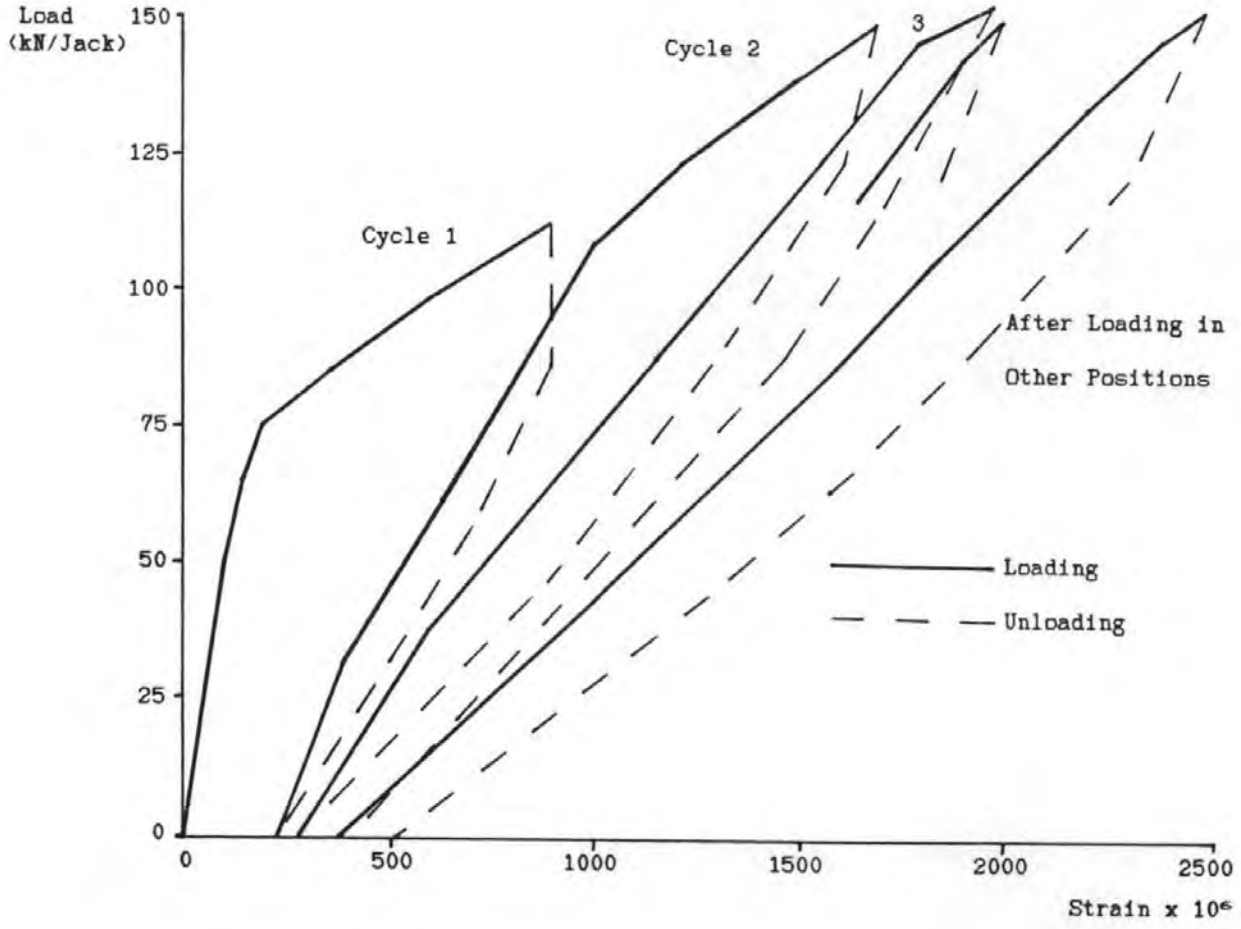

Figure 8.12: Transverse soffit strain under wheel 10
(Service load tests)

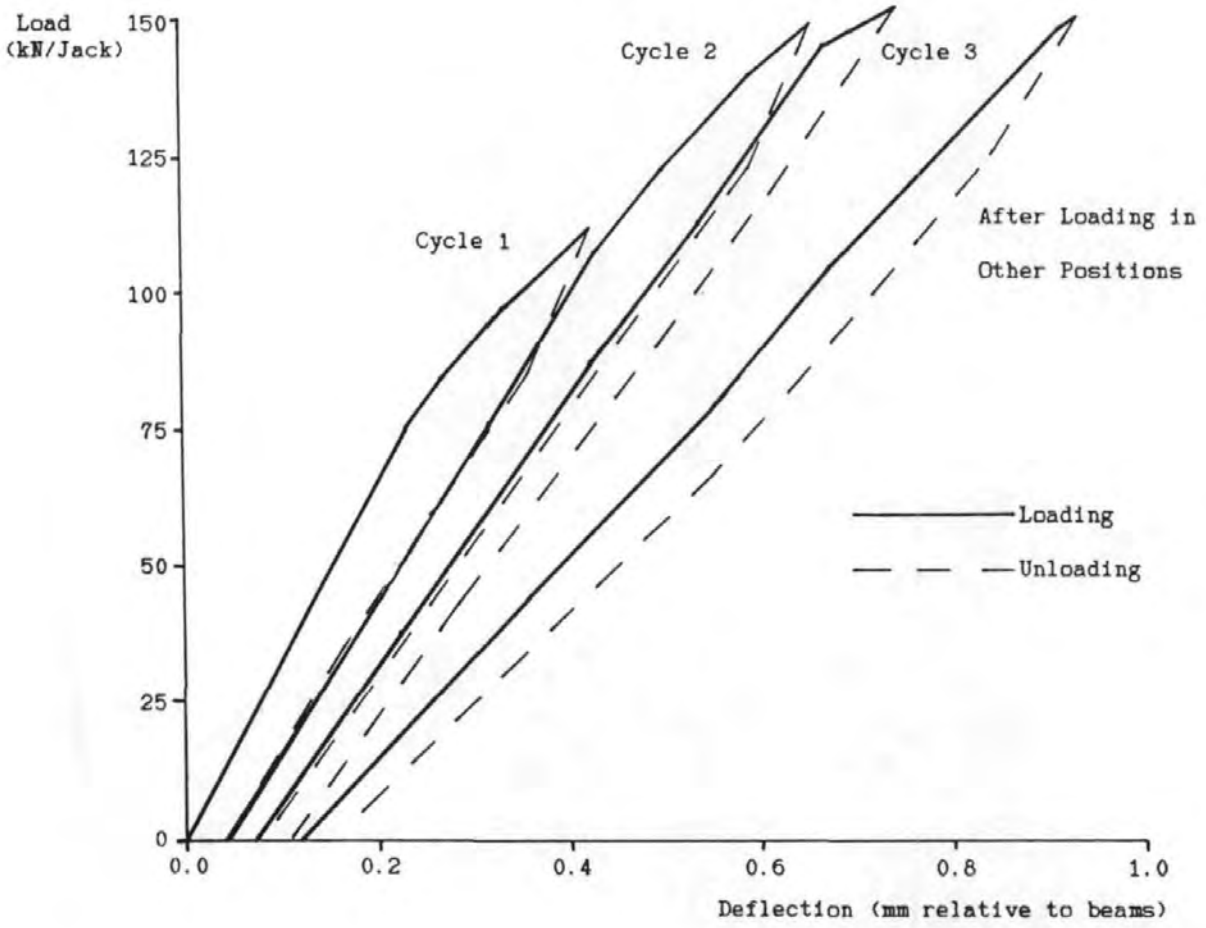

Figure 8.13: Deflection under wheel 9
(Service load tests)

The deck was then loaded to 1.2 times design service load. As the load increased above design service level, the cracks under wheels 9 and 10 grew longer and at a load of 140kN per jack they joined up. Under the maximum load (150kN/jack) the crack width under both these wheels was approximately 0.13mm whilst mid-way between them the crack was 0.08mm wide. Since the maximum crack width under the design service load had been less than 0.08mm, this (and the similar relationship between the strain readings) suggested that applying the increased load in this one position was at least equivalent, as far as this area of the deck was concerned, to rolling the service load 0.9m along the deck. If similar relative widths occurred in subsequent tests (which they did) this meant that applying 1.2 times service load in just the three positions along the deck illustrated in Figure 8.11 would be equivalent to rolling the service load along its full length.

After the cyclic loads described in 8.5.1 had been applied, a load of 1.2 times design service load was again applied. The change in the strains and displacements, compared with the load application before the cyclic tests had been performed, was so small that this application could not be plotted on Figure 8.13 without making it illegible and, for the same reason, only the peak part of this load cycle is shown in Figure 8.12. The strain measured at the start of the cycle was marginally smaller than that measured at the end of the second cycle to 1.2 times service load. Thus the 10000 cycles to "HA" service load plus 20% and 100 cycles to full HB service load had had a small effect on the behaviour compared with just two cycles to 1.2 times HB service load; the structure had actually recovered some of its strain whilst the cyclic loads were being applied.

Under full load, the cracks were not significantly wider than under the first load application and no cracks were visible on the top surface of the slab; the only visible cracks were the four longitudinal soffit cracks, one under each pair of wheels. On unloading, the cracks were again invisible even with the microscope.

b. Other Load Positions

On completion of the tests in the first position, the loading rig was moved sideways by 500mm. The same load sequence was applied in this and subsequent positions, except for the reduction from 10000 to 5000 cycles of the HA equivalent load. As can be seen from Figure 8.11 some of the

wheel positions in this load case were the same as in the first case. Thus cracks were visible under these wheels at a much earlier stage than in the previous test. Cracks were also visible in the newly loaded bay one load stage earlier than they had been in the first test. However, apart from this the behaviour was very similar.

On completion of these tests, the whole loading frame was moved along the deck by 1056mm to apply the HB load in the third position illustrated in Figure 8.11. The same load sequence was applied and the behaviour was similar. Because the instrumentation had been positioned to suit the first load position, the behaviour could not be monitored so closely. Crack widths were measured, however, and they were marginally greater than under the first load position; the maximum width being 0.15mm against 0.13. Since the first load position was a worse case for global effects, and both were identical for local effects, this suggested that the loss of restraint and distribution due to the cracking caused by the previous load cases was affecting the behaviour.

The same load sequence was then applied in the remaining positions illustrated in Figure 8.11. By the completion of these tests, all three bays of the deck slab had cracked along almost the full length of the bridge. However, these three cracks were the only cracks which had been seen. They were visible with a magnifying glass when the deck was unloaded, with a maximum width of 0.05mm and a more typical width of 0.02mm.

c. Return to First Load Position

For the final service load test, the loading frame was returned to its original position and the load was re-applied. As will be seen from Figures 8.12 and 8.13, the deformations were greater than under the first applications but still not excessive. The maximum measured crack width was 0.2mm which, as in all the tests, was slightly (25%) less than would be assumed from the strain gauge reading, indicating that the concrete on either side of the cracks was still under significant tension. The maximum crack width was equivalent to 0.4mm at full size, compared with an allowable width of 0.25mm in BS 5400: Part 4. However, that document only requires crack widths to be checked under a much lower load; 25 units of HB compared with the 1.2 times 45 unit load to which the model was subjected. Under the load used for crack width calculation, the measured

crack width was 0.12mm; the scale equivalent of 0.24mm compared with the allowable width of 0.25mm. Although it is unreasonable to expect this level of precision in crack width predictions, and a model is likely to under-estimate crack widths, the many conservative features of the tests which have been mentioned earlier mean that it is reasonable to conclude from this that the crack widths would be acceptable in a full size bridge. Thus, by this criterion, the service load behaviour of the deck was satisfactory although it clearly did not have the enormous margin of over-capacity which previous research implied it should have. Analysis, which will be considered in the next chapter, and also observation of the behaviour suggested that this difference was due to the global transverse moments resulting from the use of full HB load in this study, compared with only single wheels in other studies. However, it remained to prove conclusively that it was not due to the absence of the diaphragms recommended by others.

It was noted in Chapter 2 that crack widths are an unsatisfactory, and perhaps unnecessary, design criterion. However, by any other fundamental design criterion (such as permanent deformations) the behaviour was satisfactory. Similarly, the stresses estimated from the strain readings were well within the BS 5400 criteria. Thus the behaviour of this very lightly reinforced deck slab was clearly satisfactory. However, because of the over-provision of prestress and the conservative nature of conventional design rules for prestressed concrete, the lack of cracks in the beams did not prove that the distribution properties of the deck were either satisfactory or similar to those which had been assumed in the design of the beams. This aspect of the behaviour could only be investigated by detailed comparison with analyses and thus will be considered in Chapter 9.

8.7.2 Global Failure Test

After the service load tests had been completed, the design ultimate HB load was re-applied and the HB load was then increased in steps of approximately 25kN per jack, that is 17% of design ultimate load. The displacements of the beams are shown in Figure 8.14 whilst that of the slab under wheel 9 is shown in Figure 8.15. The loading to failure was not continuous and the points where the load was removed and re-applied are indicated by breaks in the plots in the figures.

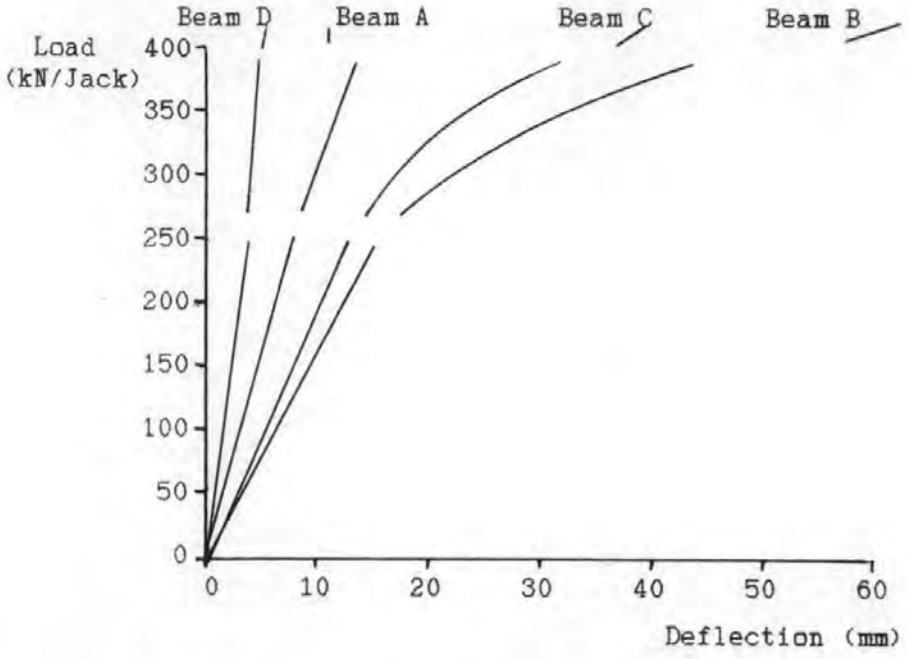

Figure 8.14: Beam deflections

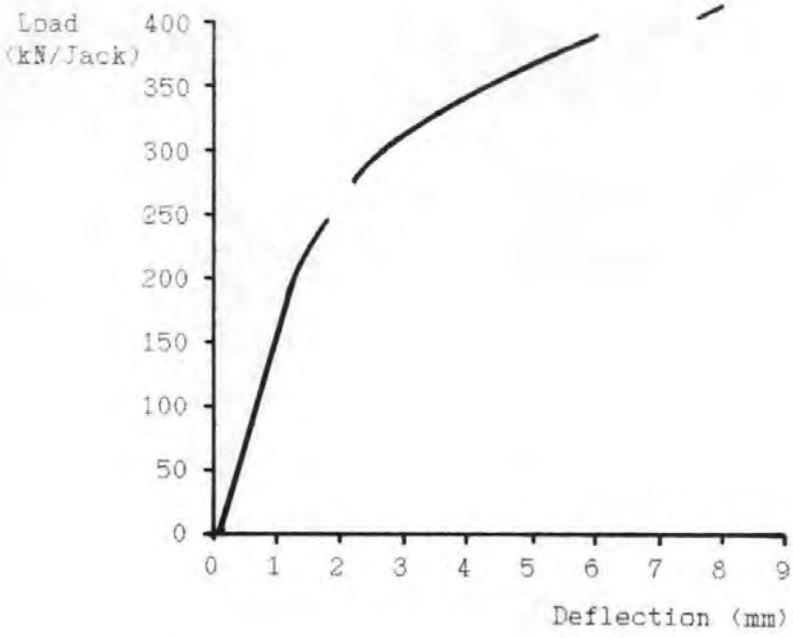

Figure 8.15: Deflection under wheel 9

As the load increased the longitudinal cracks under the slab grew wider but, at a load of 245kN per jack (1.67 times design ultimate), no new cracks were visible. At this stage the largest strain recorded by the portal gauges across the crack in the centre bay of the slab was 4600 microstrain, 80% higher than under design ultimate load, indicating (as will be seen from Figure 8.15) that the slab was beginning to depart from

the near linear behaviour it had exhibited since the completion of the service load tests. Even mid-way between the bogies, the strain across this crack was 1900 microstrain but, in contrast, the highest tensile strain recorded by the portals on the top of the slab over the edges of the webs of the beams was 300 microstrain adjacent to wheel 10. The gauge over the web of Beam B on the outside, that is adjacent to wheel 2, was reading 136 microstrain *compression* indicating that in this region the sagging moment due to transverse global effects was greater than the local moment. Longitudinal portal gauges positioned under wheels 9 and 10 were showing very small strains but that under wheel 12 showed 600 microstrain tension, the difference presumably being due to the lower global compression in this area.

A number of transverse strain gauges and demec points had been positioned in the slab near the expected points of transverse contraflexure in an attempt to estimate the membrane forces. Due to the small and erratic readings, the proximity of cracks and the transverse strains resulting from the Poisson's ratio effect of the global flange forces, these were extremely difficult to interpret. However, there did appear to be a transverse compression adjacent to the wheels.

After this load stage, the load was removed and there was over 80% recovery on all the significant readings. The load was then re-applied and increased further. At 250kN per jack, a shear crack appeared in the right hand end of Beam B (as shown in the figures) and a flexural crack was also just visible in the soffit of the same beam under wheel 6. Further shear and flexural cracks formed in the same regions at 275kN. At this stage, a shear crack also appeared in the right hand end of Beam C and in the left end of Beam B. There was also a very fine horizontal crack running along the outside of the web to Beam A adjacent to wheels 1 and 2, due to the beam's action in restraining the hogging moment in the slab. A second longitudinal crack had appeared in the soffit of the slab but still no cracks were visible on its top surface.

At 300kN per jack, twice design ultimate load, the first shear crack which had appeared in Beam B extended right through the bottom flange. What looked like shear cracks also appeared in the left end of Beam C between the support and wheel 9. However, cracks on the opposite side of the web sloped the opposite way, indicating that the cracks were largely due to

torsion although there were only the flexible bearings and thin deck slab available to resist, or apply, the torque.

Longitudinal cracks in the top of the slab also became visible at this stage. These then extended over most of the length of the deck on either side of Beam B and on one side of Beam C. A crack also appeared over the inside edge of the web to Beam A, adjacent to wheels 1 and 2, but this only extended a short distance either side of the bogie.

At a load of 2.39 times design ultimate (350kN/jack), the shear crack through the flange of Beam B became very wide with a vertical discontinuity of approximately 1mm across it. This was due to bond failure with the strands which could be seen to have drawn in by some 2mm. Since the strands used were larger in size and smaller in number than in a true half scale model, this may have occurred prematurely relative to a true model. The shear cracks are illustrated in Figure 8.16.

Figure 8.16: Shear cracks in Beam B

By this stage, flexural cracks extended over 2.2m of the length of Beam B and had also developed in Beam C. There were now five longitudinal cracks in the soffit of the outer bay of the slab under wheel 4. These fanned out beyond the wheel towards the beams and the end of the deck as illustrated in Figure 8.17. This (and less pronounced fanning at the far end of the same bay beyond wheel 1) was the only sign in the slab of transverse cracks or of the characteristic radial crack pattern observed by other researchers in single wheel tests.

Figure 8.17: Soffit cracks under wheel 4

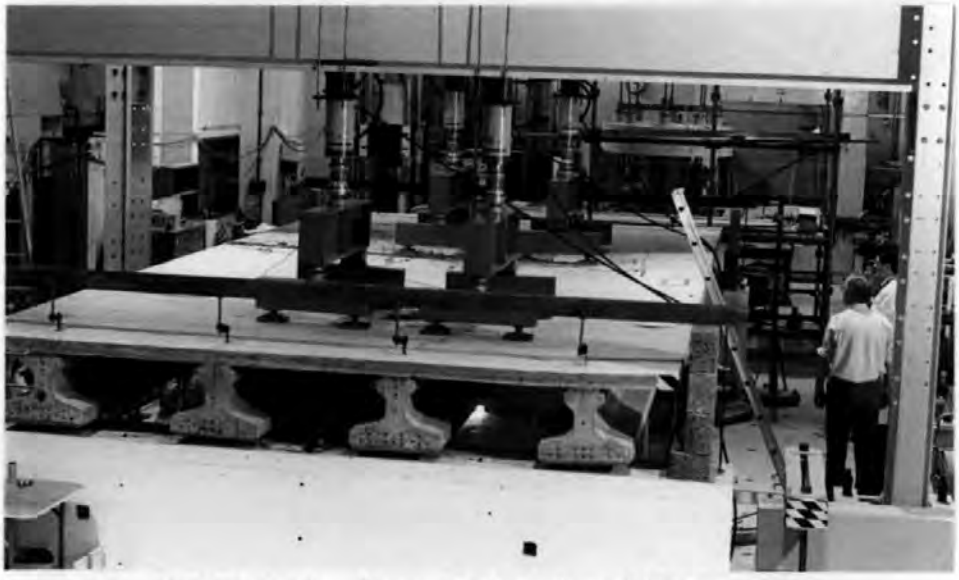

Figure 8.18: First deck under 400kN per jack

By this stage, Beam A had developed a substantial rotation which is visible in Figure 8.18. This was largely due to the differential deflection between the still uncracked Beam A and the much more heavily loaded Beam B. The local transverse hogging moment due to the wheels may have also contributed, but the crack pattern showed clearly that the slab was subjected to a net transverse sagging moment right out to Beam A adjacent to wheels 3 and 4. The slab in this region was thus contributing to restraining the rotation; the global transverse moment was dominating over the local moment. The rotation of the beam about its longitudinal axis, combined with the resulting transverse movement, was well in excess of the intended capacity of the bearing. At a load of 400kN per jack the

resulting transverse force became too much for the bearings under the other beams and the whole deck suddenly moved sideways by some 20mm. The resulting unintended eccentricity led to elastic torsional buckling in the main girders of the four load spreading rigs. The load was therefore removed and the structure recovered remarkably well; approximately 80% of the local deflections and 90% of the beam deflections. However, the maximum strain recorded by the gauge under wheel 10 reduced only from 11500 to 4400 microstrain.

On re-loading, the deck settled down to its new position but the buckling re-occurred so the load was removed again and the ball bearing under one end of the offending girders was replaced with a rocker bearing. Calculations showed that because of the low torsional stiffness of the girder (which had been the cause of the problem) the resulting unevenness of the load distribution between the four wheels would not be significant. The modified rig was therefore used for all subsequent tests, including the service tests on the second deck.

By this stage the limiting pressure of the electric pump had been reached so the loading was resumed using hand pumps. Because the sideways movement of the deck had moved the bearings off their seatings, the pronounced step in the plots in Figure 8.14 may have little significance; the displacement transducers over the bearings had come off their points so this could not be checked. However, there clearly was a deterioration in the distribution properties of the deck as well as in the stiffness of Beam B. The large differential deflections across the deck are clearly visible in Figure 8.19.

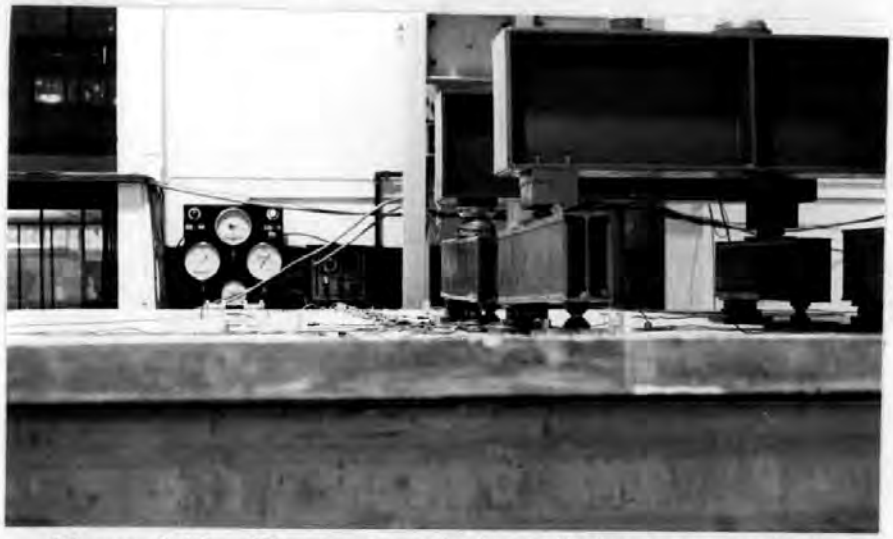

Figure 8.19: View across deck as failure approached

When the load level was only marginally higher than before, a number of "bangs" were heard from around the right hand end of Beams A and B; one so loud an observer assumed it to be due to rupture of the links either in Beam B (due to shear) or Beam A (due to separation from the slab). However, when the concrete was later broken out in this region, this proved not to be the case. It may have been due to further bond failure in the end of Beam B as the draw-in was now approaching 10mm.

By this stage difficulty was being experienced in holding the deck up to load, indicating that failure was imminent. The appearance of the right hand end of Beam B, combined with the loud bangs, suggested to some observers that this would take the form of a shear failure in this beam. However, a line of crushing concrete was just discernible between wheels 3 and 4. At a load of approximately 414kN per jack (2.83 times design ultimate) wheel 4 punched through the deck. The resulting release in the load on the beams caused the beam deflections to reduce; hence the wheel, although loaded only by a jack and thus under displacement control, punched right through the slab as shown in Figure 8.20, rupturing the steel as it went.

Figure 8.20: Failure; Wheel 4 punched through deck

The hand pumped hydraulic systems used for the two bogies were separate. The reduction in beam deflection caused by the failure therefore led to an increase in the load on the other bogie. Several minutes later, when a reading was taken, the load on this was some 25% higher than that which

had caused failure under the first bogie. Because of the high creep in concrete structures approaching failure, this indicates that the failure load would have been substantially higher.

After the structure had been unloaded, the concrete remaining under the wheel which had punched through was removed. This revealed the classic conical form of a punching shear failure as can be seen in Figure 8.21. However, the suggestion in earlier chapters that such a failure can be precipitated by concrete crushing had been reinforced by the fact that the line of crushing concrete (which is visible in Figure 8.20) had been noticed *before* the failure occurred. It also appeared that global transverse moments had significantly reduced the local strength of the slab. The rotation of the edge beam (which was due to the differential beam deflections at mid-span) had clearly led to a transverse sagging moment in the slab over the web near the wheel which failed; a region where the local moment would have been sagging. Near mid-span, where the transverse moment in the slab was causing rather than restraining the rotation of the beam, there was a transverse hogging moment over the beam; hence the higher local strength.

Figure 8.21: Failure cone viewed from below

Further confirmation of the significant reduction in strength due to the global moments (and hence, by implication, of the flexural nature of the

failures) was given when the slab strength was estimated using the methods considered in 3.2.3. Kirkpatrick et al's approach(13) over-estimated the strength by nearly 80% whilst Hewitt and Batchelor's approach(72), using a restraint factor of 0.6, was only marginally better. The restraint factor back-calculated from the failure load was approximately 0.2, compared with the "conservative" figure of 0.5 used in the Ontario Code(11) for assessing existing decks. Thus, although the test results did not suggest that decks designed to the empirical rules would be unsafe, they did imply that the Ontario assessment recommendations could be. However, since all previous research into compressive membrane action in bridge decks had suggested that support diaphragms are needed (or at least desirable) to provide the restraint, a plausible alternative explanation for the reduced strength was that the restraint in this deck was inadequate. It was decided to perform local tests to investigate this.

8.7.3 Local Failure Tests

Two single wheel tests were performed using the test rig illustrated in Figure 8.22. The position of these, which is shown in Figure 8.11, was chosen for convenience in testing and also to avoid areas of the slab which had been significantly damaged in the previous tests. However, the slab around the wheel tests had been cracked by the previous tests whilst the adjacent bay, which could be important to the restraint, had apparently been loaded very close to failure. Thus the test situation was extremely unfavourable compared with the normal situation in a real bridge deck. It was considered that the behaviour at low loads was so greatly affected by this that it had no real significance. Thus serviceability was not considered in such detail as in the global tests and the slab was loaded monotonically to failure.

The same instruments were used as for the global tests but some were repositioned and all were re-zeroed. Thus strain and displacement readings were taken relative to the start of the test, rather than relative to the initial (uncracked) state as in the global tests. Some difficulties were experienced with the logger during the first test whilst in the second test the displacement transducer under the wheel stopped working. Since the behaviour in the two tests was very similar, only the behaviour of the second test will be described in detail but the load-deflection response for the first test is illustrated in Figure 8.23.

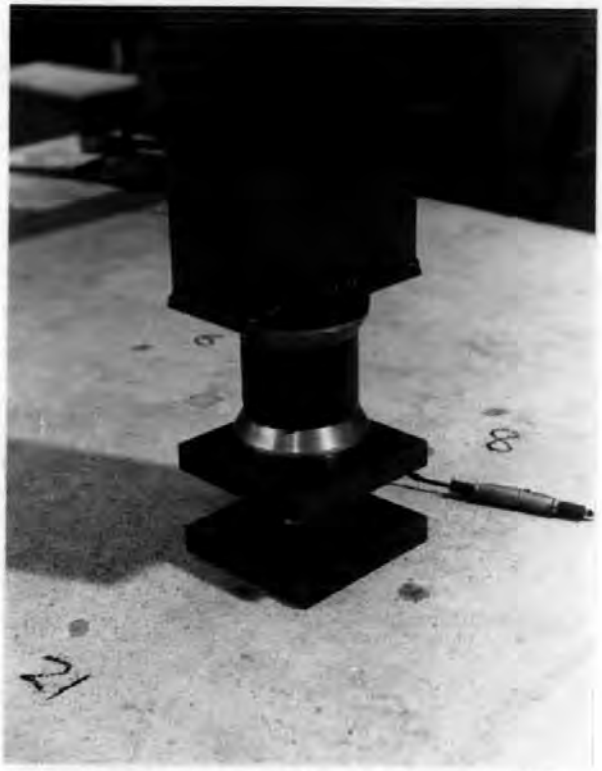

Figure 8.22: Single wheel test rig

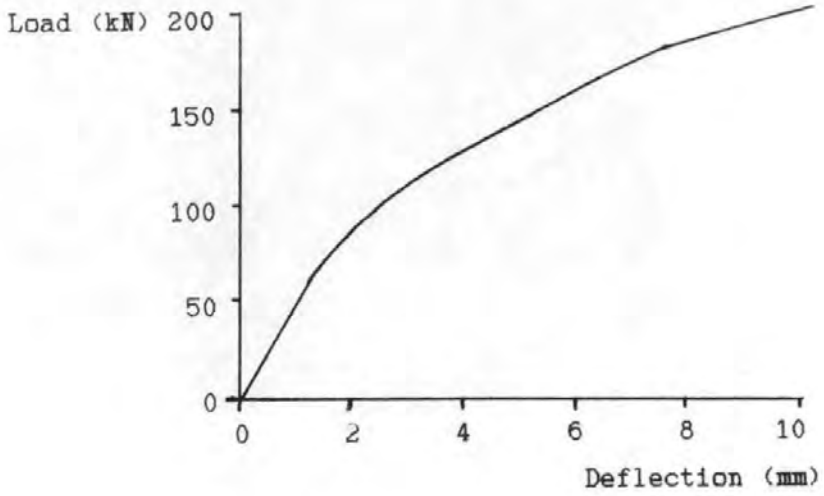

Figure 8.23: Result of single wheel test

A longitudinal crack was visible under the wheel before the test started and by a load of 43kN (which corresponds to 1.15 times the design ultimate wheel load) this crack was 0.08mm wide. This crack was thus significantly narrower than under the same load per wheel in the global test, despite the pre-cracking. At the same stage, the crack on the top of the slab over the web was 0.05mm wide, whilst the equivalent crack did not appear in the global test until nearly twice the load per wheel had been applied. However, this difference was probably largely due to damage sustained in

previous tests; the crack was visible before the load was applied. A transverse crack was just visible in the soffit under a load of 67kN. In the global tests, such a crack had not appeared until the wheel load was some 30% higher. This difference could not be explained by pre-cracking; it was due to the global flange force prestressing the slab in the local tests.

Figure 8.24: Crack pattern under single wheel

At a load of 113kN, by which point failure had occurred in the global tests, the maximum crack width was 0.3mm. By 145kN the cracks in the soffit had taken on the characteristic radial form which is illustrated in Figure 8.24. At a load of 202kN the crack in the top of the slab along the web of beam 3 had joined the similar crack due to the previously performed single wheel test. However there was no sign of this interaction reducing the strength; the wheel finally failed under a load of approximately 226kN compared with 204kN in the previous test. For comparison, the failure load in the global test was 103.5kN per wheel.

The wheel punched a neat hole through the top of the deck, coming to rest only some 10mm below the top surface of the slab. However, this difference from the failure mode under full HB was not indicative of any fundamental difference in the local behaviour. It was purely due to the different post-failure behaviour caused by the much smaller global displacement and force which was released by the local failure. Removal of the loose concrete from under the wheel revealed the classic conical failure surface illustrated in Figure 8.25 which is very similar to that observed in the global tests. The behaviour was also very similar to the global tests in that although there was plenty of warning of failure, in the sense that the structure was clearly unserviceable when subjected to only half its final failure load, the final collapse was very sudden. Even with the advantage of the strain readings, and of having observed an identical test only hours earlier, it was not easy to tell when failure was imminent.

Figure 8.25: Failure cone viewed from below

The difference between the two results may not be significant as it is not unusual to obtain much greater strength differences between nominally identical concrete specimens. However, it may have been due to the inferior restraint available to the first test which was nearer the end of the deck. The failure loads were, however, close to the 185kN predicted by Kirkpatrick et al's approach; the ratios being 1.22 and 1.10 compared with an average of 1.19 for Kirkpatrick's own tests(13). Similarly, the restraint factor back-calculated using Hewitt and Batchelor's approach, at approximately 0.65, was close to their findings. This confirms that both

approaches give good predictions for the failure load under single wheels and suggests that the restraint needed to develop this local strength is not dependent on diaphragms. Thus the lower local strength observed when all 16 wheels of the HB load had been applied must have been the result of global effects.

8.8 TESTS ON SECOND DECK

8.8.1 Global Service Load Tests

a. First Load Position

The second deck was subjected to a very similar load history to the first. However, only 5000 cycles of the reduced load were used and, because of the greater width of the deck, the load was applied in a maximum of four different positions across the width instead of two. The loading positions are illustrated in Figure 8.26.

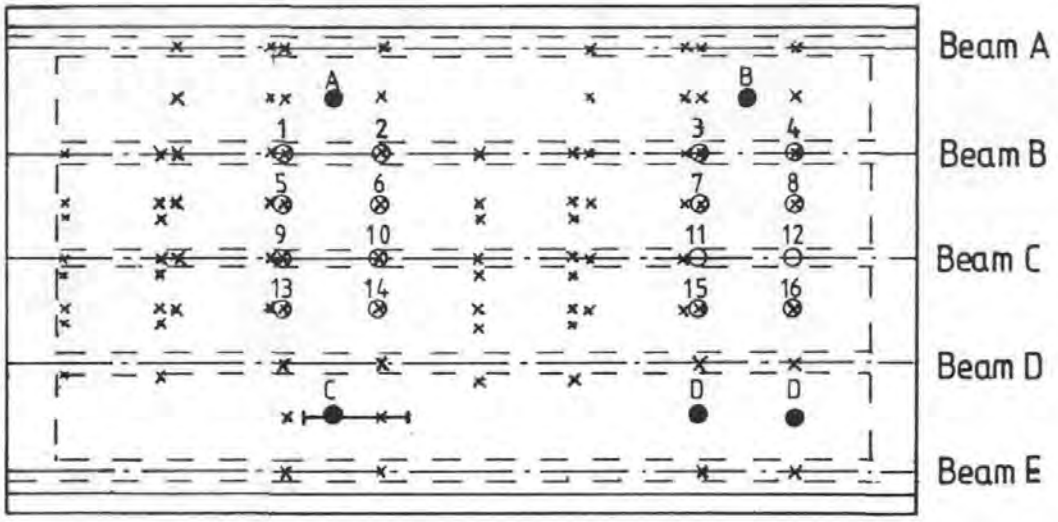

O HB wheel positions for first and last service load test and for failure test.

× Other HB wheel positions.

● Wheel positions for local tests.

⊢——⊣ Line of cuts in reinforcement.

Figure 8.26: Load positions for second deck

Like the first, this deck was initially subjected to design service load then to two cycles of a 20% higher load. A soffit crack appeared at approximately the same stage as before and under full design service load it had a width of 0.1mm: approximately twice the width as at the equivalent stage in the previous test. However, the crack widths in concrete are very variable, particularly at loads just above that which causes cracking, so this may have had little significance or may have been due to the lower tensile strength of the concrete.

The difference in crack width was less pronounced at the higher load of the second loading cycle. A more important difference from the behaviour of the first deck was that a top crack appeared at the same time as the soffit crack, whereas in the first it had required a load some 150% higher.

The measured local deflections, crack widths and transverse strains were greatest adjacent to wheel 14. These strains are shown in Figure 8.27, whilst the deflection of wheel 14 relative to the beams is shown in Figure 8.28. Initially the soffit strain exceeded the top strain by some 50% but this percentage reduced once the behaviour departed from linearity and the top strain overtook the soffit strain when the cracks became visible. It remained greater throughout the subsequent tests, the difference being greatest (even in absolute terms) when the structure was unloaded. However, these high strains were confined to the region over the inside of the web to Beam D which was the location of the only top crack. Figure 8.27 shows that the strain over the edge of the adjacent Beam C was very much lower. Indeed, nearly all the tensile strain in that region could be explained by the Poisson's ratio effect of the longitudinal compressive strain due to the global flange force.

The difference between the strains at either end of the slab span is particularly significant when it is realised that a conventional local analysis would treat the slab as symmetrical and so would predict identical strains at either end, whilst an apparently more sophisticated local analysis (treating the slab as continuous over simple supports) would predict a greater hogging moment over Beam C than over Beam D.

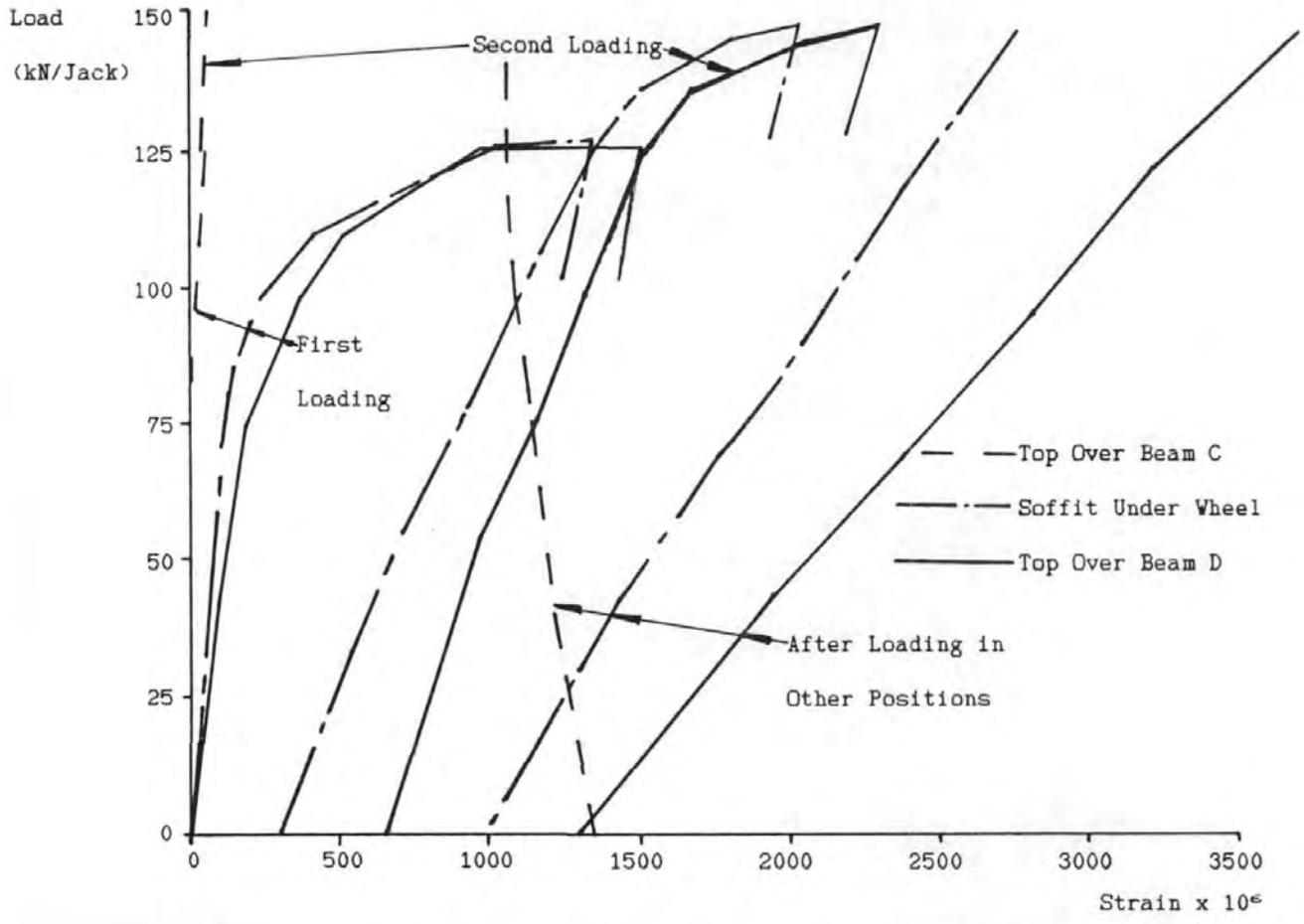

Figure 8.27: Transverse strains adjacent to wheel 14
(Service load tests)

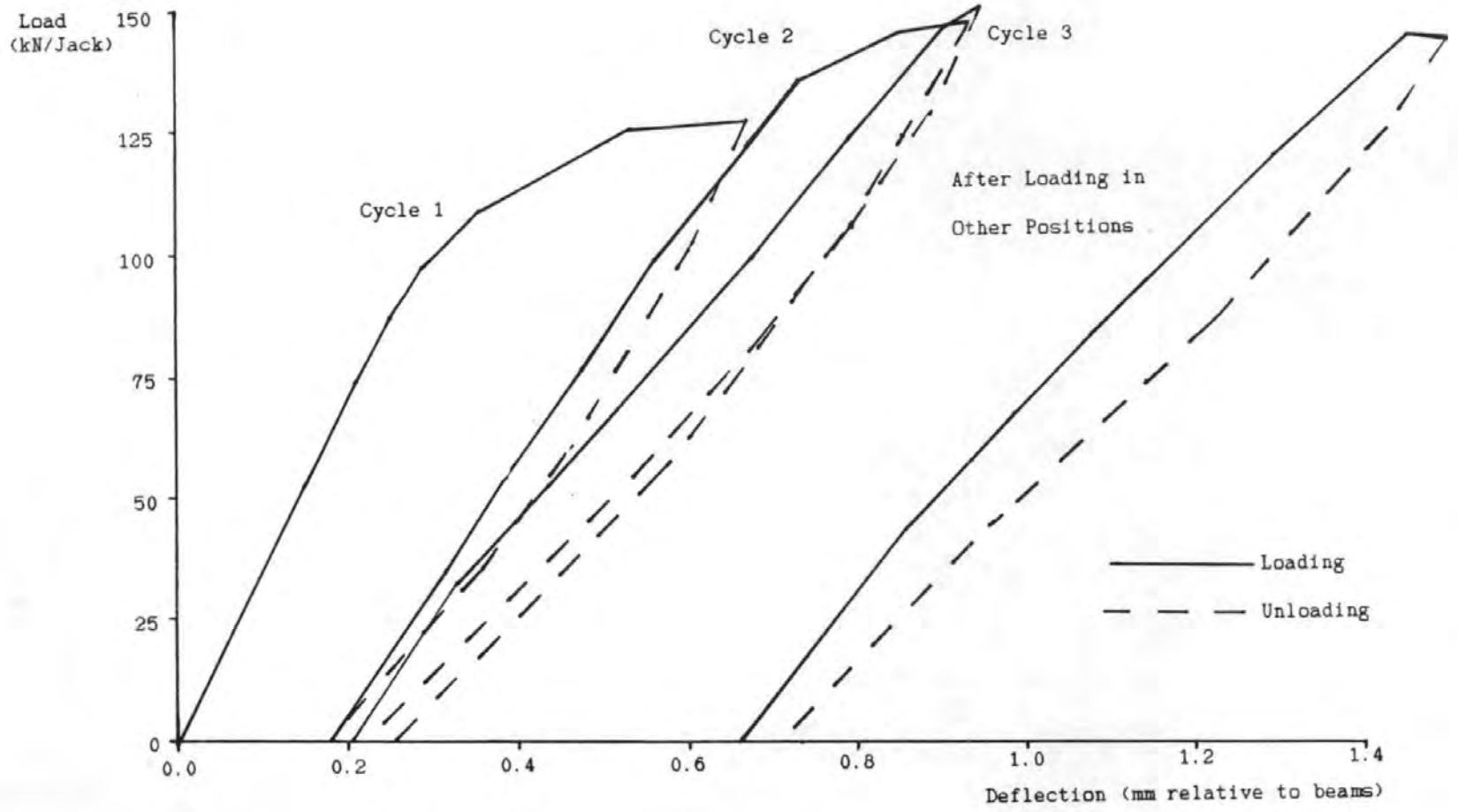

Figure 8.28: Deflection under wheel 14
(Service load tests)

The explanation for the greater strain over Beam D was that there the global transverse moment was hogging, adding to the local moment, whereas over Beam C the global moment was sagging and therefore acting against the local effect. Further evidence to suggest that the top crack over Beam D was largely due to global effects was given by the length of the crack. As soon as it appeared, it extended over most of the length of the deck. The width even mid-way between the bogies, where Pucher's charts(40) indicated that the local moment should have been sagging, was some two thirds of the maximum width adjacent to wheel 14. In contrast, as in the first deck, separate soffit cracks appeared initially under each wheel. The soffit cracks formed by the two wheels of a bogie, such as wheels 13 and 14, joined together as the load increased but the cracks formed by the two bogies did not join until the load had been applied in other positions along the length of the deck. Thus it appeared that the soffit cracks were primarily due to the local effect whilst the top crack was largely due to the global effect.

This also explains the difference in strain behaviour of the top and soffit. Initially, as predicted by elastic theory, the maximum soffit strain was greater than the maximum top strain. However, once the behaviour departed from linearity the stress peak in the soffit was smoothed out as force redistributed to the surrounding under-stressed concrete. There was less scope for redistribution of the top stresses because global moments are relatively uniform over the length of the deck; hence the rather greater increase in strain on cracking. Uncracked concrete surrounding the local cracks and trying to push them closed would also lead to better recovery of the soffit strain on unloading. However the much inferior recovery of the top strains (the top strain after each cycle of the first load position was over double the soffit strain) was undoubtedly exaggerated by the reinforcement detailing since the single layer of main steel was located some 10mm below mid-depth.

The reason why the top cracks had not appeared in the first deck until a much higher load was applied was that the lack of diaphragms meant that the beams were free to rotate. Thus local hogging moments were relieved by rotation and differential displacements of the beams led to lesser global transverse moments. The diaphragms in the second deck contributed to its superior distribution properties and the maximum beam displacement

was some 25% lower than in the first deck even though a static load distribution would predict identical deflections.

As with the first deck, the application of 5000 cycles of a reduced load had remarkably little effect on the behaviour.

b. Other Load Positions

After completion of the tests in the first position, the HB loading rig was moved a metre sideways in the direction towards the top of Figure 8.26 to apply load in the second position. The behaviour was generally similar to that in the first position. The one new top crack appeared over the edge of the centre beam when the design service load was applied, whilst the new soffit crack appeared in the bay at the top of Figure 8.26 under the full load; that is 1.2 times design service load.

The original intention had been to apply the HB load in a total of three different positions across the width of the deck. This loading sequence was designed to induce all the soffit cracking which was likely to occur in service. However, it was now apparent that top cracks due to global effects could be equally significant. The intended load sequence would have failed to induce top cracks over the inside of the web of Beam B. Since such cracks could be significant to the behaviour of the adjacent bay of slab (that between Beams B and C) and since that bay would be loaded in the final test, it was considered that this was a fault of the sequence. An intermediate load position was therefore used. The loading rig was moved back 1.5m towards the bottom of Figure 8.26 to apply the same load position as in the first test but opposite hand. Apart from the effect of the pre-cracking, which led to a softer initial response, the behaviour was very similar and the maximum crack widths were similar. The maximum strains and deflections were also similar although few direct comparisons could be made as few gauges were in equivalent positions. The global deflections were very similar; within 5%.

After completion of the tests in this position, the loading frame was moved a further metre sideways to the position nearest the bottom as shown in Figure 8.26. This position was particularly significant as it included a wheel directly over the region of the cut reinforcement.

Under the maximum load which had previously been applied, there were no cracks visible in the region of the cut reinforcement. This was slightly

surprising as the load case was identical to one which had already been tested, apart from being opposite hand, and cracks had appeared in that test at the equivalent position and load stage. It was also unfortunate as it had been intended to use the test to investigate the behaviour, under cyclic loads, of a cracked bridge deck slab with damaged reinforcement. It was therefore decided to increase the load slightly to crack the slab; the strain of 500 microstrain measured by the portal gauge under the wheel indicated that cracking was imminent. However a 10% increase in load failed to produce visible cracks despite giving a strain of 610 microstrain. Curiously, the strain under the adjacent wheel, where the reinforcement was intact, was 986 microstrain which indicated, by comparison with other cases, that cracks would have been visible. These were not noticed although the area was not inspected as thoroughly.

Clearly, cutting the main steel had not advanced the formation of cracks: indeed it appeared to have delayed it although, in view of the variability of concrete behaviour, this was probably not significant.

A further increase in load would have applied a significantly higher global load than had been intended and may have caused enough damage to significantly alter the behaviour under the later load cases. It was considered that the intended load sequence was over-severe and a further increase would have made it too unrealistic. It was therefore decided to unload the structure and disconnect three of the four jacks. This enabled a higher load to be applied on four of the wheels without causing significant damage in regions where it was likely to affect the behaviour under the later load cases.

At a load of 163kN, a marginally lower local load than that which had previously failed to crack the region, a 0.05mm crack was visible in the soffit under the cut reinforcement. The load was then increased to 178kN, equivalent to 1.22 times the design ultimate HB wheel load, which increased the crack width to 0.1mm. It also induced a crack, approximately 0.05mm wide and 1.5m long, in the top of the slab over Beam D.

The bridge was then unloaded, the other three jacks re-connected and the cyclic loads applied as in the previous positions. Despite the initial over-loading, the behaviour was entirely satisfactory and appeared similar to that when the load case had been applied opposite-hand over intact

reinforcement. There was thus no evidence that cutting the steel had adversely affected the behaviour.

For the next load position the loading frame was moved 1056mm along the deck and back to its original transverse position. The behaviour in this and subsequent positions was very similar to that in the previous positions so it will not be described in detail. Because the load cases were less severe on the beams, the top cracks were not greatly extended. It was therefore decided that it was not necessary to apply the load in as many transverse positions to simulate all the damage which could occur in practice and only two were applied. It appeared that applying 1.2 times service load in just one longitudinal position was equivalent, as far as top cracks were concerned, to applying service load in all possible longitudinal positions. However, it was still necessary to apply the load in all the positions shown in Figure 8.26 in order to ensure that the soffit cracking would be correctly simulated.

For the final loading position, the bogies were positioned to give wheel loads 250mm off-centre to the slab span. A new crack formed under some wheels but not until the load exceeded design service load. It therefore appeared that loading only at mid-span of the slabs, as in all the previous tests, had given a reasonable representation of the extent of cracking which would have occurred if the service load had been applied in all positions.

c. Return to First Position

The loading frame was returned to its original position and the full load re-applied. As will be seen from Figure 8.28, the local deflection under wheel 14 (the greatest local deflection recorded) was substantially greater than under the first loading. The maximum local deflection was also 42% greater than the equivalent deflection at the same stage in the tests on the first deck, whilst the deflection on unloading was over four times greater. It will also be seen, by comparing Figures 8.28 and 8.13, that loading in other positions had had a greater effect on this deck than it had on the first.

One reason for the greater effect on this deck of loading in other positions can be inferred from Figure 8.27: it had opened a crack over the web of Beam C. This crack tended to close as load was applied, indicating

that the global sagging moment in this region under this load case was greater than the local hogging moment. However, the tensile strain remained significant and thus continued to contribute to the local deflection throughout the load cycle.

The maximum crack width recorded was for the crack over the edge of Beam D and was equivalent to approximately 0.7mm at full size, whilst the maximum soffit crack width was equivalent to approximately 0.4mm. The pattern of top cracks after the completion of the service load tests is illustrated in Figure 8.29. Under the reduced load used for checking crack widths in BS 5400, the soffit crack width was equivalent to 0.2mm compared with the allowable width of 0.25mm. The top crack was equivalent to approximately 0.4mm but the top cover was over twice the "C_{nom}" required by BS 5400. Thus, since BS 5400 allows the crack widths to be calculated "on a hypothetical surface at a distance C_{nom} from the outermost bar", the crack width was, at worst, very close to being acceptable. Nevertheless the condition of the slab was not as obviously satisfactory as that of the first deck had been. The permanent deformations were greater and although the permanent soffit cracks were no wider top cracks, which had not occurred in the first deck at all, were up to 0.3mm wide full scale equivalent, even on unloading. It was thus somewhat debatable whether the condition of the slab could be considered acceptable.

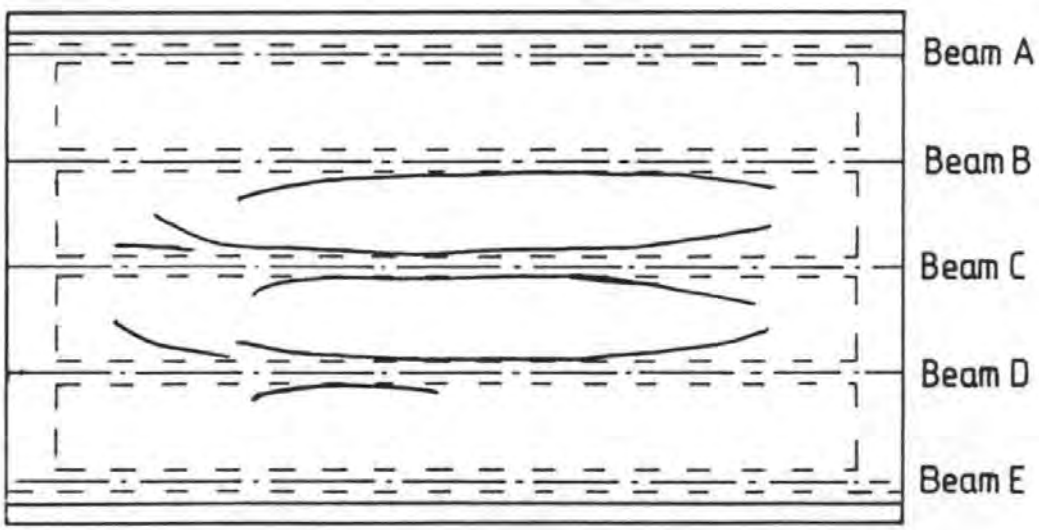

Figure 8.29: Top cracks on completion of service tests

The fact that top cracks had occurred in the second deck but not in the first was undoubtedly due to the greater transverse hogging moments resulting from the presence of diaphragms: the load which was required to

induce top cracks in the first deck was so much greater (over two and a half times as great) that none of the other differences between the decks could have been more than minor contributory factors. However, the reason for the poorer recovery of the second deck on unloading, and for its greater maximum crack widths, was less clear. It could have been due to the nature of global as opposed to local moments, but the difference in the main reinforcement and in the tensile strength of the concrete may also have been important. However, since the significant cracks all ran essentially parallel to the beams, it appeared that the substantial reduction in the secondary steel could not have been a major factor.

Unfortunately, it was not possible to test a third deck so the relative significance of the differences between the decks could only be investigated analytically. Analytical investigation was also essential to assess the distribution properties and to see how they compared with those which would normally have been assumed in design. Nevertheless, it was clear that the distribution properties were superior to those of the first deck since, despite the lower grade concrete in the slab, the deflection of the heaviest loaded beam had been consistently some 25% lower.

8.8.2 Global Failure Test

On completion of the service load tests, the load on the model was re-applied and then increased. The strains adjacent to wheel 14 are shown in Figure 8.30 whilst the beam deflections are shown in Figure 8.31. Both are plotted relative to the original zeros, which explains why they do not pass through the origin, and the break in the plot indicates a point where the load was removed before being re-applied.

The initial strain response shown in Figure 8.30 is approximately linear. However, once the load exceeded 150kN per jack, the highest load which had previously been applied, a significant departure from linearity can be observed as the cracks extended in depth and width. At this point, the tensile strain over Beam C, which had previously been reducing slightly, began to increase slightly. This would appear to indicate that the local moment in this region was increasing as moment redistributed away from the more heavily cracked regions.

The load-deflection response of Beams B and C is distinctly non-linear from a load of approximately 150kN per jack. However, this was clearly

due to deterioration of the distribution properties, rather than to softening of these beams, since the plot of the sum of the beam deflections does not become noticeably non-linear until a load of approximately 250kN. As the load increased, the proportion which the outer two beams carried clearly reduced and, above a load of 275kN per jack, the deflection of Beam E began to reduce in absolute, as well as in relative terms. This deterioration of the distribution properties was largely due to the extensive cracking in the slab but torsional cracks in the diaphragm, which began to appear from a load of 225kN per jack, also contributed.

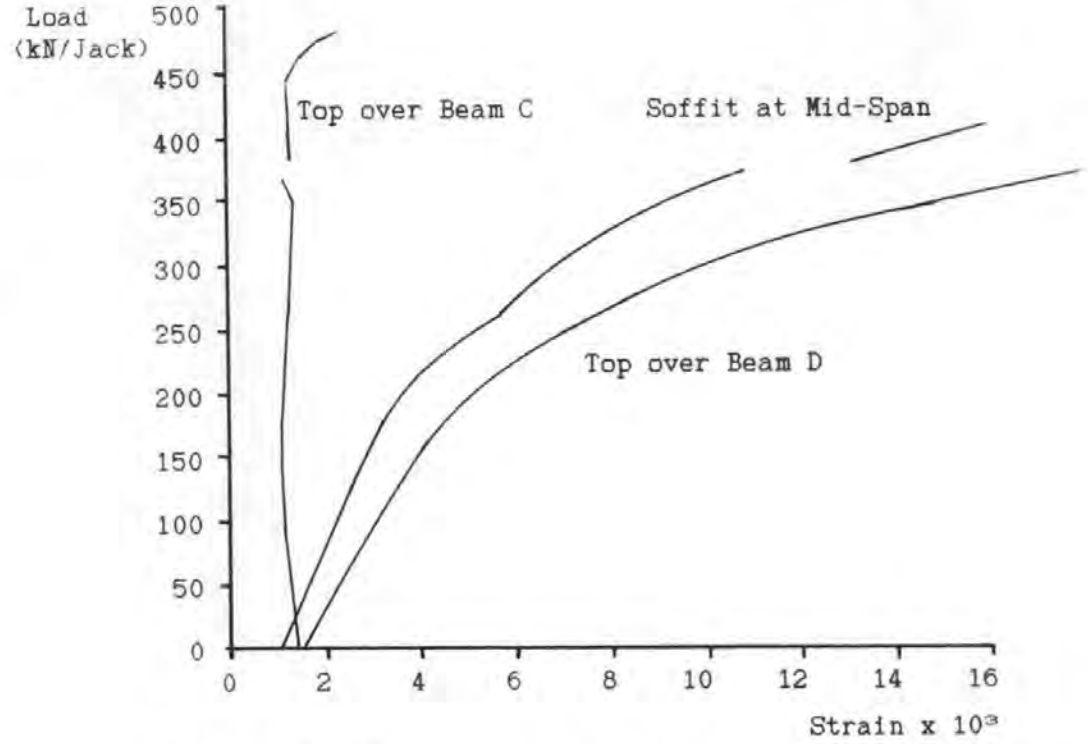

Figure 8.30: Transverse strains adjacent to wheel 14

Although, despite the lower grade concrete in the slab, the maximum global deflections were smaller than at equivalent stages in the tests on the first deck, a comparison of Figures 8.31 and 8.14 shows that they began to depart from linearity at an earlier stage. This was apparently largely because the earlier formation of top cracks meant that the distribution properties began to deteriorate at an earlier stage. However, an additional but closely-related reason was that the distribution properties of the first deck had been so poor. Thus the heaviest loaded beams carried such a high percentage of the load which a static distribution would predict that even a total loss of distribution properties would have had little effect on the deflections.

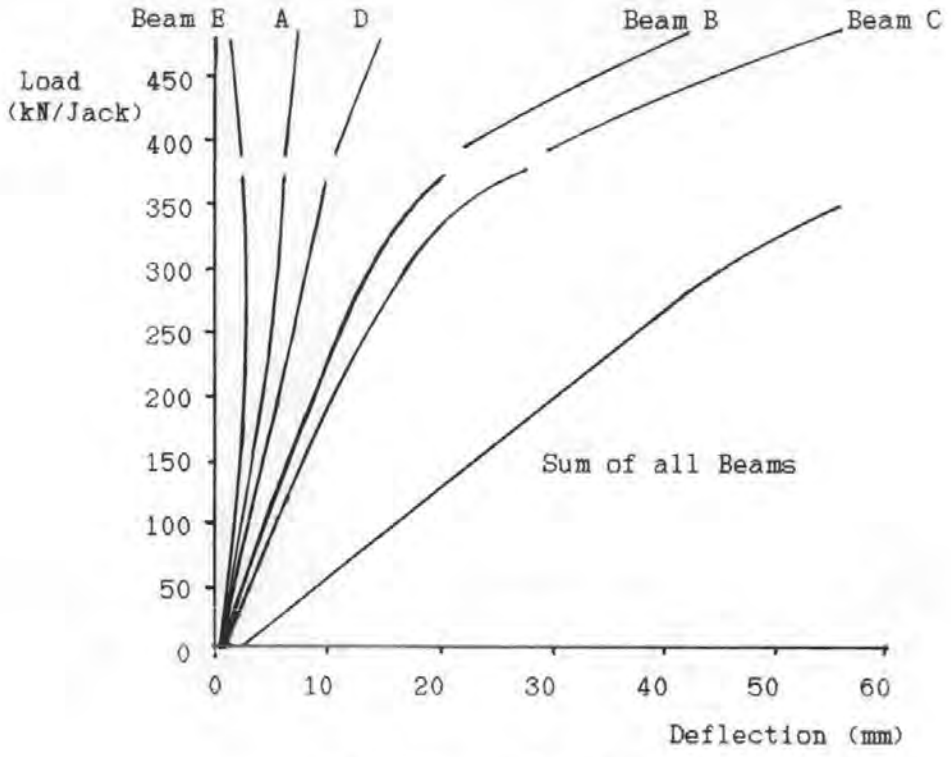

Figure 8.31: Beam deflections

As the load increased, new cracks formed. The distinct kink in the plot of the soffit strain in Figure 8.30 at a load of around 260kN per jack is due to the formation of another longitudinal crack close to, but outside, the gauge length. At a load of 300kN, there were four longitudinal cracks in each of the loaded bays of the deck. They extended over much of the length of the deck; three of the initially separate cracks caused by the two bogies in each bay having joined together. These cracks fanned out in a radial pattern at either end of the deck, between the bogies and the diaphragm, but there were no transverse cracks in the soffit and only one longitudinal crack in each bay deviated from the longitudinal direction between the bogies to meet the webs.

Whilst the pattern of soffit cracks was generally similar to that in the first deck at equivalent load stages, the pattern of cracks in the top of the slab, which is illustrated in Figure 8.32, was very different. The longitudinal crack over the web to Beam A formed at a load of 225kN per jack whilst the diagonal cracks at either end of this appeared at between 250 and 400kN per jack. Since there was no load at all applied directly to this bay of the slab, it is quite clear that these cracks were the result of global effects. Global effects also dominated the crack pattern in other bays. Thus the cracking in the bay between Beams C and D, which

had very different deflections, was far more extensive than that between Beams B and C whose deflectionss were more similar. The crack perpendicular to Beams B and C at the right hand end of the Figure was clearly due largely to global hogging in these beams as torsion in the diaphragm (which was restrained by the lightly loaded Beams A, D and E) attempted to resist the rotation of Beams B and C. Similarly, the extreme asymmetry (about the deck's longitudinal axis) of the crack pattern in the bay between Beams D and C indicated that here too, global effects were dominant.

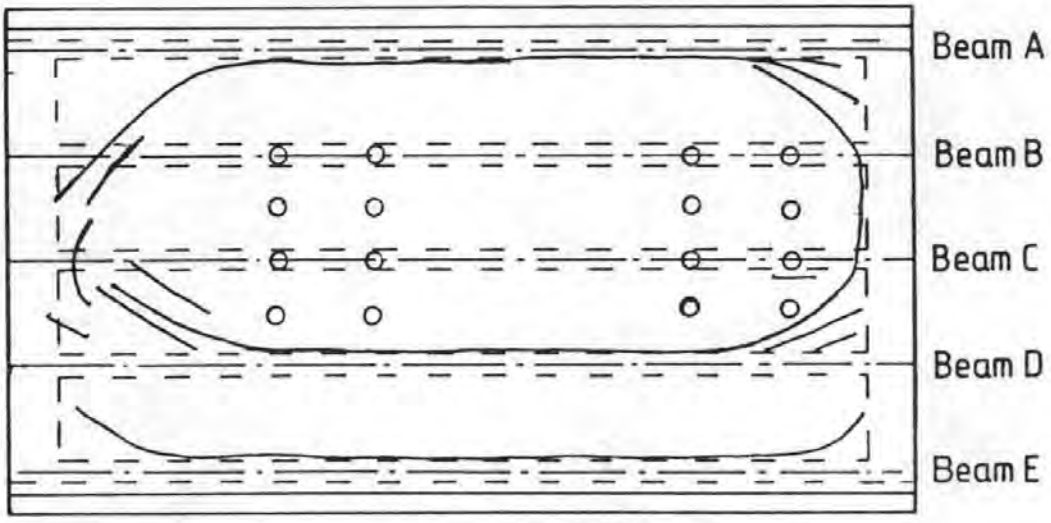

Figure 8.32: Top cracks immediately prior to failure
(note: cracks which were formed by other load positions and which were closing under this load case are not shown)

At a load of 300kN per jack, twice the design ultimate load, the first crack was observed in a beam; a flexural crack in the soffit of the centre beam under wheel 10. A shear crack appeared in the right hand end of the same beam (as shown in the Figures) at a load of 325kN. A shear crack appeared in Beam B at a load of 350kN and a flexural crack followed at approximately 375kN. By this stage, the capacity of the hydraulic system had been reached. The bridge was therefore unloaded and the jacks connected to a new electric pump which had not been available at the time of the tests on the first deck. The load was then re-applied.

By this stage, the cracking in Beams B and C had caused a significant reduction in their stiffness as can be seen from Figure 8.31. The resulting increase in the differential deflections of the beams led to further cracking in the top of the slab and the strain represented by the

crack over the web to Beam D had reached the limit of the capacity of the portal gauge. By a load of 400kN per jack, all the cracks shown in Figure 8.32 had formed except the longitudinal one over Beam E. The widest of the cracks, as throughout the test, was that over Beam D. By a load of 425kN this crack was some 3mm wide and the crack over Beam A was 1.5mm wide.

By a load of 460kN per jack, 10% higher than the failure load of the first deck, there were flexural cracks over much of the length of the centre beam joining the shear cracking at the right hand end. The flexural cracks crossed the soffit of the beam at right angles to its longitudinal axis. In contrast, those in the adjacent Beam D crossed at an angle of up to 45 degrees and tended to form first on the outside, that is away from the loaded bay. Since the very wide longitudinal crack over one side only of the web to Beam D suggested that it was subjected to a very substantial torque, this was not surprising. However, the crack pattern implied that this torque was almost entirely resisted by transverse bending and shear in the bottom flange and not by torsion as such; unlike in the first deck, the shear cracks on opposite sides of the web sloped in the same direction indicating relatively low torsional stresses in the web. The asymmetrical loading of the beam had, by this stage, caused a longitudinal crack in the web on the outside of the beam.

Up to this stage, despite the very extensive cracking, there had been no difficulty in loading the deck or in holding it up to load. However, as the load increased further this became increasingly difficult, indicating that failure was imminent. At a load of approximately 475kN per jack, a line of crushing concrete could be clearly seen on the soffit of the slab extending along the edge of Beam D for some one and a half metres adjacent to wheels 13 and 14. This section of the slab was clearly reaching the limit of its moment capacity and it is presumably the resulting redistribution of local moments which caused the increase in the strain over Beam C which can be seen in Figure 8.30.

At a load of approximately 490kN per jack, 3.35 times design ultimate load and some 18% higher than the failure load of the first deck, failure occurred in the form of wheel 14 punching through the deck. The resulting sudden reduction in the global load on the deck reduced the global deflections and hence increased the load on the other three jacks. The

local behaviour was so brittle and the failure so sudden that this caused wheels 5, 8 and 16 (one under each jack) to punch through as well, despite the fact that the four jacks were inter-connected; they punched through in such quick succession there was not time for the hydraulic pressures to equalise. The deck after failure is illustrated in Figure 8.33.

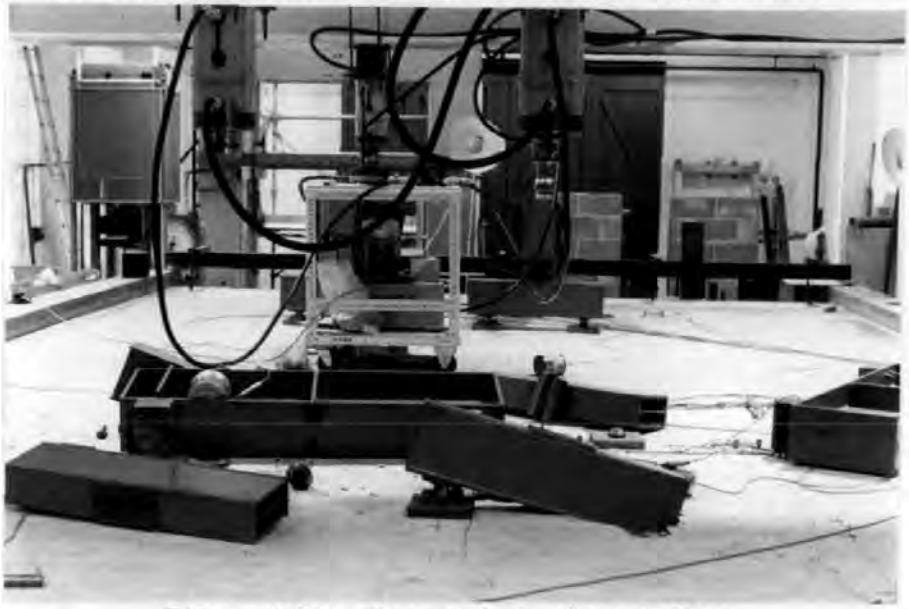

Figure 8.33: Second deck after failure

After the failure, a line of crushed concrete could be seen on the top of the slab between wheels 9 and 10 as well as between wheels 13 and 14. There was also more localised crushing adjacent to the other two wheels which punched through. However, despite a thorough inspection at the final load stage before the failure, this had not been observed until after failure although there had been some sign of very local crushing by wheel 14. It appeared that the soffit crushing which had been observed before failure had been the root cause of the collapse yet, despite this, the failure once again looked like a classic "punching shear" failure. This further confirmed that such failures could be caused by flexural effects. The fact that the critical section of slab had so clearly reached the limit of its moment capacity when the strains and crack widths at the equivalent position at the other side of the local slab span were so modest, as can be seen from Figure 8.30, again confirmed the importance of global transverse moments.

Another interesting feature of the results was that, despite a lower concrete strength and less reinforcement, this deck slab had failed at an 18% higher load than the first. As in the first deck, wheels had punched through the slab at a substantially lower load than predicted by

Kirkpatrick et al's approach but the margin was much smaller; approximately a factor of 1.22 against 1.78. It appeared that this was due to differences in the global behaviour but again an alternative explanation was the superior restraint to in-plane forces in the second deck with its diaphragms. It was decided to perform some local tests to investigate this.

8.8.3 Local Failure Tests

Despite the extensive damage caused by the global tests, it was considered that the two outer bays of the slab were in sufficiently good condition for local failure tests to be useful. This gave the opportunity to perform a total of four local tests. It was decided to perform two tests identical to those which had been performed on the first deck. These would enable the failure loads to be compared with that in the global tests and in the tests on the first deck. In addition, they would act as controls for the other two tests which would be performed; firstly a single wheel test over the region with the cut reinforcement, to investigate its effect, and secondly a two wheel test. The latter was considered important as it was not clear how much of the reduction in local strength which had occurred in the global tests could be attributed to interaction of the local effects of adjacent wheels.

Since the slab was cracked much more extensively in the bay between Beams A and B than on the other side of the deck, it was decided to perform both control tests in this bay. This meant that any reduction in the failure load per wheel of the other tests could be clearly identified as due to the effect being investigated, rather than due to the effect of previous damage. The positions used for the tests are illustrated in Figure 8.26.

The first test performed was the control single wheel test at position A in Figure 8.26. This was followed by the test over the cut reinforcement at position C in the Figure and the load-deflection response of both these tests is illustrated in Figure 8.34. The behaviour in the two tests was very much alike and also very similar, apart from the lower failure load, to that in the equivalent tests on the first deck. The fact that most of the main steel had been cut right through beneath the wheel at B appeared to have had very little effect, indeed the initial response was softer in the test with intact reinforcement although this was probably due to the greater damage sustained by this region of slab in the global tests. As

in the tests on the first deck, the failure loads were very similar to that predicted by Kirkpatrick et al's approach.

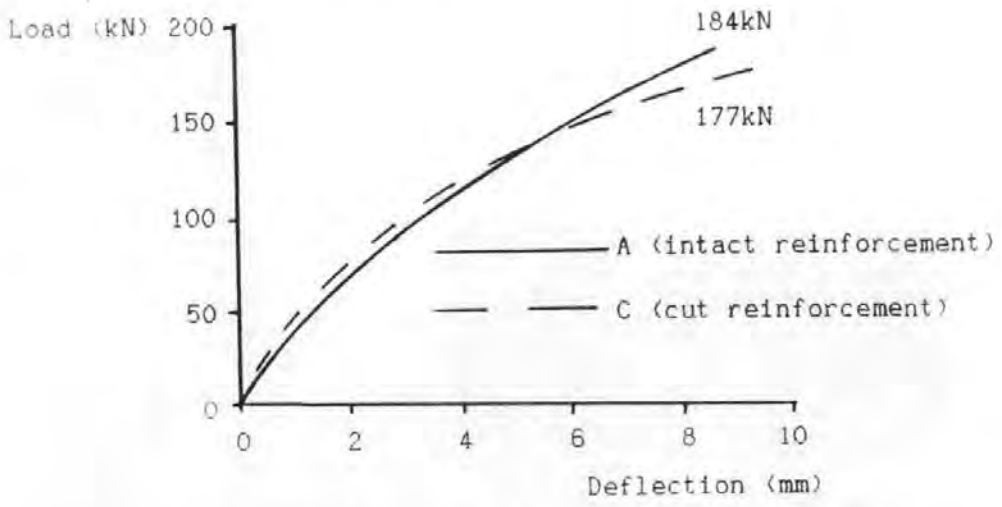

Figure 8.34: Single wheel tests A and C

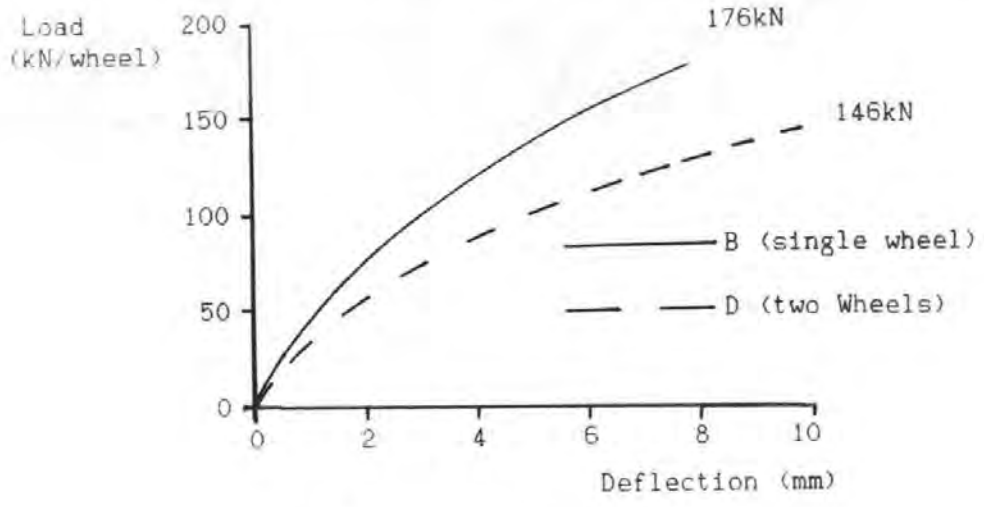

Figure 8.35: Local tests B and D

The next test performed was the control test at B and, as might be expected, this behaved in a very similar fashion. For the final test, the two wheel test, a new loading arrangement was required. Since neither the time nor the money was available to fabricate this, one of the four load spreader rigs used for the global tests was employed, the main beam being re-positioned so that over 95% of the load was applied to two of the wheels. The load-deflection response for the two tests is illustrated in Figure 8.35 and it will be seen that the presence of the second wheel had a significant effect on both the deflection and the failure load although the failure once again took the form of one wheel punching through the

deck. The reduction in strength was approximately 17% (or 19% using the average of the two control tests) which is slightly less than experienced by Kirkpatrick(13) in bays with equivalent span and depth. However, he suggested that the reduction he observed may have been due to his particular support conditions. It now appears that this was probably only a minor contributory factor. If, as his approach appears to imply, punching failures are caused directly by excessive shear stresses in the region immediately round the wheel, it is hard to explain why the presence of a second wheel should affect strength. However if, as suggested here, the failures are primarily flexural one would expect that any load which increased the bending moment would reduce the strength.

Although the presence of a second wheel reduced the failure load per wheel, it remained substantially (23%) higher than in the global tests. It thus appeared that the lower failure load per wheel in the global tests was indeed partly due to global effects although the interaction of the local effects of the two wheels was also significant.

As in the first deck, the single wheel tests were remarkably consistent with Kirkpatrick's, the average ratio of failure load to his prediction being 1.20 compared with 1.19 in his own tests(13). Considering all the single wheel tests, that is those performed on both decks, the average ratio was 1.183 with a coefficient of variation of 0.0433. This is a remarkably good result, even for a largely empirical formula developed from tests on structures which were similar to those considered here. The small variation means that the possibility of the reduction in strength observed when more wheels were applied being purely due to random variation can be eliminated. However, paradoxically, even the fact that an approach based on shear stresses gave such good predictions could be used as an argument for saying that the failures are primarily flexural: shear failure loads are inherently more variable than flexural failure loads and it would be extremely unusual to obtain such a small variation in the shear strength of even apparently identical specimens.

8.9 TESTS ON SINGLE BEAM

Although this is primarily a study of deck slab behaviour, it is clear from the previous section that global behaviour is important to this. Thus the behaviour of the beams has a significant effect and it was considered important, before analysing the complicated decks, to ensure that the

analysis was capable of modelling the relatively simple beam behaviour correctly. It was therefore decided to test a beam on its own.

The precast beam which was tested was similar to those used in the first deck, and had been cast in the same batch. It was provided with a one metre wide in situ top flange cast in the same way as the models using a similar mix which gave a cube strength at time of loading of 45.7N/mm^2. The reinforcement provided in this flange was like that used in the second deck. It was considered that the flexural behaviour, which was of prime concern, would be very similar for the two types of beams so their features were chosen for convenience.

Although it may appear obvious that the single beam should have a flange width to match the beam spacing in the decks, this is less obvious when the in-plane shear stiffness of the deck slab is considered: it was noted in 3.2.7 that the heaviest loaded beam in a beam and slab deck can effectively have a flange which is wider than the beam spacing. This means that concrete crushing failures may be less likely in bridge deck tests than in single beam tests but no allowance was made for this effect.

The beam was positioned on bearings in the same way as in the deck tests. The loads were applied with the same loading frame and jacks, although the loading rig was modified to bring the wheels closer to the longitudinal centre-line of the beam to avoid over-loading the slab. To make the results directly comparable, the longitudinal position of the loads was kept the same as in the global failure tests. Since neither the bearings nor the loading rig provided significant restraint to rotation about the longitudinal axis, a steel beam was placed across the top of the beam and held down to the floor. However, it proved acceptable to allow this system to go slack in the test.

Two 100mm travel displacement transducers were provided to measure the deflection. These were mounted over the top of the beam to avoid damage in the event of the sudden failure which was anticipated. A number of demec points were provided but no electronic strain gauges were used. The beam under test is illustrated in Figure 8.36.

Since the previous tests indicated that the beam behaviour was, for all practical purposes, perfectly linear elastic until well above design service load, there was little point in applying complicated load histories. The

beam was therefore loaded to 150kN per jack then unloaded, then loaded monotonically to failure. The mid-span deflection is plotted against the load in Figure 8.37. The response was linear elastic up to a load of approximately 200kN per jack so the first load cycle cannot be seen in the Figure.

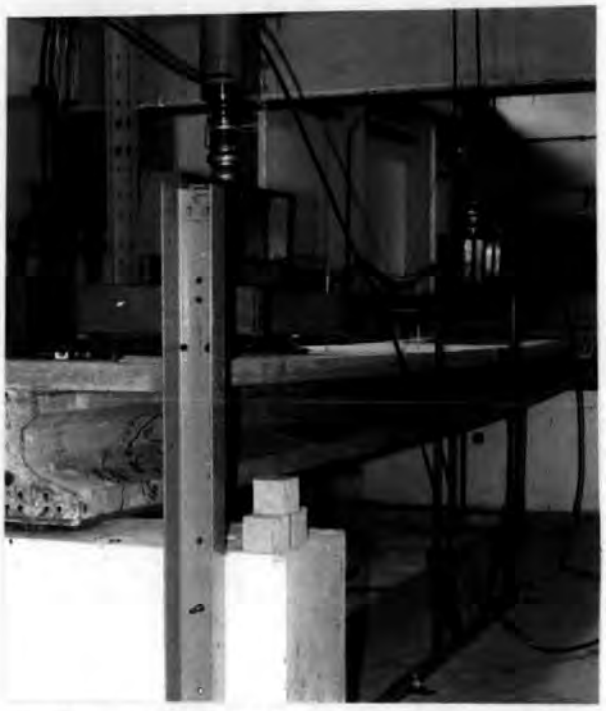

Figure 8.36: Single beam under test

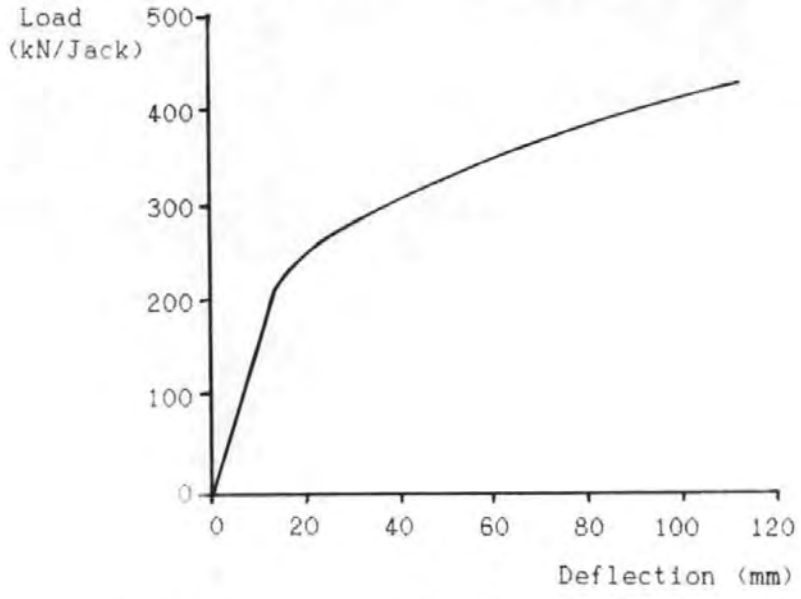

Figure 8.37: Load-deflection response of single beam

The behaviour prior to failure was remarkably similar in many respects to that of Beam B of the first deck. The crack patterns were very similar,

including the shear cracks which are illustrated in Figure 8.38. Even the loads at which the cracks appeared, expressed in kN per jack, were similar. However, the deflections were slightly higher at each load stage which suggests that the load distribution in the first deck was slightly better than that predicted by simple statics.

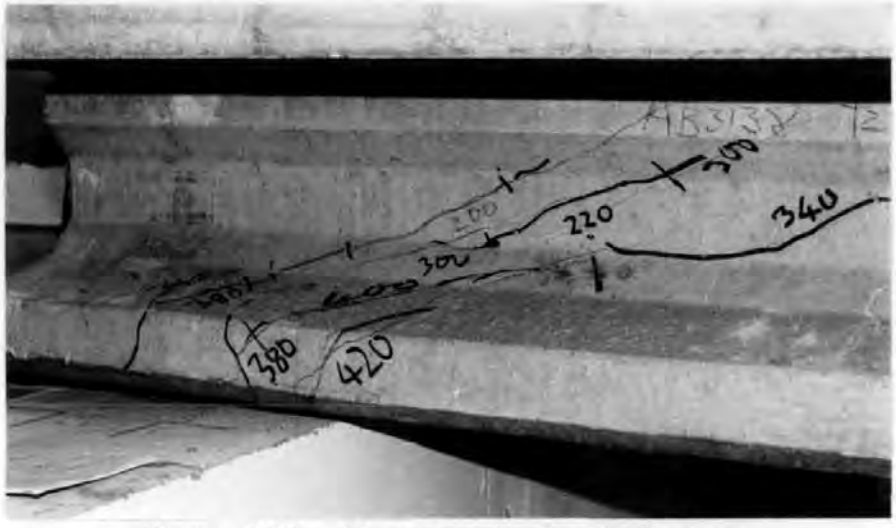

Figure 8.38: Shear cracks in single beam

Despite the extensive shear cracks and the draw-in of the tendons which had occurred by a deflection of 60mm (the global beam deflection at which failure occurred in the first deck) the load increased by another 24% before a sudden explosive failure occurred at a deflection of 110mm. The only warning of this was the increasing creep and the failure was so total that the beam fell some 500mm even though the hydraulic system used meant that the load was removed as soon as failure occurred. After failure, as illustrated in Figure 8.39, there was no concrete left at all in the critical section.

Figure 8.39: Beam after failure

It was clear that the failure had been caused by concrete crushing in the top flange; what had been observed was the classic brittle bending failure

of an over-reinforced (or in this case over-prestressed) concrete section. However, it is easy to imagine that a two-dimensional version of such a failure, that is in a slab rather than in a beam, would look like a punching shear failure. Indeed, in a sense it is a shear failure because crushing concrete fails on inclined planes. Thus there is no clear distinction between the two types of failure.

8.10 DISCUSSION AND CONCLUSIONS

8.10.1 Service Load Tests

The condition of the first deck was satisfactory at the completion of the tests. Its behaviour during the tests was also apparently satisfactory although it remains to check the distribution properties by comparison with analysis.

The behaviour of the second deck was less satisfactory because relatively large cracks opened in the top of the slab on loading and failed to close on unloading. Although the failure of these cracks to close may have been due to the reinforcement detailing, the fact that they occurred only in the second deck was clearly a result of the higher transverse moments resulting from the presence of the diaphragms.

It appears, although it remains to check this by comparison with analysis, that compressive membrane action did not greatly contribute to the resistance of either deck to global transverse moments. However, as predicted by previous researchers, compressive membrane action clearly did contribute to the resistance to local moments. Contrary to their suggestions, this contribution did not depend on the presence of diaphragms. The result was that the cracks in the top of the second deck, the feature which led to its behaviour being considered less satisfactory, were the direct result not only of an effect which has been largely ignored by previous research (global transverse moments), but also of a feature which had been positively recommended (diaphragms). Although these diaphragms improved the distribution properties, they appear to have had a detrimental effect on the serviceability of the slab.

8.10.2 Failure Tests

The most significant aspect of the failure tests was not so much the individual failure modes or loads as the relationship between them. Failure occurred in the first test when a single wheel punched through the

deck under a wheel load which represented only half the local strength of the slab: not only as predicted by previous research but also as measured by the subsequent single wheel tests. Despite its diaphragms the second deck, with its weaker concrete and smaller steel area, was weaker in the single wheel tests yet it was able to resist a higher global load. Clearly, the failures under full HB load were greatly influenced by the global behaviour but this does not mean that they did not occur until beam failure was imminent. The maximum beam deflection in the global tests was little more than half that at which failure occurred in the beam tested alone. That beam had reached only 80% of its failure load when its deflection matched that at which the decks failed.

All this fits the hypothesis that the slab failures were primarily brittle bending compression failures. In the global tests, the global transverse moments induced by the beam's differential displacements or (in the case of the first deck) rotations used up some of the bending strength of the slab. Because, by virtue of the membrane forces, the slabs behaved as though locally heavily reinforced even though actually very lightly reinforced, their local behaviour was brittle. Thus redistribution was very limited and the safe theorem of plastic design did not apply. The slabs failed under combined global and local transverse moments even though, at the failure load, the global transverse moments were not needed to maintain equilibrium.

The single wheel tests confirmed the work of previous researchers. Indeed they suggested that the enhancement to local strength caused by compressive membrane action is remarkably tolerant of features which might be expected to reduce restraint. All the tests were performed in outer slab bays which had already been extensively cracked for their full length by previous tests; half were performed after other failure tests in the same bay. Two of the tests were in a deck without diaphragms; the remaining tests (all those on the second deck) were performed close to points where wheels had punched through the adjacent bay of the slab. Despite all this, the behaviour had been entirely satisfactory. The only thing which significantly reduced the strength relative to that predicted by previous research was the presence of an adjacent wheel under load. Even with this, the failure load for the very lightly reinforced slab was equivalent to four times design ultimate load.

The global tests confirmed that the contribution of compressive membrane action to resisting global transverse moments is, at best, substantially less than the contribution to local behaviour. Because the local behaviour was so enhanced by membrane action, the crack pattern prior to failure tended to be greatly influenced, and in places dominated, by global effects. As in the service load tests, global transverse moments (which have been largely ignored by previous research) had a major influence on behaviour. However, despite the large reduction in local strength caused by this, the failure loads were still very high; a minimum of 2.83 times design ultimate load. It might, therefore, be thought that the reduction had no practical significance. This may not be the case.

The failures occurred when the combined local and global moments became too great for the slab. This has important implications because, whilst local moments are a direct effect of the load on the slab, global transverse moments are only indirectly an effect of this. They are a direct effect of the *differential deflections of the beams*. Thus anything which increases these differential deflections could reduce the local strength of the slab. The implication is that if the beams had been weaker, or less stiff, the slab would have failed in the same way but at a lower load.

Perhaps the most important conclusion from the tests is that, as predicted in 3.2.7, *global and local behaviour are not independent*. Most previous research on bridge deck behaviour has implicitly (or sometimes explicitly) assumed that they are. The result is that most of the previous research on membrane action in bridge deck slabs is only strictly applicable under single wheel loads. This does not necessarily mean that the design recommendations resulting from that research are unsafe. Indeed, even if only because of the large reserve of strength of prestressed beams designed to current rules, it seems likely that bridges designed using the empirical rules discussed in 3.2.8 will have more than adequate strength. Nevertheless it does mean that caution is required. It appears that a bridge assessed to the Ontario assessment rules(11) as having just adequate global and local strength could actually have a much lower safety factor than intended. As for service load behaviour, analytical investigation is required.

CHAPTER 9

ANALYSIS OF MODEL BRIDGE TESTS

9.1 INTRODUCTION

The tests described in the last chapter provide useful empirical evidence for the contribution of compressive membrane action to the behaviour of bridge deck slabs. They could help with the development of, and justification for, empirical design rules such as those considered in 3.2.8. However, in order to appreciate the significance of the behaviour, it is necessary to compare it with analyses. Firstly it will be compared with conventional analyses, to quantify the potential savings from using membrane action in the design of deck slab reinforcement and to see if the distribution properties predicted by conventional methods for global analysis, based on uncracked slab properties, were realised. Secondly it will be compared with the form of analysis considered in Chapter 7, both to see if that analysis would have provided a suitable design method for the models and to obtain some understanding of the behaviour.

9.2 CONVENTIONAL ANALYSIS

9.2.1 Analysis for Design of Deck Slabs

The deck slabs of both the bridges were checked using BS 5400 and the analytical methods which would normally be used with it and which were considered in 2.4. A linear grillage model was used for the global analysis and Westergaard's formula(39) was used for the local analysis.

a. First Deck

The allowable load on the first deck slab using this approach was approximately 14 units of HB. For the intended design load of 45 units of HB the reinforcement required was T10-87.5, the odd spacing giving the minimum steel area and being equivalent to 175mm at full size. This is nearly four times the steel area actually provided. The failure load implied for the reinforcement provided (setting all γ_m values to 1.0) was 14.3kN per wheel compared with the actual failure load of approximately 103.5kN per wheel in the global tests. The implied failure load under a single wheel was 21kN compared with the actual failure load of over 200kN. It is thus clear that the conventional analytical approach under-estimates local strength, apparently by a factor of up to ten. It was noted in

Chapter 2, however, that the use of linear analysis at the ultimate limit state is merely a convenient way of avoiding the requirement to check stresses under service loads. It may therefore be considered more realistic to compare the failure loads with the predictions of yield-line theory. This approach, which is normally considered to give an upper-bound solution, under-estimated the failure load in the single wheel tests by a factor of approximately two. The failure load of the slab in the global tests was reasonably close to that predicted by yield-line theory although the failure mechanism was so different that this can be little more than coincidence.

Even if yield-line analysis were used in design to BS 5400, the reinforcement provided would be little reduced since the stress limits would become critical(35). It is thus reasonable to use the T10-87.5 reinforcement as the basis of comparison with the conventional design approach. Since it has been noted in previous chapters that the critical criteria are serviceability criteria under full global load, it is most realistic to compare the observed behaviour with the conventional design approach on this basis. As the serviceability of the first deck was considered just satisfactory, the best comparison with the conventional design approach is to say that it over-estimated the steel required by a factor of nearly four.

The steel area provided approximated very closely to that required by the conventional approach to resist the global transverse moments alone.

b. Second Deck

The allowable load calculated for the second deck was approximately 16 units of HB, which is slightly higher than for the first deck. However, the calculation was based on the strength of the slab in sagging. It is common, when designing this type of slab using Westergaard's approach, to analyse only sagging and then to provide the same steel in the top. Since the single layer of steel provided was 10mm below mid-depth, this approach was not valid for this deck and analysis of hogging would have given a lower allowable load.

It was not possible to design a single layer of steel to resist 45 units of HB using normal design methods because the calculated bending moments exceeded the concrete capacity. Using two layers of steel, the requirement

was just marginally higher than for the first deck, due to slightly greater global transverse moments. However, this reinforcement was designed using a nominal value for concrete cube strength of 40N/mm², which is the normal value used in deck slabs and was slightly conservative for the concrete used in the first deck. The concrete in the second deck was weaker and using the actual cube strength in the design calculations made it impossible to design the reinforcement for 45 units of HB.

The steel area provided in this deck also approximated very closely to that required by the conventional British design approach to resist global transverse *sagging* moments. However, due to the reinforcement being located below mid-depth, the moment capacity in hogging was only some 50% of the maximum transverse global moment given by the grillage.

As in the first deck, the failure loads in the single wheel tests were approximately double the values predicted by yield-line theory.

9.2.2 Analysis for Design of Beams

Since the beams were provided with more prestress than normal, their satisfactory behaviour in the service tests proves very little. The distribution properties of the deck can only be investigated by comparing predicted and measured displacements or strains.

a. First Deck

In Figure 9.1, the maximum mid-span beam deflection in the test on the first deck is compared with the prediction of the linear grillage analysis which used 9 nodes per beam. For comparison, the prediction of a static load distribution is also shown. In order to eliminate the effect of error in predicting the stiffness of the beams, as opposed to error in predicting the distribution properties, the displacement is expressed as a factor of the average displacement of the four beams. This approach is only valid whilst the behaviour of the beams is linear-elastic but this applied throughout the range plotted in the Figure. The distribution properties are shown for the first time that each load level was applied and the breaks in the plot indicate points where, as described in Chapter 8, the loading was not continuous.

Figure 9.1 appears to show that the grillage prediction using the gross-concrete properties for the slab is very good. Initially, the distribution

was slightly better than the analysis predicts but this might be expected because the analysis ignores the shear connection between the top flanges of the beams. As the load increased, the distribution deteriorated slightly due to the reduction in transverse stiffness caused by concrete's non-linearity and cracking in tension. By 120kN per jack, the design service load, the distribution was worse than the analysis suggests but the deflection of the heaviest loaded beam was only 3.7% higher than the prediction and, even under design ultimate load, the discrepancy was less than 5%. The global transverse moments predicted by the grillage implied concrete stresses in excess of $5N/mm^2$ in the slab concrete over the beams but this concrete was apparently uncracked.

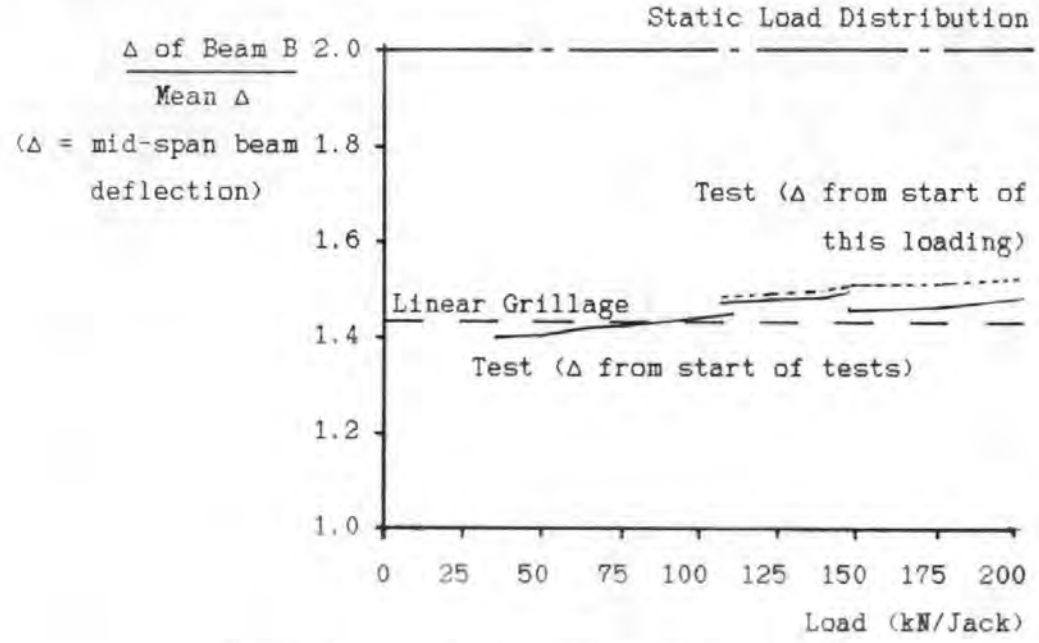

Figure 9.1: Beam deflections of first deck

(conventional analysis)

The final part of the plot in the Figure, that for loads above 150kN/jack, relates to the load application at the end of the service load tests when the load was returned to its original position. By this stage, there was a significant permanent deflection and, as will be seen from the Figure, it makes a difference to the apparent distribution properties whether the total deflections (that is, the deflections relative to the original zero) or the deflections only from the start of this load application are considered. The latter probably gives a better indication of the live-load stresses so it appears that, as might be expected, the distribution continues to deteriorate as the load increases. Despite this, the distribution remains very much better than the static load distribution.

Deflections are frequently used as an indicator of the distribution properties of beam and slab decks. However, it is the tensile stresses in the soffits of the beams which are normally the critical criteria in design so these are a better indicator. In Figure 9.2, the predicted strains on the top and the bottom of each beam at mid-span are compared with the measured strains for a particular load level. Because the beam behaviour was linear-elastic at this stage, it is reasonable to assume that stress was proportional to strain.

As in Figure 9.1, the results are expressed as a factor of the average value for the four beams. This makes the grillage predictions identical for the top and soffit.

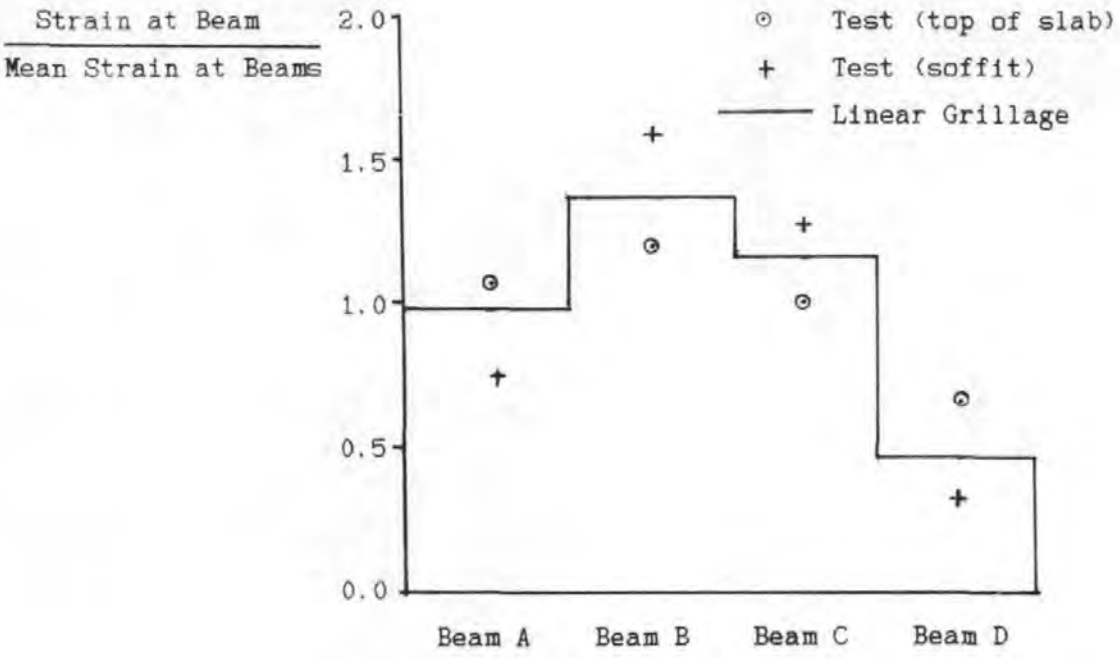

Figure 9.2: Beam strains in first deck
(end of service load tests: load = 150kN/jack)

Because the distribution properties of the deck are poor, the analysis predicts very significant differences between the stresses in adjacent beams. This is reasonable for the soffit stresses because there is no direct connection between the bottom flanges of the beams. However, the analysis implies that the stress distribution across the slab is literally as shown in the Figure; with large discontinuities between adjacent pieces of concrete. This is impossible and shear in the slab evens out the longitudinal stresses in the slab as can be seen in the Figure. However, this does not even out the soffit stresses. Indeed, because it reduces the

differential dieflections of the beams and hence reduces the contribution of global transverse moments to distribution, it can cause a deterioration of the distribution properties as expressed by soffit stresses. The result is that whilst Figure 9.1 suggests that the distribution at this load stage is only 5% worse than the grillage prediction, Figure 9.2 shows that it is 16% worse.

This may suggest that the distribution properties of this deck, with its very light reinforcement, were unsatisfactory and that the fears expressed in 3.2.7 are confirmed. However, the increase in the percentage load carried by the heaviest loaded beam was only approximately 5% between the initial linear condition and the load stage considered in Figure 9.2 which is the design ultimate load. This implies that, even if the deck slab had been so heavily reinforced that it remained effectively linear-elastic after cracking, the grillage based on gross-concrete slab properties would have under-estimated the maximum soffit stress by approximately 10%. Thus most of the discrepancy was due to a normally accepted error in analysis for design, not the reduced steel area.

b. Second Deck

In Figure 9.3, the greatest mid-span beam deflection in the tests on the second deck is compared with the prediction of a linear grillage. The prediction of the static distribution is not shown but it corresponds to a value of 2.5 in the Figure. As in Figure 9.1, the maximum beam deflection is expressed as a factor of the average deflection of all the beams. However, because of the parapet up-stands in this deck, the four beams were not identical. The approach is not, therefore, quite such a reliable guide to distribution because errors in predicting the difference between the stiffness of the edge and inner beams would show up in the Figure.

The longitudinal strains in the slab over the beams are illustrated in Figure 9.4 and the soffit strains in the beams are illustrated in Figure 9.5. The reason for using two figures, rather than one as for the first deck, is that because of the different edge beams the grillage predictions in the two figures are different. The reason for choosing a different load stage to illustrate is related to difficulties experienced in both tests with the strain gauges.

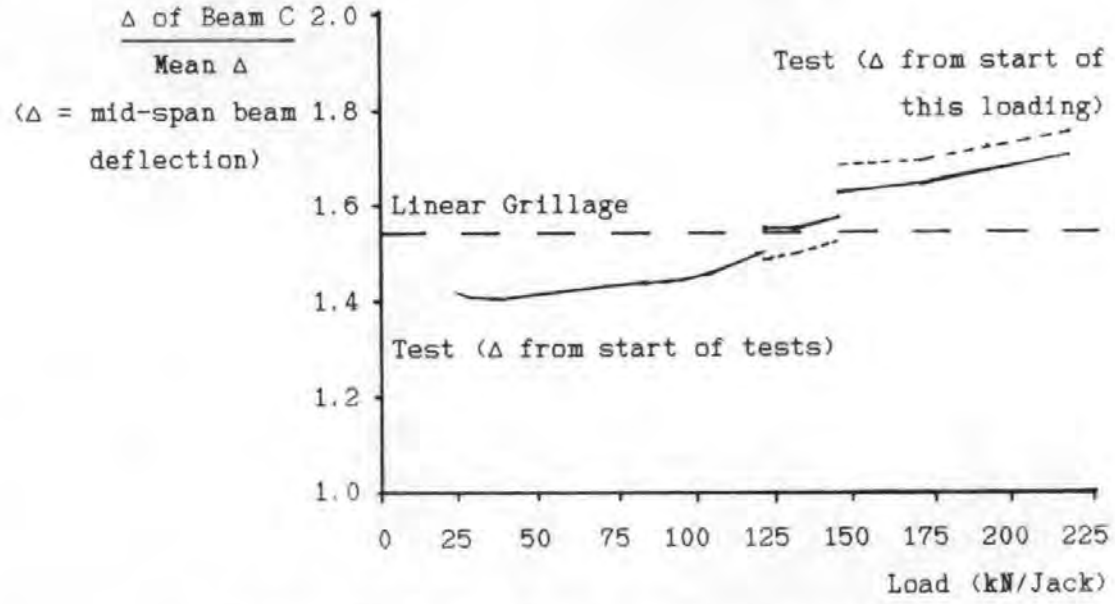

Figure 9.3: Beam deflections of second deck
(conventional analysis)

Figure 9.3 appears to suggest that the distribution was initially significantly better than the grillage prediction. Assuming that this difference was due to the shear connection between the top flanges the extent of the difference is surprising: theoretically it should be less than for the first deck. However, a detailed study of the results suggested that part of the discrepancy may have been because the analysis exaggerated the effect of the parapet up-stands and hence exaggerated the stiffness of the edge beams. This was despite the analysis using the measured E_c values for the beam and parapet concretes which were substantially more different than the nominal (or even the actual) strength difference would suggest. The reason for the small effect of the parapets was probably that they were cracked due to plastic settlement.

The first break in the plot in Figure 9.3 corresponds to the end of the first load cycle to service load. At the end of this cycle the more heavily loaded beams did not return to their original positions. The outer beams had small negative deflections suggesting that the permanent deflection was mainly due to some of the transverse curvature becoming permanent. This implies that there were locked-in stresses in the beams. Since the next part of the plot relates to a load application immediately after the first, these stresses would not have been relieved greatly by creep. Thus the solid line, relating to the distribution calculated from the total deflections, probably gives the best indication of the load

distribution in the next section of the plot. In contrast, the permanent deflections at the start of the load application represented by the final part of the plot were relatively uniform across the deck, implying that they were largely due to permanent beam curvature and thus that the dotted line gives a better indication of the load distribution at this stage. It will thus be seen that the distribution properties deteriorated progressively throughout the test and that the deterioration was greater than for the first deck. The greater deterioration might have been expected both from the extent of apparently global cracking in the slab and from the fact that the steel provided was inadequate to resist the global transverse moments predicted by the analysis.

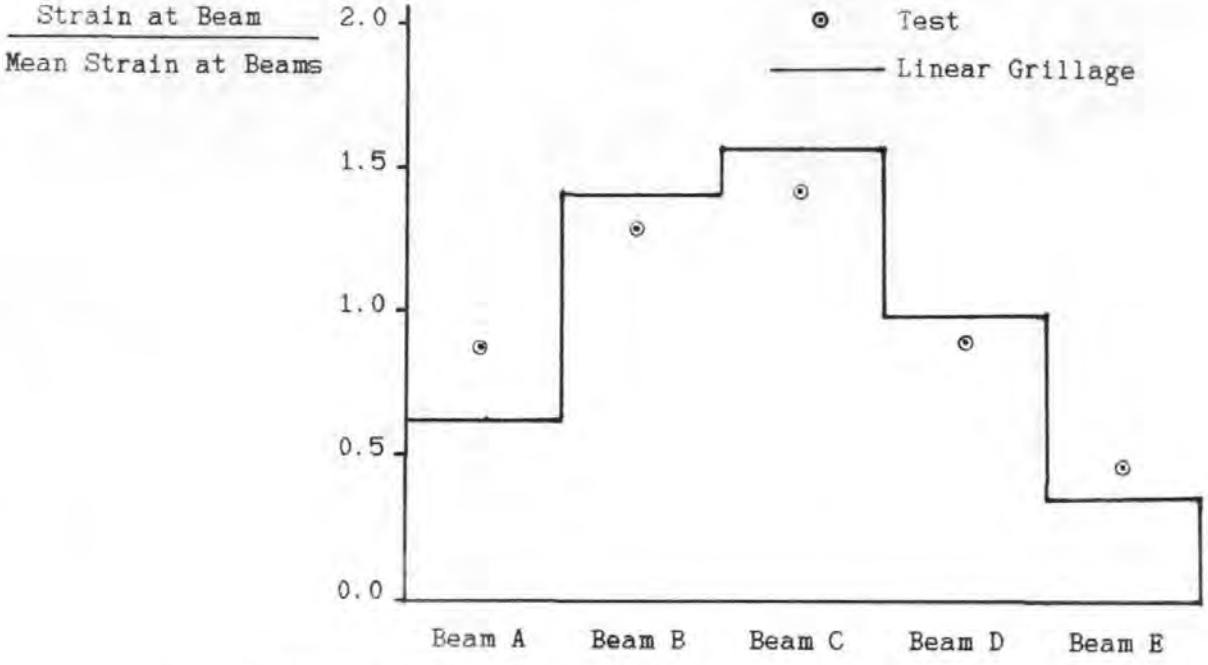

Figure 9.4: Slab strains over beams in second deck
(first loading; load = 120kN/jack)

Figure 9.4 shows that, as for the first deck and for the same reason, the stresses in the slab were more evenly distributed than the grillage predicts. Figure 9.5 shows that the maximum soffit stress was higher than the analysis predicts. The margin is so small it would not normally be considered significant. However, Figure 9.3 shows that there was further deterioration in the distribution properties after the stage to which Figure 9.5 relates. By the completion of the service load tests it appears that the worst soffit stress was approximately 10% higher than the grillage prediction although still some 30% lower than the static load distribution suggests.

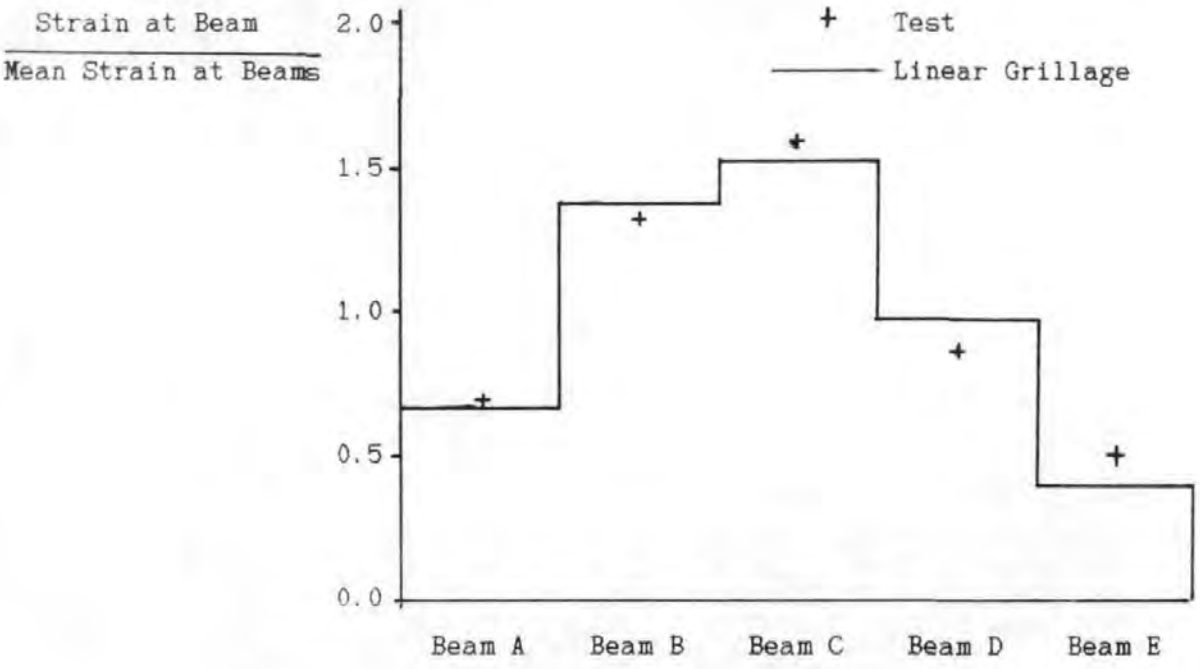

Figure 9.5: Beam soffit strains in second deck
(first loading: load = 120kN/jack)

9.3 NON-LINEAR ANALYSIS

9.3.1 Single Beam

The single beam test served to check that the analysis modelled the behaviour of the beams correctly, and thus to ensure that any errors in the predictions for the behaviour of the model bridge decks were not due to failure to model the behaviour of the beams. Because of this it is convenient to consider these tests first.

The predicted and observed load-displacement relationships are shown in Figure 9.6. They are as close together as can reasonably be expected; larger discrepancies are frequently observed between the behaviour of two nominally identical concrete specimens even when they both come from the same batch of concrete.

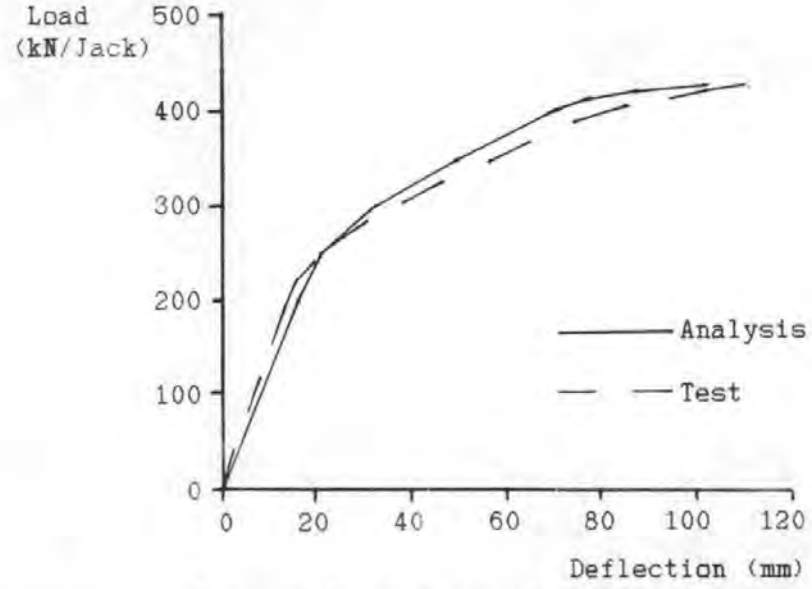

Figure 9.6: Analysis of single beam test

9.3.2 First Deck

a. Global Tests; coarse mesh analysis

The deck was initially analysed using a 15 by 12 node model. This gave four transverse elements between each beam, which was considered reasonable. However, these elements were 727mm wide so it was assumed the model would be too coarse to model the local behaviour correctly. The reason for using such a coarse mesh was that this was the largest model which would fit in the 386 desk-top computer used.

The computer model was loaded monotonically to failure under the load case used in the tests and the predicted central deflections of the beams are shown along with the test results in Figure 9.7. Considering the many approximations in the analysis, the complexity of the behaviour and the usual variability of the behaviour of concrete structures, the predictions are reasonably good. Because the analysis was performed under load-control using relatively large increments, it did not pin-point the failure load precisely. However, the best estimate of the failure load which could be obtained from the analysis was 400kN per jack compared with the actual value of 414. The analysis also predicted correctly several features of the behaviour which might otherwise have been considered surprising. It predicted that the first cracking would occur in the soffit of the slab under wheel 10 (as shown in Figure 8.11) but that at later stages of the loading the slab would be much more highly stressed in the outer bay, that is under wheels 1 to 4. It also predicted correctly that, as failure approached, the slab adjacent to wheel 4 would be subjected to transverse

sagging moments right out to Beam A. Finally, it predicted both the load at failure and the mode of failure surprisingly well; in the final increment plotted in the Figure, concrete was crushing most extensively under wheel 4 and it was in this region that the analysis failed to converge and gave large deflections in the next increment.

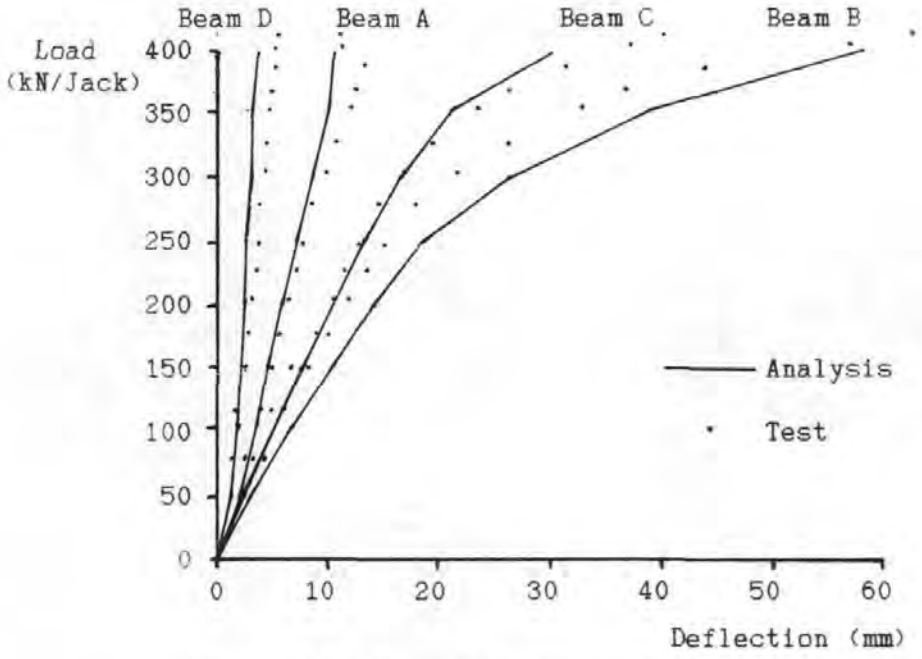

Figure 9.7: Beam deflections of first deck
(from non-linear analysis using a coarse element mesh)

With such a coarse element mesh, the correct prediction of such an apparently local failure might be considered surprising. There appear to be three explanations for it. Firstly, although the final collapse took the form of local punching due to the local shear stress, it was apparent that the concrete was crushing along a line which extended from wheel 3 to slightly beyond wheel 4. This crushing, which apparently caused the failure and which was predicted by the analysis, thus extended over the width of two elements of the computer model enabling the resulting failure to be predicted. Secondly, as was found in Chapter 7, the analysis tends to be conservative in its prediction for punching failure loads and this cancelled out the failure to model the peak of the stress concentration under the wheel; thus a finer mesh would have led to an under-estimate of failure load. Thirdly, in an attempt to cancel out the fault of the coarse model, the loads were applied as points with no allowance for the distribution over the patch area.

This ability of the analysis to predict failure load and mode is reassuring; in particular, the fact that it still gives low predictions even when a coarse mesh is used means that it is safe for use in design. However, the model tests suggest that the limiting service load for the bridge was equivalent to around 120 to 150kN per jack. In BS 5400, a design service HB load of 150kN corresponds to a design ultimate HB load of 204kN*. Even allowing for the fact that the material safety factors should be applied in the analysis for the ultimate limit state, and requiring an extra 15% strength for a brittle failure mode (which is debatable), it is clear that serviceability is critical. Thus the predictions for the lower load stages are more important.

In the analysis, there was local soffit cracking under wheel 10 at the first increment, 50kN per jack, and there was limited top cracking in the slab by the second increment, 100kN per jack. In the tests, such cracking was not observed until loads of 110 and 300kN per jack respectively. The main reason for this very large discrepancy appears to be that the analysis assumed the concrete to be linear-elastic until cracking, whereas in fact there clearly was a significant departure from linearity before cracking. The fault was exaggerated by the use of a low tensile strength for the concrete in the analysis, 0.67 times the split cylinder strength. This was chosen because it gave the best results in Chapter 6 for lightly reinforced specimens. However, because of the scope for redistribution to the steel, the use of the full split cylinder strength gave better results in heavily reinforced specimens. Although the slab of this bridge was lightly reinforced there was great scope for redistribution. It thus appears that in this respect, as in their failure mode and load, lightly reinforced restrained slabs behave like heavily reinforced unrestrained slabs.

*Footnote
The ratio of design ultimate to design service load implied by this is higher than that used in Chapter 8. This arises from the Author's interpretation of the factor γ_{fe} in BS 5400. γ_{fe} is a partial safety factor for errors in analysis which, in BS 5400: Part 4, is applied to the loads. Since the form of analysis considered here is not elastic, a factor of 1.15 is used at the ultimate limit state as specified by the code. However, when considering the load to be applied to models, the author has assumed that, since no analysis is involved, γ_{fe} can be 1.0. This might be considered debatable since γ_{fe} also covers errors in dimensions. However applying γ_{fe} to the loads used in Chapter 8 would not alter any of the conclusions.

The behaviour in the tests was clearly greatly affected by the non-linearity of concrete in tension and by its ability to transmit some tension after cracking. Although the analytical prediction of cracking under wheel 10 by a load of 50kN per jack was greatly premature, the measured strain in this region at this stage was 100 microstrain which, with the measured E_c value, implied a stress of approximately $3N/mm^2$. Assuming concrete to be linear elastic in tension until it cracks, this would certainly imply that cracking was at least imminent. In fact, although non-linearity is visible in Figure 8.12 from approximately this stage and becomes very pronounced by a load of 75kN per jack, cracking was not visible until a load of 110kN.

Although the analysis exaggerated the amount of cracking, there was not a corresponding exaggeration of the stresses in the slab. Using the analysis in the same way as a conventional linear analysis, that is calculating the stresses from the element forces given by the program using a cracked elastic section analysis ignoring the tensile strength of the concrete, the allowable service load from the BS 5400 criteria was approximately 110kN; the critical criterion being the steel stress. Although the actual steel stress in the model was unknown and probably substantially lower than the $345N/mm^2$ implied by this, it was concluded in Chapter 8 that the behaviour was just acceptable for the load history applied which had been intended to simulate the life of a bridge with a design service load of 120kN. Thus the analysis was conservative although it still allowed nearly three times the load on the deck that a conventional analysis would allow.

For reasons discussed in Chapter 6, it is not possible to adjust the material models to make the analysis reproduce the full effect of concrete's ductility in tension and hence to predict correctly the development of cracking. Indeed, it is debatable whether this is desirable since the effect is probably size dependent and thus an analysis which did this for the model would be incorrect for a full size bridge. Thus the analysis appeared to be as good as possible. However, the premature development of cracking did have an undesirable effect; it made the analysis exaggerate the rate of decay of the distribution properties, a trend which can be observed from Figure 9.7.

Before cracking, the predictions for the strain in the beams were substantially better than those of a conventional linear grillage; not

because of non-linearities but because of modelling the effect of the shear connection of the top flanges of the beams. However, by a load of 150kN per jack, the error in the predicted soffit strain was as great as that of the linear grillage although, unlike for the linear analysis, the error was in the safe direction. The premature decay of distribution properties was due to the premature development of cracking in the analysis. This was not entirely due to the material model used. It was partly due to the failure of the analysis to model the effect of the finite width of the beam webs. The predicted hogging moment in the slab at the position corresponding to the face of the web in the model was little more than half that over the centre-line of the beams. Thus a length of transverse element which was, in fact, uncracked and effectively very deep was modelled as being shallow and cracked.

b. Global Tests; fine mesh analysis

The model bridge was re-analysed using a finer mesh to give a better indication of the behaviour. Because the previous analysis had shown that the most highly stressed regions of the slab were not confined to small areas and that the most highly stressed region moved as the loading progressed, it was undesirable to restrict the fine mesh to local critical areas, as had been done in the analysis of Kirkpatrick's tests in Chapter 7. Because of this the computer model was too large to run on the desk top computer and it was transferred to a Vax 11/750 machine. This greatly increased the space available but the machine was significantly slower than the 386 and this imposed a practical limit on the size of model which could be analysed.

Six transverse elements were used between each beam and those adjacent to the beam were made shorter so that their ends coincided with the face of the web. They were given a full width 100mm deep web to represent the presence of the top flange of the beam. 32 nodes were used along the span of the bridge giving 258mm wide elements and a total of 672 nodes.

The full split cylinder value was used for the effective tensile strength of the concrete and, unlike in the coarse mesh analysis, the finite size of the load patches was represented.

The load history of the service tests was simulated by applying and removing the test load from the six different positions. However, in order

to keep the computer time used within reasonable limits, only the first and last loadings were analysed in detail. The loads were applied to and removed from the other positions in single increments.

The predicted displacement of wheel 9 relative to the beams is shown in Figure 9.8. On first loading, the analysis still under-estimated the load to cause visible cracking although not by as large a margin. It also over-estimated the loss of stiffness caused by this cracking. This is again due to its failure to model the ductility of concrete in tension. This is a far more significant factor in this highly indeterminate structure than in the simple strips considered in Chapter 6. In a simple beam, despite the ductility of concrete in tension, as soon as cracks form they extend well above the soffit. In the analysis of this bridge deck, despite the relatively brittle concrete model used, the scope for redistribution meant that it was common for cracks to form at only one of the eight integration stations through the depth of the slab. This meant that the area of concrete which is strained out of the linear range but still resisting tension is larger and further from the neutral axis. It is thus far more significant to the behaviour.

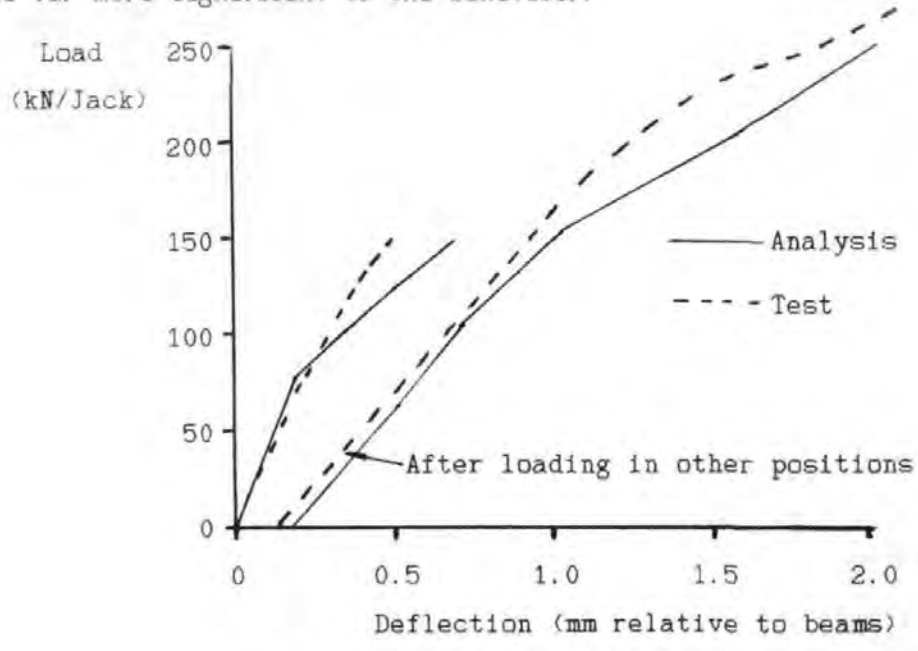

Figure 9.8: Deflection under wheel 9
(from non-linear analysis using a fine element mesh)

The over-estimate of the deflection in the final loading is also probably due to the failure to model the effect of the ductility of concrete in

tension. However, considering the many unknowns in the analysis and the complexity of the behaviour, the prediction is remarkably good.

Unfortunately, the analysis could not be taken up to failure. By a load of 300kN per jack, when the effect of cracking in the beams became significant, the convergence rate became excessively slow and it was not possible to obtain a sufficiently accurate solution using a reasonable amount of computer time. However, the analysis appeared to confirm that the allowable service load on the deck was approximately 120kN per jack and the design ultimate load corresponding to this is only 172.5kN per jack. Thus the analysis had shown that the deck had at least 50% more ultimate strength than could be used in design.

The beam deflections predicted by the analysis are shown in Figure 9.9. Because of the use of a higher tensile strength for the slab concrete, and because of the modelling of the finite width of the beams, this analysis predicted better distribution properties than the coarse analysis. The predicted beam deflections are as close to the test results as can reasonably be expected.

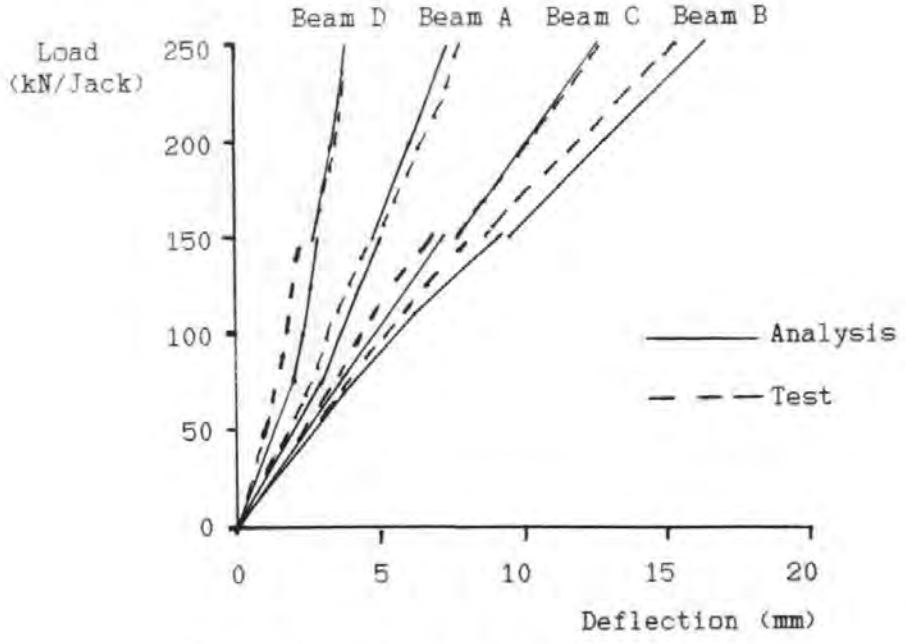

Figure 9.9: Beam deflections of first deck
(from non-linear analysis using a fine element mesh)

Since the computer models had given good predictions for the behaviour of the deck, it seemed reasonable to use them to obtain some insight into the mechanism by which this behaviour was achieved. In Figure 9.10 the

transverse restraint force across the longitudinal centre-line of the deck predicted by the computer model is shown for a particular load stage. As might be expected from previous research, there is a compressive force in the region of the wheels. However, the compressive force in the end regions of the deck (which is apparently due to the effect illustrated in Figure 3.12) is much greater. Thus, with these forces to resist, the rest of the deck is in tension. The behaviour is different from that described or implied by other researchers: with significant *compressive* force in the end regions their assumption that diaphragms are needed to resist *tension* cannot be correct. The tension required to resist the compression in the critical areas comes from material which is relatively close to those critical areas. The analysis also suggests that the restraint force is more localised than previously supposed in the transverse direction. The plot in Figure 9.10 is based on the average of the forces in the elements on either side of the centre-line. The transverse restraint force predicted for a section at the face of the web is markedly different, barely going into tension at all adjacent to the wheel positions. This appears to confirm the suggestion in 3.2.5 that membrane action under service loads is not dependent on external restraint and could still be significant in unrestrained slabs.

It is also clear from Figure 9.10 that the resistance to global transverse moments is not enhanced by compressive membrane action since much of the relevant area of the deck is in tension.

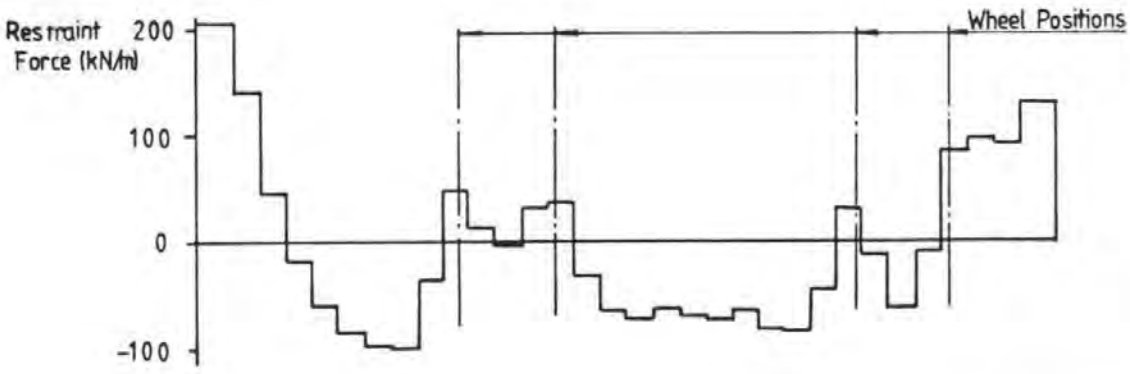

Figure 9.10: Predicted force across centre-line of first deck
(from fine analysis; load = 250kN/jack)

The coarse mesh analysis suggested that the area of slab in compression around the wheels extended in both directions as failure approached. The

restraint force also increased disproportionately as the load increased. However, the general form of Figure 9.10 remained unchanged and the end regions of the deck were subjected to an increasing compressive force.

As the predicted distribution of restraint forces was so different from that implied or described by previous researchers, it was considered highly desirable to check it by attempting to measure the restraint forces in the model. Because of the many variables in the behaviour of cracked concrete, it was considered best to do this for a section where the concrete would be uncracked. Accordingly, a series of transverse demec points were attached to the top and bottom of the slab at matching positions close to the assumed point of transverse contraflexure in the slab. Unfortunately, there were many difficulties in interpreting the results. Firstly, although the forces indicated in Figure 9.10 are sufficient to be highly significant to the behaviour of a lightly reinforced cracked section, they represent a low stress on the gross-concrete section, typically $1N/mm^2$, which makes them difficult to measure. This was made worse by the significant longitudinal compression in the deck due to global moments. It was necessary to correct for the Poisson's ratio effect of this and, although longitudinal demec points were provided to enable the longitudinal strains to be measured, the corrections were inevitably inaccurate if only because of the uncertainty in the Poisson's ratio used. Since the correction was often significantly greater than the measured transverse strain, errors in the correction had a large effect on the estimated transverse forces.

A second difficulty was caused by the effect of cracking. Although there were no visible cracks within the gauge lengths, some of the measured tensile strains were in excess of 100 microstrain which would normally be taken to imply that there would be some non-linearity in the behaviour. More seriously, cracks outside the gauge length but close enough to affect stresses within it (that is cracks within S_o of the gauge length as considered in 6.2.1) could release some of the tensile stress in the concrete transferring it to the steel. This would have the effect of making the restraint force estimated from the strain readings more compressive than the actual restraint force. It appears that this must have been a significant effect since integration of the restraint forces estimated from all the readings appeared to imply that there was a significant net transverse compression across the bridge. Since the beams

were restrained only by the flexible elastomeric bearings, this was impossible. However, it is perhaps significant that if the bridge had been provided with diaphragms one might reasonably have supposed that the "compression" in the slab was resisted by tension in the diaphragms.

The one case where the demec readings did give a reasonable indication of the transverse force was for the ends of the slab when the bridge was loaded in the first position. Since this was a free edge, the longitudinal stress was clearly zero so no Poisson's ratio correction was required. Similarly, since the nearest visible crack was over a metre away it seemed reasonable to suppose that the strain readings could not have been much affected by cracks. Another advantage was that it was possible to position demec points at mid-depth of the slab as well as on the top and bottom surface. Unfortunately, where this was done, the mid-depth gauge gave a strain which was significantly different from the mean of the top and bottom gauges. This was presumably due to non-linearities in the behaviour which invalidated the assumption that plane sections remain plane. The maximum measured tensile strain, over 150 microstrain, also implied that concrete non-linearity was possible. These difficulties meant that, even for the ends of the slab, the restraint force could only be estimated to within plus or minus some 50%. Nevertheless the results were significant; all four demec sets showed a compressive strain which was approximately as predicted by the analysis. Given that previous research implied that this region should be in tension, this alone appeared to be sufficient to show that Figure 9.10 was closer to reality than were the implications of previous research.

The restraint forces predicted by the analysis are significant to the behaviour but not, on their own, sufficient to explain the enormous enhancement relative to the predictions of conventional design methods. An equally significant mechanism is moment redistribution. An important factor here is the orthotropic nature of the cracked slab. It has already been noted that, with such light reinforcement, the cracked stiffness is only some 10% of the uncracked stiffness. It is clear from the figures in Chapter 6 that the tangent stiffness of the cracked section is lower still. Under global load, the deck slab was subjected to a very significant longitudinal compressive stress which delayed the formation of transverse cracks, hence the longitudinal stiffness remained at its full uncracked value. The result was that the distribution of the transverse moments,

both in the real slab and in the analysis, was very much more uniform than implied by a conventional analysis. This redistribution of the moments is due to cracking hence, unlike redistribution due to reinforcement yielding, it starts to take effect before there is any material damage which is unacceptable under service loads.

c. Local Test

The distribution of restraint forces indicated in Figure 9.10 is significantly different from that implied by previous research. However, the load case considered was also significantly different from that investigated by previous researchers in that 16 wheel loads were applied instead of only one or two. It is possible that this was the reason for the difference. To investigate this, it was decided to re-analyse the deck for a single wheel load. The wheel was positioned in approximately the position of single wheel A in the tests but the analysis was not directly comparable with the test. In the analysis the load was applied to the undamaged bridge whereas in the tests it was not applied until after the bridge had been loaded to failure under full global load.

Because of the uncracked slab the analysis predicted a significantly stiffer initial response than was observed in the tests. As failure approached, the crack pattern in the test began to be dominated by the single wheel and consequently the difference between the test and analysis reduced. The analysis converged under a load of 220kN but indicated that failure due to local concrete crushing round the wheel would occur before 230kN. This is remarkably good agreement with the failure load in the test which was approximately 226kN. However, although very fine for the analysis of a whole bridge deck, the element mesh used was still slightly too coarse for a local analysis as is indicated by the large difference between the restraint forces in adjacent elements in Figure 9.11. It is likely that a finer mesh would have given a slightly lower failure load. It is also possible that the failure load in the test would have been higher if the deck had not been damaged by the previous loading to failure. However, other tests and analyses suggest that this effect would have been very small.

In Figure 9.11 the restraint force predicted across the centre of the bay of slab between Beams D and E is illustrated for two different load levels. The first of these, 60kN, is close to the wheel load considered in

Figure 9.10. For this relatively low load, the forces are plotted only for the region around the wheel.

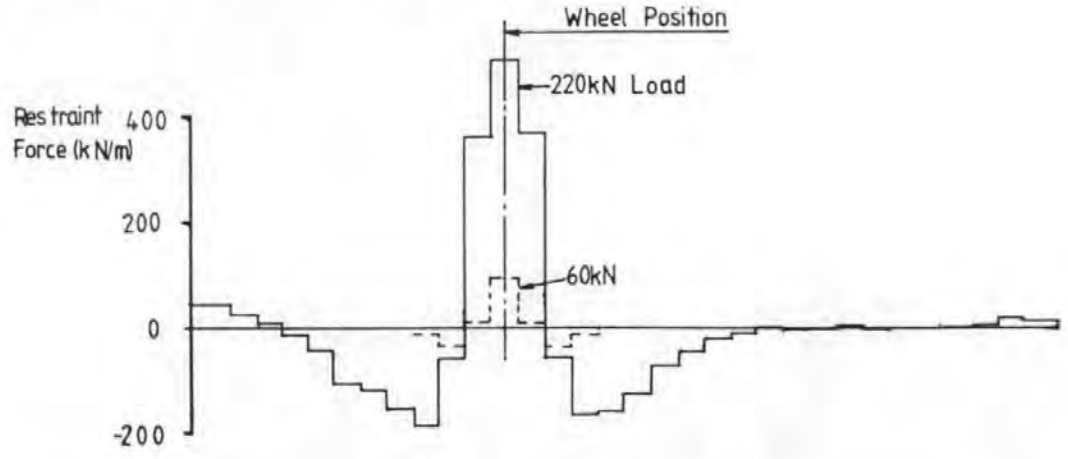

Figure 9.11: Restraint forces predicted under single wheel load

There is a compressive force in the end regions of the deck but this is very much smaller relative to the wheel load than in Figure 9.10. This confirms that the force is due to global effects which are much less significant with only one wheel loaded. The compressive force in the region of the wheel under 60kN is greater than in Figure 9.10. This is partly due to the lack of the global tension force near mid-span. However, a comparison of Figures 9.10 and 9.11 reveals another explanation. The compressive restraint force under each wheel in Figure 9.10 is superimposed on the tensile force due to an adjacent wheel. This is another reason why behaviour in single wheel tests is an unreliable guide to behaviour under multiple wheel loads.

As the load increases, the restraint force in Figure 9.11 increases disproportionately, particularly for the elements either side of the wheel. However, even as failure approaches, the area in compression around the wheel is comparatively localised. The restraint required to resist this compression comes from the slab immediately on either side of the wheel and the end regions continue to be subjected to compression. Thus, as in the global tests, the analysis shows that diaphragms are not needed to provide the restraint. The source of restraint is substantially different from that implied by previous research. However, if the critical region is considered to be applying a compressive force to the rest of the slab, the rest of the slab is analogous to a slab with a hole in it across which a compressive force has been applied. Figure 9.11 is remarkably consistent

with the result of an elastic analysis of such a case which is shown in Figure 9.12.

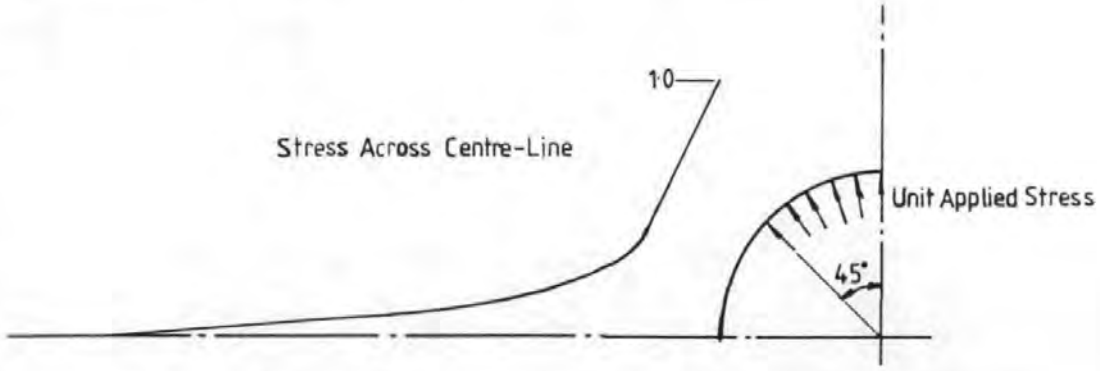

Figure 9.12: Elastic analysis of stresses around a hole
[from finite element analysis by Mehkar-Asl(130)]

Under 220kN, the analysis was very close to failure and the stress in the concrete immediately below the wheel was just starting to reduce from its peak value as the concrete began to crush. The maximum restraint force predicted was only approximately half of that suggested by the rigid-plastic strip theory considered in 3.2.1. This was entirely due to the requirement for compatibility and to the lack of ductility of the concrete. The fact that the slab failed in the analysis before reaching the full plastic moment capacity could not have been due to shear as the analysis does not model this effect.

As with the global tests, an attempt was made to ascertain whether the real restraint forces were as predicted by the analysis. Because the slab was already cracked before the tests were started, it was even more difficult to do this. All that could be established with any certainty was that the general form of Figure 9.11 is reasonable.

d. Modified Decks

In the last chapter it was suggested that if the beams had been provided with less prestress, the deck could still have failed in the same way but at a lower load. To investigate this, the bridge was re-analysed using only 60% of the prestress area. To reduce the computer time required, and to enable the analysis to be taken up to failure, the coarse element mesh was used.

The beams were not predicted to crack until the load was 175kN per jack and up to this point the behaviour was not affected by the reduction in

prestress. Thus the analysis confirmed that the behaviour in the service load tests would have been identical without the over-provision of prestress.

The analysis predicted the same form of failure as before but at a lower load of approximately 320kN per jack. The maximum beam deflection at failure was greater, indicating that the slab could withstand greater differential beam deflections when subjected to smaller local loads.

The load at which the slab was predicted to fail was *below* that predicted by yield-line theory. This is entirely consistent with the explanations of the behaviour given earlier in this thesis. It also suggests that the supposedly conservative approach to design allowing for membrane action of using yield-line theory, which was proposed by Tong and Batchelor(51), is potentially unsafe.

Analysis using the coarse element mesh was also used to investigate the effect of varying the quantity of reinforcement in the slab. Two analyses were performed, one using the actual quantity of secondary steel with double the quantity of main steel and another in which both the main and the secondary steel were reduced to half that which was actually provided. In both cases, the prestress and also the additional transverse bars in the end regions of the slab were as provided in the model. The allowable service load implied by these two analyses were approximately 190 and 60kN per jack respectively whilst the failure loads were approximately 440 and 375kN.

The service loads were obtained from normal BS 5400 criteria using the worst stress at a crack calculated ignoring the concrete in tension; the "stress at crack approach" described in 7.7.3. The steel area in the lightly reinforced slab was so low that this approach predicted high steel stresses as soon as the concrete cracked, that is before the cracking was extensive enough to develop much membrane action. Because of this the service load of 60kN predicted in this way is very approximate and probably too low. However, this behaviour might be taken to imply that the steel area was below the desirable absolute minimum. At 0.18% it was above the code nominal steel area but the low d/h ratio in a thin deck slab means that the minimum steel area expressed as a percentage of the net section should be higher than normal.

The analysis with increased steel area suggested that doubling the area of main steel increased the service load by over 50%. Although well below the near linear relationship given by normal design methods, this is a greater effect than implied by previous research. This is because the steel contributes to the resistance to global moments and also to the restraint. Under single wheel loads, as tested by previous researchers, the global moments are insignificant and there is relatively more slab available to provide the restraint. Thus these effects are less pronounced.

A final analysis was performed using a single layer of deck slab reinforcement as provided in the second deck, although still with the extra bars in the end regions of the slab. This analysis suggested a slightly higher allowable service load than for the steel actually provided, in contrast to the analysis of the second deck which will be described in the next section. The failure load was, however, reduced to approximately 375kN per jack.

All the analyses predicted the same failure mode with the same wheel punching through the deck. However, the failures were clearly greatly influenced by global transverse moments. A major effect of increasing the steel area was to improve the distribution properties of the decks, particularly in the later stages of the analysis as failure approached. Thus, although the most heavily reinforced slab had the smallest rotation capacity, and hence failed when the differential beam deflections were relatively small, it failed at the highest load. At failure, the predicted deflection of the heaviest loaded beam (Beam B) was similar to that in the test and analysis of the actual model but the deflections of all the other beams were significantly greater.

e. Analysis with no Concrete Tensile Strength

The coarse mesh analysis was also used to investigate the effect of reducing the tensile strength of concrete to zero. This analysis gave a failure load of approximately 375kN which is a reduction of less than 10% compared with the original analysis. The implied service load was reduced by a similar percentage. These relatively small reductions indicate that the tensile strength of concrete is not as important to the restraint as might have been supposed. This arises because the global moments meant that the slab was cracked over much of its length, reducing the

contribution of concrete in tension. It implies that much of the restraint actually comes from the under-stressed reinforcement away from the critical areas and confirms that reinforcement is necessary in deck slabs.

It was noted in Chapter 7 that this form of analysis has the major practical advantage of not being load history dependent. In this case, it did provide conservative answers and would have been a reasonable design approach. However, it was also noted in Chapter 7 that this may not always be the case. Another disadvantage of this form of analysis is that it gives over-conservative predictions for the distribution properties. In this case it over-estimated the worst beam moment under service loads by 10%.

9.3.3 Second Deck

Only one computer model was used for the second deck. This used the same width of transverse elements as the fine mesh analysis of the first deck, 258mm, but it used only four elements across a slab span. This gave a total of 608 nodes. The use of six elements across a slab span, as in the fine mesh analysis of the first deck, would have required 864 nodes and a significantly greater band width, which would have needed an excessive amount of computer time. The major disadvantage of using only four elements across a slab span is that it prevented the model from representing the finite width of the beam webs.

As with the fine mesh analysis of the first deck, a complete load history analysis was performed. The predictions for local deflection were not as good as for the first deck with the deflection under wheel 14 being consistently over-estimated, typically by 50%. This was undoubtedly largely due the failure to represent the finite width of the beam web. The analysis implied a transverse moment at the face of the beam web which was only some 50% of that over the centre-line of the beam. This was more significant than in the first deck because the critical slab section was over the beam rather than at mid-span of the slab.

The analysis predicted lower steel stresses than in the first deck. However, using conventional BS 5400 design criteria, the allowable service load would still have been lower at just under 100kN per jack compared with 120kN for the first deck. The critical criterion was the concrete stress in the soffit of the slab over Beam D adjacent to wheel 14. This

contrasts with the hypothetical analysis of the first deck with only one steel layer which gave a higher service load. This is due to the greater hogging moments in the second deck and the fact that the single layer of steel was below mid-depth. Another factor was the higher concrete grade in the first deck.

By 150kN per jack the concrete in the critical region was stressed significantly beyond the limit of linear elastic behaviour used in the computer model. This, and the more extensive cracking in this bridge, meant that the analysis predicted a much greater difference between the behaviour under the first and last applications of the service load than for the first deck. This reflected the real behaviour of the bridge and confirmed the implication of both the analysis and the test results that the 150kN per jack applied in the tests was above the desirable service load for this structure.

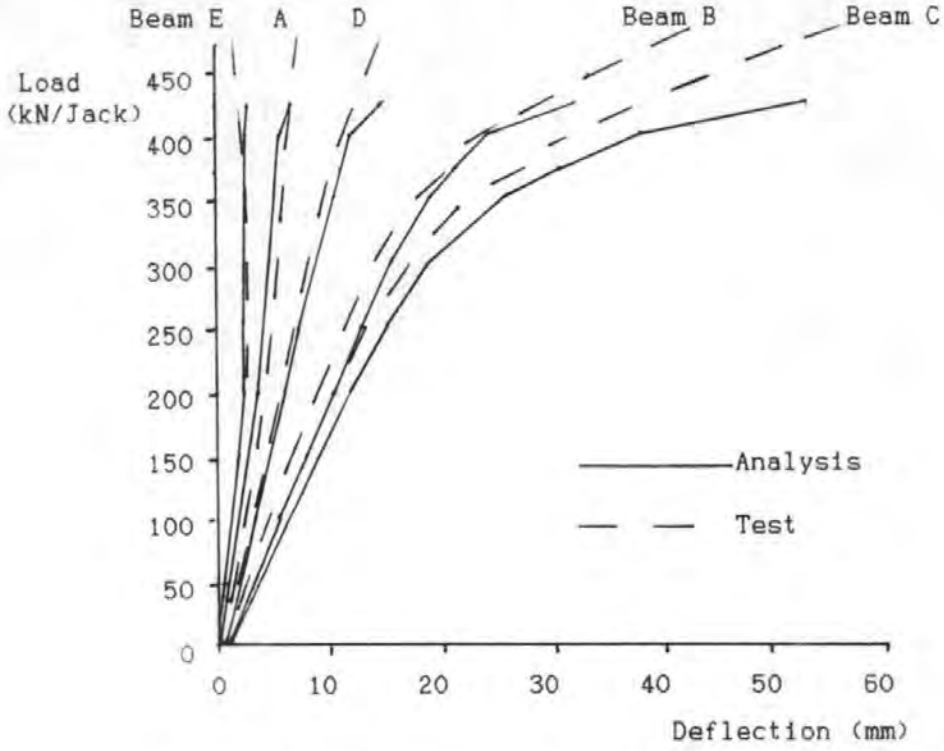

Figure 9.13: Beam deflections of second deck
(from non-linear analysis)

On completion of the analysis of the service load tests, the computer model was loaded monotonically to failure and the predicted beam deflections are shown in Figure 9.13. As for the first deck, the analysis correctly predicted the failure mode; it predicted concrete crushing on the slab soffit over Beam D followed by excessive local deflection under wheel

14. However, the prediction of failure load was not quite as good, the analysis under-estimating this by over 10%. Indeed it would be more realistic to say that the analysis under-estimated failure load by nearly 20% since it did not converge properly under the last load increment plotted in Figure 9.13 and at this stage it also gave an excessive deflection under wheel 14 of over 20mm relative to the beams.

This greater conservatism of the analysis compared with the coarse mesh analysis of the first deck might have been attributed to the finer element mesh or to the greater significance to this deck of the failure to model the web width. However, the fact that the analysis predicted significant increases in the deflections of Beams B and D as well as C in the final load increment plotted in Figure 9.13 suggests that it was the prediction of the beam behaviour which was at fault. If the low predicted failure load had been due to the analysis under-estimating slab strength and consequently under-estimating distribution properties, the analysis should have under-estimated the deflection of Beam D. In fact it slightly over-estimated the deflection of that beam. It appears that the reason the analysis predicted an earlier failure than actually occurred was that it predicted that the concrete in the slab would start to crush due to the global flange forces under a lower load than was the case. In the tests, there was no obvious sign of this crushing although it seems likely that it was beginning to occur when the bridge failed. The reason this happened at a lower deflection than in either the first bridge or the single beam test was that the slab concrete was significantly weaker and the analysis appears to have exaggerated the effect of this. However, although this global crushing was a major reason for the failure in the analysis, the analysis still correctly predicted that the final collapse would look like a local failure; once again it showed that global and local behaviours are not independent.

Since the predicted failure load, although 20% below the actual failure load, was nearly four times the allowable service load given by the analysis its value had no practical significance. The reasonably good predictions for the behaviour at lower loads are more important. The analysis suggested that the slab as tested was inadequate for the intended load and this confirms the findings from the tests suggesting that the analysis would have provided a satisfactory design method.

As with the first deck, the analysis was considered to have given sufficiently good predictions of behaviour to suggest that it was reasonable to use it to obtain some insight into how that behaviour was obtained.

In Figure 9.14 the predicted transverse force across the centre of the slab span between Beams C and D is shown for a particular load stage in the final loading. In order to make the plot directly comparable with Figure 9.10 (the equivalent plot for the first deck) the same load level is used. It will be seen that the restraint force in the region of the wheels is much greater and much less localised than for the first deck. The diaphragm at the right hand support, which is relatively close to a wheel, is resisting a significant tension as implied by previous researchers but that at the opposite end of the deck is resisting very little axial force. The distribution of forces might be considered less different from that implied by previous research than was that predicted for the first deck. However, the central portion of the deck between the two bogies of the HB vehicle is still subjected to a significant transverse tension, showing that compressive membrane action is not contributing to the resistance to global transverse moments.

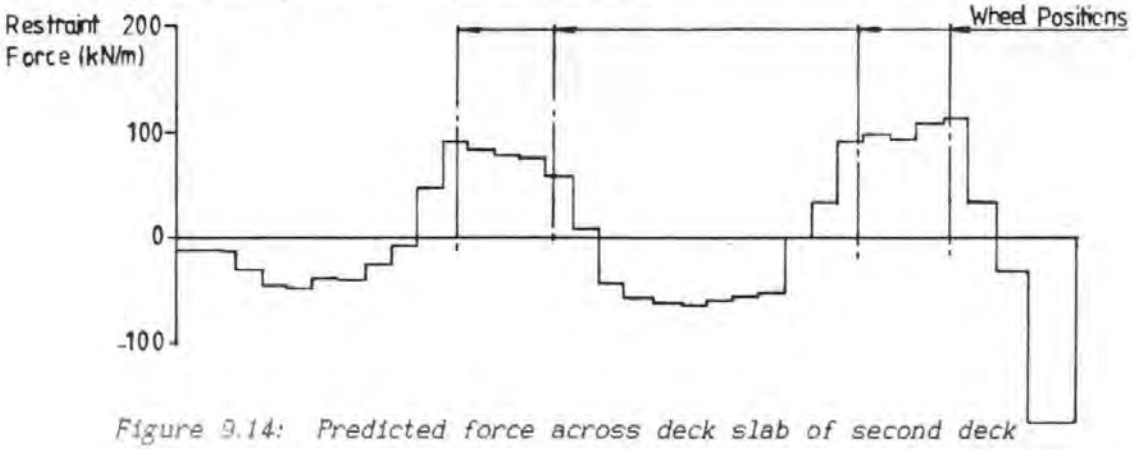

Figure 9.14: Predicted force across deck slab of second deck
(load = 250kN/jack)

At first sight, the obvious reason for the greater compressive membrane forces in this deck than in the first deck is that the diaphragms provided better restraint to these forces. However, this is not a satisfactory explanation; adding in-plane transverse stiffness to a region of the first deck which which was subjected to significant *compression* could not have this effect. Also, Figure 9.14 shows that only one of the diaphragms was resisting a significant tension. There are two other explanations. Firstly, the weaker concrete and less effective reinforcement in the second

deck meant that it was more extensively cracked at this load stage and consequently there was more membrane action. Secondly, the diaphragms reduced the difference between the moments in adjacent beams and consequently the global effect which led to tension at mid-span of the first deck was less pronounced.

As with the first deck, an attempt was made to see if the membrane forces predicted by the analysis were realised in practice. However, the more extensive cracking made this even more difficult. All that could be determined was that the form of Figure 9.14 was reasonable.

Although the compressive membrane forces shown in Figure 9.14 are sufficient to cause a very significant enhancement in the behaviour they are not, on their own, sufficient to explain all the difference between the actual behaviour of the slab and that predicted by normal design methods. The re-distribution of moments away from the critical region is equally significant.

9.4 CONCLUSIONS

Conventional analyses of the models, as expected, give extremely conservative predictions for the slab behaviour. Also as expected, if gross-concrete slab properties are used the predicted distribution properties are slightly better than were realised in practice. However, the discrepancies are relatively small and no greater than other faults of conventional analysis which are normally considered acceptable.

The non-linear analyses gave reasonably good predictions for behaviour and appear to give a reasonably good basis for design. They also give a good insight into the behaviour. They suggest that the restraint required to develop compressive membrane action comes from material which is relatively close to the areas being restrained. This explains why, as was clear from the results of the tests on the first deck, membrane action is not dependent on the presence of diaphragms. It also confirms, as suggested in the last chapter, that membrane action does not contribute to the resistance to global transverse moments.

The analyses also confirm that the failures observed were primarily brittle bending compression failures and that they were greatly influenced by global behaviour. They suggest that a large part of the difference

between the real behaviour of bridge deck slabs and that predicted by conventional elastic analysis is actually due to moment redistribution rather than to pure membrane action. This redistribution, like membrane action, is not dependent on reinforcement yielding; it starts to occur as soon as the behaviour of the concrete becomes non-linear in tension which is well before the slab becomes unserviceable in any way.

CHAPTER 10

USE OF MEMBRANE ACTION

IN

DESIGN AND ASSESSMENT

10.1 INTRODUCTION

Previous chapters have shown that membrane action, and the closely related mechanism of moment redistribution, have a significant beneficial effect on the behaviour of bridge deck slabs. They have also shown that the effect is sufficiently reliable to justify its use in design and assessment. This chapter will consider the use of the effect in design and assessment. Only the application to concrete bridges will be considered as steel-concrete composite bridges are considered to be outside the scope of this thesis.

10.2 USE IN DESIGN

10.2.1 M Beam Type Decks

Under present design rules, the quantity of main reinforcement in the deck slabs of otherwise identical bridges designed for identical loads in Northern Ireland and in the rest of Britain differ by a factor of over two. This is clearly unsatisfactory and should be resolved.

It appears that non-linear analysis such as the form of analysis described in Chapter 7, is needed to give a realistic prediction of the behaviour of a deck slab under full HB load. Although it is feasible to use this form of analysis in design, it is probably not justified for such a routine, simple and relatively standardised structure as the deck slab of an M beam type bridge. That standardisation enables simple prescriptive rules to be developed.

Although Chapter 8 showed that deck slabs can fail at substantially lower wheel loads than are predicted by the research on which the Northern Irish rules are based, the rules are so conservative compared with that research that they remain adequate. Indeed they appear to be over-cautious. The first of the two decks tested in this study remained serviceable after the deliberately excessively severe load history had been applied, despite having only 60% of the steel area recommended by the Northern Irish rules.

It also had more than adequate ultimate strength. It might be argued, considering the observed significance of global and local interaction, that the tests were unrealistic because of the over-provision of prestress. However, since the beams' behaviour remained linear elastic up to some 1.3 times design ultimate load, the behaviour under service loads would have been virtually identical with substantially less prestress. The ultimate strength undoubtedly would have been lower. However, the analysis in 9.3.2d suggested that even with less than the normal amount of prestress, the bridge would have been over twice as strong as was required. It thus appears that T12-250 reinforcement is adequate compared with the T12-150 specified by the Northern Irish rules. Nevertheless, and allowing for the fact that analysis shows that global transverse moments could be greater in a wider deck, it is prudent to continue to specify T12-150 main steel. If this reinforcement is provided in M beam deck slabs there is no need to do any analysis for the design of the slab.

Although this steel area can be justified from the test results alone, there may be a preference for a design method which is based on some form of analysis. Such a method can be obtained by consideration of the tests described in Chapter 8. The first deck, whose behaviour was considered satisfactory, was provided with just enough transverse reinforcement to resist the global transverse moments predicted by a conventional grillage analysis. The second deck, whose behaviour was less satisfactory, was provided with substantially less steel. A possible design approach is thus to require that the reinforcement be designed for the global transverse moments only; the opposite of the conventional North American approach. This would give very light steel areas in some decks so a minimum nominal area would also have to be specified. Although one might put a case for using the steel percentage specified by the Ontario Code, it is considered prudent to specify a minimum of T12-250 which corresponds to the steel area used in the first test deck and is the lightest steel area which has been demonstrated to be satisfactory by tests. In practice, the requirement to resist global moments means that the main steel would normally be slightly heavier than this.

It is more difficult to justify the continued specification of the same quantity of secondary steel. It appears that the Ontario researchers had two reasons for specifying isotropic reinforcement. Firstly, their research used an axi-symmetrical analysis and so they chose to use isotropic

reinforcement to get closer to the assumptions of the analysis. Secondly, and more significantly, they began by specifying main steel equal to the minimum nominal steel required by their code so they could hardly have specified less secondary steel. When Kirkpatrick et al wisely specified a larger area of main steel, to allow for global transverse moments, they rather arbitrarily decided to continue to use isotropic reinforcement. Both the tests reported in Chapter 8 and the analysis reported in Chapter 9 suggest that the secondary steel in the deck slab of a simply supported M beam deck is very lightly stressed and contributes little to the behaviour. It could be reduced to that provided in the first of the models considered here, equivalent to T12-250 at full size, whichever approach is used for the design of the main steel. Even this is probably over-conservative; there is no evidence from this study that any secondary reinforcement is required.

The same basic approach to deck slab reinforcement design is valid in regions of global longitudinal hogging. This is clear from previous research and also because, as was discussed in 3.2.7, the critical load cases for global longitudinal hogging do not impose any wheel loads in the region of the slab which is in tension. It is prudent, although probably conservative, to require the nominal longitudinal slab steel to be additional to that required for global moments and also to require a proportion of the latter, say 30%, to be placed close to the bottom face of the slab. The reason for this restriction is that, although intended only to resist local effects, the nominal steel will be stressed by global effects. Thus the reserve strength available for local effects could be very small if only this very small quantity of already highly stressed steel was provided in the soffit.

The basic limitations imposed by Kirkpatrick et al on the use of the empirical rules appear to be reasonable; one could debate the limiting span given but since, with M beams, this is well above the limitation imposed by web shear strength there is little to be gained by so doing. The one restriction which is worth reconsidering is the requirement for diaphragms.

The analyses and tests reported in this thesis show that diaphragms are far less important to the development of compressive membrane action than has previously been believed. The empirical rules could be extended to cover bridges with only nominal diaphragms, or with no diaphragms at all.

In the latter case the end section of the slab would not receive the full benefit of restraint and would require extra reinforcement. It is suggested that a strip of slab extending 0.5m from the end of the deck should be provided with enough reinforcement to enable it to support a wheel acting as a single beam. This is marginally more steel than was provided in the first test deck considered in Chapter 8.

From a purely theoretical viewpoint, the use of these empirical design rules in combination with global analysis based on gross-concrete section properties cannot be justified. However, analysis shows that the use of cracked transformed transverse properties is conservative and in 9.2.2 it was found that the errors resulting from the cracking are no greater than other normally accepted faults of grillage analysis. A reasonable approach is to use half the transverse stiffnesses calculated for the gross-concrete properties. The economic consequences of the slightly worse distribution properties resulting from this compared with the conventional approach are extremely small and significantly less than might be inferred from the results of the tests considered in this thesis. This is because the tests considered HB alone, the worst case for the slab, whilst the critical load case for the beams is HA plus HB. Improving the distribution properties reduces the effect of the HB load in the critical area but it increases the effect of the associated HA. Due to a continuing increase in the HA load which is applied in combination with the HB load, the benefits of good distribution properties have reduced with every new loading standard introduced in Britain since the 1950s. Nevertheless, the suggestion that reduced transverse properties should be used does imply that the beams of bridges designed to the existing Northern Irish rules could be subjected to slightly greater moments than those for which they were designed. In the author's view this is unimportant since the design criteria currently used for this type of beam (class 1 and 2 criteria in combination with an extremely severe service load) are unduly conservative. However, a discussion of this subject is outside the scope of this thesis.

Where half the gross-concrete transverse properties are used in the global analysis, it appears prudent to continue to require the transverse steel to be capable of resisting the global transverse moments predicted by a conventional analysis based on gross-concrete properties. To avoid the need to perform two separate analyses, these can be taken conservatively

to be double the moments calculated using half the gross-concrete properties.

10.2.2 Other Beam and Slab Decks

The slabs of bridges built with U Beams or the proposed new Y Beams are so similar to those of M beam decks that the same design rules can be applied. The only modification required being that, with U beams, the main steel may have to be increased to enable it to act as part of the torsion links of the beams.

Other types of beam and slab bridges normally have thicker deck slabs with wider-spaced beams. This means that the global transverse moments are likely to be less significant but it is difficult to prove this. It is prudent, therefore, to recommend a check that the main steel in the deck slab is always sufficient to resist the transverse moments given by the global analysis. The suggested minimum steel area to be specified is 0.3% of the gross-section. This corresponds to T12-250 (the minimum suggested for M Beam slabs) for a thickness of 160mm so the rules are consistent.

These suggestions are more conservative than the Ontario rules but this is justified due to the significance of global transverse moments noted in this thesis and by the nature of the HB load which is exceptionally severe for this effect.

The restriction on the use of these rules can be as for the Ontario rules except for relaxing the requirement for diaphragms as with M Beam decks. However, where these restrictions are not complied with it does not mean that membrane action cannot be used in design; merely that the empirical rules are not applicable. Analysis such as that described in Chapter 7 could still be used. Where the span to depth ratio is outside that required to use the empirical rules the analysis should consider large displacements.

10.2.3 Other Types of Deck

It has been noted in earlier chapters that compressive membrane action is potentially significant to other types of bridges, apart from beam on slab structures. These range from simple slab decks to major concrete box girder structures. The detailed consideration of these is considered beyond the scope of this thesis and, in any case, they are probably not

sufficiently standardised to enable prescriptive rules to be developed; non-linear analysis would be required. However, a simple conservative approach can be developed using normal analytical methods. This approach could also be used for beam and slab decks if desired.

The mechanism by which the behaviour of deck slabs is enhanced relative to the predictions of elastic plate theory is essentially one of stresses redistributing away from the critical areas. It was demonstrated in Chapter 9 that the restraint force required to develop compressive membrane force comes from material which is relatively close to these critical areas; not from the diaphragms. This suggests a very simple over-conservative way of allowing for the effect. Design could be based on a normal elastic slab analysis but ignoring, or rather smoothing out, the peaks in the moment over a finite width. If it was only moment redistribution which was being considered this width would be related to the span and to the ductility of the sections. With arching action, however, the critical factor is the depth. It is suggested, therefore, that elastic analysis could be used with the design based on the moment averaged over a width equal to the lesser of 6d or half the slab span. This is undoubtedly extremely conservative; it was demonstrated in 8.8.3 that removing the steel completely over a width of 12h had little effect on behaviour.

10.3 ASSESSMENTS

The approaches suggested in 10.2 are equally applicable to the assessment of existing bridges. However, purely empirical approaches are less suitable for assessment because it is not possible to adjust the structure to fit the limitations imposed for the rules. It will therefore be necessary to resort to non-linear analysis more frequently than in design.

The use of the assessment approach given in the Ontario Highway Bridge Design Code(11), which relies on the strength predictions of Hewitt and Batchelor's approach, is not normally advised. This is because of its failure to consider global transverse moments. However, in assessing a bridge which has intermediate diaphragms, it is reasonable to assume that the global transverse moments in the deck slab are insignificant and so the approach is more reliable. Even then, if the spacing of the design wheel loads is less than the slab span, some allowance should be made for the effect of the second wheel.

CHAPTER 11

CONCLUSIONS AND RECOMMENDATIONS

11.1 CONCLUSIONS

The first conclusion to be drawn from this study is that bridge deck slabs are able to support loads by compressive membrane action and, as a result, that they are able to support very much greater loads than is suggested by conventional design methods which are based on flexural theory. Judged against the background of the research which was reviewed in Chapter 3, this conclusion is unremarkable. However, the conclusions to be drawn from any study depend as much on the the background against which the study is assessed as on the study itself. Judged against the background of conventional design practice, which was reviewed in Chapter 2, the enormous strengths of deck slabs, particularly lightly reinforced deck slabs, compared with the predictions of conventional flexural theory remains the most significant conclusion. It is re-stated here to put some of the other conclusions into perspective; it should be remembered, for example, that when the deck slab of the first model considered in Chapter 8 failed at little over half the load which might have been expected from some previous research, it was resisting some five times its ultimate load according to normal design methods.

The remaining conclusions are:

1. Compressive membrane action and the closely allied mechanism of moment redistribution start to enhance the behaviour of deck slabs relative to the predictions of linear analysis as soon as the concrete's behaviour becomes non-linear in tension. This, at least in thin slabs, is well before there are visible cracks. It does not depend on any material behaviour which is unacceptable under service loads. Because of this, membrane action significantly increases the service load, as well as the ultimate load, which a slab can carry.

2. Compressive membrane action is sufficiently reliable to justify its consideration in design and assessment. The model tests described in Chapter 8 were an exceptionally severe test yet the behaviour was substantially better than could be anticipated by purely flexural analysis.

3. The restraint required to develop compressive membrane action comes from the under-stressed reinforcement and concrete surrounding the critical areas of the slab. It is not dependent on the presence of diaphragms.

4. Compressive membrane action could even enhance the service load behaviour of slabs with no external restraint. However, it cannot increase the failure load of such slabs above that predicted by yield-line theory.

5. Compressive membrane action does not greatly enhance the resistance to global transverse moments.

6. Because of 3 and 5 above, and contrary to the implications of some earlier research, reinforcement is needed in bridge deck slabs. However, because it is required to resist global transverse moments and to provide restraint (rather than to resist local moments), the behaviour is not sensitive to the exact position of the reinforcement. Thus the behaviour of bridge deck slabs is remarkably insensitive to local reinforcement corrosion.

7. The failure loads of bridge deck slabs subjected to single wheel loads are reasonably well predicted by the approaches which were considered in 3.2.3. The cases where these approaches gave unsafe predictions were restricted to impractically lightly reinforced slabs with large span to depth ratios and relatively poor restraint. The methods do not, however, give good predictions of other aspects of behaviour; for example, Hewitt's approach under-estimated the deflection at failure by a factor of up to 10.

8. Non-linear analyses of the forms considered in Chapters 5 and 7 are also capable of predicting these failure loads and are better able to predict other aspects of behaviour. The form considered in Chapter 5 is theoretically more rigorous and realistic than that considered in Chapter 7 but the latter has many practical advantages in a design situation; it is simpler, more compatible with design standards and also appears to be more consistently safe.

9. The local failures observed in deck slabs are primarily brittle bending compression failures. They can be predicted by analyses which do not consider shear, the load at which they occur can be reduced by the

presence of other moments (such as global transverse moments) and, in many cases, crushing concrete is visible before failure.

10. Bridges which are subjected to multiple wheel loads, such as HB, can fail by wheels punching through their slabs at wheel loads which are substantially below the local strength of their slabs; both as measured in single wheel tests and as predicted by the approaches developed by previous research.

11. The form of failure considered in 10 above can occur even when the beams have a reserve of strength and the global transverse moments are thus not needed to maintain equilibrium. This is contrary to the safe theorem of plastic design but the behaviour is too brittle for this to apply.

12. Non-linear analysis is capable of predicting the behaviour of bridge decks reasonably well. In particular, it appears to be the only form of analysis which is capable of modelling the interaction of global and local effects and of predicting the restraint.

11.2 RECOMMENDATIONS

11.2.1 Recommendations for Design and Assessment

Less conservative design methods for bridge deck slab reinforcement should be introduced which allow for the beneficial effects of compressive membrane action. Possible details of these methods were considered in Chapter 10 and will not be discussed here.

11.2.1 Recommendations for Further Research

There are many aspects of the behaviour of the type of slabs considered in detail in this and previous studies which could be considered to require further research. However, such research is not needed to justify the use of membrane action in design or assessment. To recommend it would merely serve to perpetuate the use of conventional design methods which have been shown to be extremely unrealistic and conservative.

This study has suggested that membrane action could have a significant beneficial effect on the behaviour of a wide range of bridge deck slabs in addition to those for which it has so far been investigated in detail. Any future studies of membrane action in bridge deck slabs should consider types of slab which have not previously been researched. This includes

the thin long-span slabs typical of longer span concrete bridges. However, this study has shown that the restraint required to develop compressive membrane action comes from under-stressed material surrounding the critical areas of the slab. At service load levels, which are critical in design, it is not dependent on any external restraint. It follows that the behaviour of simply supported and even cantilever slabs could be significantly enhanced by the effect and this should be investigated.

REFERENCES

1. WESTERGAARD, H.M. and SLATER, W.A. Moments and stresses in slabs. *Proceedings, American Concrete Institute.* Vol. 17. 1921. pp. 415-538.

2. TURNER, C.A.P. Advance in reinforced concrete construction: an argument for multiple-way reinforcement in floor slabs. *Engineering News.* Vol. 61, No. 7. Feb. 18, 1909. pp. 178-181.

3. SOZEN, M.A. and SEISS, C.P. Investigation of multiple-panel reinforced concrete floor slabs. Design methods - their evolution and comparison. *Proceedings, American Concrete Institute.* Vol. 60. 1963. pp. 999-1020.

4. NICHOLS. J.R. Statical limitations upon the steel requirement in reinforced concrete floor slabs. *Transactions, American Society of Civil Engineers.* Vol. 77. 1914. pp. 1670-1736.

5. LORD, A.R. A test of a flat slab floor in a reinforced concrete building. *National Association of Cement Users (American Concrete Institute).* Vol. 7. 1910. pp. 156-179.

6. BEEBY, A.W. *A proposal for change in the basis of the design of slabs.* Wexham Springs, C & CA, April 1982. p. 28. Technical Report 42.547.

7. STATE CONSTRUCTION COMMITTEE OF THE USSR. Building standards and regulations BS & R II-21-75. *The structural use of concrete.* Moscow, 1976.

8. BRAESTRUP, M.W. Dome effect in reinforced concrete slabs: rigid-plastic analysis. *Journal of the Structural Division, American Society of Civil Engineers.* Vol. 106, No. ST6. June 1980. pp. 1237-1253.

9. OCKLESTON, A.J. Load tests on a three-storey reinforced concrete building in Johannesburg. *The Structural Engineer.* Vol. 33, No. 10. October 1955. pp. 304-322.

10. GUYON, Y. Tests on continuous slabs. Method of analysis. *Prestressed Concrete. Vol. 2, Statically Indeterminate Structures.* English translation by C. Von Amerongen. London, C. R. Books Ltd. 1960. pp. 515-567.

11. ONTARIO MINISTRY OF TRANSPORTATION AND COMMUNICATIONS. *Ontario Highway Bridge Design Code.* Downsview, Ontario, Canada, 1st Edition 1979, 2nd Edition 1983.

12. DEPARTMENT OF THE ENVIRONMENT FOR NORTHERN IRELAND. *Design of M beam bridge decks.* Amendment 3 to B.D.C, Belfast, Northern Ireland Road Services Headquarters. March 1986.

13. KIRKPATRICK, J. RANKIN, G.I.B. and LONG, A.E. Strength evaluation of M-beam bridge deck slabs. *The Structural Engineer.* Vol. 62B, No. 3. September 1984. pp. 60-68.

14. KIRKPATRICK, J., LONG, A.E., and THOMPSON, A. Load distribution characteristics of spaced M-beam bridge decks. *The Structural Engineer.* Vol. 62B, No. 4. Dec. 1984. pp. 86-88.

15. PRITCHARD, B.P. Combatting road salt corrosion in U.K. concrete bridges - the way ahead. *Proceedings, Institution of Highways & Transportation National Workshop on Bridge Maintenance Initiatives.* April 1986. pp. 119-159.

16. GEE, A.F. Bridge winners and losers. *The Structural Engineer.* Vol. 65A, No. 4. April 1987. pp. 141-145.

17. BEEBY, A.W. The function of research in the construction industry. *A testimonial volume for Professor Rehm's 60th birthday.* Berlin, Ernst & Sohn. 1984.

18. FREYSSINET, E. Prestressed concrete principles and applications. *Journal of the Institution of Civil Engineers.* Vol. 33, No. 4. February 1950. pp. 331-380.

19. EMERSON, M. *Temperature differences in bridges: basis of design requirements.* Crowthorne, Transport and Road Research Laboratory, 1977. Laboratory report 765.

20. LOW, A. Prestress design for continuous concrete members. *Arup Journal.* April 1983. pp. 18-21.

21. DEPARTMENT OF THE ENVIRONMENT. Technical Memorandum (Bridges) BE5/73. *Standard Highway Loadings.* London, August 1973.

22. DEPARTMENT OF TRANSPORT. Departmental Standard BD17/83. *Design of Concrete Bridges. Use of BS 5400: Part 4: 1978.* London, 1983.

23. BRITISH STANDARDS INSTITUTION. BS 5400: Part 4: 1978. *Code of practice for the design of concrete bridges.* London, 1978.

24. BRITISH STANDARDS INSTITUTION. BS 5400: Part 2: 1978. *Specification for Loads.* London, 1978.

25. DEPARTMENT OF TRANSPORT. Departmental Standard BD14/82. *Loads for Highway Bridges. Use of BS 5400: Part 2: 1978.* London, October 1982.

26. BRITISH STANDARDS INSTITUTION. BS 5400: Part 4: 1984. *Code of practice for the design of concrete bridges.* London, 1984.

27. DEPARTMENT OF TRANSPORT. Departmental Standard BD24/84. *Design of Concrete Bridges. Use of BS 5400: Part 4: 1978.* London, 1984.

28. DEPARTMENT OF THE ENVIRONMENT. Technical Memorandum (Bridges) BE1/73. *Reinforced concrete for highway structures.* London, 1973.

29. DEPARTMENT OF THE ENVIRONMENT. Technical Memorandum (Bridges) BE2/73. *Prestressed concrete for highway structures.* London, 1973.

30. BEAL, A.N. The new concrete code - is it all it's cracked up to be? *The Structural Engineer.* Vol. 64A, No. 8. August 1986. pp. 199-201.

31. BRITISH STANDARDS INSTITUTION. CP110: Part 1: 1972. *The structural use of concrete: Part 1, Design materials and workmanship.* London, 1972.

32. BRITISH STANDARDS INSTITUTION. BS 8110: Part 1: 1985. *Structural use of concrete: Part 1, Code of practice for design and construction.* London, 1985.

33. BEEBY, A.W. Cracking and corrosion. *Concrete in the oceans.* Technical Report 1. Wexham Springs, CIRIA, C & CA, DoE, 1978.

34. BEEBY, A.W. The prediction of crack widths in hardened concrete. *The Structural Engineer.* Vol. 57A, No. 1. January 1979. pp. 9-17..

35. JACKSON, P.A. The stress limits for reinforced concrete in BS 5400. *The Structural Engineer.* Vol. 65A, No. 7. July 1987. pp. 259-263.

36. EDWARDS, K.R. *Non-linear analysis of eccentrically stiffened reinforced concrete bridge decks.* PhD Thesis, University of Liverpool. 1983.

37. COPE, R.J., RAO, P.V., and CLARK, L.A. Non-linear design of concrete structures. *CSCE-ASCE-ACI-CEB International Symposium.* University of Waterloo, Ontario, Canada. 1979.

38. CLARK, L.A., Elastic analysis of concrete bridges and the ultimate limit state. *The Highway Engineer*. October 1977. pp. 22-24.

39. WESTERGAARD, H.M. Computation of stress in bridge slabs due to wheel loads. *Public Roads*. Vol. 2, No. 1. March 1930. pp. 1-23.

40. PUCHER, A. *Influence surfaces of elastic plates*. Wien and New York, Springer Verlag, 1964.

41. MORICE, P.B. and LITTLE, G. *Analysis of right bridge decks subject to abnormal loading*. London, C & CA, July 1956. Publication 32-002.

42. PENNELLS, E. *Concrete bridge designer's manual*. London, Viewpoint Publications, 1978. p. 111.

43. WEST, R. *The use of grillage analogy for the analysis of slab and pseudo-slab bridge decks*. London, 1973. C & CA Research Report 21, Publication 41.021.

44. HAMBLY, E.C. *Bridge deck behaviour*. London, Chapman & Hall, 1976. pp. 83-85.

45. AMERICAN ASSOCIATION OF STATE HIGHWAY AND TRANSPORTATION OFFICIALS. *Standard specification for highway bridges*. Washington DC, 13th Edition, 1983.

46. CONCRETE SOCIETY. *Design and cost studies of lightweight concrete highway bridges*. London, 1986.

47. DORTON, R.A., HOLOWKA, M. and KING, J.P.C. The Conestogo River Bridge design and testing. *Canadian Journal of Civil Engineering*. Vol. 4. 1977. pp. 18-39.

48. BUCKLE, I.G., DICKSON, A.R. and PHILIPS, M.H. Ultimate strength of three reinforced concrete highway bridges. *Canadian Journal of Civil Engineeering*. Vol. 12. 1985. pp. 63-72.

49. KIRKPATRICK, J., RANKIN, G.I.B. and LONG, A.E. The influence of compressive membrane action on the serviceability of beam and slab bridge decks. *The Structural Engineer*. Vol. 64B, No. 1. March 1986. pp. 6-12.

50. HOPKINS, D.C. and PARK, R. Tests on reinforced concrete slab and beam floor designed with allowance for membrane action. *Cracking deflection and ultimate loads of concrete slab systems*. Detroit, American Concrete Institute, 1971. Publication SP 30. pp. 223-250.

51. TONG, P.Y. and BATCHELOR, B. de V. Compressive membrane enhancement in two-way bridge slabs. *Cracking deflection and ultimate loads of concrete slab systems.* Detroit, American Concrete Institute, 1971. Publication SP 30. pp. 271-286.

52. BEAL, D.B. Load capacity of concrete bridge decks. *Journal of the Structural Division, American Society of Civil Engineers.* Vol. 108, No. ST4. April 1982. pp. 814-832.

53. ROBERTS, E.H. Load-carrying capacity of slab strips restrained against longitudinal expansion. *Concrete.* Vol. 3, No. 9. September 1969. pp. 369-378.

54. PARK, R. Ultimate strength of rectangular concrete slabs under short term uniform loading with edges restrained against lateral movement. *Proceedings, Institution of Civil Engineers.* Vol. 28. June 1964. pp. 125-150.

55. TAYLOR, R. and HAYES, B. Some tests on the effect of edge restraint on punching shear in reinforced concrete slabs. *Magazine of Concrete Research.* Vol. 17, No. 50. March 1965. pp. 39-40.

56. BROTCHIE, J.F. and HOLLEY, M.J. Membrane action in slabs. *Cracking deflection and ultimate loads of concrete slab systems.* Detroit, American Concrete Institute, 1971. Publication SP 30. pp. 345-378.

57. JOHANSEN, K.W. *Yield-Line Theory.* London, C & CA, 1962. (Translation from Danish first published in 1943).

58. WOOD, R.H. *Plastic and elastic design of slabs and plates with particular reference to reinforced concrete floor slabs.* London, Thames and Hudson, 1961. p. 344.

59. MORLEY, C.T. Yield line theory for reinforced concrete slabs at moderately large deflexions. *Magazine of Concrete Research.* Vol. 19, No. 61. December 1967. pp. 211-222.

60. PARK, R. and GAMBLE, W.L. Membrane action in slabs. *Reinforced concretete slabs.* New York, J. Wiley & Sons, 1980. pp. 562-612

61. MASSONNET, C.H. General theory of elastic-plastic membrane plates. *Engineering Plasticity.* Cambridge, Cambridge University Press, 1968. Editors Heyman and Leckie. pp. 443-471.

62. MOY, S.S.J. and MAYFIELD, B. Load deflection characteristics of reinforced concrete slabs. *Magazine of Concrete Research.* Vol. 24, No. 81. December 1972. pp. 209-218.

63. CHRISTIANSEN, K.P. The effect of membrane stress on the ultimate strength of the interior panel in a reinforced concrete slab. *The Structural Engineer.* Vol. 41, No. 8. August 1963. pp. 261-265

64. Mc DOWELL, E.L., Mc KEE K.E. and SEVIN, E. Arching action theory in masonry walls. *Journal of the Structural Division, American Society of Civil Engineers.* No. ST2. March 1956. pp. 915/1-18.

65. RANKIN, G.I.B. *Punching failure and compressive membrane enhancement in slabs.* PhD Thesis, Department of Civil Engineering, Queens University of Belfast. 1982.

66. SKATES, A., RANKIN, G.I.B. and LONG, A.E. Utilising the effects of membrane action in the design of offshore cellular structures. *Proceedings, Marine Concrete '86 International Conference on Concrete in the Marine Environment.* London. Concrete Society, September 1986. pp. 79-90.

67. WHITNEY, C.S. Design of reinforced concrete members under flexure or combined flexure and direct compression. *Journal of the American Concrete Institute.* Vol. 33, No. 2. March/April 1937. pp. 483-498.

68. AOKI, Y. and SEKI, H. Shearing strength and cracking in two-way slabs subjected to concentrated load. *Cracking deflection and ultimate loads of concrete slab systems.* Detroit, American Concrete Institute, 1971. Publication SP 30. pp. 103-126.

69. MOE, J. *Shearing strength of reinforced concrete slabs and footings under concentrated loads.* Skokie, Portland Cement Association, April 1961. Development Department Bulletin D47.

70. YOUNG, D.M. *The strength of two-way slabs with fixed edges subjected to concentrated loads.* MSc Thesis, Queens University of Kingston, Ontario, Canada. 1965.

71. BATCHELOR, B. de V. and TISSINGTON, I.R. Shear strength of two way bridge slabs *Journal of the Structural Division, American Society of Civil Engineers.* Vol. 102, No. ST12. December 1976. pp. 2315-2331.

72. HEWITT, B.E. and BATCHELOR, B. de V. Punching Shear Strength of Restrained Slabs. *Journal of the Structural Division, American*

Society of Civil Engineers. Vol. 101, No. 6T9. September 1975. pp. 1837-1852.

73. KINNUNEN, S. and NYLANDER, H. Punching of concrete slabs without shear reinforcement. *Transactions of the Royal Institute of Technology.* No. 158. Stockholm, 1960.

74. LONG, A.E. A two-phase approach to the prediction of the punching strength of slabs. *Journal of the American Concrete Institute.* Vol. 72, No. 2. February 1975. pp. 37-45.

75. CHANA, P.S. *Shear failure in reinforced concrete beams.* PhD Thesis, University College London. October 1986.

76. BATCHELOR, B. de V. Membrane enhancement in top slabs of concrete bridges. *Concrete Bridge Engineering, Performance and Advances..* London and New York, Elsevier, 1987. Editor Cope, R. J. pp. 189-210.

77. BEAL, A.N. *Strength of Concrete Bridge Decks.* New York. Engineering Research and Development Bureau, New York State Department of Transportation. July 1981. Research Report 89.

78. BATCHELOR, B. de V., HEWITT, B.E., CSAGOLY, P. and HOLOWKA, M. *Investigation of the ultimate strength of deck slabs of composite steel/concrete bridges.* Bridge Engineering Conference. September 1978. Transportation Research Record 664. pp. 162-179.

79. PETCU, V. and STANCULESCU, G. Critical steel ratios in the limit design of two-way reinforced concrete slabs. *Cracking deflection and ultimate loads of concrete slab systems.* Detroit, American Concrete Institute, 1971. Publication SP 30. pp. 287-300.

80. NIBLOCK, R.A. and LONG, A.E. A Design Method for Uniformly Loaded Laterally Restrained Concrete Slabs. *Proceedings, 6th International Offshore Mechanics and Arctic Engineering Symposium.* Houston. Vol. 13. 1987. pp. 177-184.

81. HOLOWKA, M. and CSAGOLY, P. *Testing of a composite prestressed concrete AASHTO girder bridge.* Downsview, Ontario, Canada, Ontario Ministry of Transportation and Communications, 1980. Research Report 222.

82. CAIRNS, J. *Measurement of service strains in the deck slab of a highway bridge.* Wexham Springs, C & CA, 1986. pp. 127-133. Research Seminar.

83. PARK, R. The lateral stiffness and strength required to ensure membrane action at the ultimate load of a reinforced concrete slab-and-beam floor system. *Magazine of Concrete Research. Vol. 17, No. 50. March 1965. pp. 29-38.*

84. BATCHELOR, B. de V., HEWITT, B.E. and CSAGOLY, P. *An investigation of the fatigue strength of deck slabs of composite steel/concrete bridges.* Bridge Engineering Conference. September 1978. Transportation Research Record 664. pp. 153-161.

85. CRANSTON, W.B. Developments in concrete bridges. *Proceedings, Institution of Highway and Transportation National Workshop on Bridge Construction and Maintenance.* April, 1984. pp. 40-51.

86. NGO, D. and SCORDELIS, A.C. Finite element analysis of reinforced concrete beams. *Journal of the American Concrete Institute* Vol. 64, No. 3. March 1967. pp. 152-163.

87. ABDEL RAHMEN, H.H. *Computational models for the non-linear analysis of slab systems.* PhD Thesis, University College, Swansea. 1982.

88. MINDLIN, R.D. Influence of rotary inertia and shear on flexural motions of isotropic elastic plates. *Journal of Applied Mechanics.* Vol. 18. 1951. pp. 31-38.

89. COPE, R.J. and CLARK, L.A. *Concrete slabs, analysis and design.* London, Elsevier, 1984.

90. BUCKLE, I.G. and JACKSON, A.T. A filament element for the non-linear analysis of reinforced concrete beam and slab structures. *Proceedings, International Conference on Finite Element Methods.* Shanghai, 1982. pp. 4-15.

91. POPOVICS, S. A review of stress-strain relationships for concrete. *Proceedings, American Concrete Institute. Vol. 67, No. 3. 1970. pp. 243-248.*

92. NILSON, A.H., TASUJI, M.E. and SLATE, F.O. Biaxial stress-strain relationship for concrete. *Magazine of Concrete Research.* Vol. 31, No. 109. 1969. pp. 217-224.

93. COPE, R.J., RAO, P.U., CLARK, L.A. and NORRIS, P. Modelling of reinforced concrete behaviour for finite element analysis of bridge slabs. *Numerical Methods for Non-Linear Problems.* Swansea, Pineridge Press. 1980. pp. 457-470.

94. COPE, M. and COPE. R.J. *Design and assessment of one way prestressed bridge slabs. Vol. 2. Analytical investigations and conclusions.* Contractor's report 74, Crowthorne, Transport and Road Research Laboratory, 1988.

95. CRISFIELD, M.A. Local instabilities in the non-linear analysis of reinforced concrete beams and slabs. *Proceedings, Institution of Civil Engineers.* Part 2. March, 1982. pp. 135-145.

96. COPE, R.J. Non-linear analysis of reinforced concrete slabs. *Computational models of reinforced concrete structures.* Swansea, Pineridge Press, 1986. Editors Hinton, E. and Owen, R. pp. 3-43

97. BAZANT, Z.P., PAN, J. and PIJAUDIER-CABOT, G. Softening in reinforced concrete beams and frames. *Journal of Structural Engineering, American Society of Civil Engineers.* Vol. 113, No. 12. Dec. 1987. pp. 2333-2364

98. JACKSON, A.T. *Finite Element Analysis of Compression Membrane Action in Slabs.* University of Auckland. 1979. School of Engineering Research Report 207.

99. COPE. R.J. and EDWARDS K.R. Non-Linear Finite Element Analysis of Eccentrically Stiffened Bridge Decks. *Proceedings of international conference on finite elements in computational mechanics.* Oxford, Pergamon Press. 1985. pp. 431-448

100. BEDARD, C. and KOTSOVOS, M.D. Application of NLFEA to concrete structures. *Journal of the Structural Division, American Society of Civil Engineers.* Vol. 111, No. 12. Dec. 1985. pp. 2691-2707.

101. GILBERT, R.I. and WARNER, R.F. Tension stiffening in reinforced concrete slabs. *Journal of the Structural Division, American Society of Civil Engineers.* Vol. 104, No. ST12. Dec. 1978.

102. MARATHE, M. *Stress-strain characteristics of concrete in tension.* PhD Thesis, University of Leeds. 1967.

103. VETTER, C.P. Stresses in reinforced concrete due to volume changes. *Transactions, American Society of Civil Engineers.* No. 98. 1933. pp. 1039-1080.

104. BRITISH STANDARDS INSTITUTION. BS 8110: 1985. *Structural use of concrete: Part 2, Code of practice for special circumstances.* London, 1985.

105. HARTL, G.. Die arbeitslinie eingebetteter stähle unter erst-und kurzzeitbelastung (Force-Deformation diagram "embeded bars" under first time and short term loading). *Beton-und Stahlbetonbau.* 78. No. 8. 1983. pp. 221-224.

106. CERVENKA, V. Constitutive model for cracked reinforced concrete. *Journal of the American Concrete Institute.* Vol. 82 No.6. Nov./Dec. 1985. pp. 877-882.

107. COPE, R.J. and RAO, P.V. A two-stage procedure for non-linear analysis of slab bridges. *Proceedings, Institution of Civil Engineers, Part 2.* Vol. 75 No. 6. December 1983. pp. 671-688.

108. American Association of State Highway Officials. *AASHO interim guide for the design of rigid pavement structures.* Washington D.C., 1962.

109. WILLIAMS, A. *Tests on large reinforced concrete elements subjected to direct tension.* Wexham Springs, C & CA, April 1986. Technical Report 562.

110. CLARK, L.A. and SPIERS, D.M. *Tension stiffening in reinforced concrete beams and slabs under short-term load.* Wexham Springs, C & CA, July 1978. Technical Report 521.

111. CLARK, L.A. AND CRANSTON, W.B. The influence of bar spacing on tension stiffening in reinforced concrete slabs, *Advances in concrete slab technology.* Oxford, Pergamon Press, 1979, Editors R. K. Dhir and J.G.L. Munday, pp. 118-128.

112. GIFFORD AND PARTNERS. *The assessment of Mound Bridge for Transport and Road Research Laboratory.* Report GP 3988.02, Southampton, November 1988. (written by P.A. Jackson).

113. BRITISH STANDARDS INSTITUTION. BS 4975: 1973. *Specification for prestressed concrete pressure vessels for nuclear reactors.* London, 1973.

114. GANABA, T.H. and MAY, I.M. *An improved numerical integration over the thickness of plates and shells in finite element analysis.* University of Warwick. 1984. Report No. 8.

115. CRISFIELD, M.A. A fast incremental/iterative procedure that handles "snap through" *Computers and Structures.* No. 13. 1981. pp. 55-62.

116. DUDDECK, H. GRIENOW, G. and SCHAPER, G. Material and time dependent nonlinear behaviour of cracked reinforced concrete slabs. *Nonlinear*

behaviour of reinforced concrete spatial structures. Vol. 1, Preliminary Report IASS Symposium. DÜsseldorf, Werner-Verlag, July 1978. Editors G. Mehlorn, H. RÜhle and W. Zerna. pp. 101-113.

117. MUELLER, G. *Numerical Problems in Nonlinear Analysis of Reinforced Concrete.* Department of Civil Engineering, University of California, September 1977. Report No. UC SESM, 77-5.

118. RAEGEN, P.E. and REZAI-JORABI, H. Shear resistance of one way slabs under concentrated loads. *Structural Journal of the American Concrete Institute.* March/April 1988. pp. 150-157.

119. HUGHES, G. *Longitudinal shear in composite concrete bridge beams. Part 2; Experimental investigation and recommendations.* Contractors report 52. Crowthornne, Transport and Road Research Laboratory, 1987.

120. GREEN, J.K. *Detailing for standard prestressed concrete bridge beams.* London, C & CA, December 1973. Publication 46.018.

121. CLARK, L.A. and WEST, R. *The torsional stiffness of support diaphragms in beam and slab bridges.* Wexham Springs, C & CA, August 1975. Technical Report 42.510.

122. BEAL, A.N. *Reinforcement for Concrete Bridge Decks.* New York. Engineering Research and Development Bureau, New York State Department of Transportation. July 1983. Research Report 105.

123. JACKSON, P.A. Some aspects of the assessment of concrete bridges. *Highways.* Vol. 56 No. 1936. April 1988. pp. 32-33

124. P.S.C. FREYSSINET, *Elastomeric Bearings.* Iver, P.S.C. Freyssinet, 1982 and 1983.

125. BRITISH STANDARDS INSTITUTION. BS 1881; Part 111; 1983. *Methods for curing test specimens.* London, 1983.

126. BRITISH STANDARDS INSTITUTION. BS 5400: Part 10: 1980. *Code of practice for fatigue.* London, 1980.

127. DEPARTMENT OF TRANSPORT. *Background and synopsis of proposed new loading for highway bridges in the UK.* London, 1983.

128. PERDIKARIS, P.C. and BEIM, S. Reinforced concrete bridge decks under pulsating and moving load. *Journal of the Structural Division, American Society of Civil Engineers.* Vol. 114, No. 3. March 1988. pp. 591-607.

129. COOK, C.F. An electrical demountable strain transducer. *15th Annual Conference, British Society of Strain Measurement.* Bristol Polytechnic. September 1979.

130. MEHKAR-ASL, S. *Direct measurement of stress in concrete structures.* PhD Thesis, University of Surrey, September 1988.

APPENDICES

A. RESTRAINED SLAB STRIP TO ELASTIC THEORY

A1 Stresses

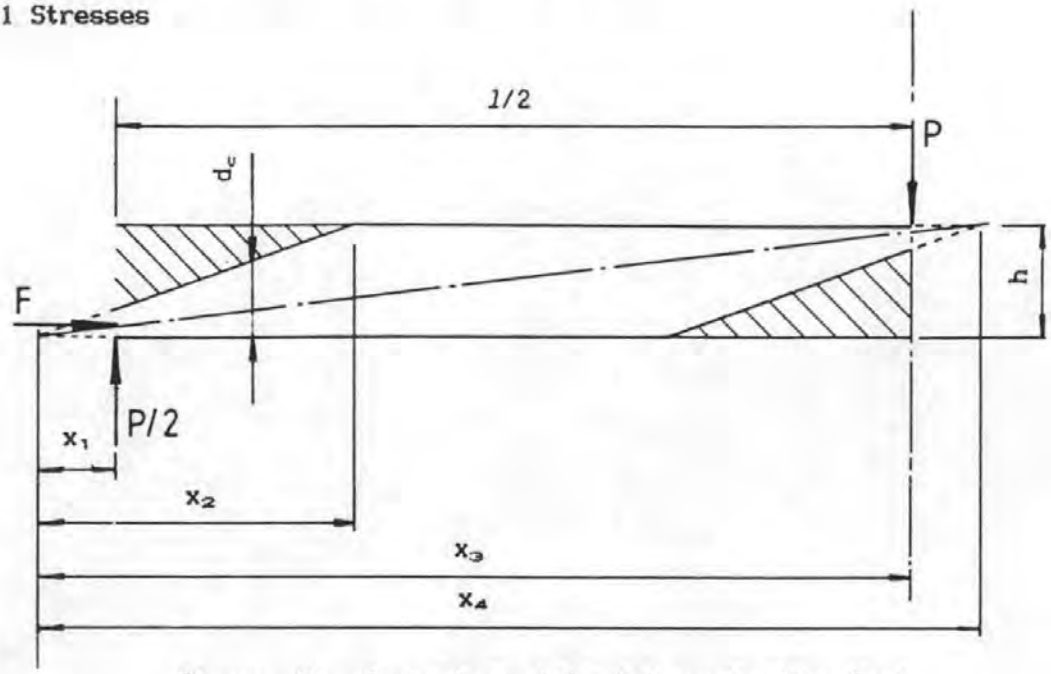

Figure: A1: Restrained slab strip under line load
(half section: elastic theory)

Consider the slab strip shown in Figure A.1. For convenience the origin of the x axis is located at the intersection of the extended line of thrust of the restraint force and the projection of the soffit of the slab.

Since the support is fully fixed in rotation, and the section at mid-span cannot rotate either because this would violate the symmetry of the system;

$$x_3 - x_1 = l/2$$

and $$x_1 = x_4 - x_3$$

Now, from the geometry of the line of thrust:

$$P/2 = Fh/x_4$$

Therefore $$F = Px_4/2h$$

Now, from x = 0 to x = x_2 the depth of concrete in compression, d_c,

$$= hx/x_2$$

$$= 3hx/x_4$$

since $$x_2 = x_4/3$$

Now the stress on the compression face of the section, f_{cc},

$$= 2F/d_c$$

$$= \frac{2F}{3hx/x_4}$$

Substituting for F, this gives:

$$f_{cc} = Px_4^2/3h^2x$$

Now, the strain at mid-depth of the slab

$$= (f_{cc}/E_c)(1-h/2d_c)$$

Note: For a wide slab, the Young's modulus, E_c, of the concrete should strictly be replaced by $E_c/(1-\nu^2)$ since the slab is forced to bend cylindrically because the transverse strains, which occur in a narrow slab due to the Poisson's ratio effect, are prevented.

Substituting for f_{cc}, d_c and F, leads to:

$$\varepsilon_c = \frac{Px_4^2}{3E_ch^2x}\left[1 - \frac{h}{2(3hx/x_4)}\right]$$

$$= \frac{Px_4^2}{3E_ch^2x}\left[1 - \frac{x_4}{6x}\right]$$

$$= \frac{Px_4^2}{3E_ch^2}\left[\frac{1}{x} - \frac{x_4}{6x^2}\right]$$

From $x = x_4/3$ to $x = 2x_4/3$ the section is uncracked so its centroid is at mid-depth. Hence the stress there is:

$$= F/h$$

so $$\varepsilon_c = Px_4/2E_ch^2$$

Now the slab's extension from the centre-line to the support;

$$= -2\int_{x_1}^{x_4/2} \varepsilon_c \, dx$$

$$= -\frac{2Px_4}{E_ch^2}\left[\frac{x_4}{3}\int_{x_1}^{x_4/3}\left(\frac{1}{x} - \frac{x_4}{6x^2}\right)dx + \int_{x_4/3}^{x_4/2}\frac{1}{2}\,dx\right]$$

$$= -\frac{2Px_4}{E_ch^2}\left\{\frac{x_4}{3}\left[\ln x + \frac{x_4}{6x}\right]_{x_1}^{x_4/3} + \left[\frac{x}{2}\right]_{x_4/3}^{x/2}\right\}$$

$$= \frac{-2Px_4^2}{E_c h^2}\left\{\frac{1}{3}\left[\ln\left(\frac{x_4}{3x_1}\right)+\frac{1}{2}-\frac{x_4}{6x_1}\right]+\frac{1}{2}\left[\frac{1}{2}-\frac{1}{3}\right]\right\}$$

$$= \frac{-2Px_4^2}{E_c h^2}\left[\frac{1}{3}\ln\left(\frac{x_4}{3x_1}\right)+\frac{1}{6}-\frac{x_4}{18x_1}+\frac{1}{12}\right]$$

$$= \frac{-2Px_4^2}{3E_c h^2}\left[\ln\frac{x_4}{x_1}-\ln 3+\frac{3}{4}-\frac{x_4}{6x_1}\right]$$

$$= \frac{-2Px_4^2}{3E_c h^2}\left[\ln(x_4/x_1)-0.3486-(x_4/6x_1)\right]$$

If the slab is rigidly restrained this must be equal to zero. Hence;

$$0 = \ln(x_4/x_1)-0.3486-(x_4/6x_1)$$

and numerical solution of this equation leads to;

$$x_4/x_1 = 13.54$$

so, at the support and at mid-span;

$$d_c = \frac{3h}{13.54}$$

$$= \underline{\underline{0.222h}}$$

now;

$$F = \frac{P}{2}\,\frac{l/2}{[h-(2/3)d_c]}$$

$$= \frac{P}{2}\,\frac{l/2}{h[1-(2/3)\times 0.222]}$$

$$= \underline{\underline{Pl/3.41h}}$$

and the maximum concrete stress

$$= 2F/d_c$$

$$= \frac{2Pl}{3.41\times 0.222h^2}$$

$$= \underline{\underline{2.64Pl/h^2}}$$

A2 Deflection

From $x = 0$ to $x = x_4/3$

$$d_c = 3hx/x_4$$

and;

$$f_{cc} = \frac{Px_4^2}{3h^2x}$$

now, the curvature

$$= \frac{f_{cc}/E_c}{d_c}$$

$$= \frac{Px_4^2 \; x_4}{E_c 3h^2 x \; 3hx}$$

$$= \frac{Px_4^3}{9E_c h^3 x^2}$$

From $x = x_4/3$ to $x = x_4/2$, where the section is uncracked, the curvature

$$= \frac{12F\ e}{E_c h^3}$$

where the eccentricity, e;

$$= \frac{h}{6}\left[1 - \frac{(x - x_4/3)}{x_4/6}\right]$$

$$= h\left[\frac{1}{2} - \frac{x}{x_4}\right]$$

and $F = \frac{Px_4}{2h}$

Thus the curvature $= \frac{12Px_4}{2E_c h^3}\left[\frac{1}{2} - \frac{x}{x_4}\right]$

$$= \frac{6P}{E_c h^3}\left[\frac{x_4}{2} - x\right]$$

From $x = x_1$ to $x = x_4/3$ the slope

$$= \int_{x_1}^{x} \text{curvature}\ dx$$

since it is zero at $x = x_1$

thus the slope $= \int_{x_1}^{x} \frac{Px_4^3}{9E_c h^3 x^2}\ dx$

$$= \frac{Px_4^3}{9E_c h^3}\left[\frac{-1}{x}\right]_{x_1}^{x}$$

$$= \frac{Px_4^3}{9E_c h^3}\left[\frac{1}{x_1} - \frac{1}{x}\right]$$

From $x = x_4/3$ to $x = x_4/2$;

$$\text{slope} = (\text{slope at } x = x_4/3) + \int_{x_4/3}^{x} \text{curvature}\ dx$$

$$= \frac{Px_4^3}{9E_ch^3}\left[\frac{1}{x_1} - \frac{3}{x_4}\right] + \int_{x_4/3}^{x} \frac{6P(x_4/2 - x)}{E_ch^3}\,dx$$

$$= \frac{Px_4^3}{9E_ch^3}\left[\frac{1}{x_1} - \frac{3}{x_4}\right] + \frac{6P}{E_ch^3}\left[\frac{x_4x}{2} - \frac{x^2}{2}\right]_{x_4/3}^{x}$$

$$= \frac{Px_4^3}{9E_ch^3}\left[\frac{1}{x_1} - \frac{3}{x_4}\right] + \frac{3P}{E_ch^3}\left[x_4x - x^2 - \frac{x_4^2}{3} + \frac{x_4^2}{9}\right]$$

$$= \frac{P}{E_ch^3}\left[\frac{x_4^3}{9x_1} - x_4^2 + 3x_4x - 3x^2\right]$$

From $x = x_1$ to $x = x_4/3$, the deflection

$$= \int_{x_1}^{x} \text{slope}\,dx$$

$$= \frac{Px_4^3}{9E_ch^3}\int_{x_1}^{x} \frac{1}{x_1} - \frac{1}{x}\,dx$$

$$= \frac{Px_4^3}{9E_ch^3}\left[\frac{x}{x_1} - \ln x\right]_{x_1}^{x}$$

at $x = x_4/3$ this is

$$= \frac{Px_4^3}{9E_ch^3}\left[\frac{x_4}{3x_1} - \ln\frac{x_4}{3} - 1 + \ln x_1\right]$$

$$= \frac{Px_4^3}{9E_ch^3}\left[\frac{x_4}{3x_1} - 1 + \ln\frac{3x_1}{x_4}\right]$$

From $x = x_4/3$ to $x = x_4/2$, the deflection relative to that at $x = x_4/3$

$$= \int_{x_4/3}^{x} \text{slope}\,dx$$

$$= \frac{P}{E_ch^3}\int_{x_4/3}^{x} \frac{x_4^3}{9x_1} - x_4^2 + 3x_4x - 3x^2\,dx$$

$$= \frac{P}{E_ch^3}\left[\frac{xx_4^3}{9x_1} - xx_4^2 + \frac{3x_4x^2}{2} - x^3\right]_{x_4/3}^{x}$$

at $x = x_4/2$ this is

$$= \frac{P}{E_c h^3}\left[\frac{x_4^4}{18x_1} - \frac{x_4^3}{2} - \frac{3x_4^3}{8} - \frac{x_4^3}{8} + \frac{x_4^3}{27x_1} + \frac{x_4^3}{3} - \frac{x_4^3}{6} + \frac{x_4^3}{27}\right]$$

$$= \frac{Px_4^3}{E_c h^3}\left[\frac{x_4}{54x_1} - \frac{5}{108}\right]$$

so the total deflection, w

$$= \frac{2Px_4^3}{E_c h^3}\left[\frac{x_4}{27x_1} - \frac{1}{9} + \frac{1}{9}\ln\frac{3x_1}{x_4} + \frac{x_4}{54x_1} - \frac{5}{108}\right]$$

$$= \frac{2Px_4^3}{E_c h^3}\left[\frac{x_4}{18x_1} - \frac{17}{108} + \frac{1}{9}\ln\frac{3x_1}{x_4}\right]$$

now, with full restraint,

$$x_4/x_1 = 13.54 \qquad \text{(from Appendix A1)}$$

substituting this into the expression for deflection gives;

$$w = \frac{0.8547\ Px_4^3}{E_c h^3}$$

now $l/2 = x_4\left[1 - \frac{2x_1}{x_4}\right]$

so $l = 1.7046\ x_4$

and $w = \frac{Pl^3}{E_c h^3}\ \frac{0.8547}{1.7046^3}$

$$= \underline{\underline{0.1726\ \frac{Pl^3}{E_c h^3}}}$$

Note. This expression can also be obtained by an algebraically simpler method using the virtual work approach.

A3 Effect of Restraint Flexibility on Stress

In Appendix A1 it was shown that the slab's extension from the centre-line to the support

$$= \frac{-2Px_4^2}{3E_c h^2}\left[\ln(x_4/x_1) - 0.3486 - (x_4/6x_1)\right]$$

This is equal to the lateral movement of each support so, if the supports develop a restraint force, F, of K times the movement whilst still giving full rotational restraint, this leads to;

$$F/K = \frac{-2Px_4^2}{3E_c h^2}\left[\ln(x_4/x_1) - 0.3486 - (x_4/6x_1)\right]$$

and, substituting for F using Appendix A1, this leads to;

$$\frac{Px_4}{2Kh} = \frac{-2Px_4^2}{3E_ch^2}\left[\ln(x_4/x_1) - 0.3486 - (x_4/6x_1)\right]$$

Therefore:

$$3E_ch = -4Kx_4\ [\ln(x_4/x_1) - 0.3486 - (x_4/6x_1)]$$

Therefore

$$K = \frac{-3E_ch}{4x_4[\ln(x_4/x_1) - 0.3486 - (x_4/6x_1)]}$$

now

$$l/2 = x_4[1 - 2x_1/x_4]$$

Therefore, substituting for x_4 and expressing the restraint stiffness relative to the axial stiffness of the uncracked slab strip:

$$\frac{Kl}{E_ch} = \frac{-3[1 - 2x_1/x_4]}{2[\ln(x_4/x_1) - 0.3486 - (x_4/6x_1)]}$$

Numerical solution of this equation gives a value of x_1/x_4 for any given restraint stiffness. By substituting this into the expressions in Appendix A1 the restraint forces and the stresses can be obtained.

APPENDIX B. TRANSVERSE SHEAR DEFORMATION OF LINE ELEMENTS

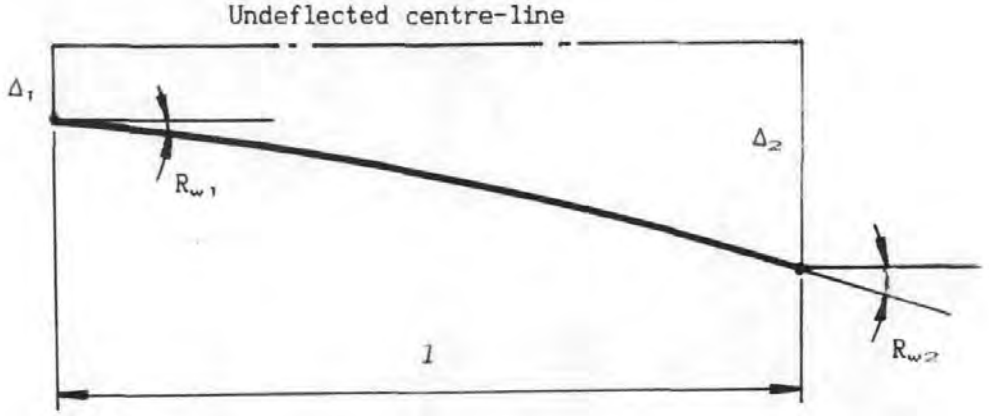

Figure B1: Plan of line element

Assume the element illustrated in Figure B1 has only a uniform curvature, C, and shear deformation, S. Then:

$$R_{w2} = R_{w1} + Cl$$

and:

$$\Delta_2 = \Delta_1 + Cl^2/2 + Sl$$

Substituting for Cl gives

$$\Delta_2 = \Delta_1 + R_{w1}l + (R_{w1} - R_{w2})l/2 + Sl$$

Rearranging gives:

$$Sl = \Delta_2 - \Delta_1 - (R_{w1} + R_{w2})l/2$$

Therefore:

$$S = (\Delta_2 - \Delta_1)/l - (R_{w1} + R_{w2})/2$$

This deformation is used to calculate the shear force, F, using the elastic shear stiffness of the slab. In the program described here, this stiffness is based on the gross area of uncracked concrete plus one third of the area of cracked concrete.

To maintain equilibrium, the moments

$$M_{w1} = M_{w2} = Fl/2$$

are applied to the nodes. This automatically results in the complimentary shears being applied to the orthogonal elements.

The element provides no resistance to the uniform curvature, C. Thus the structure provides no resistance to the form of deformation shown in Figure B2 and this deformation would not affect the results. However, this could lead to numerical instability. To avoid this a nominal resistance to uniform curvature is added.

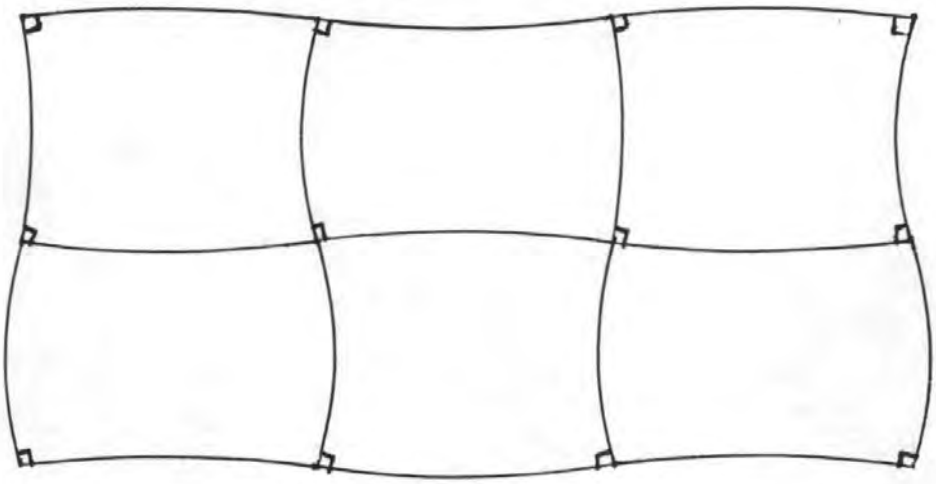

Figure B2: Unrestrained deformation

The relevant terms of the stiffness matrix are then as follows;

	M_{w1}	F_1	M_{w2}	F_2
R_{w1}	ASG *l*/4 + EI_n/l	ASG/2	ASG *l*/4 - EI_n/l	-ASG/2
Δ_1		ASG/*l*	ASG/2	-ASG/*l*
R_{w2}		(symmetrical)	ASG *l*/4 + EI_n/l	-ASG/2
Δ_2				ASG/*l*

Where:

AS is the the effective transverse shear area of the slab taken as the width of the slab in the element multiplied by $[d_c + (h - d_c)/3]$; that is the uncracked slab area plus one third of the cracked area.

G is the shear modulus of the concrete.

EI_n is the nominal transverse bending stiffness of the slab in the element which is set to a very low value, less than 1% of the elastic transverse bending stiffness.

F is the transverse force

and the other notation is as used previously.

APPENDIX C. LARGE DISPLACEMENTS

C1 Example Showing Effect of Vertical Component of Axial Force

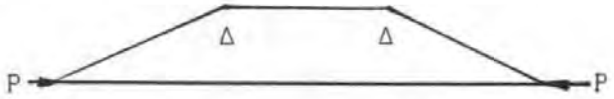

a. deflected shape

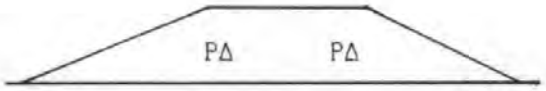

b. bending moment about deflected centre-line

c. vertical component of axial force applied to nodes

Figure C1: Three element strut

Assume the initially horizontal strut illustrated in Figure C1a is subjected only to the axial force P. Clearly, the true bending moment about the deflected centre-line of the strut is as shown in Figure C1b. The axial force in the strut is equal to P and, in an analysis using small displacement theory, this is taken as acting along the line of the elements.

The vertical component of the axial force in the outer elements is $P\Delta/l$, where l is the length of each element. If this force, which is ignored in an analysis using small displacement theory, is applied to the nodes of a computer model (which otherwise uses small displacement theory) the

resulting vertical forces are as shown in Figure C1c. These give the bending moments which are illustrated in Figure C1b and which are the true bending moments in the real strut. They also give shear forces in the outer two elements of $P\Delta/l$. Thus the resultant line of thrust acts horizontally because, as in the real strut, the vertical component of the thrust in the line of the elements is equal and opposite to the shear in the elements. Thus adding the vertical component of the axial force has reproduced the true forces in the elements.

C2 Effect of Slope on Axial Extension

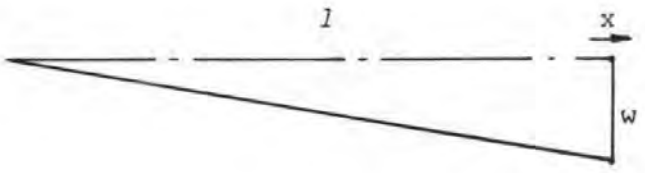

Figure C2: Inclined element

Consider the element shown in Figure C2. For convenience the left hand node is assummed to be undeflected.

According to small displacement theory, the axial extension of the element is equal to the x displacement of the right hand node. However, there is an additional extension due to the slope. Taking the horizontal length of the element as l and the inclined length as l_m *we obtain:*

$$l_m^2 = l^2 + w^2$$

Therfore $$l_m = (l^2 + w^2)^{0.5}$$

Neglecting second order terms gives:

$$l_m = l + w^2/2l$$

Hence the total axial extenxsion of the element

$$= x + w^2/2l$$

APPENDIX D. NOTATION

Because of the many references to BS 5400, the notation used has been made consistent with that document wherever possible. The main symbols used are as follows:

A_s	reinforcement area
b	width of section
c	diameter of circular contact area of load
d	depth to tension steel
d_c	depth of concrete in compression
E_c	Young's modulus of concrete
E_s	Young's modulus of steel
f	stress
f_c'	concrete stress on rectangular stress block ($0.6f_{cu}$)
f_{ct}	tensile strength of concrete (normally effective value)
f_{cu}	cube strength of concrete
f_{cyl}	cylinder strength of concrete
f_y	yield stress of reinforcement
F	force (normally restraint force)
h	overall depth of section
K	restraint stiffness
l	span (also used as element length)
M	bending moment
P	load
R	restraint factor (used in reference 72)
S_o	distance over which a crack affects the stress
w	vertical deflection
x	x direction (always horizontal, normally along element)
y	y direction (horizontal and perpendicular to x)
γ_{fL}	partial safety factor for loads
γ_{f3}	partial safety factor for errors in analysis
γ_m	partial safety factor for materials
Δ	displacement
ε	strain
ρ	reinforcement area (as percentage of concrete area, bd)